

# **Permeation Properties and Stability of Nanostructured Polyhedral Oligomeric Silsesquioxane Incorporated Poly(Vinyl Alcohol) Membranes**

Thesis submitted to  
**University of Calicut**  
in partial fulfillment of the requirements  
for the award of the degree of

**DOCTOR OF PHILOSOPHY IN CHEMISTRY**  
under the Faculty of Science

by

**SWAPNA V P**



**Post Graduate & Research Department of Chemistry  
St. Joseph's College (Autonomous), Devagiri  
Calicut, Kerala, India- 673 008**

**September 2018**

**UNIVERSITY OF CALICUT  
CERTIFICATE OF PLAGIARISM CHECK**

1	Name of the Research Scholar	SWAPNA V P		
2	Title of Thesis/ Dissertation	Permeation Properties and Stability of Nanostructured Polyhedral Oligomeric Silsesquioxane Incorporated Poly (Vinyl Alcohol) Membranes		
3	Name of the Supervisor	Dr. RANIMOL STEPHEN		
4	Department/Institution	Department of Chemistry, St. Joseph's College, Devagiri, Calicut, Kerala		
5	Similar content (%) identified	Introduction	Materials and Methods	Result/Discussion /Summary/ Conclusion
		1% (one)	1% (one)	1% (one)
	Acceptable maximum limit(%)	25	25	10
6	Software used	Urkund		
7	Date of verification	21-08-2018		

\*Report on plagiarism check, items with % of similarity is attached

Checked by (with Name, designation & signature)

Name & Signature of the Researcher *Swapna V P*

Name & Signature of the Supervisor

Name & Signature of the HoD/HoI  
(Chairperson of the Doctoral committee)



*Sibichen M Thomas*  
Dr. Sibichen M Thomas  
PRINCIPAL  
St. Joseph's College, (Autonomous)  
Devagiri, Calicut-673 008

*Dr. Ranimol Stephen*  
DR. RANIMOL STEPHEN  
Assistant Professor  
Post Graduate & Research Dept. of Chemistry  
St. Joseph's College (Autonomous)  
Devagiri, Calicut-673008

*Dr. Abdul Aziz T.*  
Dr. ABDUL AZIZ T.  
University Librarian (i/c)  
St. Joseph's College (Autonomous)  
University of Calicut  
Devagiri, Calicut-673008

**Dr. RANIMOL STEPHEN**

Assistant Professor

**Department of Chemistry**

St. Joseph's College, Devagiri

Calicut- 673 008

Tel: 9446288448

E-mail: ranistephen@gmail.com

---

## Certificate

This is to certify that the thesis entitled “**Permeation Properties and Stability of Nanostructured Polyhedral Oligomeric Silsesquioxane Incorporated Poly(Vinyl Alcohol) Membranes**” is an authentic record of the research work carried out by **Ms. Swapna V P**, under my supervision and guidance in partial fulfilment of the requirements for the award of the degree of **Doctor of Philosophy in Chemistry** under the **Faculty of Science**, University of Calicut, Kerala. The work presented in this thesis has not been submitted for any other degree or diploma earlier. It is also certified that Ms. Swapna V P has fulfilled the course requirements and qualified the course work examination for the Ph.D. degree of the University.

Calicut

15<sup>th</sup> September 2018

**Dr. Ranimol Stephen**

(Supervising Teacher)

## Declaration

I hereby declare that the thesis entitled “**Permeation Properties and Stability of Nanostructured Polyhedral Oligomeric Silsesquioxane Incorporated Poly(Vinyl Alcohol) Membranes**” is an authentic research work carried out by me under the supervision of **Dr. Ranimol Stephen**, Assistant Professor, Department of Chemistry, St. Joseph’s College, Devagiri, Calicut. This work is entirely original in its contents and has not been submitted before either in part or in full to any University or Institute for the award of any degree or diploma.

Calicut  
15<sup>th</sup> September 2018

**SWAPNA V P**



## Acknowledgement

*First and foremost, I praise God, The Almighty for showering blessings on me and giving the opportunity and granting me the capability to achieve this dream. I express my sincere and deepest sense of gratitude to my esteemed supervisor and mentor Dr. Ranimol Stephen, Assistant professor, St. Joseph's College, Devagiri, Calicut. Throughout my time as a research student, she has been providing her unlimited support, love, warm motivation, insightful decision, critical comments, correction of the thesis and above all her inspiration and patient guidance. Without her kind support, I could not dream to be at this stage. Apart, from the academic, I learned a lot from her, which I am sure will be useful in my life. She has also taken keen interest in my personal success. I also extend my thanks to her family.*

*I extend my sincere thanks to Dr. Jose John Mallikasseri, Head, Department of Chemistry, St. Joseph's College, Devagiri, and Dr. Babu I Maliakkal, former Head, Department of Chemistry, St. Joseph's College, Devagiri, for care and encouragement and all the facilities offered for my research work.*

*I am very grateful to the Management, the Principal Dr. Sibichen M Thomas, the Vice-principal Fr. Anto N.J and the former Principal, Fr. Benny Sebastian Thottanani for their permission and valuable help and encouragement during my research tenure. I am thankful to the Manager Fr. Joseph Paikada for his constant encouragement and support. I also wish to place on record my sincere thanks to all the teachers and non-teaching staff of Department of Chemistry, St. Joseph's College, Devagiri for their good wishes and generosity.*

*I acknowledge the Librarian and the entire library staff of St. Joseph's College, Devagiri and the Librarian of University of Calicut for their help during the research programme. I am grateful to all office staff of St. Joseph's College, Devagiri for their support, good wishes and generosity.*

*I express my deep sense of gratitude to all collaborators of my research work, especially I remember Prof. (Dr.) Sabu Thomas, Dr.Soney C George and their research students Abitha V K, Thomasukutty Jose, Grace Moni and Dr.*

*Hanna J. Maria for their help and fruitful discussions during my research stay at their reputed institutions.*

*My sincere thanks to Prof. (Dr.) P.M.G. Nambissan, Dr.Selvin P Thomas, Dr. Deepalekshmi Ponnamma, Dr. Kishor Kumar Sadasivuni, Dr. Subash C.K, Thulasi Radhakrishnan for their invaluable help to do various characterisation of my samples. Support and help extended by Dr. Harikumar P S, Dr. Resmi T R Scientist, CWRDM is sincerely acknowledged. I remember with gratitude the help, caring, support and constant encouragement provided by my long-time friends Vintu, Jayanthi, Shilpa, Merlin, Jaise, Meenu, Anju, Meril, Annie, Abhisha, Amritha, Sruthi, Theertha, Meera and Linda. I am extremely thankful to my friends and colleagues for their support and fruitful suggestions during the Ph.D programme. I place on record my thanks to all my teachers from schooldays through college for their blessings and support.*

*Thanks to DST-SERB for the Junior Research Fellowship to complete the research work. Special thanks to Mr Rajesh, Beena Printing for his help in neat processing of my thesis.*

*I am thankful to staff of Rubber Park India (P) Ltd, Ernakulam and Sophisticated Test and Instrumentation Centre (STIC), Cochin, for helping to do various characterisations of my samples. Finally and most importantly, I owe my deep sense of gratitude and regards to my beloved Parents, Parents-in-law and my loving husband Vimal, whose untiring patience, prayers, affection, encouragement, inspiration and support, smoothly paved my path towards the successful completion of this research work. Hearty thanks to my brothers and sister-in-laws for their unconditional love, care, affection, motivation, encouragement and support which always energised me during the entire research work.*

*There are many more people whom I have met in the course of my research work especially at conferences and seminars whose names I am not specifically taking being large in numbers. Their suggestions and comments have also helped me a lot to complete this work successfully. Thank you all.*

**Swapna V P**

..... *To My Husband and Parents*

# Preface

Polymer membrane based liquid and gas separation technique is an advent of new era in the field of science and technology due to their efficiency to separate the azeotropic mixtures and the separation of CO<sub>2</sub> from air mixtures. The current research problem arises from the fact that conventional methods are not so effective to separate azeotropic mixtures as well as the separation of CO<sub>2</sub> from gas mixtures in industries. Membrane based separation technique has established a strong platform for gas and liquid mixture separation in industries in order to protect the environment. As compared with energy-exhausting conventional methods like distillation, the membrane separation technology reduces the consumption of energy remarkably. The conventional separation process leads to many environmental, economical and technical threats to the society. Trade-off behaviour between the permeability and the selectivity of polymeric membrane is one of the most predominant restrictions for the fabrication of high performance membranes in the field of separation. The incorporation of nanoscale inorganic moieties in organic polymers has been found to be one of the most important regulation methods to overcome the trade-off behaviour, and to maintain good mechanical strength, thermal and chemical stability to the membranes. Therefore, current research focused on the development of inorganic moieties embedded polymer membrane. It is an attempt to modify the stability, pervaporation and gas mixture separation performance of PVA by incorporating chemically modified polyhedral oligomeric silsesquioxane (POSS) particles and blending with polyethylene oxide (PEO). The hybrid POSS material can contribute excellent mechanical stability and separation property to polymers. The rigid silica core of POSS imparts enhanced mechanical strength, thermal and water stability while the versatile and

adjustable outer functional groups on POSS provide good compatibilisation with PVA. The presence of ethylene glycol unit (PEO) in the PVA membrane enhances the affinity of membrane towards CO<sub>2</sub> and water molecules. Strategy adopted for the modification of PVA membrane by the incorporation of POSS and blending with PEO leads to high performance PVA membrane to separate gas and liquid mixtures without sacrificing stability, permeance and selectivity during separation.

The thesis entitled “*Permeation Properties and Stability of Nanostructured Polyhedral Oligomeric Silsesquioxane Incorporated Poly(Vinyl Alcohol) Membranes*” consists of nine chapters. **Chapter one** is a brief introduction about significance of the inorganic nanoparticle embedded polymer membrane in separation field. An updated survey of literature covering the transport theories, permeation properties of organic-inorganic hybrid membranes, properties of poly(vinyl alcohol) and polyhedral oligomeric silsesquioxane are presented. At the end of this chapter motivation, objectives and scope of this work are explained. **Chapter two** provides comprehensive information of the materials, experimental methods and characterization techniques used for the fabrication of POSS embedded PVA membranes.

**Chapter three** discuss the characterisation, mechanical and viscoelastic behaviour of PVA/POSS system. The objective of this chapter is to examine the effect of poly(ethylene glycol) (PEG) and anionic octa(tetramethylammonium) (Octa-TMA) functionalised POSS on the mechanical and viscoelastic behaviour of PVA membrane. The PVA-POSS chemical interaction, the membrane crystallinity, nature of dispersion of POSS in the PVA matrix are well analysed using various characterisation technique. **Chapter four** outlines the pervaporation separation of THF-water azeotropic mixture using PVA/POSS system. **Chapter five** provides an overview of the effect of cetyltrimethylammonium bromide (CTAB)

modified Octa-TMA-POSS (m-POSS) on the properties of PVA membrane. Characterisation, mechanical properties and pervaporation performance of PVA/m-POSS membranes are discussed in this chapter.

**In chapter six** the gas transport properties of PVA/POSS and PVA/m-POSS membranes are discussed and correlated with free volumes analysed by PALS measurements. **Chapter seven** deals with the properties of POSS embedded PVA-PEO blend membranes. In **chapter eight** the thermal degradation and water stability of PVA/POSS, PVA/m-POSS and PVA-PEO/POSS membranes are analysed and discussed in detail. **Chapter nine** is the final chapter of this thesis work, which deals with overall conclusion of the major findings discussed in all other chapters followed by future outlook of research in this field.

# Contents

<b>Chapter 1: Introduction</b>	<b>1-90</b>
1.1. Polymer modification	4
1.1.1 Grafting	5
1.1.2 Blending	6
1.1.3 Cross-linking	8
1.1.4 Copolymerization	8
1.1.5 Nanoparticle incorporation	8
1.2. Theory of transport phenomena	12
1.2.1 Transport through dense membranes solution-diffusion mechanism	12
1.2.2 Liquid mixture separation using porous membrane: Pore-flow model	15
1.2.3 Porous membrane gas mixture separation mechanism: Poiseuille flow, Knudsen diffusion and molecular sieving	16
1.3. Factors affecting transport properties of the polymer membrane	17
1.3.1 Effect of free volume	17
1.3.2 Nature of polymers	18
1.3.3 Nature of filler particles	19
1.3.4 Effect of temperature	20
1.3.5 Nature of penetrants	21
1.3.6 Degree of crosslinking	21
1.4. Applications of permeation properties of polymers	21
1.4.1. Food packaging	21
1.4.2. Membrane separation	22
1.4.2.1 Electrodialysis and reverse osmosis	22
1.4.2.2 Pervaporation	23

1.4.2.2.1 Dehydration of alcohols and tetrahydrofuran (THF)	26
1.4.2.2.2 Literature review on pervaporation study of PVA based systems	28
1.4.2.2.3 Literature review on pervaporation study of POSS embedded polymeric systems	31
1.4.2.3 Gas separation	31
1.4.2.3.1 Mechanism of gas transport in polymer nanocomposite membrane	35
1.4.2.3.1.1 Maxwell's model	35
1.4.2.3.1.2 Free-volume model	35
1.4.2.3.1.3 Solubility increase mechanism	36
1.4.2.3.2 Literature review on gas transport study of PVA based systems	36
1.4.2.3.3 Literature review on gas transport study of POSS embedded polymer systems	37
1.5. Poly (vinyl alcohol)	40
1.5.1 Structure and synthesis	41
1.5.2 Properties	43
1.5.3 Applications	45
1.6. Polyhedral oligomeric silsesquioxane (POSS)	47
1.6.1 Different types of POSS	50
1.6.2 Synthesis of POSS	52
1.6.3 Literature review on POSS based polymernanocomposites	55
1.6.4 Applications of POSS	56
1.7. Motivation of work	58
1.8. Gap areas	59
1.9. Objectives of the work	59
1.10. Scope of the work	60
1.11. References	61



<b>Chapter 2: Materials, Methods and Characterisation Techniques</b>	<b>91-121</b>
2.1. Materials	91
2.1.1 Poly(vinyl alcohol) (PVA)	91
2.1.2 Poly (ethylene oxide) (PEO)	92
2.1.3 Glutaraldehyde (GLA)	92
2.1.4 Amphiphilic POSS	93
2.1.4.1 Poly ethylene glycol-polyhedral oligomeric silsesquioxane (PEG-POSS)	93
2.1.4.2 Octa tetra methyl ammonium-polyhedral oligomeric silsesquioxane ((Octa- TMA-POSS)	94
2.1.5 Cetyltrimethylammonium bromide (C <sub>16</sub> H <sub>33</sub> N(CH <sub>3</sub> ) <sub>3</sub> Br, CTAB)	95
2.1.6 Carboxymethyl cellulose sodium salt (CMC)	95
2.2. Methods	96
2.2.1. Preparation of poly(vinyl alcohol) (PVA)-polyhedral oligomeric silsesquioxane (POSS) membranes	96
2.2.2. Modification of Octa-TMA-POSS using cetyltrimethylammonium bromide (C <sub>16</sub> H <sub>33</sub> N(CH <sub>3</sub> ) <sub>3</sub> Br, CTAB)	97
2.2.3. Fabrication of crosslinked PVA/m-POSS membranes	98
2.2.4. Fabrication of PVA-PEO/POSS membranes	99
2.3. Characterisation	100
2.3.1 Spectroscopic analysis	100
2.3.1.1 Fourier transform infrared (FTIR) spectroscopy	100
2.3.1.2 <sup>1</sup> H- NMR Spectroscopy	101
2.3.1.3 Positron annihilation lifetime spectroscopy (PALS)	101
2.3.2 Microscopic analysis	103
2.3.2.1 Transmission electron microscopy	103

	(TEM)	
	2.3.2.2 Scanning Electron Microscopy (SEM)	104
	2.3.2.3 Atomic force microscopy (AFM)	104
	2.3.3 X-ray diffraction (XRD)	105
	2.3.4 Water contact angles ( $\theta$ ) measurement	106
	2.3.5 Differential scanning calorimetry (DSC)	108
	2.3.6 Water uptake study	109
	2.3.7 Swelling study	109
	2.3.8 Mechanical properties	109
	2.3.9 Dynamic mechanical analysis (DMA)	110
	2.3.10 Pervaporation studies	110
	2.3.10.1 Flux and separation factor	112
	2.3.10.2 Permeance and selectivity	113
	2.3.10.3 Diffusion coefficient measurement	114
	2.3.10.4 Swelled membranes density measurements	115
	2.3.11 Gas permeability analysis	116
	2.3.12 Thermo gravimetric analysis (TGA)	118
2.4.	References	119
	<b>Chapter 3: Characterization, Mechanical and Viscoelastic Behaviour of PVA/POSS System</b>	<b>122-160</b>
3.1.	Introduction	123
3.2.	Results and discussion	124
	3.2.1 Characterization	124
	3.2.2 Properties	140
	3.2.2.1 Mechanical properties	140
	3.2.2.2 Dynamic mechanical analysis	149
3.3.	Conclusion	156
3.4	References	157

<b>Chapter 4: Pervaporation Separation of Azeotropic Mixture of Tetrahydrofuran-Water System Using PVA/POSS Membrane</b>	<b>161-177</b>
4.1. Introduction	162
4.2. Results and discussion	164
4.2.1. Effect of POSS on pervaporation performance of PVA membrane	164
4.2.3 Application of modified Maxwell-Stefan equation for pervaporation separation of THF-water azeotropic mixture	170
4.3. Conclusion	173
4.4. References	175
<b>Chapter 5: Characterization, Mechanical and Pervaporation Performance of Chemically Modified PVA/POSS Membranes</b>	<b>178-202</b>
5.1. Introduction	179
5.2. Results and discussion	181
5.2.1. Characterisation	181
5.2.2. Morphology	183
5.2.3 Water uptake and contact angle studies	185
5.2.4 Differential scanning calorimetry (DSC)	187
5.2.5 Mechanical studies	189
5.2.6 Pervaporation performance	192
5.2.7 Modified Maxwell-Stefan model to assess the permeation flux during the IPA-water azeotropic mixture PV separation	197
5.3. Conclusion	198
5.4. References	199
<b>Chapter 6: Gas Transport Properties and Free volume Studies of PVA/POSS and PVA/m-POSS Membranes</b>	<b>203-223</b>
6.1. Introduction.	204
6.2. Results and discussion	206
6.2.1. Positron annihilation lifetime spectroscopic (PALS) analysis	206

6.2.2. Gas separation performance of PVA/POSS membranes	208
6.3. Conclusion	218
6.4. References	220
<b>Chapter 7: Mechanical Properties and Permeation Performance of PVA-PEO/POSS Membranes</b>	<b>224-248</b>
7.1. Introduction	225
7.2. Results and discussion	227
7.2.1. FT-IR analysis	227
7.2.2. Morphology	228
7.2.3. Hydrophilicity	231
7.2.4. Differential scanning calorimetry (DSC)	231
7.2.5. Mechanical properties	233
7.2.6 Free volume studies	237
7.2.7 Gas transport properties	238
7.2.8 Pervaporation separation of THF-water azeotropic Mixture	240
7.3. Conclusion	244
7.4. References	245
<b>Chapter 8 Thermal and Water Stability of PVA/POSS, PVA/m-POSS and PVA-PEO/POSS Systems</b>	<b>249-275</b>
8.1. Introduction	250
8.2. Results and discussion	251
8.2.1 Thermo gravimetric analysis (TGA) analysis	251
8.2.1.1 POSS molecules	251
8.2.1.2 PVA/POSS systems	253
8.2.1.3 Crosslinked PVA/POSS systems	257
8.2.1.4 PVA/m-POSS systems	260
8.2.1.5 PVA-PEO/POSS systems	262
8.2.6 Analysis of residue of all systems	264
8.2.7 Activation energy for thermal degradation	265
8.2.8 Mechanical properties in the hydrated state	268
8.4. Conclusion	271
8.5. Reference	272

<b>Chapter 9 Conclusions and Future Outlook</b>	<b>276-282</b>
9.1. PVA/PEG-POSS and Octa- TMA-POSS system	277
9.2. PVA/m-POSS system	278
9.3. PVA-PEO/PEG-POSS and Octa-TMA-POSS system	280
9.4. Mechanical stability and permeation properties- A comparison	280
9.5 Future aspects	282

# Symbols and Abbreviations

AFM	-	Atomic force microscopy
ATR	-	Attenuated total reflection
BA	-	Boric acid
BTEE	-	1,2-bis (triethoxysilyl) ethane
C	-	Concentration
CMC	-	Carboxymethyl cellulose sodium salt
CNT	-	Carbon nanotubes
CTAB	-	Cetyltrimethylammonium bromide
D	-	Diffusion coefficient
$D_K$	-	Kundsen diffusion coefficient
DBE-PEG	-	Polyethylene glycol dibutyl ether
DD	-	Double distilled
$\overline{D_{iM}}$	-	Average diffusion coefficient
DMA	-	Dynamic mechanical analysis
DMU	-	Dimethylol urea
DN	-	Double network
DS	-	Degree of swelling
DSC	-	Differential scanning calorimetry
$E'$	-	Storage modulus
$E''$	-	Loss modulus
$E_a$	-	Activation energy
EBM	-	Equivalent box model
$E_c$	-	Modulus of composite
$E_m$	-	Modulus of pure PVA
FS	-	Fumed silica
FTIR	-	Fourier transform infrared
$f_v$	-	Fractional free volume
FVE	-	Free volume elements
GC	-	Gas chromatography
GLA /GLU	-	Glutaraldehyde
GO	-	Graphene oxide
GONS	-	Graphene oxide nanosheet
GPU	-	Gas permeation unit
HEMA	-	2-hydroxyethyl methacrylate
HM	-	Horowitz and Metzger

	-	Hours
hrs		
IPA	-	Isopropanol
J	-	Flux
$J_{H_2O}$	-	Component flux of water
$J_i$	-	Molar flux of the component i
$J_{THF}$	-	Component flux of THF
$K_E$	-	Einstein coefficient or intrinsic viscosity
$K_H$	-	Higuchi constant
$l$	-	Membrane thickness
M	-	Monomer
MMA	-	Methyl methacrylate
MPA	-	Mega pascal
m-POSS	-	Modified polyhedral oligomeric silsesquioxane
MW	-	Molecular weight
NP	-	Nanoparticles
OCP	-	CTAB modified octa-TMA-POSS
OCTA-TMA	-	Octa tetra methyl ammonium
OPC	-	Oxygen permeability coefficients
O-PS	-	Ortho- positronium
OTR	-	O <sub>2</sub> transmission rate
P	-	Permeability/Permeation coefficient
P0	-	Pure poly(vinyl alcohol)
PA	-	Polyamide
PAA	-	Poly(acrylic acid)
PALS	-	Positron annihilation lifetime spectroscopy
PANI	-	Polyaniline
$P_c$	-	Permeability of pure poly (vinyl alcohol)
PEBAX	-	Poly(amide-b- ethylene oxide)
PEG	-	Poly(ethylene glycol)
PEA	-	Polyetheramine
PEO	-	Poly(ethylene oxide)
PG	-	Glutaraldehyde crosslinked poly(vinyl alcohol)
PGO1	-	Octa-TMA-POSS incorporated crosslinked poly (vinyl alcohol)
PGP1	-	PEG-POSS incorporated crosslinked poly(vinyl alcohol)
PHEMA	-	Poly (2-hydroxyethylmethacrylate)
PI	-	Polyimide
$P_{il}$	-	Vapour pressure of the component i over permeate

	-	side of the membrane
$P_{i0}$	-	vapour pressure of the component i over feed and permeate side of the membrane
POSS	-	Polyhedral oligomeric silsesquioxane
POCPG	-	M-POSS incorporated crosslinked poly(vinyl alcohol)
POTP	-	Octa-TMA-POSS incorporated poly(vinyl alcohol)
PPP	-	PEG-POSS incorporated poly(vinyl alcohol)
PPCOP3	-	Octa-TMA-POSS incorporated poly(vinyl alcohol)-Poly(ethylene oxide)
PPCPP3	-	PEG-POSS incorporated poly(vinyl alcohol)-Poly(ethylene oxide)
P-PS	-	Para-positronium
PS	-	Positronium
PSI	-	Pervaporation separation index
PSS	-	Polysilsesquioxane
PU	-	Polyurethane
PV	-	Pervaporation
PVA	-	Poly (vinyl alcohol)
R	-	Free volume radius/Pore radius
R	-	Universal gas constant
$R_a$	-	Average deviation of height
RO	-	Reverse osmosis
$R_q$	-	Root-mean-square surface roughness
S	-	Solubility coefficient
SEM	-	Scanning electron microscopy
SNS	-	Silica nanospheres
SPEEK	-	Functionalised silica in poly(ether ether ketone)
T	-	Time
$T_{MAX}$	-	Temperature at maximum rate of weight loss
$T_c$	-	Crystallization peak temperature
TEM	-	Transmission electron microscopy
TEOS	-	Tetraethoxysilane
THF	-	Tetrahydrofuran
$T_g$	-	Glass transition temperature
TGA	-	Thermo gravimetric analysis
$T_m$	-	Melting peak temperature
TMS	-	Tetramethylsilane
$W_A$	-	Work of adhesion
WAC	-	Water absorption capacity



W.r.to	-	With respect to
Wt%	-	Weight percentage
X	-	Distance
$X_c$	-	Crystallinity
XRD	-	X-ray diffraction
$\theta_c$	-	Contact angle in the Cassie–Baxter model
$\Delta H_C$	-	Heat of crystallisation
$\Delta H_F$	-	Heat of fusion
$\Lambda$	-	Mean free path
$\theta_y$	-	Youngs contact angle
$\theta_w$	-	Apparent contact angle
$\phi$	-	Volume fraction of filler
$\phi_{\max}$	-	Maximum packing fraction of the filler
$\mu$	-	Viscosity
$\mu_i$	-	Chemical potential of component i
$\frac{d\mu_i}{dz}$	-	Chemical potential gradient of component i
T	-	Tortuosity
A	-	Separation factor
$\alpha_{wt}$	-	Water selectivity
$\beta$	-	Enrichment factor
$\gamma_s$	-	Surface free energy
$\gamma_{sl}$	-	Interfacial free energy
$\rho_w$	-	Density of water
$\bar{\rho}_M$	-	Average density of the swollen polymer membrane
$\nu$	-	Poisson's ratio
$\sigma_m$	-	Tensile strength
$\tau_1$	-	Para-positronium lifetime
$\tau_2$	-	Free positron lifetime
$\tau_3$	-	Ortho- positronium lifetime

## Chapter 1

# Introduction

---

Membrane separation technology has so far been a rapidly developing area in the field of separation due to its economical and environmental advantages and their ability to overcome the limitations of conventional separation methods like distillation. Separation process is the main component in the manufacturing process in chemical industries. It is mainly aimed at the elimination of contaminants from factory effluent water and air, removal of contaminants from raw materials and purification of primary products. Development of polymer membrane based separation technique is considered to be one of the rewards to our world and it contributes a lot to our society. Membranes can be defined as a thin layer of semi-permeable material allowing the selective transport of one or more chemical component in contact with it.<sup>1-2</sup> Membranes consist of distinct thin interfaces that manage the permeation of chemical substances through it. According to Mulder, membrane is a selective barrier between two phases.<sup>3</sup> **Figure 1.1** depicts the classification of membranes based on various criteria like origin, material, geometry, structural factors and applications. Conventional separation processes such as liquid-liquid extraction, distillation, adsorption and solvent absorption are energy-exhausting processes, that involve many complicated operations and produce many environmental, economical and technical issues as well as ineffective in separation of azeotropic mixtures. The membrane technology has demonstrated outstanding advantages over conventional separation methods, which include efficiency in separation, ease of processability, moderate cost, low maintenance necessity and low energy consumption. The membrane technology is an environment friendly method

---

*A part of this chapter has been accepted as a chapter 'Polymer/ POSS Nanocomposite Membranes for Pervaporation' in the eBook Polymer/ POSS Nanocomposite Membranes for Pervaporation, ISBN: 9780128167854, Elsevier (March 2020)*

---

where no additives are required and offers contaminant elimination without generating any hazardous by-products.<sup>4-8</sup>

**Table 1.1** presented the characteristics and classification of membrane based separation processes mainly based on the driving force, mechanism and nature of membrane (porous/dense). Separation includes microfiltration, ultrafiltration, nanofiltration, reverse osmosis (RO), membrane distillation, diffusion dialysis, electrodialysis, solvent extraction, pervaporation (PV) and gas separation. In the past few decades, polymeric membrane based separation and purification technologies have gained considerable research attention because of its remarkable applications in various fields such as medical, electronics and food industry. Physicochemical properties of the polymers and affinity of membranes towards penetrants are the important factors that determine the separation performance of the membrane. The rate of transport of liquid or gases through polymers is governed by number of factors, which includes driving forces (concentration gradients, temperature and pressure), features of permeating substance (molecular size, chemical nature, and molecular shape), properties of polymer membrane (free volume, physical aging, crystalline/amorphous structure and porous/nonporous structure) and the composition of the feed mixture.<sup>9-13</sup> The general features of membrane to exhibit efficiency in gas and liquid separation are,

- presence of amide or hydroxyl functionality
- degree of polarity (e.g., nitrile, chloride, fluoride, acrylic and ester)
- high chain stiffness and crystallinity
- inertness to the diffusing substance
- strong attraction or bonding between polymer chains
- high glass transition temperature ( $T_g$ )

Therefore, polymers such as polyimides, poly(vinyl alcohol), polysulfone, polyamides, polyaniline, poly(dimethyl siloxane) and polycarbonates are widely used for the fabrication of membranes for separation processes.<sup>14-20</sup>

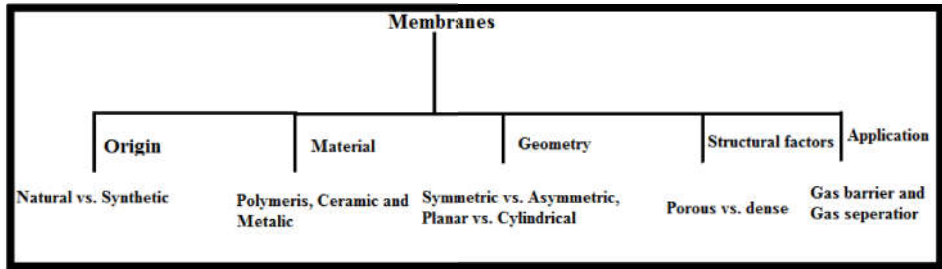


**Figure 1.1:** Classification of membranes based on various criteria

**Table 1.1:** Characteristics of various membrane separation processes

Process	Transport mechanism	Driving force	Pore size	Pressure difference
Micro filtration	Sieving	Pressure difference	0.1-10 $\mu$ m	0.5-2 bar
Ultra filtration	Sieving	Pressure difference	1-100nm	1-10 bar
Nanofiltration	Solution diffusion	Pressure difference	0.7-2nm	10-70 bar
Reverse Osmosis	Solution diffusion	Pressure difference	<2nm	15-100 bar
Dialysis	Diffusion	Chemical potential	1.5-10 nm	Atmospheric
Pervaporation	Solution diffusion	Activity difference	Non-porous	Vacuum/ Atmospheric
Gas separation	Solution diffusion	Fugacity difference	Non-porous	1-20 bar

---

The simplicity and cost-effectiveness of the membrane separation process makes it extremely attractive for industrialists and other scientific community. However, efficiency of the membrane is a major concern for its end use applications. For instance, membrane fouling is one of the major drawbacks associated with the membrane based liquid mixture separation. Several kinds of fouling has been observed in membrane system including crystalline, organic and microbial fouling. The attachment of solutes onto the surface or internal structure of the membrane results in fouling. Consequently, these materials block the transport of solvent across the pores of the membrane, resulting in reduced selectivity, flux and overall service life of the membrane.<sup>21-24</sup> A lot of polymers have been investigated for their separation performance but only a small number of pure polymer membranes are applied in industry for liquid and gas mixture separation. Therefore, current researches in polymeric membranes are focused on its performance i.e., better selectivity without sacrificing permeability and durability under the process conditions. Unfortunately, intrinsic trade-off behaviour between permeability and selectivity and decreased product purity are the major restrictions for development of high performance polymer membranes.<sup>25-28</sup> Moreover, plasticization and aging factors also significantly reduce the efficiency of separation. This drawback of the polymer can be overwhelmed by certain modifications.

The development of high performance membranes by embedding nanoscale inorganic moieties in organic polymers have been found to be a successful strategy to overcome the limitation.

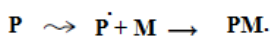
### **1.1 Polymer modification**

Most widely used polymer modification strategies are grafting, blending, crosslinking, copolymerisation and nanoparticle incorporation.<sup>29-36</sup>

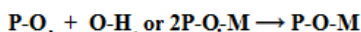
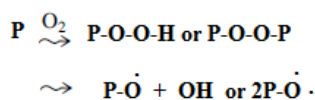
### 1.1.1 Grafting

In this method, oligomeric chains are attached irregularly to the main chain of the polymer through chemical reaction or irradiation process. Grafting by chemical reaction can be achieved only if grafted molecule contains functional group and is capable to react with functional groups present in the polymer chain. In the case of insoluble polymer, irradiation technique such as free radical grafting, ionic grafting and photochemical grafting is usually employed to graft oligomer. For instance; the mechanism of free radical grafting in three different ways are shown in **Figure 1.2**. As shown in **Figure 1.2 (a)**, in pre-irradiation method: polymer (P) is initially irradiated in vacuum to form free radical, then the monomer (M) is treated with the irradiated polymer in a suitable solvent. The second method is peroxidation grafting (**Figure 1.2 (b)**), here polymer is first converted to hydroperoxides or diperoxides by the application of high-energy radiation in presence of air followed by the high temperature treatment of the formed stable peroxides with monomer to decompose the peroxide to radicals and it then starts grafting. **Figure 1.2 (c)** shows the mutual irradiation method: both the monomer and polymer irradiate together and produce free radicals, following the addition process.<sup>37</sup>

**(a) Grafting (pre-irradiation)**



**(b) Grafting (peroxidation)**



**(c) Grafting (mutual irradiation)**

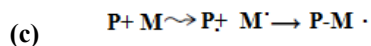


**Figure 1.2:** The mechanisms of free radical grafting

---

### 1.1.2 Blending:

Blending of polymers is an efficient technique to produce material with optimum properties such as hydrophilicity, high selectivity and permeance together. Yave *et al.* fabricated Pebax®/PEG blend membranes for CO<sub>2</sub> separation. They achieved good permeability and selectivity for CO<sub>2</sub> due to the presence of highly CO<sub>2</sub>-philic PEG plasticizer, which will enhance the free volume and chain mobility of polymer.<sup>38</sup> Zereshki *et al.* examined the pervaporation performance of poly(lactic acid)/poly(vinyl pyrrolidone) blend membranes for the separation of ethanol/ethyl tert-butyl ether azeotropic mixture, the membrane shows good flux and satisfactory selectivity during separation performance.<sup>39</sup> The separation performance of polymer blends are mainly controlled by its phase behaviour, ie; miscible or phase separated. In miscible blend, equation (1.1) is applied to predict the permeability,

$$\ln P_b = \phi_1 \ln P_1 + \phi_2 \ln P_2 \quad (1.1)$$

where  $\phi_1$  and  $\phi_2$  are volume fraction of polymer components 1 and 2 in the polymer blend.  $P_1$ ,  $P_2$  and  $P_b$  are permeability of polymer 1, 2 and blend respectively.

Phase separated blend membranes permeability expression is quite complex because the continuous phase changes from polymer 1 to polymer 2. Hence there are many models developed for their expression such as parallel (eq.1.2), series (eq.1.3), Maxwell's (eq.1.4) and equivalent box model (EBM) (eq.1.5). First three models consider that one phase is entirely continuous whereas EBM model is based on co-continuous morphology

$$P_b = \phi_1 P_1 + \phi_2 P_2 \quad (1.2)$$

$$P_b = P_1 P_2 / (\phi_1 P_2 + \phi_2 P_1) \quad (1.3)$$

$$P_b = P_m \left[ \frac{P_d + 2P_m - 2\phi_d(P_m - P_d)}{P_d + 2P_m + \phi_d(P_m - P_d)} \right] \quad (1.4)$$

Maxwell's model can be applied for dispersed phases with spherical nature, where  $P_d$  and  $\phi_d$  are dispersed phase permeability and volume fraction.  $P_m$  is the permeability of matrix phase.

$$P_b = P_1\phi_{1p} + P_2\phi_{2p} + \phi_s^2 \left[ \frac{\phi_{1s}}{P_1} + \frac{\phi_{2s}}{P_2} \right] \quad (1.5)$$

where  $\phi_s = \phi_{1s} + \phi_{2s}$

$$\phi_{1p} = [(\phi_1 - \phi_{1cr}) / (1 - \phi_{1cr})]^{T_1}; \quad \phi_{1s} = \phi_1 - \phi_{1p}$$

$$\phi_{2p} = [(\phi_2 - \phi_{2cr}) / (1 - \phi_{2cr})]^{T_2}; \quad \phi_{2s} = \phi_2 - \phi_{2p}$$

$\phi_{1cr}$  and  $\phi_{2cr}$  represent critical threshold percolation values of polymer 1 and 2.  $T_1$  and  $T_2$  indicate polymer components critical percolation exponents.<sup>40</sup> Different models are schematically presented in **Figure 1.3**.<sup>41</sup>

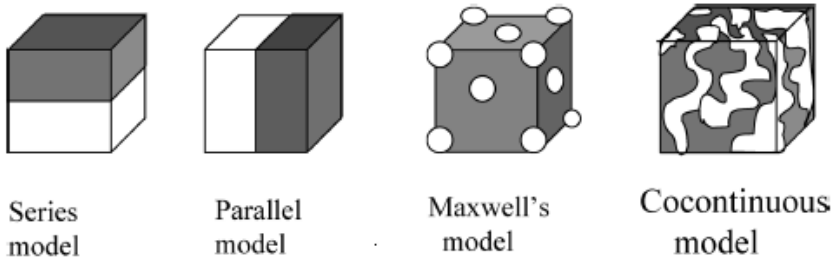


**Figure 1.3:** Various permeability models of phase separated blend.<sup>41</sup>



---

### 1.1.3 Cross-linking

The reason for introducing crosslink in macromolecular chains is to reduce degree of swelling, resist solubility of polymers in the feed mixture, to suppress the plasticization phenomenon during pervaporation and gas separation processes and finally to enhance selectivity. Tortuous path is high in crosslinked polymer matrices during mass transport. Crosslinking of polymers can be carried out mainly through three methods, which includes chemical (two polymer chains are connected through chemical compound), physical and irradiation process. Vanherck *et al.* reviewed the features of different crosslinking methods and its effect on the properties of polyimide membranes.<sup>42</sup>

### 1.1.4 Copolymerisation

Unlike polymer blends, in copolymerised systems, covalent bonds exists between two polymer components, which will enhance the overall properties of the polymer. This technique can be employed for the synthesis of random, graft and block copolymers. Degree of crystallinity is a major characteristic of copolymerisation. Random copolymers produce materials with fully amorphous nature whereas graft copolymers produce materials with definite degree of crystallinity. For the PV application, it is necessary to have a polymer with some extent of crystallinity to achieve high selectivity.<sup>43</sup>

### 1.1.5 Nanoparticle incorporation

Nanoparticle incorporation in polymer matrix has been an efficient path for enhancing the polymer membrane performance for a wide range of processes, such as gas separation and pervaporation. As the particle size reduces, the number of atoms on the particle surface increases leading to exceptionally high interfacial area in composites. The particles might enhance the polymer permeability, diffusion rate, permselectivity, tensile strength and fouling resistance.<sup>44-47</sup> Filler characteristics (size, volume fraction, surface area and

---

agglomeration), method of incorporation of nanoparticle in polymer matrix and the interaction between polymer matrix and filler particle are the crucial factors that determine the transport properties of polymeric nanocomposites.

The interaction existing between nanoparticle and organic polymers may be strong chemical (covalent/co-ordination/ionic bonds) or weak physical (van-der-Waals force/ hydrogen-bonds/ hydrophilic-hydrophobic balance) interactions.<sup>48</sup> Schematic representation of different types of polymer-filler interactions are shown in **Figure 1.4**. The interfacial interaction between polymer and inorganic filler and the nature of dispersion of the nanofillers in the polymer matrix are the important factors that control the reinforcing efficiency of nanoparticle in the polymer matrix. The major issue encountered by researchers in the fabrication of inorganic–organic systems are in the mixing between two dissimilar phases because the nanoparticles usually tend to aggregate in polymer matrix, in order to reduce very high surface energy. This particle aggregation reduces the mechanical and other properties of the resulting material. This problem can be addressed by using functionalised polymers or surface modified inorganic particles with appropriate organic groups.<sup>49-50</sup> The surface modification of particle can be achieved through grafting and in situ functionalization during their development (**Figure 1.5**). Organic modification of inorganic nanoparticle made it more compatible with the polymer matrices. The improved interface between particle and polymer system leads to the improvement in mechanical, transport and other properties of polymer.<sup>51-54</sup>

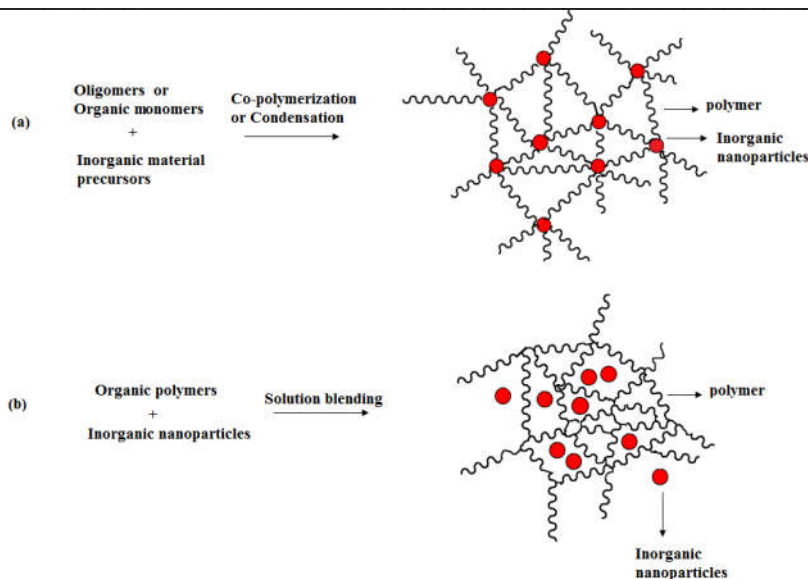


**Figure 1.4:** Schematic demonstration of various methods for the incorporation of inorganic materials in polymer systems, where organic and inorganic phases are linked via (a) covalent bonds and (b) van der Waals force or hydrogen bonds.

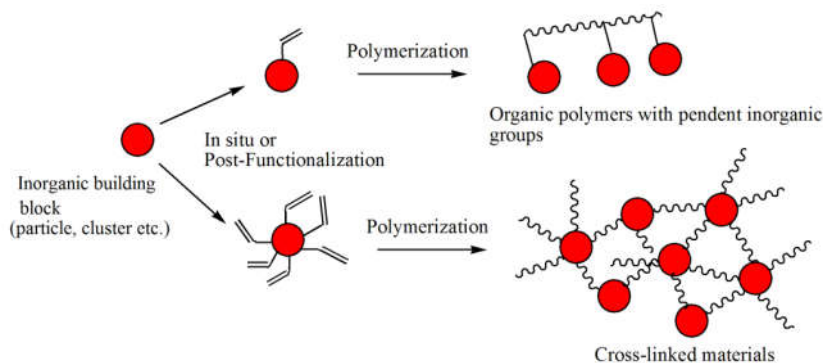


**Figure 1.5:** Surface modification of nanoparticle through grafting and in situ functionalization.

Semsarzadeh *et al.* synthesized silica particles through in-situ method using tetraethoxysilane (TEOS) precursor in the presence of poly(vinyl alcohol)(PVA) and cetyltrimethyl ammonium bromide (CTAB) as templating

agents (**Figure 1.6**).<sup>55</sup> The prepared particles were incorporated into polyurethane (PU) membrane by solution casting method. This membrane exhibited enhanced CO<sub>2</sub> solubility in PU as compared with pristine PU due to the presence of polar hydroxyl groups in PVA template and in silica particle.

Khoonsap *et al.* synthesised a membrane by incorporating poly(2-hydroxyethylmethacrylate) (PHEMA) grafted fumed silica (FS) in PVA matrix.<sup>56</sup> The membrane has been employed for the pervaporation separation of water-acetone mixture, and found that the membrane exhibit higher water permeation and selectivity over unmodified FS doped PVA membrane.

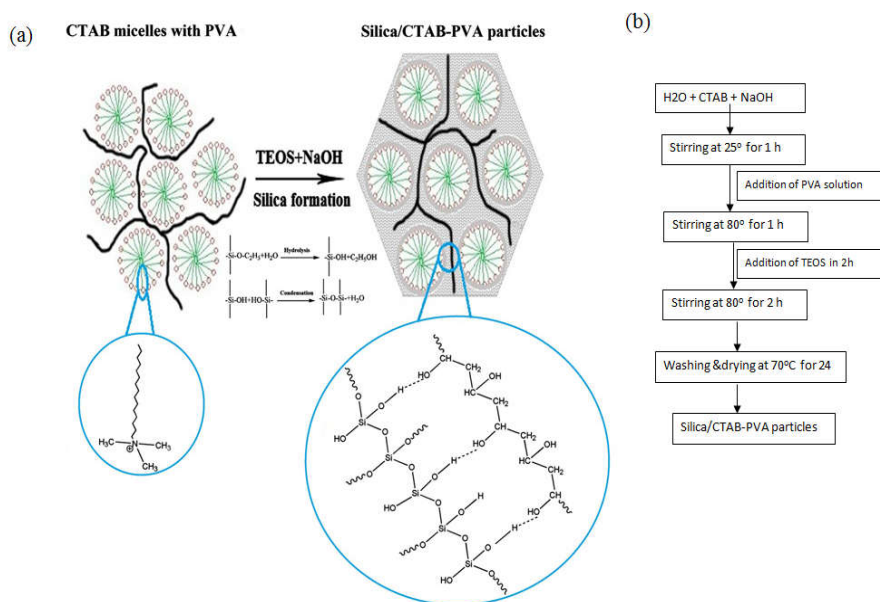


**Figure 1.6:** The illustration of (a) formation mechanism (b) schematic flow diagram, for the preparation of silica particle from TEOS precursor in the presence of PVA and CTAB as templating agents.<sup>55</sup>

## 1.2 Theory of transport phenomena

### 1.2.1 Transport through dense membranes: Solution-diffusion mechanism

The transport of liquid and gas mixtures across the non-porous dense polymeric membranes are based on the solution diffusion mechanism introduced by Thomas Graham and afterwards Paul and Koros.<sup>57-58</sup> The process occurs in three steps and is schematically presented in **Figure 1.7**.<sup>59-62</sup>

- (i) sorption of solute in the upstream face of the membrane surface
- (ii) diffusion of permeate across the membrane based on gradient of concentration
- (iii) desorption of permeate from the downstream surface of the membrane

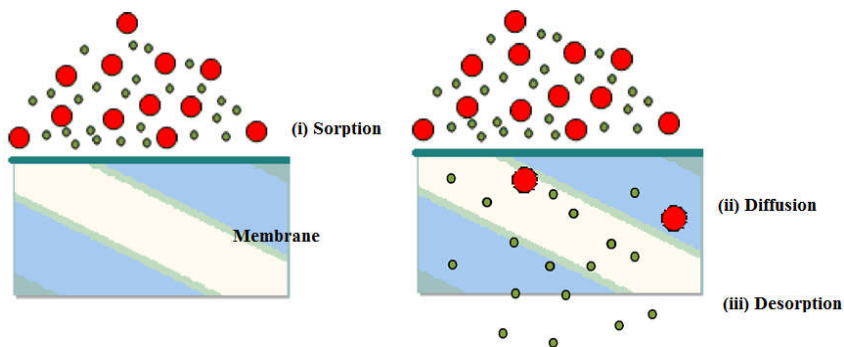


**Figure 1.7:** Schematic illustration of solution diffusion mechanism.

Chemical potential or concentration gradient between upper and downstream side of the membrane is the basic driving force for separation, which is created by the application of partial pressure difference to the diffusing species across the membrane. The application of vacuum pump or an inert purge on the downstream permeate side of the membrane helps to establish the partial pressure difference. In this process, second step (diffusion) is the

rate controlling step. The product of diffusion coefficient 'D' (kinetic factor) and solubility coefficient 'S' (thermodynamic factor) parameters gives the permeability (P) of the membrane. Morphology, mobility of polymer chains, free volume, orientation of additives and the penetrant-polymer interaction are the major factors that control the diffusion and permeation properties of polymer membranes.<sup>63, 47</sup>

**Sorption:** Sorption is a concomitant term for adsorption (physical process) and absorption (chemical process), in which one substance takes up another. Generally thermodynamic sorption expresses penetration and dispersal of permeant species into the membrane. Sorption coefficient (S) depends strongly on the interactions between penetrant and the polymer. S is the ratio of weight of the solvent taken up at equilibrium swelling ( $M_{\infty}$ ) to the weight of the membrane at initial stage ( $M_0$ ) and is given by the equation,

$$S = M_{\infty} / M_0 \quad (1.6)$$

Crystallinity, free volume, swelling degree and glass transition temperature of the polymer membrane are the important factors that influence the sorption performance of the polymer membrane.<sup>64-66</sup>

Sorption ability of the membrane gets reduced with increasing crystalline regions in the membrane. Porous membrane exhibit selective sorption of molecules based on their size while in the case of nonporous membrane, it is based on the affinity or interaction of membrane towards gas or liquid molecules.

**Diffusion:** Diffusion is a kinetic parameter and in the process molecule is transported between different regions of polymer phase by random molecular motions.

Fick's first and second laws of diffusion explains the steady state and non-steady state diffusion processes.<sup>67-68</sup> Fick's first law expressed the relationship between gradient of concentration ( $\frac{\partial C}{\partial x}$ ) in the membrane and flux of the diffusing species at steady-state condition,

$$J = -D \frac{\partial C}{\partial x} \quad (1.7)$$

C indicates concentration of diffusing species, J is the flux, D (cm<sup>2</sup>/s) corresponds to diffusion coefficient/diffusivity and x is the thickness of the membrane. At nonsteady-state condition, Fick's second law is applicable,

$$\frac{\partial C}{\partial t} = D \frac{\partial^2 C}{\partial x^2} \quad (1.8)$$

where  $\frac{\partial C}{\partial t}$  is the rate of change of permeant concentration at any point in the membrane. In the case of nonsteady-state condition, the concentration gradient across the membrane varies with time, but second law is derived by assuming that the membrane is isotopic, flow is unidirectional and D is a constant independent of concentration (C), time (t) and distance (x). Fick's law of diffusion is generally applied for rubbery polymers. While in glassy polymers, non-Fickian kinetics for diffusion is generally applied.<sup>69-70</sup>

Diffusivity (D) is measured from the following equation,

$$D = \pi \left( \frac{h\theta}{4Q_\infty} \right)^2 \quad (1.9)$$

where  $\theta$  is the slope of the initial linear portion of the sorption curve  $Q_t$  % against square root of time.  $Q_\infty$  is the number of moles of liquid sorbed per

gram of sample at equilibrium and  $h$  is the thickness of the sample. The  $S$  and  $D$  are the two important terms explain the permeation process. The permeation coefficient ( $P$ ) is the product of the  $D$  and  $S$  ( $P = D \times S$ )

### 1.2.2 Liquid mixture separation using porous membrane: Pore-flow model

In 1991 Okada and Matsuura have introduced pore-flow model for pervaporation. This model assumes that in the membrane a selective layer contains a bunch of straight cylindrical pores through which transport of molecules takes place under an isothermal condition. The driving force for the separation of permeant is the difference in pressure over the membrane which leads to phase change for liquid permeate to vapour state across the transport in the membrane. In the pores of the membrane filtrate one component from the feed and other component is preferentially sorbed by the membrane, which move across the membrane through capillary flow mechanism.<sup>71-72</sup> The flux equation for pore-flow model is given below

$$J = \left[ \frac{Q}{Z} (P_f - P_{sat,mix}) + \frac{B_i}{Z} (P_{i,f}^2 - P_{i,p}^2) + \frac{B_j}{Z} (P_{j,f}^2 - P_{j,p}^2) \right] (x_j M_i + x_i M_j) \quad (1.10)$$

where  $J$  is the total flux,  $P_f$  is the pressure of permeate in the membrane pore's inlet, partial pressures on the feed and permeate side of the component 'i' is represented by  $P_{i,f}$  and  $P_{i,p}$  respectively,  $M$  is the molecular weight,  $Z$  is thickness of the membrane,  $Q$  is a constant,  $B_i$  and  $B_j$  are the membrane selectivity of  $i^{\text{th}}$  and  $j^{\text{th}}$  component.



---

### 1.2.3 Porous membrane gas mixture separation mechanism: Poiseuille flow, Knudsen diffusion and Molecular sieving

Poiseuille flow, Knudsen diffusion and molecular sieving are three important mechanisms employed to analyse gas mixture separation performance of the membrane based on the diameter of gas molecule and free volume radius of the membrane.

Poiseuille flow mechanism is applied in porous membranes with membrane pore radius ( $r$ ) is greater than  $5 \mu\text{m}$  and  $r^4$  proportional to permeate flux. If the gas molecules mean free path ( $\lambda$ ) is lower than ' $r$ ', gas molecule undergoes the viscous flow or Poiseuille.<sup>3,73</sup> Expression for the mean free path is,

$$\lambda = \frac{3\mu}{2p} \sqrt{\frac{\pi RT}{2M_w}} \quad (1.11)$$

where  $M_w$  is the molecular weight of gas molecule,  $T$  is the temperature,  $R$  is the universal gas constant,  $\mu$  is viscosity of gas molecules and  $p$  is pressure.

Knudsen diffusion predominated, when the gas molecules mean free path ( $\lambda$ ) is greater than  $r$  of membrane. This mechanism mainly occurs in a membrane having 5-10 nm range pore diameter. In this mechanism transport occurs due to the higher interaction of gas molecules with surface of the pore.<sup>74</sup> The equation for Knudsen diffusion coefficient ( $D_k$ ) is,

$$D_k = 97r \sqrt{\frac{T}{M_w}} \quad (1.12)$$

Molecular sieving mechanism is employed in porous membranes when membrane pore radius ( $r$ ) is less than 4 nm and very small molecules are selectively transported across the membrane. The membranes with high

---

selectivity during gas separation can be potentially explained using this mechanism. Molecular sieving mechanism is applied in carbon molecular sieve and zeolite membranes when used in gas transport study.

### 1.3 Factors affecting transport properties of the polymer membrane

Permeability and solubility of gases or liquids vary with the nature of the polymer and permeants. There are many key parameters that has great influence on the transport of gas or liquid molecule across the polymer membrane such as polymer chain mobility, amount of free volume within the membrane, crystallinity, molecular weight, glass transition temperature ( $T_g$ ), nature of cross-links, penetrant feature, composition of the feed, casting solvents employed for membrane fabrication, temperature, polarity of permeant and affinity of membrane towards diffusing molecule.<sup>75-77</sup> Yampolskii has reported the relation between structure and transport of various polymeric systems.<sup>78</sup>

#### 1.3.1 Effect of free volume

Free volume in a polymer can be defined as volume of the total mass, that is not occupied by polymer chains themselves and hence diffusing molecules can be situated there. It can generally be said to the gap or pores occupied between the chains of polymers. The direct examination of pore in the membrane is impossible because the gaps are occur at molecular scale. The schematic representation of the free volume in a polymer is shown in **Figure 1.8**. It is an intrinsic, transient and dynamic property. The physical state and density of the polymer greatly influence the free volume properties of membrane. The process of reduction of excess free volume in the membrane can be referred as physical aging, which originates from the lattice contraction and diffusion of the free volume from membrane interior to the surface.<sup>79</sup>

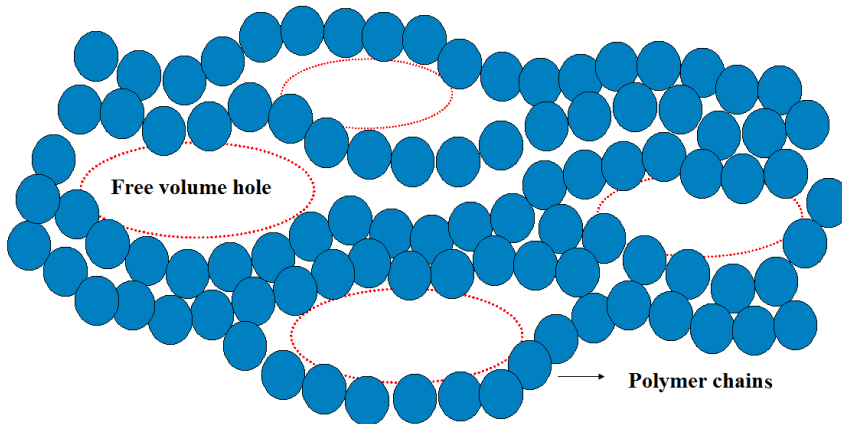


**Figure 1.8:** Schematic representation of the free volume in a polymer

The diffusion ability of membrane can be described by free volume theory and molecular model. According to free volume theory, diffusion occurs in polymer due to the random redistribution of free volume voids. On the other hand, the molecular model describes diffusion as a thermally activated phenomenon. This parameter reflects the movement of polymer chains and hence it has a strong influence on gas or liquid molecule transport and the overall performance of the membrane. The diffusing molecule can travel distances less than the diameter of the void itself. These voids are termed as free volume elements (FVE) or “holes” and their sum is termed as free volume. FVE in a polymer randomly forms and die out because of the possibility of thermally activated chain motion or molecular oscillation in them. Free volume in the membrane decreases with an increase in the intermolecular cohesion. The diffusing molecule passes one FVE to another based on the size of the cavity sufficient to occupy the molecule.<sup>80</sup>

### 1.3.2 Nature of polymers

The permeation properties of polymers differ from one to another. The polymer's internal composition is a key factor that influences the permeation

---

process of polymers. Polar polymers show strong affinity or increased diffusion towards permeant gas with polar groups. Strong interaction between polymer and permeating molecule also cause swelling, partial dissolution or crazing of the polymer. High degree of unsaturation in polymers results in reduced diffusion.

Glass transition temperature, crystallinity and molecular weight of polymers play a vital role in diffusion process. As the crystallinity,  $T_g$  and molecular weight of polymer increases permeation decreases. The distribution and number of voids in the polymers have great influence in the permeability.<sup>81-83</sup> The presence of crystalline phase opposes the diffusion of permeant species. A polymer contains both crystalline and amorphous regions, wherein amorphous region shows higher permeability due to the presence of higher amount of fractional free volume. However, in the crystalline region permeability is less due to uniform rigid chain packing. Both crystalline and semicrystalline materials are usually found in packaging applications due to their ability to prevent permeation of molecules. Glass transition temperature ( $T_g$ ) of the polymer has a significant influence on the transport properties. As  $T_g$  decreases the diffusion coefficient of the permeant increases due to high segmental motion, which leads to high fractional free volume. The number of chain ends represents the degree of discontinuity in the polymer chain, which means that chain ends decreases with increase in polymer molecular weight. Therefore, as the molecular weight increases the sorption sites within the polymer decreases.

### **1.3.3 Nature of filler particles**

Nanoparticles are usually added to polymers to improve properties. The nanofiller either improve or reduce transport properties of polymers, which depends on polymer-filler interaction and nature of filler. Uniform dispersion of fillers in the polymer matrix has a major role in the permeation of

---

molecules because of the increase in the tortuosity of path for permeating molecules and decrease in the permeation crosssection. Generally, inorganic particles resist and organic particle facilitate permeation properties of polymer membrane. The shape of the filler is another key factor that plays a vital role in influencing the barrier property. Platelet fillers exhibit high barrier property due to the long diffusion pathway. The parallel orientation of nanofillers with respect to diffusing molecule in the matrix will increase the permeation whereas perpendicular orientation reduces the permeation.<sup>84-86</sup>

Nanoparticle embedded polymer matrix reduce their free volume and creates a tortuous path for the diffusing molecules. In the reverse case, incompatible nanoparticle introduced polymer matrix, creates voids at the interface and increases free volume of the polymer matrix.

#### 1.3.4 Effect of temperature

Temperature has vital role in the permeation of gas/liquid molecule across the polymer membrane. As the temperature increases, mobility and flexibility of polymer chain increases, which will result in more free volume and easier diffusion of molecule across the membrane. The temperature has significant effect on selectivity; selectivity decreases with increase in temperature.

As the temperature increases free volume increases due to the thermal expansion and reduced density in the membrane, consequently permeation increases.

The relationship between solubility coefficient (S) and temperature is,

$$S = S_0 \exp\left[-\frac{\Delta H_s}{RT}\right] \quad (1.13)$$

---

Similarly, Arrhenius equations express the relation between temperature and diffusion coefficient (D),

$$D = D_0 \exp\left[-\frac{ED}{RT}\right] \quad (1.14)$$

where  $ED$  corresponds to energy barrier to diffusion.

### 1.3.5 Nature of penetrants

Generally shape, size, molecular weight and phase of the penetrants have strong effect on permeation property of the polymer. As the size of gas/liquid penetrant molecule increases, diffusivity of molecule decreases. Diameter of molecule in the gaseous or liquid mixture is also an important factor that influences the transport. It is usually observed that, those components in the feed with small molecular dimension are highly permeable across the membrane.<sup>87-88</sup>

### 1.3.6 Degree of crosslinking

It is an important factor that influences the membrane selectivity. Generally, higher level of cross-linking between the polymer chains results in higher membrane selectivity. Crosslinked polymer can attain high strength and stability due to compact network structure, resulting in reduced swelling.<sup>89</sup>

## 1.4 Applications of permeation properties of polymers

### 1.4.1 Food packaging

The use of polymer based food packaging material in market is a major area of research over a decade since the safety of food is essential during its storage and transportation. The food packaging material requires good oxygen and water vapour barrier properties in order to preserve the product quality from adverse physico-chemical changes due to oxidation and hydrolysis reactions. However, CO<sub>2</sub> permeation actually suppresses the

degradation of product and enhances its shelf life. In accordance with environmental condition, proper fabrication of polymer membrane is necessary in order to ensure the food quality during storage. Oxygen permeability coefficient (OPC) is a parameter to calculate oxygen barrier properties of a packaging material. The correlation between OPC with oxygen transmission rate (OTR) is given in the equation below,

$$OPC = \frac{OTR \cdot l}{\Delta P} \quad (1.15)$$

Where  $\Delta P$  is the partial pressure difference of the oxygen across the membrane (in pascal) and  $l$  is the thickness of the membrane.

Lim *et al.* synthesised hybrid films of cross linked poly(vinyl alcohol) (PVA)/boric acid with a 22.8% suppression in the OTR and significant improvement in water resistance at 1wt% of BA loading.<sup>90</sup>

## 1.4.2 Membrane separation

### 1.4.2.1 Electrodialysis and reverse osmosis

Electrodialysis is a process of demineralization of water and other fluids by applying a constant electric field and using ion-selective membranes. The process is not a cost effective method because huge amount of electricity is required with increase in the ions present in the fluids. Ion-exchange polymer membranes with ionogenic group can seize and exchange ions during demineralization of water. The membrane quality, efficiency, chemical stability and mechanical strength are the key factors that affect the electrodialysis process.<sup>91</sup>

Membrane based reverse osmosis (RO) process is applied for the separation of saline water by the application of pressure higher than the osmotic pressure on the feed side of semipermeable membrane, resulting in the diffusion of fresh water occurs in the opposite direction of osmotic flow. This process

---

require low amount of energy as compared to distillation for the separation of dissolved substance in water.<sup>92</sup>

### 1.4.2.2 Pervaporation

Pervaporation (PV) is an important energy efficient, chemical potential or activity-driven membrane based green separation technique. It has found great application in many industrial scenarios for dehydration of organic solvents, separation of organic-organic mixtures, structural isomers, mixture containing close boiling constituents or azeotropes and water purification. In PV technique, liquid mixture is separated by partial vapourization using a dense nonporous or porous polymer membrane. Vapour and liquid phases are involved in the technique. Liquid phase exists at the feed side which undergo phase transition to vapour in the permeate side. Physical structure and intrinsic properties of the membrane, feed mixture interaction and affinity of feed components towards the membrane are the important parameters that control the PV separation. Azeotropic mixture separation through currently existing distillation technique is difficult to be made possible without adding additional entrainers.<sup>93-98</sup> Now a days, existing separation processes are not effective for the separation of water from organic solvents due to its high energy cost. Pervaporation process effectively overcomes the drawback. Hydrophilic membranes are usually employed for the solvent dehydration, which preferentially allow water diffusion across the membrane. Membranes with glass transition temperature above room temperature are usually employed for this purpose. There should be a specific interaction between membrane and water, which is the key factor accountable for the separation of water. To attain high water selectivity, it is very necessary to have an active functional group in the polymer to interact with water. Dipole-dipole, hydrogen bonding and ion-dipole interactions are the mostly existing chemical interaction between the hydrophilic membranes and water.<sup>99-100</sup> Hydrogen bonding interactions are observed in poly(vinyl alcohol) (due to the presence of hydroxylic group), cellulose acetate (due to the presence of



carboxylic groups) and polyamides (due to the presence of imide/amide groups) with water. The materials such as Nafion (ion exchange membranes), quarternized ammonium group containing materials, chitosan and cellulose sulfate (polyelectrolyte complexes) exhibit ion-dipole interaction with water. Shan *et al.* synthesised high performance superhydrophilic membrane using (poly(acrylic acid)/poly(ethyleneimine))<sub>n</sub>/polyacrylonitrile polyelectrolyte membrane through the biomineralization of calcium carbonate onto the membrane by spray-assisted technique. Ethanol-water mixtures can be separated using the membrane by overcoming the trade off relation between selectivity and permeability. The membrane exhibited 98.8 wt% water content and 1317 g/(m<sup>2</sup> h) flux in the permeate for the 95% ethanol/water mixture feed. While the pure electrolyte membrane shows only 95.1wt% and 275 g/(m<sup>2</sup>h) water content and flux in the permeate respectively.<sup>101</sup>

In 1917, Kober invented the term pervaporation (PV) and the word is originated from the combination of terms permeation (P) and vapourisation (V). Schematic representation of PV process is shown in **Figure 1.9**, the membrane selectively permeate and evaporate a particular component from the liquid feed than its counterpart, finally the permeated component pass through the membrane and change its phase from liquid to vapour. Among the component in the feed which gets preferentially absorbed and diffused through the membrane and condense at the otherside of the membrane is called the permeate. The preferential transport of one component is caused by the vacuum applied on other side of the membrane. The component that can not pass across the membrane is called retentate.<sup>102-107</sup> Generally, dense polymeric membranes are employed for the PV separation of liquid mixtures. High mechanical strength, chemical resistance and sorption capacity are the essential requirements for the membrane for the efficient liquid mixture separation application. Molecule with high affinity to the membrane will preferably diffuse across the membrane. During PV, feed component undergoes solubility and diffusivity process in the polymer membrane.

Solubility parameters are employed for the qualitative analysis of solubility of feed components in the membrane. Hansen solubility parameters describe solubility of feed components in the membrane and it can be expressed as follows,<sup>108</sup>

$$\partial^2 = \partial_d^2 + \partial_h^2 + \partial_p^2 \quad (1.16)$$

where  $\partial_d$ ,  $\partial_h$  and  $\partial_p$  are corresponding contributions of dispersive, hydrogen bonding and polar interactions. The equation given below shows the interaction or affinity between two components.

$$\Delta = (\partial_{d,1} - \partial_{d,2})^2 + (\partial_{h,1} - \partial_{h,2})^2 + (\partial_{p,1} - \partial_{p,2})^2 \quad (1.17)$$

where  $\Delta$  decreases with increase in affinity between two components.

The solubility of organic solvent in a polymer membrane can be well described by Flory-Huggins,

$$\chi_{i,3} = \frac{[-\ln(1 - \nu_3) + \nu_3]}{\nu_3^2} \quad (1.18)$$

where  $\chi_{i,3}$  parameter indicates the binary interaction between the polymer and the components. Components are indicated by  $i$  and volume fraction of the polymer is indicated by  $\nu_3$ . The increase in interaction between penetrant and polymer leads to increase in amount of liquid entering into the polymer, which will reduce  $\chi_{i,3}$ . Polarities of membrane and feed components have significant effect on separation performance. The polarity of membrane and particular component in the feed should match for the separations to be easier.

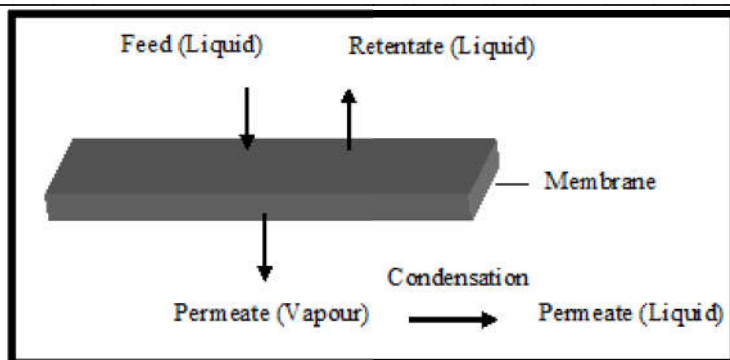


**Figure 1.9:** Schematic representation of pervaporation process

#### 1.4.2.2.1 Dehydration of alcohols and tetrahydrofuran (THF)

Ethanol, isopropanol (IPA) and tetrahydrofuran (THF) form an azeotrope with water at 96, 88 and 94.7 wt% in mole fraction respectively. Chemicals like cyclohexane are required in the conventional distillation process for the complete liquid mixture separation. The addition of carcinogenic chemicals as an entrainer can lead to impurity in one component and is difficult to isolate. Thus, membrane based pervaporation (PV) has been turned as a promising alternative technique for the efficient separation of these azeotropes without requiring additional entrainers.<sup>109</sup>

Magalada *et al.* studied the PV separation performance of ethanol-water azeotropic mixture using phosphomolybdic acid (PMA) loaded poly (vinyl alcohol)–poly (vinyl pyrrolidone) blend membrane. The nascent membrane exhibit very low selectivity while upon the addition of 4wt% of PMA its selectivity increases significantly.<sup>110</sup>

Isopropanol (IPA) is a non-toxic and rapidly evaporating alcohol produced through microorganism's fermentation as well as from water and propene reaction. It is an extensively used solvent in various industrial applications such as intermediate for the synthesis of vitamin B<sub>12</sub>, isopropyl acetate and rubbing alcohol, employed as an additive in disinfecting pads and as a

---

powerful cleaner in electronic devices. Everyday, large quantity of IPA is produced as a by-product from various industries. Hence, recycling and reusing of IPA is found to be an essential factor.<sup>111</sup> Zhang *et al.* reported PV separation of IPA-water system using poly (vinyl alcohol)-silicone hybrid membranes.  $\gamma$ -aminopropyl-triethoxysilane (APTEOS) is used as a precursor for the preparation of PVA/silicone membrane. The membrane exhibited high water permselectivity and flux concomitantly as compared with pristine PVA. The membrane exhibited separation factor of 1580 and permeation flux of 0.0265 kg/m<sup>2</sup>h at 5wt% of APTEOS for PV separation of isopropanol (90 wt %)–water system.<sup>112</sup> Amirilargani *et al.* synthesised zeolitic imidazolate frameworks (ZIF-8) nanoparticle and it is introduced into the PVA matrix. The PVA/ZIF-8 membrane is employed for the separation of IPA-water mixture. The membranes show improved permeance without much reduction in the separation factor.<sup>26</sup>

THF is a expensive volatile polar aprotic solvent frequently used in many chemical processes including pharmaceutical products, synthesis of drug, adhesives, paints and inks due to its high dissolving power for non-polar and polar species. Recycling of highly pure THF is very essential to overcome the economical and environmental challenges. It is very difficult to separate highly pure THF especially from water. Usually, it is separated by multistage distillation process. The distillation process possess many environmental, economical and technical challenges including explosion due to the reaction of THF with atmospheric oxygen. The distillation separation of THF-water azeotropic mixture needs a third component (entrainer), which lead to contamination during the separation of THF. The pervaporation technique is a suitable alternative for distillation separation of THF.

Zhang *et al.* studied the PV dehydration of THF (90wt%) using polysilsesquioxane (PSS) incorporated PVA membrane. The PSS introduction in PVA membrane improves its hydrophilicity, reduce crystalline region and overcome the inverse relation between permeance and

---

selectivity. At 2wt% loading of PSS, the membrane achieve maximum separation factor (1810) with improved flux.<sup>113</sup>

#### 1.4.2.2.2 Literature review on pervaporation study of PVA based systems

Poly(vinyl alcohol) (PVA) is an extensively used membrane for PV dehydration of organic solvents. However its swelling nature in aqueous solutions leads to poor water permselectivity, stability and mechanical properties. To solve these limitations, many modification strategies including crosslinking, introducing inorganic nanofiller and blending with other polymers are employed.

Zhang *et al.* successfully prepared PVA/1,2-bis (triethoxysilyl) ethane (BTEE) hybrid membrane for the dehydration of ethanol through PV process. The hybrid membrane exhibit reduced swelling, improved separation performance and high thermal stability.<sup>114</sup> Premakshi *et al.* synthesised an anion-exchange membrane from PVA and AESP ammonium functionalised silica precursor by sol-gel technique. The membrane has been applied for the PV dehydration of 10 mass% of water containing isopropanol mixture and achieved maximum separation factor (2991) and  $10.76 \times 10^{-2} \text{ kgm}^{-2}\text{h}^{-1}\text{flux}$ . The membranes overcome the trade-off effect between permeance and selectivity.<sup>115</sup> Das *et al.* analysed the effect of various crosslinking agents (oxalic acid (OA), dimethylol urea (DMU), glutaraldehyde (GLU) and tetra ethyl ortho silicate (TEOS)) and fillers on the IPA-water azeotropic mixture pervaporation separation performance of poly (vinyl alcohol) membranes. **Figures 1.10** represents the crosslinking reaction of PVA with various crosslinking agents. Among this, 2wt% GLU crosslinked PVA exhibit optimum PV performance and hence aluminosilicate filler was introduced to the system. GLU crosslinked PVA system with 6wt% aluminosilicate exhibit optimum PV performance.<sup>32</sup>

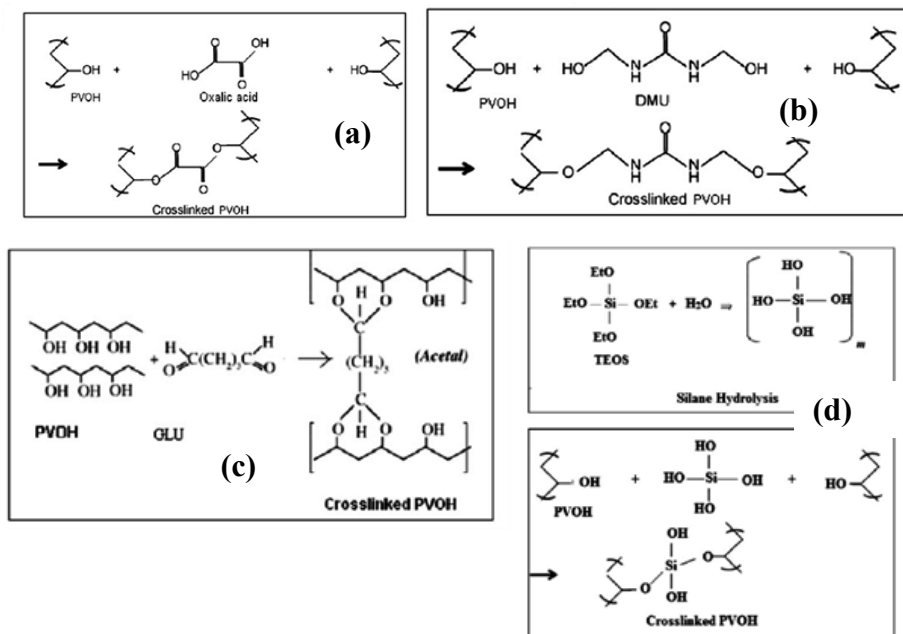


**Figure 1.10:** Crosslinking of PVA with (a) oxalic acid (OA), (b) dimethylol urea (DMU) (c) glutaraldehyde (GLU) and (d) tetra ethyl ortho silicate (TEOS).<sup>32</sup>

Recently Narkkun and co-workers reported a double network (DN) PVA nanocomposite membrane for PV dehydration of 90wt% ethanol. The DN is constructed from two PVA networks by sequential method. First network is formed by crosslinking of high molecular weight PVA (HPVA) with silica nanospheres (SNS) and second network is formed from low molecular weight PVA (LPVA) by thermal crosslinking. The membrane exhibit improved mechanical property, crystallinity, water selectivity and maintained swelling. The presence of SNS in PVA-DN membrane strongly enhance its water permselectivity as compared with pure HPVA-DN.<sup>116</sup> Kursun and Isiklan fabricated poly (vinyl alcohol)-g-poly (N-isopropylacrylamide) co-polymer membrane for the pervaporation separation of azeotrope of IPA-water

---

system. The membrane attained a separation factor of 95 and flux of 0.011 kg/m<sup>2</sup> h at 40°C.<sup>117</sup>

Shirazi and co-workers reported PV dehydration of IPA (10 wt% water-in-IPA-water mixture) using PVA/carbon nanotube (CNT) nanocomposite membrane system. The maximum separation selectivity of 1794 has been achieved for PVA membrane at 2wt% of CNT incorporation. It can be attributed to the rigidification effect of CNT in PVA matrix by reducing polymer free volume, resulting in reduced flux and improved selectivity. However, at higher loading (4wt%) of CNT in PVA resulted in improved flux and reduced selectivity due to the agglomeration of CNT in PVA matrix, thereby free volume and flux of PVA membrane get increased.<sup>118</sup> Olukman and Sanl reported Fe<sub>3</sub>O<sub>4</sub> nanoparticles incorporated in 2-hydroxyethyl methacrylate (HEMA) and acrylonitrile (AN) grafted PVA membrane (PVA-g-AN/HEMA-Fe<sub>3</sub>O<sub>4</sub>) for PV dehydration of acetone. The membrane exhibited improved separation factor on increasing the acetone concentration in the feed. The maximum separation factor of 120 was achieved at 80 wt% acetone concentration in the feed.<sup>119</sup>

Recently, Wu *et al.* synthesised a potential surface modified MIL-53(Al)-NH<sub>2</sub> (MIL-53-NHCOH, MIL-53-NHCOC<sub>4</sub>H<sub>9</sub> and MIL-53-NHCOC<sub>6</sub>H<sub>11</sub>) incorporated PVA membrane for PV dehydration of 92.5wt% ethanol. Among the modified system, MIL-53-NHCOH, and MIL-53-NHCOC<sub>4</sub>H<sub>9</sub> incorporated PVA exhibited outstanding separation performance. As compared with pure PVA, MIL-53-NHCOH (4wt%)/PVA system exhibited 206% and 200% improvement in water permeance and selectivity respectively and MIL-53-NHCOC<sub>4</sub>H<sub>9</sub> (7.5wt%)/PVA system exhibited 340% and 170% increase in water permeance and selectivity respectively. The difference in hydrophilicity of the surface substituent is the reason behind the significant difference in separation performance. MIL-53-NHCOC<sub>4</sub>H<sub>9</sub> and

---

MIL-53-NHCOC<sub>6</sub>H<sub>11</sub> possess high hydrophobic constant for the surface functional group and hence it reduces water selectivity of PVA while hydrophilic nature of MIL-53-NHCOH enhance the water permeance and selectivity of PVA.<sup>120</sup>

#### **1.4.2.2.3 Literature review on pervaporation study of POSS embedded polymeric systems**

Various organic group functionalised POSS embedded polymer membranes find high potential for PV dehydration of organic solvents. Recently Wang and co-workers reported hydrophilic PEG-POSS embedded sodium alginate (SA) membrane for the PV dehydration of ethanol. The PEG side group on the POSS significantly enhance water affinity while it reduces the crystallinity of the membrane resulting in increase in free volume of the membrane.<sup>121</sup>

Le *et al.* successfully developed two types of POSS (disilanolisobutyl (SO1440) and octa(3-hydroxy-3-methylbutyldimethylsiloxy) (AL0136) incorporated polyether-block-amide (Pebax 2533) system. They analysed PV performance of the membrane for the dehydration of ethanol by varying the feed composition, POSS loading and temperature. They found that Pebax/AL0136 exhibit higher separation efficiency than Pebax/SO1440. This can be attributed to the high affinity of Pebax/AL0136 system towards ethanol molecule. The best performance of the membrane obtained at 2wt% filler loading. Membrane show improved flux and reduced selectivity on increasing the ethanol concentration in the feed.<sup>122</sup>

#### **1.4.2.3 Gas separation**

Today, polymeric membrane based gas separation progressively receives great attention in various industries such as petrochemical, food packaging



---

and biomedical field. Membranes are used for different purposes, which includes oxygen enrichment, combustion processes, solar cells, CO<sub>2</sub>/N<sub>2</sub> and CO<sub>2</sub>/CH<sub>4</sub> separation during flue gas and bio gas treatment, lithium air batteries, natural gas drying and roofing membranes.<sup>123-127</sup> As mentioned above the challenging issue for the material scientists is the intrinsic trade-off effect between permeability and selectivity during membrane based separation.

Robeson in 1991 and then in 2008 developed a selectivity versus permeability plot of different gas separation membranes and it is presented in **Figure 1.11**. The plot elucidated inevitable trade-off effect or inverse correlation between permeability and selectivity of polymeric membranes (high selective polymers are simultaneously less permeable and vice versa). Most of the polymer membranes exhibit their separation performance below this upper bound, called as Robeson's upper bound and exhibit reduced gas separation performance in practical.<sup>128-129</sup> Several successful polymer membrane modification strategies as mentioned earlier have introduced for the efficient separation of gas mixtures by overcoming the limitation of Robeson's upper bound.<sup>130-132</sup> The materials like poly (ethylene oxide)s (PEO) and amines are highly CO<sub>2</sub>-philic species, hence their addition in polymer membranes can often improve CO<sub>2</sub>/gas selectivity because of their enhanced solubility and selectivity.<sup>133-136</sup> The increased CO<sub>2</sub> solubility in PEO is because of the strong quadrupole-dipole interaction that exists between CO<sub>2</sub> and ethylene oxide group.<sup>137-139</sup> For instance; the introduction of PEG into the poly(amide-b- ethylene oxide) (Pebax) copolymer shows outstanding CO<sub>2</sub> selectivity and permeance due to the occurrence of polar ether linkages in the structure, it has strong affinity towards CO<sub>2</sub> molecule.<sup>140</sup> During the last years many novel CO<sub>2</sub>-philic polymer membranes have been reported. For example; polyethylene glycol dibutyl ether (DBE-PEG) incorporated poly(ethylene oxide)-poly(butylenes terephthalate) multiblock copolymer exhibit 750 barrer CO<sub>2</sub> permeance without the dropping of selectivity while

---

pure copolymer exhibits only 150 barrer CO<sub>2</sub> permeance.<sup>141-143</sup> Very recently, Gye *et al.* reported PEG and the imidazolium groups (ionic liquids) introduced polyimide membrane, which exhibited 42.0 and 37.1 CO<sub>2</sub>/CH<sub>4</sub> and CO<sub>2</sub>/N<sub>2</sub> permselectivity values respectively and 464 Barrer permeance.<sup>144</sup> The organic polymer matrix incorporated with well dispersed inorganic particle is a good material for gas separation. It exhibit superior performance such as high flux, permselectivity and stability over pristine polymer.<sup>145-149</sup>

Generally observed that, impermeable nanoparticles in polymer may limit diffusion of larger gas molecules across the membrane due to the increase in the tortuous path of the gas molecule in the polymer matrix. Schematic representation of tortuous path is presented in **Figure 1.12**. Shape, dispersion state, orientation and volume fraction of nanofillers are the factors that determine the tortuosity of the path. Tortuosity ( $\tau = L_1/L_2$ ) is the ratio of diffusion path length of permeating molecule in the nanocomposite membrane ( $L_1$ ) to the diffusion path length of permeating molecule in the pristine polymer ( $L_2$ ). The presence of well oriented nanoparticle such as nanoplatelets and elongated particles situated perpendicular to the direction of permeating molecules in the hybrid membranes have great influence on the decrease in the permeability of the membrane.<sup>150</sup> Nanoclay is efficient nanofiller to reduce permeability of polymer membrane due to its high surface area as compared with spherical nanoparticles.<sup>151-152</sup>

Spherical particles incorporated polymer systems often increase the permeability of permeating molecules because of the minor effect of spherical particle on the tortuosity. Nanosized silica particles can enhance the gas separation as well as thermal and mechanical stabilities of the polymer membrane.<sup>153-157</sup> Xing and Ho reported fumed silica nanoparticles (FS) with a size of 7 nm introduced crosslinked poly (vinyl alcohol)-poly(siloxane) membrane for high-pressure CO<sub>2</sub>/H<sub>2</sub> separation. The membrane exhibited 87 and 1296 Barrers CO<sub>2</sub> selectivity and permeance respectively for 22.3 wt% FS loading at 107°C and 220 psia.<sup>158</sup> There are few reports showing the

reduction in the gas permeability of polymer systems by the incorporation of spherical nanoparticles.<sup>159</sup>

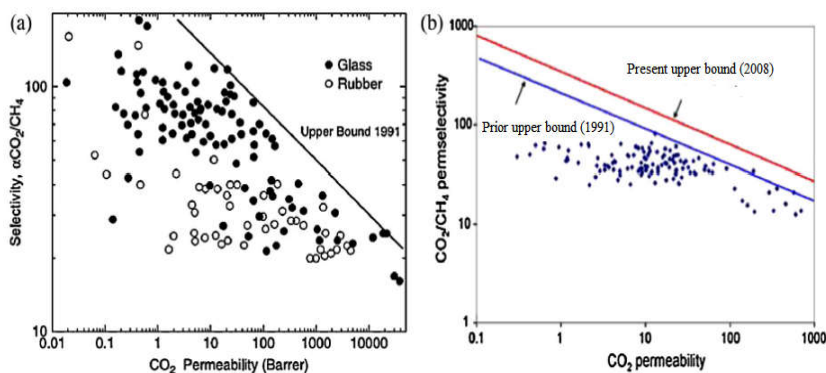


**Figure 1.11:** Robeson in 1991(a) and then in 2008 (updated) (b) developed selectivity versus permeability plot for  $\text{CO}_2/\text{CH}_4$  gas separation membranes, which elucidated trade-off effect between permeability and selectivity of polymeric membranes.<sup>128-129</sup>

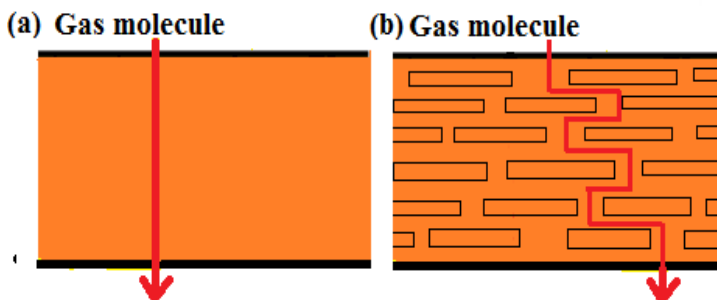


**Figure 1.12:** (a) Diffusion of gas molecule in pure polymeric film and (b) diffusion of gas molecule in polymer nanocomposites (eg: polymer/clay nanocomposites) through tortuous path.

### 1.4.2.3.1 Mechanism of gas transport in polymer nanocomposite membranes

#### 1.4.2.3.1.1 Maxwell's model

In 1873 Maxwell analysed the permeability of membranes prepared by dispersing spherical impermeable particles in a continuous matrix phase.<sup>160</sup>

$$P_c = P_0 \left( \frac{1 - \phi_f}{1 + 0.5\phi_f} \right) \quad (1.19)$$

Where  $P_0$  and  $P_c$  are the permeability of pure polymer and filler incorporated polymer system respectively.  $\phi_f$  is the volume fraction of filler. There are few demerits for this model ie, it is applicable only for spherical particle dispersed nanocomposite membranes and the model completely neglect the polymer-filler interaction.

#### 1.4.2.3.1.2 Free-volume model

Cohen and Turnbull described the effect of free volume of the membrane on the diffusion of the penetrate molecule across the membrane and its expression is shown below.<sup>161</sup>

$$D = A \exp\left(\frac{-\gamma V^*}{V_f}\right) \quad (1.20)$$

where  $A$  indicated pre-exponential factor,  $V_f$  is the average free volume in the membrane available for the transport of penetrants,  $V^*$  the smallest free volume element size that can hold a penetrant molecule and  $\gamma$  is an overlap factor used to prevent double-including of elements of free volume. A qualitative awareness of the polymer-filler interaction is provided by this model. The introduction of nanofiller disrupts the chain packing of the polymer that will improve free volume in the membrane, as a result diffusion of gas molecule increased.<sup>162</sup>

---

#### 1.4.2.3.1.3 Solubility increase mechanism

This mechanism describes the increased gas permeability of the nanocomposite membrane due to the interaction of penetrant molecule with the functional groups present on the polymer membrane.<sup>48</sup> Yave *et al.* fabricated Pebax®/PEG blend system, exhibited high CO<sub>2</sub> separation efficiency due to the presence of ethylene oxide unit within the membrane. CO<sub>2</sub> interacted with PEG unit of the membrane via dipole-quadrupole interaction, which increased the solubility of CO<sub>2</sub> molecule in the polymer blend membrane.<sup>38</sup>

#### 1.4.2.3.2 Literature review on gas transport study of PVA based systems

Semsarzadeh and Ghalei synthesised silica particle by micelle-templating process using tetraethoxysilane (TEOS) as precursor. First cetyltrimethyl ammonium bromide (CTAB)-with poly(vinyl alcohol) (PVA) form template on which silica particle is synthesised. A nanocomposite membrane has been synthesised using this synthesised silica/CTAB–PVA hybrid particles and polyurethane (PU). The membrane exhibited high CO<sub>2</sub> selectivity due to the presence of PVA in the silica particle. The –OH group of PVA can interact with polar CO<sub>2</sub>. Therefore, the membrane exhibited good selectivity for gas mixtures.<sup>55</sup>

Lai *et al.* successfully prepared highly transparent, flexible as well as high gas barrier borate ion crosslinked PVA/graphene oxide (GO) system. The crosslinker makes the membrane impermeable, ordered and dense. The amount of crosslinker and time for crosslinking greatly influenced the gas transport rate. The system at 1wt% borax loading exhibited O<sub>2</sub> transmission rate (OTR) < 0.005 cc m<sup>-2</sup> day<sup>-1</sup> and transmittance >85% at 550 nm. The barrier films have high potential for the commercial production of flexible electronic materials such as solar cells and LCD.<sup>163</sup>

---

#### 1.4.2.3 Literature review on gas transport study of POSS embedded polymer systems

Li *et al.* recently synthesised highly CO<sub>2</sub>-philic hybrid membrane consisting of amino-functional polyhedral oligomeric silsesquioxanes (POSS-NH<sub>2</sub>) and crosslinked poly (ethylene oxide) (PEO); synthetic route is presented in **Figure 1.13**. The combined high CO<sub>2</sub> affinity of PEO and porous characteristic of POSS-NH<sub>2</sub>, significantly improves the hybrid membrane CO<sub>2</sub> permeability and selectivity. As compared with crosslinked PEO, POSS incorporated crosslinked PEO exhibit 242% (385.8 Barrer) improvement in permeability.<sup>164</sup>

Iyer *et al.* analysed the gas transport performance of octa amino group functionalised POSS (OAPS) incorporated polyimide (PI) nanocomposite membrane. Related to the base PI, the composite membrane give reduced permeability and improved selectivity for all gases except for CO<sub>2</sub> as the weight percentage of OAPS increases from 0 to 20wt%. The POSS molecule restricts the motion of PI chain by making the chain so rigid resulting in reduced gas diffusion and improved diffusivity and selectivity for O<sub>2</sub>/N<sub>2</sub> and CO<sub>2</sub>/CH<sub>4</sub>. In contrast, CO<sub>2</sub> gases show exceptional characteristics which show higher permeability and selectivity at lower loading of POSS due to the interaction between surface amino group on the POSS and CO<sub>2</sub>. While at higher loading (20wt%) there is a significant reduction in the CO<sub>2</sub> permeability due to the decreased free volume by the aggregation of OAPS.<sup>165</sup>

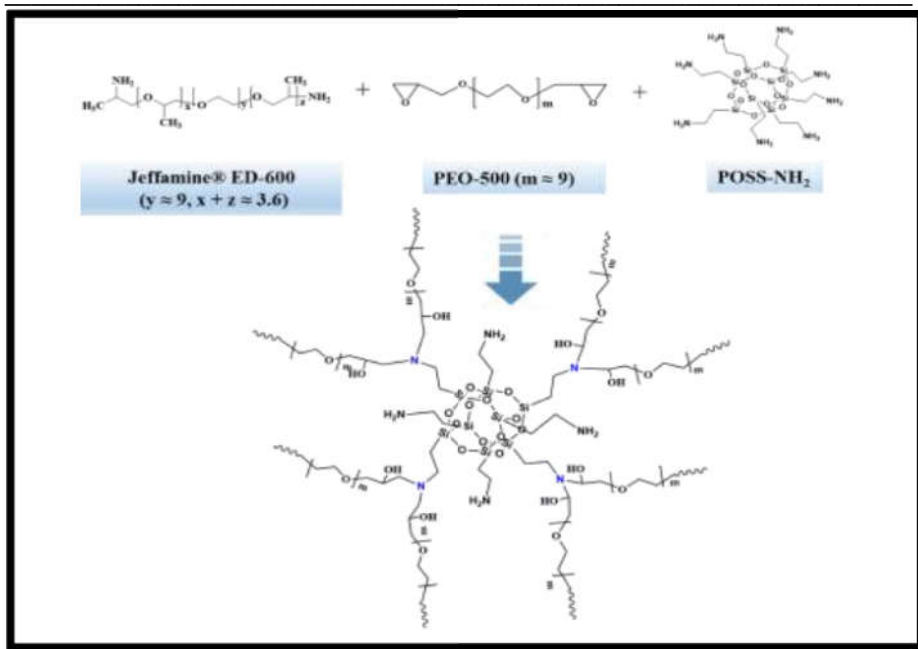


**Figure 1.13:** Hybrid crosslinked membrane synthesis from amino-functional polyhedral oligomeric silsesquioxanes (POSS-NH<sub>2</sub>) and crosslinked poly(ethylene oxide) (PEO).<sup>164</sup>

Chua and co-workers fabricated a membrane for the separation of CO<sub>2</sub> from N<sub>2</sub> and H<sub>2</sub>, using highly CO<sub>2</sub>-philic polyetheramine (PEA) and polyhedral oligomeric silsesquioxane (POSS). The chemical structures of the POSS and PEA employed for the study are shown in **Figure 1.14**. The membrane exhibited improved mechanical stability, CO<sub>2</sub> separation performance and reduced crystallinity. They achieved 7.0 and 39.1 CO<sub>2</sub>/N<sub>2</sub> and CO<sub>2</sub>/H<sub>2</sub> selectivity respectively with 380 Barrer permeability using this membrane.<sup>132</sup>

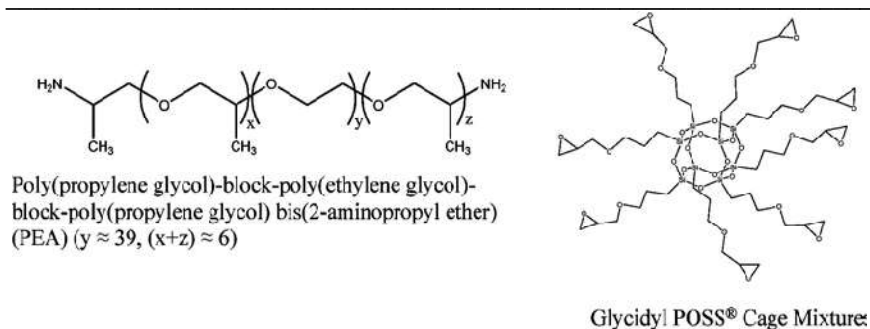


**Figure 1.14:** Chemical structure of polyetheramine (PEA) and polyhedral oligomeric silsesquioxane (POSS) used for the preparation of membrane for the separation of CO<sub>2</sub> from N<sub>2</sub> and H<sub>2</sub>.<sup>132</sup>

Rahman *et al.* successfully functionalised poly (ethylene glycol) (PEG) on the surface of polyhedral oligomeric silsesquioxane (POSS) nanoparticle through epoxy ring opening reaction of glycidyl POSS and glycidyl dimethylsilyl POSS in presence of boron trifluoride diethyletherate catalyst in different solvents (THF, toluene and chloroform). They fabricated a membrane by incorporating this PEG modified POSS in poly (ether-block-amide) multiblock copolymer PEBAX-MH 1657 and analysed its CO<sub>2</sub>/N<sub>2</sub> and CO<sub>2</sub>/H<sub>2</sub> gas separation performance. The THF complex and dimethylsilyl spacer present in the membrane provide improved CO<sub>2</sub> separation efficiency to the membrane.<sup>166</sup>

Bandyopadhyay *et al.* prepared amino functionalised POSS incorporated polyamide (PA) nanocomposite. The membrane exhibited improved gas permeability and reduced selectivity (trade-off relation) with respect to pristine polymer membrane. The increase in permeability is ascribed to the increase in the fractional free volume (FFV) of the system. The membrane gives higher diffusion to O<sub>2</sub> gas than CO<sub>2</sub>, even though kinetic diameter of CO<sub>2</sub> (3.3 Å) is smaller than O<sub>2</sub> (3.46 Å). This decrease in CO<sub>2</sub> could be explained by the quadrupolar interactions existing between CO<sub>2</sub> and amide in the PA. Interfacial area between polymer and filler, Si–O cage of POSS and



---

agglomeration of POSS are the three main pathways through which transport of gas molecule can occur.<sup>167</sup>

Xing *et al.* analysed CO<sub>2</sub>/CH<sub>4</sub> separation performance on zeolite filled and unfilled poly(vinylalcohol)/poly(ethylene glycol) (PEG) blend membranes. Strong quadrupole–dipole interaction exists between PEG (MW200) and CO<sub>2</sub> results in high permeance to CO<sub>2</sub>. The PVA chain provides good mechanical stability to the blend membrane. Zeolite 5A incorporation also makes significant change in separation performance. As the zeolite 5A content increases, selectivity decreases, in contrast CO<sub>2</sub> permeability first reduced and then increases significantly at higher loading.<sup>168</sup>

### 1.5 Poly (vinyl alcohol)

Poly(vinyl alcohol) (PVA) is an extensively used hydrophilic, semicrystalline ecofriendly synthetic polymer with high technological potential. The thermoplastic PVA found particular interest in various industrial fields due to its water processability, good film forming nature, high-abrasion resistance, high level of biocompatibility, biodegradability, H-bonding ability with variety of additives, good mechanical properties and gas barrier property.<sup>169-173</sup> It can be participated in chemical reaction using its large number of secondary alcohol functional groups. It is widely employed in engineering, drug delivery, biomedical devices, food packaging, textile sectors and for the fabrication of membranes in separation process.<sup>174-178</sup> The separation efficiency of membranes vary significantly depending on the polymerization degree, degree of hydrolysis, molecular weight of polymer, membrane structure and cross linking degree. Based on the degree of hydrolysis and viscosity, various grades of PVA is commercially available. The atactic grade is the largely supplied PVA. Viscosity of the PVA membrane increases with increasing polymerisation degree. Consequently, prominent change in the fractional free volume and separation performance of membrane can be observed. The excess swelling nature of PVA membranes in high water

containing environment leads to its reduced chemical and mechanical stability and separation performance. The problem can be rectified by the modification of PVA through grafting, blending or cross-linking.<sup>179-184</sup> Recently, the introduction of inorganic nanofillers to the polymers are found to have great success to improve thermal stability, mechanical strength and separation performance of the membrane even in the aqueous solution due to the advantages of both components.<sup>185-186</sup> Nevertheless, several limitations still exists for this systems such as incompatibility or uniform dispersion of fillers in the polymer matrix and poor interaction between polymers and fillers. So trade-off effect exists between permeability and selectivity.

### 1.5.1 Structure and synthesis

Structure of PVA is presented in **Figure 1.15**. As vinyl alcohol can not stand in free state (in presence of air, it transformed to acetaldehyde), the synthesis of PVA by polymerization of vinyl alcohol monomer unit is found to be very difficult. In 1924, the German scientists Hermann and Haehnel were first developed a strategy for the preparation of PVA throughfull or partial hydrolysis of polyvinyl ester (polyvinyl acetate) with potassium hydroxide in ethanol. Chemical reaction steps are presented in **Figures 1.16**.<sup>187</sup> Both fully and partially hydrolysed PVA are commercially available and their chemical structures are presented in **Figures 1.17**. In fully hydrolysed grade of PVA, about 98% mole of acetal in poly (vinyl acetate) are replaced with alcohol. It contains severe inter molecular hydrogen bonding and higher crystallinity, resulting in insolubility in water at room temperature while solubility in hot water. In the case of partially hydrolysed PVA grade, about 87-89% mole of acetal in poly (vinyl acetate) are replaced with alcohol. It dissolves in water at room temperature and exhibit reduced melting point, degree of crystallinity, strength and easier processability over fully hydrolysed PVA due to the presence of residual acetate groups.<sup>188-192</sup> Extent of hydrolysis (amount of residual vinyl acetate) is an important parameter, which controls the properties of PVA such as flexibility, solubility and molecular weight (**Table**

1.2). Poly(vinyl acetate) is prepared by the polymerisation of vinyl acetate through refluxing at 80°C in the presence of potassium persulfate free radical as initiator.

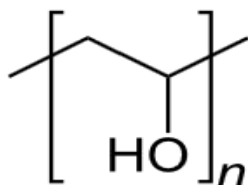


Figure 1.15: Structure polyvinyl alcohol (PVA)

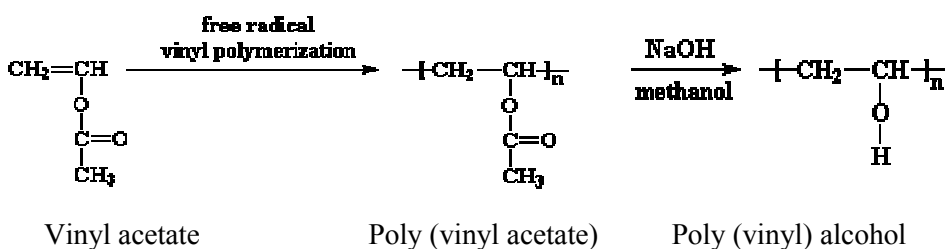


Figure 1.16: PVA synthesis from vinyl acetate

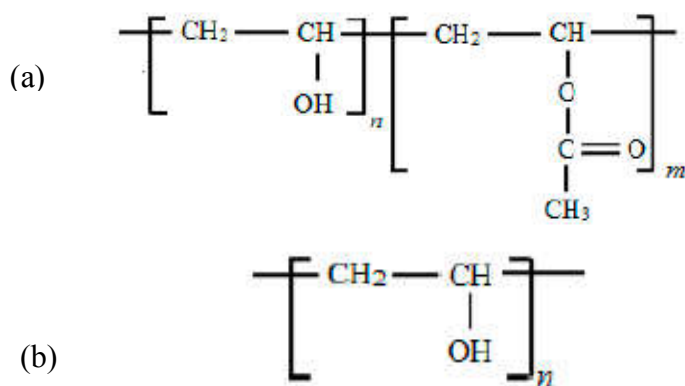


Figure 1.17: Structure of (a) partially (b) completely hydrolysed PVA

**Table 1.2:** Variation in the properties of PVA, based on its molecular weight and hydrolysis.<sup>191</sup>

<p>Increased viscosity          Increased block resistance          Increased tensile strength          Increased water resistance          Increased adhesive strength          Increased solvent resistance          Increased dispersing power</p>	<p>Increased flexibility          Increased water sensitivity          Increased ease of solvation</p>
<p>Molecular weight</p> <p>← Decreasing      Increasing →</p>	
<p>Increased water resistance          Increased tensile strength          Increased block resistance          Increased solvent resistance          Increased adhesive to hydrophilic surfaces</p>	<p>Increased flexibility          Increased dispersing power          Increased water sensitivity          Increased adhesion to hydrophobic surfaces</p>
<p>Hydrolysis%</p>	

### 1.5.2 Properties

PVA is a tasteless, odorless and nonhazardous linear polymer having high solubility in water and insolubility in most organic solvents. Properties of PVA vary based on certain factors such as molecular weight, degree of polymerisation, hydroxylation and hydrolysis. Water solubility of PVA get reduced on increasing the degree of polymerisation and hydroxylation. Based on the degree of hydrolysis, melting point of PVA varies from 180 to 240°C. It possesses excellent adhesive, film forming and emulsifying properties. Hence it is widely used in food packaging, paper adhesives, textile and paper coating sectors.<sup>193-194</sup> Through pyrolysis, it undergoes rapid decomposition above 200°C. Commercially, PVA films are synthesised by solution blending method due to its high water solubility. The film exhibits good strength, flexibility, solvent mixture separation properties, high gas and moisture barrier characteristic. It undergoes biodegradation both in anaerobic

(landfill) and aerobic (composting) environment. PVA undergoes fast decomposition through hydrolysis because of the occurrence of hydroxyl group. According to reported literature the degradation period of PVA is 5-6 weeks.<sup>195-196</sup> The chemical, thermal and mechanical stability of PVA is essential for its application in packaging, separation and pharmaceutical sectors. In order to achieve improved stability, it can be modified by chemical or physical cross-linking, blending and grafting.<sup>197-199</sup>

Physical and chemical methods are employed for the crosslinking of PVA. Heat treatment and freeze–thaw are well known existing important physical crosslinking method. Chemical crosslinking can be carried out using chemical agents such as glutaraldehyde, formaldehyde, maleic acid etc, these can be strongly interact with hydroxyl functional group of PVA. Crosslinks are bonds that connect polymer chains, consequently network structures are formed by its multidirectional chain extension and it reduced the mobility as an individual chain.<sup>200</sup>

Glutaraldehyde (GLA) with acid catalyst (sulfuric acid and acetic acid) is extensively employed for the chemical crosslinking of PVA, which is shown in **Figure 1.18**.<sup>201</sup> In these case, secondary hydroxyl group of PVA interact with GLA. Nearly 0.1mol of GLA ( $\text{OHC}-(\text{CH}_2)_3-\text{CHO}$ ) is used per mole of PVA (very high MW, 88% hydrolysed) for crosslinking. At high pH, GLA is subjected to self condensation by an aldol condensation. This crosslinked PVA give reduced swelling products than uncrosslinked PVA. Hence it can be employed for waste water treatment. Recently, Figueiredo *et al.* reported crosslinking of PVA with GLA without using acid catalyst or any organic solvent and is useful for the application of PVA in biomedical field.<sup>202</sup> Sonker *et al.* prepared glutaric acid ( $\text{C}_5\text{H}_8\text{O}_4$ ) crosslinked tungsten disulphide nanotubes (WSNTs) incorporated PVA composite. The interactions present

in the composite are shown in the **Figure 1.19**. The composite exhibited excellent thermal and mechanical properties as compared to pure PVA.<sup>203</sup>

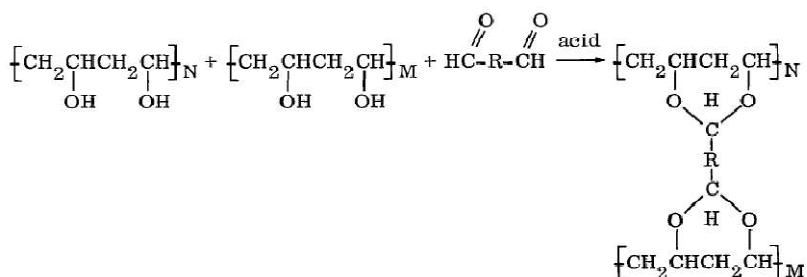


**Figure 1.18:** Cross linking of PVA using GLA in presence of an acid

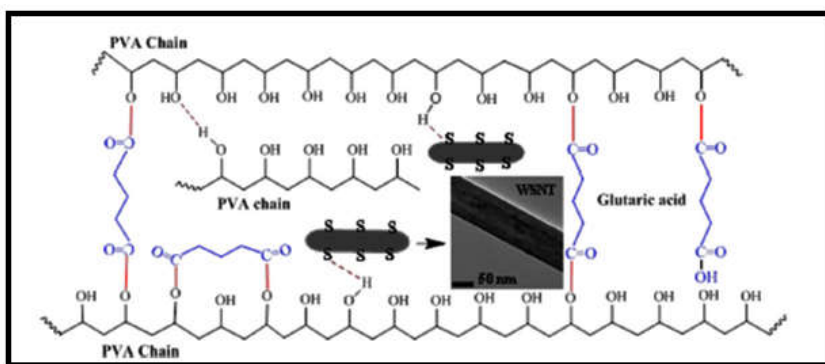


**Figure 1.19:** Schematic representation of chemical interaction present in glutaric acid crosslinked WSNT-PVA composite: esterification reaction between PVA and glutaric acid, intermolecular hydrogen bonding between PVA chains and hydrogen bonding between WSNT and PVA.<sup>203</sup>

### 1.5.3 Applications

PVA has found wide range of applications, mainly in pharmaceuticals, biomedical areas, waste water treatment, adhesives, textile, food packaging, paper coating, dehydration of organic solvents and separation of gas mixtures. In the world, around 6, 50,000 tons of PVA are produced yearly.<sup>204-</sup>

<sup>208</sup> Recently, Moulay *et al.* extensively reviewed various chemical

modifications, uses and applications of PVA.<sup>209</sup> Largest producer and consumer country of PVA is China; they consume around half of the total world's consumption. PVA is widely employed in medical and food industry because of its biodegradability, biocompatibility, hydrophilicity, barrier properties, nontoxicity, swelling, flexibility and chemical resistance. **Figure 1.20** demonstrated the PVA market volume in US which is approximately 172.8 kilo tons in 2016 and it is expected to grow from 2016 to 2025 with a compound annual growth rate (CAGR) of 5.4%.<sup>210</sup>

PVA extensively used in food packaging market due to its water solubility, nontoxicity, biodegradability and oxygen and aroma barrier properties. The governments are highly interested in green package, which is the major reason behind the market growth of biodegradable PVA.

PVA hydrogels behaves as a good bioadhesive, shows elastic and rubbery nature, possess high mechanical strength by hydrogen bonding influenced by crosslinking, it is non-carcinogenic and has an easy mode of processability. It has wide application in the field of tissue engineering, drug delivery, as hemodialysis membranes, contact lenses and in pharmaceutical industry.

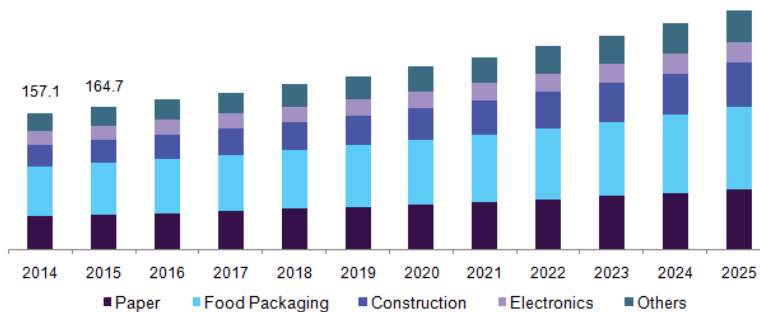


**Figure 1.20:** PVA market volume by end-use in U.S, 2014 - 2025 in Kilo Tons.<sup>210</sup>

---

## 1.6 Polyhedral oligomeric silsesquioxane (POSS)

Polyhedral oligomeric silsesquioxane is a new class of high potential organic-inorganic silica based hybrid material, commonly referred by the abbreviation “POSS”. The hybrid materials possess intermediate property between that of ceramics and organic polymers; it is presented in **Figure 1.21**. The name polyhedral oligomeric silsesquioxane is originated from its characteristic structure that contain silicon, oxygen and alkane. Polyhedral refers to multi-sided (3-D) geometric shapes like cubes, sphere. ‘Oligo’ denotes the small number of silsesquioxane units present in the compound and the term silsesquioxane refers to each silicon atom connected to one-and a half (sesqui) of oxygen (ox) and one hydrocarbon (ane) groups to the silicon vertex. POSS is considered as a well defined, smallest, zero-dimensional (sphere like structure), highly symmetrical and multiple functional nanoparticle of silica.<sup>211-214</sup> POSS have nanometer sized polyhedral inorganic core made up of tetravalent silicone and oxygen with the formula  $(\text{SiO}_{1.5})_x$ . The core is surrounded by organic functional groups (R) at all the apex of silicon atom. In POSS molecule, Si-O-Si-O-Si network core is found to be very rigid and inert due to the strong overlapping of two lone pair electrons on the oxygen with vacant d orbital of Si. As compared with the bond energy of Si-C ( $326 \text{ kJmol}^{-1}$ ) and C-C ( $346 \text{ kJmol}^{-1}$ ), Si-O bond energy ( $444 \text{ kJmol}^{-1}$ ) is found to be very high. The architecture of the substituent attached on each silicon vertex determines the final chemical and physical properties of POSS. The anatomy of POSS molecule is given in **Figure 1.22**.<sup>215-219</sup> Its diameter is in the range 1-3 nm and the Si-Si diameter of 0.53nm and the ratio of Si:O is 2:3. Zhang and Müller recently reviewed the properties and application of POSS embedded polymers.<sup>220</sup> Tanaka and Chujo well reviewed the POSS based advanced functional materials and their unique properties.<sup>221</sup> Two special characteristic of POSS molecule are the following: (i) It is physically



---

large as compared with polymer dimensions and almost equivalent in size to most polymer segments and coils and (ii) the chemical composition ( $\text{RSiO}_{1.5}$ ) is a hybrid intermediate between that of silicone ( $\text{R}_2\text{SiO}$ ) and silica ( $\text{SiO}_2$ ). Unlike usual traditional inorganic fillers, POSS is very flexible and offer many incomparable advantages. Peculiarities like monodispersion with well defined structure, high thermal stability, low density, controllable surface properties and easiness with which POSS can be decorated with appropriate organic functionalities make it a promising material for the modification of polymers.<sup>222-227</sup>

POSS has been widely used as inorganic nanofiller for the construction of organic/inorganic hybrid materials. Its incorporation in polymer materials is to produce hybrid material with valuable properties. The well controllable functionality makes them compatible with diverse polymer matrices at the molecular level by creating reactive sites or modifies the interfacial properties. The functional group significantly affects the characteristic phase transitions and molecular packing. The organic functional group on the POSS can be reactive (e.g., for copolymerization) such as acids, epoxy, acrylate, styrene, amine, alcohol and methacrylate, or inert (e.g., for polymer blending) such as cyclopentyl, phenyl, methyl, isobutyl and cyclohexyl. The reactive organic group on the POSS surface enables its grafting or polymerisation with polymers by strong interaction. The non reactive functional group makes them readily compatible and dispersible in various polymers at molecular level.<sup>228-235</sup> Recently, Zhou and coworkers reviewed the preparation, properties and application of POSS-polymer hybrid systems.<sup>236</sup> Kuo and Chang published a review in 2011 about synthesis of different functionalised POSS and various POSS incorporated polymer systems such as poly(ethylene oxide)/POSS, polyimide/POSS, polyester/POSS, polyurethane/POSS, epoxy/POSS, polyamide/POSS, polystyrene/POSS, polyolefin/POSS and

---

poly(acrylate)/POSS. Their miscibility, hydrogen bonding interaction and properties such as thermal, electrical, dynamic mechanical and surface properties and applications are well analysed.<sup>237</sup>

The POSS-polymer systems offer the benefits of both the inorganic and organic phase. POSS can be introduced into the polymer matrix through blending, crosslinking, grafting, chemical coupling or copolymerisation. It can create higher dimensionality (1,2 or 3-D scaffolds) in polymer matrix through crystallisation or aggregation that may reduce the possible advantages related with nanoscale incorporation.<sup>238-240</sup> The rigid centre siloxane core provides good chemical, thermal and mechanical stability.<sup>241-249</sup> Unlike conventional organic compounds, most of the POSS derivatives are ecofriendly, odourless and nonvolatile. The nanosized POSS embedded polymers show significant enhancement in thermal stability, mechanical property, increased decomposition temperature, lower density, oxidative resistance, surface hardening, reduction in flammability, increased gas permeability, optical properties and surface hardening. Hence it is a suitable material for fire-resistant and high-temperature applications.<sup>250-251</sup> However, the strong molecular interaction (van der Waals, dipolar, hydrogen bonding) of POSS, the different degree of compatibility between organic and inorganic parts of POSS cage and the rigidity of silicon-oxygen cores lead to the aggregation of particles in polymer matrix. This may reduce many properties of the nanocomposite.

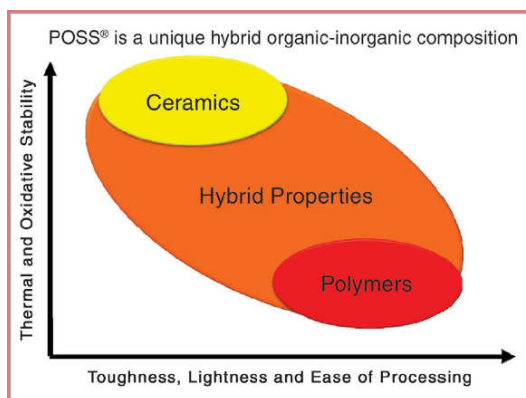


**Figure 1.21:** Schematic representation of organic-inorganic hybrid, bridging the gap between organic polymers and ceramics.<sup>211</sup>

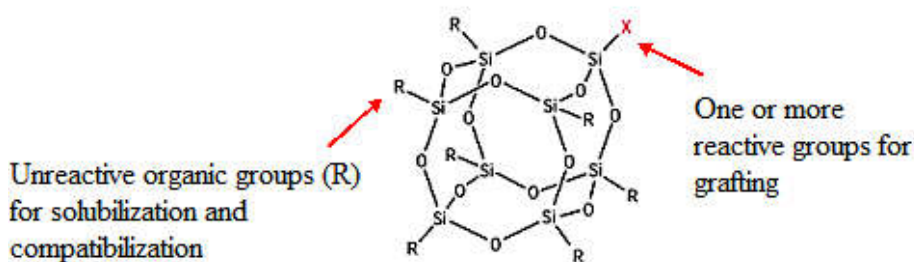


**Figure 1.22:** The anatomy of polyhedral oligomeric silsesquioxane (POSS).<sup>241</sup>

### 1.6.1 Different types of POSS

POSS belongs to the broad family of silsesquioxanes, The term silsesquioxane refers to the molecules with the chemical structure  $(\text{RSiO}_{1.5})_n$  or  $\text{R}_n\text{T}_n$ , where R is called vertex group for polyhedral molecule, it may be hydrogen or an organic group such as alkyl, aryl or any of their derivatives.<sup>252-253</sup> On the basis of molecular architecture, silsesquioxanes have been classified into caged and noncaged structure (**Figure 1.23**). In the noncaged structure, it is further divided into random, ladder and partial-cage

---

structure. Baney *et al.* in 1995 reviewed the synthesis, structure and application of silsesquioxanes.<sup>254</sup> The ladder and cage like structures are the most common structure for silsesquioxanes. Silsesquioxane with caged structure (completely and incompletely condensed) is known as POSS, which is commonly represented by  $T_8$ ,  $T_{10}$  and  $T_{12}$  based on the number of silicon atom attached to the vertex of the cage (**Figure 1.23**).<sup>255-258</sup> The most familiar varieties are  $T_8$  type, which consists of eight  $RSiO_{1.5}$  units forming a cage like inorganic central part surrounded by eight organic vertex groups. In the  $T_8$  type, POSS molecule can bear same kind of eight reactive or unreactive groups ( $T_8R_8$ ), or one reactive and seven unreactive groups (monofunctional POSS molecules,  $T_8R_7R'$ ). Compared to  $T_{10}$  and  $T_{12}$  type,  $T_8$  cubic silsesquioxanes are most preferable form due to the stability of the  $Si_4O_4$  ring structure. The rigid crystalline silica frame work is the reason behind the outstanding chemical and thermal stability of POSS molecules. A large diversity is possible for POSS for the modification of polymers, because one or more vertex group can be replaced by reactive functional groups (such as alcohol, phenol, amine, epoxy and styrene) for grafting or co-polymerisation. POSS can be classified into (a) molecular silica: all the organic groups on each silicon atom are nonreactive (b) monofunctional POSS: one of the organic group is reactive (c) multifunctional POSS: all the organic groups on each silicon atom are reactive.

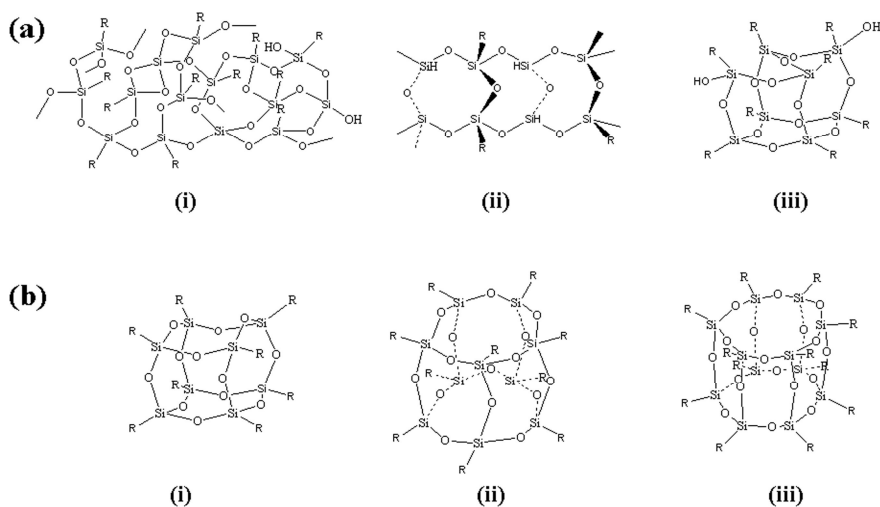


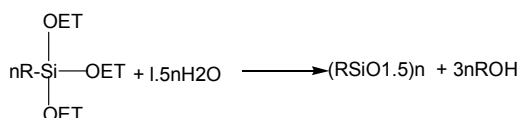
**Figure 1.23:** Structures of silsesquioxanes (a) non-caged silsesquioxanes: (i) random, (ii) ladder; (iii) partial caged structures, and (b) caged silsesquioxanes: (i) T<sub>8</sub>, (ii) T<sub>10</sub>, (iii) T<sub>12</sub> structures.<sup>231</sup>

### 1.6.2 Synthesis of POSS

Scott was the first person who introduced the synthetic method of POSS synthesis with empirical formula  $(\text{CH}_3\text{SiO}_{1.5})_n$  by the thermolysis of polymeric product obtained by dimethyl chlorosilane and methyl trichlorosilane co-hydrolysis. Even though Scott discovered the first POSS molecule  $((\text{CH}_3\text{SiO}_{1.5})_n)$  in 1946 at US air force research laboratory for aerospace applications, only in the last twenty years scientists have widely studied and commercialised the extensive applications of POSS molecules. In 1991, Feher's group and Lichtenhan have made significant effort for the development of POSS incorporated polymer systems. Hybrid plastic is the POSS manufacturing company first established in 1998 at Fountain valley and then in 2004, in Southern California and city of Hattiesburg, Mississippi. The company made dramatic enhancement in the production of large variety of POSS.<sup>259-265</sup>

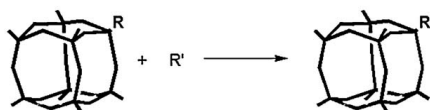
Many scientists reviewed the synthesis of monofunctionalised and multifunctionalised POSS nanostructure through silane chemistry and found that many factors such as monomer concentration, solvent nature, catalyst, temperature and the quantity of water addition affect the properties of the final product.<sup>266-270</sup>

The most common method for the production of monofunctional POSS is the hydrolysis and condensation of trifunctional monomers  $\text{RSiX}_3$ , where 'X' is a very reactive substituent such as Cl or alkoxy and R is chemically stable substituent such as methyl, phenyl or vinyl. About 48% of monosubstituted product is obtained from the above mentioned method. Another method is the substitution reaction on the silicon atom with the retention of siloxane cage such as hydrosilylation reactions. Corner-capping reactions also produce fully condensed monosubstituted POSS starting from incompletely condensed molecule such as  $\text{R}_7\text{Si}_7\text{O}_9(\text{OH})_3$  with  $\text{RSiCl}_3$ . Trifunctional organo silicon monomers produce incompletely and completely condensed POSS molecules in first and second step respectively. Different synthesis methods are presented in **Schemes 1.1-1.5**.<sup>237, 252, 271-272</sup>

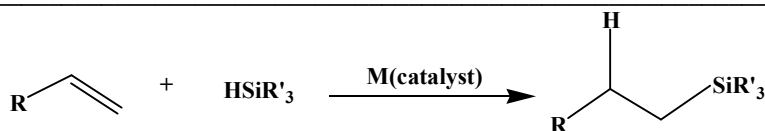


R is an organic group such as alkyl, aryl, amine, acid, epoxides, isocyanates, thiols or sulphonic acid

**Scheme 1.1:** Synthesis of POSS molecule using the hydrolytic condensation reactions of trifunctional organosilicon monomers.<sup>237</sup>



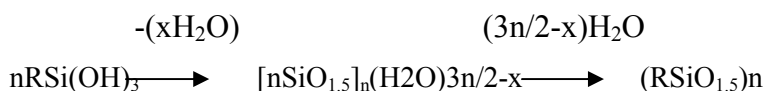
**Scheme 1.2:** Synthesis of POSS molecule by hydrolysis and condensation of organotrialkoxysilane.



**Scheme 1.3:** Hydrosilylation reaction (example for substitution reactions with retention of the siloxane cage)



**Scheme 1.4:** Corner capping reaction.<sup>237</sup>



**Scheme 1.5:** Production of incompletely and completely condensed POSS molecules in first and second step respectively.

POSS-polymer nanocomposites can be classified into three based on the functionality of POSS or method used for the incorporation of POSS in polymer matrix. (a) Star like polymer nanocomposites: polymerisation is initiated from the surface of the multi-functional POSS, so it act as a microinitiator and produce star type macromolecule (b) Crosslinked polymer nanocomposites: polymerization of multireactive POSS with polymers forms a thickly cross-linked network (c) Pendent type: polymerization of monofunctional POSS onto a polymer backbone produce pedant POSS cages contains polymer system. These three systems are presented in **Figure 1.24**.<sup>242</sup>

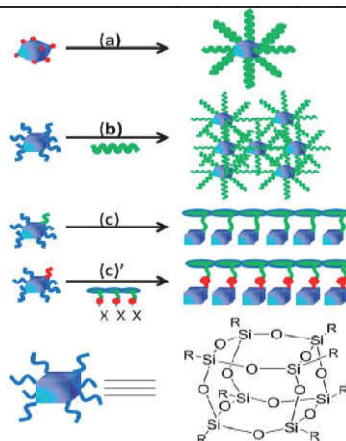


**Figure 1.24:** The three main types of POSS-based nanocomposites (a) Star-like polymer nanocomposites (b) Cross-linked nanocomposites (c) Pendant type.<sup>242</sup>

### 1.6.3 Literature review on POSS based polymer nanocomposites

Ullah *et al.* recently made a detailed review on the synthesis, self-assembly and applications of water soluble POSS incorporated amphiphilic hybrid polymers.<sup>273</sup>

Sheikh and co-workers prepared spherical nanoparticles through dialysis approach, using POSS as an inner hydrophobic core and PVA as a hydrophilic outer shell, schematically presented in **Figure 1.25**. Urethane bond is formed between the POSS and PVA. This amphiphilic nanoparticle is a good drug carrier. Controlled release of Paclitaxel drug for more than 40 days was achieved by employing the prepared nanoparticles.<sup>274</sup>

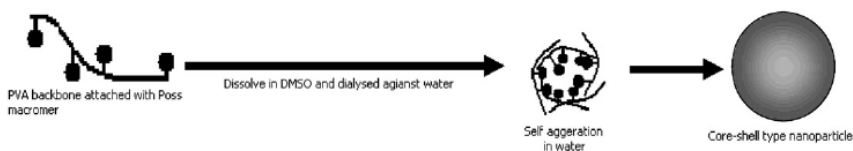


**Figure 1.25:** Synthesis of POSS-grafted-PVA nanoparticle.<sup>274</sup>



---

Kim *et al.* synthesized the amphiphilic PVA-POSS hybrids by introducing different weight percentage of POSS. Urethane linkage is formed between monoisocyanate group of POSS macromer and hydroxyl group of PVA. It was found that the water solubility or hydrophobicity of the PVA-POSS hybrids altered significantly depending on the hydrophobic POSS content incorporated into the PVA.<sup>275</sup>

Zhou *et al.* analysed the effect of octaammonium functionalised polyhedral oligomeric silsesquioxane (POSS) and layered silicates on the surface wettability of polyamide-6. It was found that both the fillers improve the hydrophilicity of polymer significantly. Types of nanofiller, the interaction between POSS and polymer are the major factors that determine the surface properties of polymer nanocomposites. H-bonding interaction in layered silicates and aggregation of POSS molecule at the surface are the major factors that improve the hydrophilicity of polyamide-6.<sup>276</sup>

You *et al.* synthesised PEG-POSS incorporated polyamide (PA) membrane through interfacial polymerization. The membrane exhibits high water flux and excellent fouling resistance as compared to pure PA.<sup>277</sup>

#### 1.6.4 Applications of POSS

POSS nanostructures are found to be a promising material for many applications from biomedical to aerospace technologies. The unique properties of POSS-polymer nanocomposite materials offer interdisciplinary technological applications (**Figure 1.26**).<sup>278-280</sup> Therefore, scientists explore the potential application in various fields, for instance, reinforcing agent or good nanofiller in polymer nanocomposites, mechanics, sensors, catalysts, photo resists, semiconductors, high temperature lubricants and electron beam lithography. With respect to carbon nanofibres and nanotubes, POSS chemical is an ecofriendly nanofiller, it is odourless, non-poisonous and

cytocompatible moieties and does not produce any volatile organic components. Hence it is a good choice for the fabrication of biomaterials.<sup>281</sup> Material scientists explore the POSS-polymer systems in tissue engineering and biomedical fields. POSS form dental nanocomposites with methacrylate based polymers that overcome the weakness (lack of strength, toxicity) of dental monomer, methyl methacrylate (MMA).<sup>282-283</sup> POSS/PMMA composites dramatically enhance the strength of PMMA. POSS/Poly(carbonate-urea) urethane nanocomposites are ideal material in cardiovascular bypass grafts and microvessels.<sup>284</sup> Ammonium-POSS like cationic POSS found great application in the field of gene delivery, drug delivery and DNA detection.<sup>285</sup>

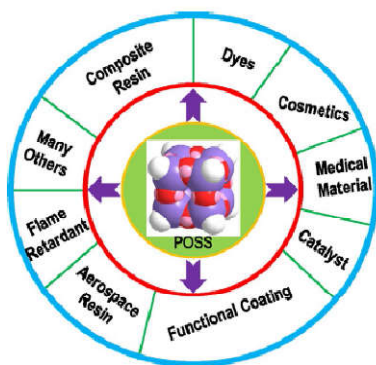


**Figure 1.26:** Various application of POSS nanomaterial.<sup>243</sup>

POSS nanocomposites based coating film hold advanced conductive, protective and mechanical properties, so it found many future opportunities in habitation missions and lunar exploration.<sup>286-287</sup> The very low dielectric constant and high thermal stability of POSS-polymer nanocomposite bring its use in modern microelectronics. POSS/polyfluorenes shows high thermal and optoelectronic properties, hence it is extensively used in electroluminescent devices.<sup>288</sup> Xiong *et al.* discovered polyaniline (PANI)-

---

POSS based complementary electrochromic device with high colouration ability.<sup>289</sup> The US Airforce has recognised the space application of POSS. POSS incorporated polymers show high atomic oxygen resistance. POSS form thin SiO<sub>2</sub> network that resist further decay of polymers from atomic oxygen erosion. POSS-polyimide nanocomposites also possess high protective power from atomic oxygen erosion.<sup>290</sup>

### 1.7 Motivation of Work

Membrane based separation processes combines excellent properties, which includes efficiency in separation, eco-friendliness, cost effectiveness, low maintenance necessity and low energy consumption. Possibilities of this technology overcome the limitations of traditional separation processes such as distillation and adsorption, which involve many economical, environmental as well as technical challenges. Moreover, conventional methods are not so effective to separate azeotropic mixtures. During the last decades, the scientific community focused to develop membranes with good stability, permeance and selectivity. Permeability-selectivity trade-off is the major challenge for the development of high performance polymer membranes. Several successful modification strategies such as grafting, crosslinking, polymer blending and mixed-matrix polymer membranes containing various nanoscale additives have been adopted for the fabrication of potential membranes. The addition of nanofillers to polymers enhance the thermal and mechanical stability as well as permeance and selectivity of the membranes. However, several limitations exist in the membrane systems such as incompatibility of fillers in the polymer matrix.

The present study focus on the introduction of organically functionalised polyhedral oligomeric silsesquioxane (POSS) molecule into the poly(vinyl alcohol) (PVA) matrix to generate stable membranes for separation process.

---

Nanostructured POSS molecule with their hybrid organic-inorganic nature and flexible functionalisation could help to enhance the dispersion in PVA. Therefore, the challenge of this work is to make use of nanostructured POSS to reinforce hydrophilic PVA and also to enhance its separation performance. Gas permeation and pervaporation accomplishment of the membranes are investigated for various gases and azeotropic mixtures respectively. Selectivity of the membrane for different gases as well as water in azeotropic mixtures have been analysed in detail. Membranes were characterised by various analytical techniques and other properties such as mechanical, viscoelastic and thermal were studied and discussed in detail.

### 1.8 Gap areas

- Trade-off effect between permeability and selectivity during pervaporation separation of liquid mixtures
- Modification of polymer membranes for efficient CO<sub>2</sub> separation
- Stability of membranes for separation process

### 1.9 Objectives of the work

- To prepare polyethylene glycol (PEG) and anionic-octa(tetramethylammonium) (Octa-TMA) functionalised polyhedral oligomeric silsesquioxane (POSS) incorporated poly(vinyl alcohol) (PVA) membrane.
- Modification of Octa-TMA-POSS (m-POSS) using cetyltrimethylammonium bromide (CTAB) and incorporation into crosslinked PVA membrane.
- To characterise the membranes using FTIR, X-ray diffraction, DSC, contact angle measurements, SEM, TEM, AFM and PALS

---

techniques. To analyse mechanical, dynamic mechanical, free volume and swelling properties of the membrane.

- To investigate the pervaporation separation efficiency of the PVA/POSS and PVA/m-POSS membrane using THF-water and IPA-water azeotropic mixture respectively.
- To investigate the gas transport ( $\text{CO}_2/\text{N}_2$  and  $\text{CO}_2/\text{O}_2$ ) properties of these membranes and correlate it with free volumes analysed by PALS measurements.
- To synthesis PEG-POSS and Octa-TMA-POSS embedded PVA-PEO blend membrane.
- Characterisation of PVA-PEO/POSS membranes using FTIR, DSC, contact angle measurements, SEM, AFM and PALS techniques.
- Analyse mechanical, free volume and swelling properties of the PVA-PEO/POSS membrane.
- To investigate the gas transport ( $\text{CO}_2/\text{N}_2$  and  $\text{CO}_2/\text{O}_2$ ) properties and THF-water azeotropic mixture pervaporation separation efficiency of the membrane.
- To analyse thermal degradation and water stability of PVA/POSS, PVA/m-POSS and PVA-PEO/POSS membranes.

### **1.10 Scope of the work**

The fabricated, mechanically and thermally stable PVA/POSS and PVA-PEO/POSS membranes exhibited efficient separation performance for  $\text{CO}_2$  and azeotropic mixtures (THF/water and IPA/water). The present thesis demonstrates the potential of highly efficient, cost effective and environment friendly membrane based separation technology over conventional methods such as adsorption and distillation.

---

**1.11 References**

1. S. Thomas W. Runcy, A. Kumar S, S. George, Transport properties of polymeric membranes, Elsevier (2017) ISBN: 9780128098851 (eBook)
2. K. Nath, Membrane separation processes, PHI Learning Private Limited (2017) ISBN:978-81-203-5291-9
3. M. Mulder, Basic principles of membrane technology, Kluwer Academic Publishers (1996) ISBN: 978-94-009-1766-8
4. E. Drioli, L. Giorno, E. Fontananova, Comprehensive membrane science and engineering, Elsevier (2017) ISBN:978-0-444-63775-8
5. M. Kárászová, M. Kacirková, K. Friess, P. Izák, Progress in separation of gases by permeation and liquids by pervaporation using ionic liquids: A review, *Separa.Purif.Techno.*, 132 (2014) 93-101
6. B. Bolto, M. Hoang, Z. Xie, A review of membrane selection for the dehydration of aqueous ethanol by pervaporation, *Chem. Eng. Process.*,50 (2011) 227–235
7. S. Bano, A. Mahmood, K. H. Lee, Vapor permeation separation of methanol–water mixtures: effect of experimental conditions, *Ind. Eng. Chem. Res.*, 52 (2013)10450–10459
8. X. Jiang, S. Li, L. Shao, Pushing CO<sub>2</sub>-philic membrane performance to the limit by designing semi-interpenetrating networks (SIPN) for sustainable CO<sub>2</sub> separations,*Energ. Environ. Sci.*,10(2017)1339-1344
9. S. Kim, Y. M. Lee, Rigid and microporous polymers for gas separation membranes,*Prog. Polym.Sci.*,43 (2015) 1-32
10. S. Kanehashi, K. Nagai, Gas and Vapor Transport in Membranes,*Membrane Characterization* (2017) 309-336
11. S. Wang, X. Li, H. Wu, Z. Tian, Q. Xin, G. He, D.Peng, S. Chen, Y. Yin, Z. Jiang, M. D. Guiver, Advances in high permeability polymer-based membrane materials for CO<sub>2</sub> separations,*Energy Environ. Sci.*, 9(2016) 1863-1890
12. J.Yin, B. Deng, Polymer-matrix nanocomposite membranes for water treatment,*J. Mem. Sci.*, 479 (2015) 256-275

13. Q. Xu, H. Xu, J. Chen, Y. Lv, C. Dong, T. S. Sreeprasad, Graphene and grapheme oxide: advanced membranes for gas separation and water purification, *Inorg. Chem. Front.*, 2 (2015)417-424
14. Y. M. Xu, T. S. Chung, High-performance UiO-66/polyimide mixed matrix membranes for ethanol, isopropanol and n-butanol dehydration via pervaporation, *J. Mem. Sci.*, 531 (2017)16-26
15. L. L. Xia, C. L. Li, Y. Wang, In-situ crosslinked PVA/organosilica hybrid membranes for pervaporation separations, *J. Mem. Sci.*, 498 (2016) 263-275
16. K. Golzar, S. A. Iranagh, M. Amani, H. Modarress, Molecular simulation study of penetrant gas transport properties into the pure and nanosized silica particles filled polysulfone membranes, *J. Mem. Sci.*, 451(2014)117-134
17. J. Yin, G. Zhu, B. Deng, Graphene oxide (GO) enhanced polyamide (PA) thin-film nanocomposite (TFN) membrane for water purification, *Desalination* 379 (2016) 93-101
18. V. Giel, J. Kredatusová, M. Trchová, J. Brus, J. Žitka, J. Peter, Polyaniline/polybenzimidazole blends: characterisation of its physico-chemical properties and gas separation behaviour, *Euro. Poly. J.*, 77 (2016) 98-113
19. E. Tilahun, A. Bayrakdar, E. Sahinkaya, B. Çalli, Performance of polydimethylsiloxane membrane contactor process for selective hydrogen sulfide removal from biogas, *Waste Management* 61 (2017) 250-257
20. A. Behboudi, Y. Jafarzadeh, R. Yegani, Polyvinylchloride/polycarbonate blend ultrafiltration membranes for water treatment, *J. Mem. Sci.*, 534 (2017) 18-24
21. J. H. Jhaveri, ZVP Murthy, A comprehensive review on anti-fouling nanocomposite membranes for pressure driven membrane separation processes, *Desalination* 379 (2016) 137-154
22. B. R. A. Heitz, M. O. Tade, S. Liu, Improved separation and antifouling performance of PVA thin film nanocomposite Membranes incorporated with carboxylated TiO<sub>2</sub> nanoparticles, *J. Mem. Sci.*, 485(2015) 48-59

23. B. Díez, N. Roldán, A. Martín, A. Sotto, J. A. P. Melón, J. Arsuaga, R. Rosal, Fouling and biofouling resistance of metal-doped mesostructured silica/polyethersulfone ultrafiltration membranes, *J. Mem. Sci.*, 526 (2017) 252-263
24. M. F. S. Dubreuil, P. Vandezande, W. H. S. V. Hecke, W. J. P. Carrero, C. T. E. Dotremont, Study on ageing/fouling phenomena and the effect of upstream nanofiltration on in-situ product recovery of n-butanol through poly[1-(trimethylsilyl)-1-propyne] pervaporation membranes, *J. Mem. Sci.*, 447 (2013) 134-143
25. D. Wu, Y. Han, W. Salim, K. K. Chen, J. Li, W. S. W. Ho, Hydrophilic and morphological modification of nanoporous polyethersulfone substrates for composite membranes in CO<sub>2</sub> separation, *J. Mem. Sci.*, 565 (2018) 439-449
26. M. Amirilargani, B. Sadatnia, Poly (vinyl alcohol)/zeolitic imidazolate frameworks (ZIF-8) mixed matrix membranes for pervaporation dehydration of isopropanol, *J. Mem. Sci.*, 469 (2014) 1-10
27. A. M. Sajjan, B. K. J. Kumar, A. A. Kittur, M. Y. Kariduraganavar, Development of novel grafted hybrid PVA membranes using glycidyltrimethylammonium chloride for pervaporation separation of water–isopropanol mixtures, *J. Indus. Eng. Chem.*, 19 (2013) 427-437
28. G. Liu, Z. Jiang, K. Cao, S. Nair, X. Cheng, J. Zhao, H. Goma, H. Wu, F. Pan, Pervaporation performance comparison of hybrid membranes filled with two-dimensional ZIF-L nanosheets and zero-dimensional ZIF-8 nanoparticles, *J. Mem. Sci.*, 523 (2017) 185-196
29. Y. M. Xu, N. L. Le, J. Zuo, T. S. Chung, Aromatic polyimide and crosslinked thermally rearranged poly (benzoxazole-co-imide) membranes for isopropanol dehydration via pervaporation, *J. Mem. Sci.*, 499 (2016) 317–325
30. M. M. Khani, D. Woo, E. L. Mumpower, B. C. Benicewicz, Poly (alkyl methacrylate)-grafted silica nanoparticles in polyethylene nanocomposites, *Polymer* 109 (2017) 339-348
31. X. Li, A. Sotto, J. Li, B. V. Bruggen, Progress and perspectives for synthesis of sustainable antifouling composite membranes containing in situ generated nanoparticles, *J. Mem. Sci.*, 524 (2017) 502-528



32. P. Das, S. K. Ray, S. B. Kuila, H. S. Samanta, N. R. Singha, Systematic choice of crosslinker and filler for pervaporation membrane: A case study with dehydration of isopropyl alcohol–water mixtures by polyvinyl alcohol membranes, *Separat.Purif. Tech.*, 81 (2011) 159–173
33. P. Salehian, T. S. Chung, Thermally treated ammonia functionalized graphene oxide/polyimide membranes for pervaporation dehydration of isopropanol, *J. Mem. Sci.*, 528(2017) 231-242
34. W. F. Yong, K. Kar H. Andrel, K. S. Liao, T. S. Chung, Suppression of aging and plasticization in highly permeable polymers, *Polymer* 77(2015)377-386
35. P. Das, S. K. Ray, Pervaporative recovery of tetrahydrofuran from water with plasticized and filled polyvinylchloride membranes, *J. Indus. Eng. Chem.*, 34 (2016) 321-336
36. Z. Liu , L. Qi, X. An, C. Liu, Y. Hu, Surface engineering of thin film composite polyamide membranes with silver nanoparticles through layer-by-layer interfacial polymerization for antibacterial properties, *ACS Appl. Mater. Interface.*, 9 (46) (2017) 40987–40997
37. A. Bhattacharya, B.N. Misra, Grafting: a versatile means to modify polymers Techniques, factors and applications, *Prog. Poly. Sci.*, 29 (2004) 767-814
38. W. Yave, A. Car, K. V. Peinemanna, M. Q. Shaikh, K. Rätzke, F. Faupel, Gas permeability and free volume in poly(amide-b-ethylene oxide)/polyethylene glycol blend membranes , *J. Mem. Sci.*, 339 (2009) 177–183
39. S. Zereshki, A. Figoli, S. S. Madaeni, F. Galianoc, E. Drioli, Pervaporation separation of ethanol/ETBE mixture using poly(lactic acid)/poly(vinyl pyrrolidone) blend membranes, *J. Mem. Sci.*, 373 (2011) 29–35
40. L. M. Robeson, Polymer blends in membrane transport processes, *Ind. Eng. Chem. Res.*, 49(2010)11859-11865
41. L. M. Robeson, H. H. Hwu, J. E. M. Grath, Upper bound relationship for proton exchange membranes: empirical relationship and relevance of phase separated blends, *J. Mem. Sci.*, 302 (2007) 70-77

- 
42. K. Vanherck, G. Koeckelberghs, I. F.J. Vankelecom, Crosslinking polyimides for membrane applications: A review, *Prog. Poly. Sci.*, 38 (2013) 874-896
  43. S. Ray, S.K. Ray, Effect of copolymer type and composition on separation characteristics of pervaporation membranes- a case study with separation of acetone-water mixtures, *J. Mem. Sci.*, 270 (2006) 73
  44. H. Zhou, J. Zhang, Y. Wan, W. Jin, Fabrication of high silicalite-1 content filled PDMS thin composite pervaporation membrane for the separation of ethanol from aqueous solutions, *J. Mem. Sci.*, 524(2017) 1-11
  45. C. Shin, X. C. Chen, J. M. Prausnitz, N. P. Balsara, Effect of block copolymer morphology controlled by casting-solvent quality on pervaporation of butanol/water mixtures, *J. Mem. Sci.*, 523 (2017) 588-595
  46. T. S. Chung, L. Y. Jiang, Y. Li, S. Kulprathipanja, Mixed matrix membranes (MMMs) comprising organic polymers with dispersed inorganic fillers for gas separation, *Prog. Poly. Sci.*, 32 (2007) 483–507
  47. H. Nagasawa, N. Matsuda, M. Kanezashi, T. Yoshioka, T. Tsuru, Pervaporation and vapor permeation characteristics of BTESE-derived organosilica membranes and their long-term stability in a high-water-content IPA/water mixture, *J. Mem. Sci.*, 498(2016)336–344
  48. H. Cong, M. Radosz, B. F. Towler, Y. Shen, Polymer–inorganic nanocomposite membranes for gas separation, *Separ. Purif. Tech.*, 55 (2007) 281–291
  49. M. Z Rong, M. Q Zhang, Y. X Zheng, H. M Zeng, R Walter, K Friedrich, Structure-property relationships of irradiation grafted nano inorganic particle filled polypropylene composites, *Polymer* 42 (2001)167–83.
  50. S. Kangoa, S. Kaliab, A. Celli, J. Njugunad, Y. Habibie, R. Kumara, Surface modification of inorganic nanoparticles for development of organic–inorganic nanocomposites—A review, *Prog. Poly. Sci.*, 38 (2013) 232-1261

51. K. Müller, E. Bugnicourt, M. Latorre, M. Jorda, Y. E. Sanz, J. M. Lagaron, O. Miesbauer, A. Bianchin, S. Hankin, U. Bölz, G. Pérez, M. Jesdinszki, M. Lindner, Z. Scheuerer, S. Castelló, M. Schmid, Review on the processing and properties of polymer nanocomposites and nanocoatings and their applications in the packaging, Automotive and Solar Energy Fields, *Nanomaterials (Basel)* 7(4)(2017) 74
52. D. Pitsa, M. G. Danikas, Interfaces features in polymer nanocomposites: a review of proposed models, *NANO* 06 (2011)497-508
53. P. Song, Y. Yu, T. Zhang, S. Fu, Z. Fang, Q. Wu, Permeability, viscoelasticity, and flammability performances and their relationship to polymer nanocomposites, *Ind. Eng. Chem. Res.*, 51 (2012) 7255–7263
54. V. Monteil, J. Stumbaum, R. Thomann, S. Mecking, Silica/polyethylene nanocomposite particles from catalytic emulsion polymerization, *Macromolecules* 39 (2006)2056-2062
55. M. A. Semsarzadeh, B. Ghalei, Preparation, characterization and gas permeation properties of polyurethane–silica/polyvinyl alcohol mixed matrix membranes, *J. Mem. Sci.*, 432 (2013) 115–125
56. S. Khoonsap, N. Supanchaiyamat, A. J. Hunt, S. Klinrisuk, S. Amnuaypanich, Improving water selectivity of poly (vinyl alcohol) (pva)-fumed silica (fs) nanocomposite membranes by grafting of poly (2-hydroxyethyl methacrylate) (phema) on fumed silica particles, *Chem. Eng. Sci.*,122 (2015) 373-383
57. D. R. Paul, Transport properties of polymers, Tess and Poehlein; applied polymer science, in: ACS Symposium Series, American Chemical Society, Washington, DC, (1985)
58. W. J. Koros, G. K. Fleming, S. M. Jordan, T. H. Kim, H. H. Hoehn, Polymeric membrane materials for solution-diffusion based permeation separations, *Progress in Polymer Science* 13 (4) (1988) 339-401.
59. B. Freeman, Y. Yampolskii, I. Pinnau, Materials science of membranes for gas and vapor separation, (2006) ISBN:9780470853450

- 
60. L. Y. Jiang, Y. Wang, T. S. Chung, X. Yi Qiao, J. Y. Lai, Polyimides membranes for pervaporation and biofuels separation, *Prog. Poly. Sci.*, 34(2009)1135-1160
  61. P. Shao, R. Y. M. Huang, Polymeric membrane pervaporation, *J. Mem. Sci.*, 287 (2007) 162-179
  62. Y. K. Ong, G. M. Shi, N. L. Le, Y. P. Tang, J. Zuo, S. P. Nunes, T. S. Chung, Recent membrane development for pervaporation processes, *Prog. Poly. Sci.*, 57(2016) 1-31
  63. P. Schaetzel, C. Vauclair, Q. T. Nguyen, R. Bouzerar, A simplified solution-diffusion theory in pervaporation: the total solvent volume fraction model, *J. Mem. Sci.*, 244 (2004) 117-127
  64. A. W. Grabczyk, S. Smigasiwicz, J. Muszynski, An improvement of the Mc Bain's microbalance to study transport of solvent vapours into polymeric films, *Polym. Bull.*, 40 (4) (1998) 591-598.
  65. K. Friess, J. C. Jansen, O. Vopicka, A. Randova, V. Hynek, M. Sipek, L. Bartovska, P. Izak, M. Dingemans, J. Dewulf, H. Van Langenhove, E. Drioli, Comparative study of sorption and permeation techniques for the determination of heptane and toluene transport in polyethylene membranes, *J. Mem. Sci.*, 338 (1-2) (2009) 161-174.
  66. A. F. M. Barton, *Handbook of solubility parameters and other cohesion parameters*, CRC Press LLC, (1991) ISBN: 9780849301766
  67. S. Thomas, R. Stephen, *Rubber Nanocomposite: preparation, properties and applications*, John Wiley and Sons (Asia) Pt Ltd., Singapore., (2010) ISBN: 978-0-470-82345-3
  68. V. G. Geethamma, S. Thomas, Diffusion of water and artificial seawater through coir fiber reinforced natural rubber composites, *Polymer composites* 26 (2005) 136-143.
  69. R. Stephen, S. Varghese, K. Joseph, Z. Oommen, S. Thomas, Diffusion and transport through nanocomposites of natural rubber (NR), carboxylated styrene butadiene rubber (XSBR) and their blends, *J. Mem. Sci.*, 282 (2006) 162-170
  70. T. M. Aminabhavi, R. S. Khinnavar, Diffusion and sorption of organic liquids through polymer membranes: 10. Polyurethane,

- 
- nitrile-butadiene rubber and epichlorohydrin versus aliphatic alcohols (C<sub>1</sub>-C<sub>5</sub>), *Polymer* 34 (1993) 1005.
71. T. Okada, T. Matsuura, Predictability of transport equations for pervaporation on the basis of pore-flow mechanism, *J. Mem. Sci.*, 70 (2-3) (1992) 163-175.
72. T. Okada, M. Yoshikawa, T. Matsuura, A study on the pervaporation of ethanol/water mixtures on the basis of pore flow model, *J. Mem. Sci.*, 59 (2) (1991) 151-168
73. G. W. M. Thomson, The antoine equation for vapor-pressure data, *Chem. Rev.*, 38 (1946) 1-39
74. S. Reinecke, B.E. Sleep, Knudsen diffusion, gas permeability, and water content in an unconsolidated porous medium, *Wat. Resour. Resea.*, 38 (2002) 1-15
75. L. Cui, J. T. Yeh, K. Wang, F. C. Tsai, Q. Fu, Relation of free volume and barrier properties in the miscible blends of poly(vinyl alcohol) and nylon 6-clay nanocomposites film, *J. Mem. Sci.*, 327 (2009) 226–233
76. S. Y. Hu, Y. Zhang, D. Lawless, X. Feng, Composite membranes comprising of polyvinylamine-poly(vinyl alcohol) incorporated with carbon nanotubes for dehydration of ethylene glycol by pervaporation, *J. Mem. Sci.*, 417–418 (2012) 34–44
77. Q. An, J.T.Chen, M. D. Guzman, W.S. Hung, K.R.Lee, J.Y. Lai, Multilayered poly(vinylidene fluoride) composite membranes with improved interfacial compatibility: correlating pervaporation performance with free volume properties, *Langmuir* 27 (2011) 11062–11070
78. Y. Yampolskii, Polymeric gas separation membranes, *Macromolecules* 45 (2012) 3298–3311
79. F. Peng, Z. Jiang, E. M. V. Hoek, Tuning the molecular structure, separation performance and interfacial properties of poly(vinyl alcohol)–polysulfone interfacial composite membranes, *J. Mem. Sci.*, 368 (2011) 26–33
80. J. L. Duda, J. M. Zielinski, Free-volume theory. In Neogi, P., editor, *Diffusion in Polymers*, Marcel Dekker, New York, N. Y. (1996) 143–171

- 
81. A. Thran, G. Kroll, F. Faupel, Correlation between fractional free volume and diffusivity of gas molecules in glassy polymers, *J.Poly. Sci.B: Poly. Phys.*, 37 (1999) 3344-3358.
  82. Y. Jean, J. Yuan, J. Liu, Q. Deng, H. Yang, Correlations between gas permeation and free-volume hole properties probed by positron annihilation spectroscopy, *J.Poly. Sci. B: Poly. Phys.*, 33 (1995) 2365-2371.
  83. Y. Kobayashi, K. Haraya, S. Hattori, Evaluation of polymer free volume by positron annihilation and gas diffusivity measurements, *Polymer* 35 (1994) 925-928.
  84. S. Khoonsap, S. Rugmai, W.S. Hung, K.R. Lee, S.Klinsrisuk, S.Amnuaypanich, Promoting permeability-selectivity anti-trade-off behavior in polyvinyl alcohol (PVA) nanocomposite membranes, *J. Mem. Sci.*, 544(2017) 287-296
  85. Q. Xin, Y. Zhang, Y. Shi, H. Ye, L. Lin, X. Ding, Y. Zhang, H. Wu, Z. Jiang, Tuning the performance of CO<sub>2</sub> separation membranes by incorporating multifunctional modified silica microspheres into polymer matrix, *J. Mem. Sci.*, 514(2016)73–85
  86. D. Peng, S. Wang, Z. Tian, X. Wu, Y. Wu, H. Wu, Q. Xin, J. Chen, X. Cao, Z. Jiang, Facilitated transport membranes by incorporating graphene nanosheets with high zinc ion loading for enhanced CO<sub>2</sub> separation, *J. Mem. Sci.*, 522(2017) 351-362
  87. C. H. Ji, S. M.Xue, Z. L. Xu, Novel swelling-resistant sodium alginate membrane branching modified by glycogen for highly aqueous ethanol solution pervaporation, *ACS Appli.Mater. Interfac.*, 8 (2016) 27243-27253
  88. P. Garg, R. P.Singh, V. Choudhary, Selective polydimethylsiloxane/polyimide blended IPN pervaporation membrane for methanol/toluene azeotrope separation, *Separ. Purifi. Tech.*, 76 (2011) 407-418
  89. K. Cao, Z. Jiang, X. Zhang, Y. Zhang, J. Zhao, R. Xing, S. Yang, C. Gao, F. Pan, Highly water-selective hybrid membrane by incorporating g-C<sub>3</sub>N<sub>4</sub> nanosheets into polymer Matrix, *J. Mem. Sci.*, 490 ( 2015) 72-83
  90. M. Lim, H. Kwon, D. Kim, J. Seo, H. Han, S. B. Khan, Highly-enhanced water resistant and oxygen barrier properties of cross-

- 
- linked poly(vinyl alcohol) hybrid films for packaging applications, *Prog. Orga. Coat.*, 85 (2015) 68–75
91. S. K. Nataraj, S. Sridhar, I. N. Shaikha, D. S. Reddy, T. M. Aminabhavi, Membrane-based microfiltration/electrodialysis hybrid process for the treatment of paper industry waste water, *Separat. Purifi.Tech.*,57(2007) 185-192
92. K. P. Lee, T. C. Arnot, D. Mattia, A review of reverse osmosis membrane materials for desalination—Development to date and future potential, *J. Mem. Sci.*, 370 (2011) 1-22
93. K. Cao, Z. Jiang, J. Zhao, C. Zhao, C. Gao, F. Pan, B. Wang, X. Cao, J. Yang, Enhanced water permeation through sodium alginate membranes by incorporating graphene oxides, *J. Mem. Sci.*, 469(2014) 272-283
94. X. Cheng, F. Pan, M. Wang, W. Li, Y. Song, G. Liu, H. Yang, B. Gao, H. Wu, Z. Jiang, Hybrid membranes for pervaporation separations, 541 (2017) 329-346
95. R. C. Muñoz, F. Galiano, V. Fila, E. Drioli, A. Figoli, Matrimid®5218 dense membrane for the separation of azeotropic MeOH-MTBE mixtures by pervaporation, *Separat. Purifi.Tech.*, 199 (2018) 27-36
96. J. Yin, B. Deng, Polymer-matrix nanocomposite membranes for water treatment, *J. Mem. Sci.*, 479 (2015) 256-275
97. X. Cheng, Z. Jiang, X. Cheng, H. Yang, L. Tang, G. Liu, M. Wang, H. Wu, F. Pan, X. Cao, Water-selective permeation in hybrid membrane incorporating multi-functional hollow ZIF-8 nanospheres, *J. Mem. Sci.*, 555 (2018) 146-156
98. I. L. Vane1, V. Nambodiri1, G. Lin, M. Abar, F. Alvarez, Preparation of water-selective polybutadiene membranes and their use in drying alcohols by pervaporation and vapor permeation technologies, *ACS Susta. Chem. Eng.*, 4 (8) (2016) 4442–4450
99. W. Zhang, Y. Ying, J. Ma, X. Guo, H. Huang, D. Liu, C. Zhong, mixed matrix membranes incorporated with polydopamine-coated metal organic frame work for dehydration of ethylene glycol by pervaporation, *J. Mem. Sci.*, 527 (2017) 8-17
100. Y. L. Liao, C. C. Hu, J. Y. Lai, Y. L. Liu, Crosslinked polybenzoxazine based membrane exhibiting in-situ self promoted

- 
- separation performance for pervaporation dehydration on isopropanol aqueous solutions, *J. Mem. Sci.*, 531 (2017) 10–15
101. L. Shan, L. Gong, H. Fan, S. Ji, G. Zhang, Spray-assisted biomimetic mineralization of a superhydrophilic water uptake layer for enhanced pervaporation dehydration, *J. Mem. Sci.*, 522 (2017) 183–191
102. S. Roy, N. R. Singha, Polymeric Nanocomposite Membranes for Next Generation Pervaporation Process: Strategies, Challenges and Future Prospects, *Membranes* 7(3) (2017) 53
103. P. Schaetzel, C. Vauclair, Q. Trong, N. Roger, Bouzerar, A simplified solution–diffusion theory in pervaporation: the total solvent volume fraction model, *J. Mem. Sci.*, 244 (2004) 117–127
104. S. Xu, L. Liu, Y. Wang, Network cross-linking of polyimide membranes for pervaporation dehydration, *Separat. Purif. Technol.*, 185 (2017) 215–226
105. A. V. Penkova, M. E. Dmitrenko, N. A. Savon, A. B. Missyul, A. S. Mazur, A. I. Kuzminova, A. A. Zolotarev, V. Mikhailovskii, E. Lahderanta, D. A. Markelov, K. N. Semenov, S. S. Ermakov, Novel mixed-matrix membranes based on polyvinyl alcohol modified by carboxyfullerene for pervaporation dehydration, *Separat. Purif. Technol.*, 204 (2018) 1–12
106. M. Wang, H. Wu, X. Jin, C. Yang, X. He, F. Pan, Z. Jiang, C. Wang, M. Chen, P. Zhang, X. Cao, Enhanced dehydration performance of hybrid membranes by incorporating fillers with hydrophilic-hydrophobic regions, *Chem. Eng. Sci.*, 178 (2018) 273–283
107. R. W. Baker, J. G. Wijmans, Y. Huang, Permeability, permselectivity and selectivity: A preferred way of reporting pervaporation performance data, *J. Mem. Sci.*, 348 (2010) 346–352.
108. C. M. Hansen, A. Beerbower, *Encyclopedia of chemical technology*, (1971) Supplement volume.
109. T. Jose, S. C. George, M. G. Maya, H. J. Maria, R. Wilson, S. Thomas, effect of bentonite clay on the mechanical, thermal, and pervaporation performance of the poly(vinyl alcohol) nanocomposite membranes, *Indu. Eng. Chem. Resear.*, 53 (2014) 16820–16831



110. V. T. Magalada, G. S. Gokavia,, K.V.S.N. Rajub, T. M. Aminabhavia,, Mixed matrix blend membranes of poly(vinyl alcohol)–poly(vinyl pyrrolidone) loaded with phosphomolybdic acid used in pervaporation dehydration of ethanol, *J. Mem. Sci.*, 354 (2010) 150–161
111. Y. M. Xu, N. L. Le, J. Zuo, T. S. Chung, Aromatic polyimide and crosslinked thermally rearranged poly (benzoxazole-co-imide) membranes for isopropanol dehydration via pervaporation, *J. Mem. Sci.*, 499 (2016) 317–325
112. Q. G. Zhang, Q. L. Liu, Y. Chen, J. H. Chen, Dehydration of isopropanol by novel poly(vinyl alcohol)–silicone hybrid membranes, *Ind. Eng. Chem. Res.*, 46 (3) (2007)913–920
113. Q. G. Zhang, Q. L.Liu, F. F. Shi, Y. Xiong, Structure and permeation of organic–inorganic hybrid membranes composed of poly(vinyl alcohol) and polysilisesquioxane, *J. Mater. Chem.*, 18 (2008) 4646-4653
114. Q. G. Zhang, Q. L. Liu, A. M. Zhu, Y. Xiong, X. H. Zhang, characterization and permeation performance of novel organic-inorganic hybrid membranes of poly(vinyl alcohol)/1,2-bis(triethoxysilyl)ethane, *J. Phys. Chem. B.*, 112 (2008) 16559–16565
115. H. G. Premakshi, M. Y. Kariduraganavar, G. R. Mitchell,Development of composite anion-exchange membranes using poly(vinyl alcohol) and silica precursor for pervaporation separation of water– isopropanol mixtures, *RSC Adv.*, 6 (2016) 11802-11814
116. T. Narkkun, W. Jenwiriyakul, S. Amnuaypanich, Dehydration performance of double-network poly (vinyl alcohol) nanocomposite membranes (PVAs-DN), *J. Mem. Sci.*, 528 (2017) 284-295
117. F. Kursun, N. Isiklan, Development of thermo-responsive poly(vinyl alcohol)-g-poly(N-isopropylacrylamide) copolymeric membranes for separation of isopropyl alcohol/water mixtures via pervaporation, *J. Indus. Eng. Chem.*, 41 (2016) 91–104
118. Y. Shirazi, M. A. Tofighy, T. Mohammadi, Synthesis and characterization of carbon nanotubes/poly vinyl alcohol

- 
- nanocomposite membranes for dehydration of isopropanol, *J. Mem. Sci.*, 378 (2011) 551– 561
119. M. Olukman O. Sanl, A novel in situ synthesized magnetite containing acrylonitrile and 2-hydroxyethyl methacrylate grafted poly(vinyl alcohol) nanocomposite membranes for pervaporation separation of acetone/water mixtures, *Chem.Eng. Process.Process Intensifi.*, 98 (2015) 60-70
120. G. Wu, M. Jiang, T. Zhang, Z. Jia, Tunable Pervaporation Performance of Modified MIL-53(Al)-NH<sub>2</sub>/Poly(vinyl Alcohol) Mixed Matrix Membranes, *J.Mem. Sci.*, 507(2016) 72-80
121. M. Wang, R. Xing, H.Wu, F.Pan, J.Zhang, H. Ding, Z. Jiang, Nanocomposite membranes based on alginate matrix and high loading of pegylated POSS for pervaporation dehydration, *J. Mem. Sci.*, 538(2017) 86-95
122. N. L. Le, Y. Wang, T. S. Chung, Pebax/POSS mixed matrix membranes for ethanol recovery from aqueous solutions via pervaporation, *J.Mem. Sci.*, 379 (2011) 174-183
123. G. Dong, H. Liab and V. Chen, Challenges and opportunities for mixed-matrix membranes for gas separation, *J. Mater. Chem. A.*, 1(2013) 4610-4630
124. M. Vinoba, M. Bhagiyalakshmi, Y. Alqaheem, A. A. Alomair, A. Pérez, M. S. Rana, Recent progress of fillers in mixed matrix membranes for CO<sub>2</sub> separation: A review, *Separ. Purif. Techno.*, 188 (2017) 431-450
125. D. F. Sanders , Z. P. Smith , R. Guo , L. M. Robeson , J. E. McGrath , D. R. Paul, B. D. Freeman, Energy-efficient polymeric gas separation membranes for a sustainable future: A review, *Polymer* 54 (2013) 4729-4761
126. D. Wu, C. Sun, P. K. Dutta, W. S. W. Ho, SO<sub>2</sub> interference on separation performance of amine-containing facilitated transport membranes for CO<sub>2</sub> capture from flue gas, *J. Mem. Sci.*, 534 (2017) 33-45
127. E. G. Estahbanati, M. Omidkhah, A. E. Amooghin, Interfacial design of ternary mixed matrix membranes containing pebax 1657/silver-nanopowder/[BMIM][BF<sub>4</sub>] for improved CO<sub>2</sub> separation

- 
- performance, *ACS Appl. Mater. Interface.*, 9(11) (2017) 10094–10105
128. L. M. Robeson, Correlation of Separation factor versus permeability for polymeric membranes, *J. Mem. Sci.*, 62 (1991) 165-185.
129. L. M. Robeson, The upperbound revisited, *J. Mem. Sci.*, 320 (2008) 390-400.
130. Z. Dai, L. Ansaloni, D. L. Gin, R. D. Noble, L. Deng, Facile fabrication of CO<sub>2</sub> separation membranes by cross-linking of poly(ethylene glycol) diglycidyl ether with a diamine and a polyamine-based ionic liquid, *J. Mem. Sci.*, 523 (2017) 551-560
131. V. Giel, Z. Morávková, J. Peter, M. Trchová, Thermally treated polyaniline/polybenzimidazole blend membranes: Structural changes and gas transport properties, *J. Mem. Sci.*, 537 (2017) 315-322
132. M. L. Chua, L. Shao, B. T. Low, Y. Xiao, T. S. Chung, Polyetheramine–polyhedral oligomeric silsesquioxane organic–inorganic hybrid membranes for CO<sub>2</sub>/H<sub>2</sub> and CO<sub>2</sub>/N<sub>2</sub> separation, *J. Mem. Sci.*, 385–386 (2011) 40-48
133. Z. Dai, H. Aboukeila, L. Ansaloni, J. Deng, M. G. Baschetti, L. Deng, Nafion/PEG hybrid membrane for CO<sub>2</sub> separation: Effect of PEG on membrane micro-structure and performance, *Separat. Purif. Technol.*, (2018) <https://doi.org/10.1016/j.seppur.2018.03.062>
134. J. Cheng, L. Hu, Y. Li, J. Liu, J. Zhou, K. Cen, CO<sub>2</sub> absorbents Improving CO<sub>2</sub> permeation and separation performance of CO<sub>2</sub>-philic polymer membrane by blending CO<sub>2</sub> absorbents, *Appl. Surf. Sci.*, 410 (2017) 206–214
135. Md. M. Rahman, V. Filiz, S. Shishatskiy, C. Abetz, P. Georgopoulos, M. M. Khan, S. Neumann, V. Abetz, Influence of poly(ethylene glycol) segment length on CO<sub>2</sub> permeation and stability of polyactive membranes and their nanocomposites with PEG POSS, *ACS Appl. Mater. Interfac.*, 7(23) (2015) 12289-12298
136. D. Zhao, J. Ren, Y. Wang, Y. Qiu, H. Li, K. Hua, X. Li, J. Ji, M. Deng, High CO<sub>2</sub> separation performance of Pebax®/CNTs/GTA mixed matrix membranes, *J. Mem. Sci.*, 521 (2017) 104-113

- 
137. S. L. Liu, L. Shao, M. L. Chua, C. H. Lau, H. Wang, S. Quan, Recent progress in the design of advanced PEO-containing membranes for CO<sub>2</sub> removal, *Prog. Polym. Sci.*, 38 (2013) 1089–1120
138. S. B. Hamouda, Q. T. Nguyen, D. Langevin, S. Roudesli, Poly(vinylalcohol)/poly(ethyleneglycol)/poly(ethyleneimine) blend membranes- structure and CO<sub>2</sub> facilitated transport, *Compt. Rend. Chimie.*, 13 (2010) 372–379
139. N. Du, H. B. Park, M. M. D. Cin, M. D. Guiver, Advances in high permeability polymeric membrane materials for CO<sub>2</sub> Separations, *Ener. Environ. Sci.*, 5 (2012) 7306-7322
140. L. Kwisnek, J. Goetz, K. P. Meyers, S. R. Heinz, J. S. Wiggins, S. Nazarenko, PEG containing thiol-ene network membranes for CO<sub>2</sub> separation: effect of cross-linking on thermal, mechanical, and gas transport properties, *Macromolecules* 47(2014) 3243–3253
141. A. Car, C. Stropnik, W. Yave, K. V. Peinemann, PEG modified poly (amide-b-ethylene oxide) membranes for CO<sub>2</sub> separation, *J. Mem. Sci.*, 307 (2008) 88-95.
142. W. Yave, A. Car, S. S. Funari, S. P. Nunes, K.V. Peinemann, CO<sub>2</sub>-philic polymer membrane with extremely high separation performance, *Macromolecules* 4(2010)326–333
143. A. Mondal, B. Mandal, CO<sub>2</sub> separation using thermally stable crosslinked poly(vinylalcohol) membrane blended with polyvinylpyrrolidone/polyethyleneimine/tetraethylenepentamine, *J. Mem. Sci.*, 460(2014)126–138
144. B. Gye, I. Kammakam, H. You, S. Y. Nam, T. H. Kim, PEG-imidazolium-incorporated polyimides as high- performance CO<sub>2</sub>-selective polymer membranes: The effects of PEG-imidazolium content, *Separa. Purifi. Tech.*, 179 (2017) 283–290
145. S. Wang, X. Li, H. Wu, Z. Tian, Q. Xin, G. He, D. Peng, S. Chen, Y. Yin, Z. Jiang, M. D. Guiver, Advances in high permeability polymer-based membranematerials for CO<sub>2</sub> separations, *Ener. Environ. Sci.*, 9 (2016)1863-1890
146. Y. Kinoshita, K. Wakimoto, A. H. Gibbons, A. P. Isfahani, H. Kusuda, E. Sivaniah, B. Ghalei, Enhanced PIM-1 membrane gas

- 
- separation selectivity through efficient dispersion of functionalized POSS fillers, *J. Mem. Sci.*, 539(2017) 178-186
147. M. Wang, Z. Wang, N. Li, J. Liao, S. Zhao, J. Wang, S. Wang, Relationship between polymer-filler interfaces in separation layers and gas transport properties of mixed matrix composite membranes, *J. Mem. Sci.*, 495 (2015) 252-268
148. W. R. Kang, A. S. Lee, S. Park, S. H. Park, K. Y. Baek, K. B. Lee, S. H. Lee, J. H. Lee, S. S. Hwang, J. S. Lee, Free-standing, polysilsesquioxane-based inorganic/organic hybrid membranes for gas separations, *J. Mem. Sci.*, 475 (2015) 384–394
149. N. Konnertz, Y. Ding, W. J. Harrison, P. M. Budd, A. Schönhals, M. Böhning, Molecular mobility and gas transport properties of nanocomposites based on pim-1 and polyhedral oligomeric phenethyl-silsesquioxanes (POSS), *J. Mem. Sci.*, (2017) 274-285
150. J. H. Lee, D. Jung, C. E. Hong, K. Y. Rhee, S. G. Advani, Properties of polyethylene-layered silicate nanocomposites prepared by melt intercalation with a PP-g-MA compatibilizer, *Compos. Sci. Technol.*, 65 (2005) 1996–2002.
151. B. Tan, N. L. Thomas, A review of the water barrier properties of polymer/clay and polymer/graphene nanocomposites, *J. Mem. Sci.*, 514 (2016) 595-612
152. C. Wolf, N. Gontard, F. Doghieri, V. Guillard, How the shape of fillers affects the barrier properties of polymer/non-porous particles nanocomposites: A review, *J. Mem. Sci.*, 556 (2018) 393-418
153. P. G. Ren, X. H. Liu, Biodegradable graphene oxide nanosheets/poly-(butylene adipate-co-terephthalate) nanocomposite film with enhanced gas and water vapor barrier properties, *Poly. Test.*, 58 (2017) 173-180
154. H. D. Huang, P. G. Ren, J. Chen, W. Q. Zhang, X. Ji, Z. M. Li, High barrier graphene oxide nanosheet/poly(vinyl alcohol) nanocomposite films, *J. Mem. Sci.*, 409–410 (2012) 156–163
155. Y. Cui, S. Kumar, B. R. Konac, D. van Houckee, Gas barrier properties of polymer/clay nanocomposites, *RSC Adv.*, 5(2015)63669-63690

- 
156. S. Hasebe, S. Aoyama, M. Tanaka, H. Kawakami, CO<sub>2</sub> Separation of Polymer Membranes Containing Silica Nanoparticles with Gas Permeable Nano- Space, *J.Mem.Sci.*, 536 (2017) 148-155
  157. M. G. D. Angelis, G. C. Sarti, Gas sorption and permeation in mixed matrix membranes based on glassy polymers and silica nanoparticles, *Curr. Opin. Chem. Eng.*, 1 (2012)148–155
  158. R. Xing, W. S. W. Ho, Crosslinked polyvinylalcohol– polysiloxane/fumed silica mixed matrix membranes containing amines for CO<sub>2</sub>/H<sub>2</sub> separation, *J.Mem.Sci.*, 367 (2011) 91-102
  159. M. Sadeghi, M. Semsarzadeh, M. Barikani, M. Chenar. Gas separation properties of polyether-based polyurethane-silica nanocomposite membrane. *J. Mem. Sci.*, 376 (2011)188–95
  160. H. V. Thang, S. Kaliaguine, Predictive models for mixed-matrix membrane performance: a review, *Chem. Rev.*,113 (7) (2013)4980–5028
  161. M. H. Cohen, D. Turnbull, Molecular transport in liquids and glasses, *J. Chem. Phys.*, 31 (1959) 1164–1169
  162. H. Chen, W. S. Hung, C. H. Lo, S. H. Huang, M. L. Cheng, G. Liu, K. R. Lee, J. Y. Lai, Y. M. Sun, C. C. Hu, R. Suzuki, T. Ohdaira, N. Oshima, Y. C. Jean, Free-volume depth profile of polymeric membranes studied by positron annihilation spectroscopy: layer structure from interfacial polymerization, *Macromolecules* 40(2007)7542-7557
  163. C. L. Lai, J. T. Chen, Y. J. Fu, W. R. Liu, Y. R. Zhong, S. H. Huang, W. S. Hung, S.J.Lue, C. C.Hu, K. R. Lee, Bio-inspired cross-linking with borate for enhancing gas-barrier properties of poly(vinyl alcohol)/graphene oxide composite films, *Carbon* 82 (2015) 513-522
  164. S. Li, X. Jiang, Q. Yang, L. Shao, Effects of amino functionalized polyhedral oligomeric silsesquioxanes on cross-linked poly (ethylene oxide) membranes for highly-efficient CO<sub>2</sub> separation, *Chem. Eng. Resea. Desig.*, 122 (2017) 280-288
  165. P.Iyer, G. Iyer, M. Coleman, Gas transport properties of polyimide–POSS nanocomposites, *J. Mem. Sci.*, 358 (2010) 26–32
  166. M. M. Rahman., V. Filiz, M. M. Khan, B. N. Gacal, V. Abetz, Functionalization of POSS nanoparticles and fabrication of block

- 
- copolymer nanocomposite membranes for CO<sub>2</sub> separation, *Reac. Function. Polym.*, 86 (2015) 125-133
167. P. Bandyopadhyay, S. Banerjee, Synthesis, characterization and gas transport properties of polyamide-tethered polyhedral oligomeric silsesquioxane (POSS) nanocomposites, *Ind. Eng. Chem. Res.*, 53 (2014)18273–18282
168. R. Xing, W. S. W. Ho, Synthesis and characterization of crosslinked polyvinylalcohol/polyethyleneglycol blend membranes for CO<sub>2</sub>/CH<sub>4</sub> separation, *J.Taiwan Institut.Chem. Eng.*, 40 (2009) 654–662
169. C. A. Finch, Ed. Polyvinyl alcohol, Wiley, London, (1973)
170. J. G. Pritchard, Poly(vinyl alcohol), basic properties and uses; Macdonald Technical and Scientific: London, (1970)
171. C. A. Finch, Ed. Properties and applications of polyvinyl alcohol. S. C. I. Monograph No. 30, Society of Chemical Industry: London, (1968)
172. M. Liu, Q. Chen, L. Wang, S. Yu, C. Gao, Improving fouling resistance and chlorine stability of aromatic polyamide thin-film composite RO membrane by surface grafting of polyvinyl alcohol (PVA), *Desalination*367 (2015) 11-20
173. K. Halake, M. Birajdar, B. S. Kim, H. Bae, C. C. Lee, Y. J. Kim, S. Kim, H. J. Kim, S. Ahn, S. Y. An, J. Lee, Recent application developments of water-soluble synthetic polymers, *J. Indus. Eng. Chem.*, 20 (2014)3913-3918
174. E. Marin, J. Rojas, Y. Ciro, A review of polyvinyl alcohol derivatives: Promising materials for pharmaceutical and biomedical applications, *Afri. J. Pharma. Pharmaco.*, 8(24) (2014)674-684
175. A. Singhal, M. Kaur, K. A. Dubey, Y. K. Bhardwaj, D. Jain, C. G. S. Pillaia, A. K. Tyagi, Polyvinyl alcohol–In<sub>2</sub>O<sub>3</sub> nanocomposite films: synthesis, characterization and gas sensing properties, *RSC Adv.*, 2 (2012)7180–7189
176. A. Quanfu, L. Feng, J. Yanli, C. Huanlin, Influence of polyvinyl alcohol on the surface morphology, separation and anti-fouling performance of the composite polyamide nanofiltration membranes, *J. Mem. Sci.*, 367 (2011)158-165

- 
177. K. Deshmukh, M. B. Ahamed, R. R. Deshmukh, S. K. K. Pasha, K. K. Sadasivuni, D. Ponnamma, K. Chidambaram, Synergistic effect of vanadium pentoxide and graphene oxide in polyvinyl alcohol for energy storage application, *Europ. Poly. J.*, 76 (2016) 14-27
178. S. Gupta, S. Sindhu, K. A. Varman, P. C. Ramamurthy, G. Madras, Hybrid nanocomposite films of polyvinyl alcohol and ZnO as interactive gas barrier layers for electronics device passivation, *RSC Adv.*, 2 (2012) 11536–11543
179. S. D. Jiang, Z. M. Bai, G. Tang, Y. Hu, L. Song Fabrication and characterization of graphene oxide-reinforced poly (vinyl alcohol)-based hybrid composites by the sol-gel method, *Compos. Sci. Tech.*, 102 (2014) 51–58
180. H. Lu, C. A. Wilkie, M. Ding, L. Song, Thermal properties and flammability performance of poly (vinyl alcohol)/ $\alpha$ -zirconium phosphate nanocomposites, *Poly. Degrad. Stab.*, 96 (2011) 885-891
181. M. K. Mandal, S. B. Sant, P. K. Bhattacharya, Dehydration of aqueous acetonitrile solution by pervaporation using PVA-iron oxide nanocomposite membrane, *Collo. Surfa. A: Physicochem. Eng. Aspec.*, 373 (2011) 11-21
182. S. Huang, X. Cen, H. Zhu, Z. Yang, Y. Yang, W. W. Tjiu, T. Liu, Facile preparation of poly(vinyl alcohol) nanocomposites with pristine layered double hydroxides, *Mater. Chem. Phys.*, 130 (2011) 890–896
183. R. K. Layek, A. K. Das, M. U. Park, N. H. Kim, J. H. Lee, Layer-structured graphene oxide/polyvinyl alcohol nanocomposites: dramatic enhancement of hydrogen gas barrier properties, *J. Mater. Chem. A.*, 2(2014) 12158-12161
184. A. Mandal, D. Chakrabarty, Studies on the mechanical, thermal, morphological and barrier properties of nanocomposites based on poly(vinyl alcohol) and nanocellulose from sugarcane bagasse, *J. Indus. Eng. Chem.*, 20 (2014) 462-473
185. M. J. Cho, B. D. Park, Tensile and thermal properties of nanocellulose-reinforced poly(vinyl alcohol) nanocomposites, *J. Indus. Eng. Chem.*, 2017 (2011) 36–40
186. Y. Hu, K. Lu, F. Yan, Y. Shi, P. Yu, S. Yu, S. Li, C. Gao, Enhancing the performance of aromatic polyamide reverse osmosis membrane by



- 
- surface modification via covalent attachment of polyvinyl alcohol (PVA), *J. Mem. Sci.*, 501 (2016) 209-219
187. T. Narkkun, W. Jenwiriyakul, S. Amnuaypanich, Dehydration performance of double-network poly(vinyl alcohol) nanocomposite membranes (PVAs-DN, *J. Mem. Sci.*, 528 (2017) 284–295
188. T. S. Gaaz, A. B. Sulong, M. N. Akhtar, A. A. H. Kadhum, A. B. Mohamad, A.A. Al-Amiery, Properties and Applications of Polyvinyl Alcohol, Halloysite Nanotubes and Their Nanocomposites, *Molecules* 20(12) (2015) 22833-22847.
189. C. C. Thong, D. C. L. Teo, C.K. Ng, Application of polyvinyl alcohol (PVA) in cement-based composite materials: A review of its engineering properties and microstructure behavior, *Construc. Build. Mater.*, 107 (2016) 172–180
190. K. S. Hemalatha, K. Rukmani, Synthesis, characterization and optical properties of polyvinyl alcohol–cerium oxide nanocomposite films, *RSC Adv.*, 6 (2016) 74354-74366
191. X. Tang, S. Alavi, Recent advances in starch, polyvinyl alcohol based polymer blends, nanocomposites and their biodegradability, *Carbohyd. Poly.*, 85 (2011) 7–16
192. C. Ying, H. L. Hong, Z. Y. Hong, Properties of poly(vinyl alcohol) plasticized by glycerin, *J. Fores. Prod. Indus.*, 3(3) (2014) 151-153
193. M. I. Baker, S. P. Walsh, Z. Schwartz, B. D. Boyan, A review of polyvinyl alcohol and its uses in cartilage and orthopedic applications, *J. Biomed. Mater. Resea. Part B: Appli. Biomater.*, 100(5)(2012) 1451-1457
194. M. Flieger, M. Kantorova, A. Prell, T. Rezanka and J. Votruba, Biodegradable plastics from renewable sources, *Folia Microbiologica.*, 48(1) (2003) 27–44
195. N. B. Halima, Poly(vinyl alcohol): Review of its promising applications and insights into biodegradation, *RSC Adv.*, 6 (2016) 39823-39832
196. S. D. Jiang, G. Tang, Z.M. Bai, Y.Y. Wang, Y. Hu, L. Song, Surface functionalization of MoS<sub>2</sub> with POSS for enhancing thermal, flame-retardant and mechanical properties in PVA composites, *RSC Adv.*, 4 (2014) 3253-3262

- 
197. S. Mallakpoura, M. Dinaria, The synergetic effect of chiral organoclay and surface modified- $\text{Al}_2\text{O}_3$  nanoparticles on thermal and physical properties of poly(vinyl alcohol) based nanocomposite films, *Prog. Organ. Coati.*, 76 (2013) 263–268
  198. D. Ghanbari, M. S. Niasari, M. Sabet, Preparation of flower-like magnesium hydroxide nanostructure and its influence on the thermal stability of poly vinyl acetate and poly vinyl alcohol, *Compos. Part B.*, 45 (2013) 550–555
  199. B. Bolto, T. Tran, M. Hoang, Z. Xie, Crosslinked poly(vinyl alcohol) membranes, *Prog. Poly. Sci.*, 34(2009) 969–981
  200. J. Xu, H. Ni, X. Luo, Z. Wang, H. Zhang, Preparation, characterization and enhanced performance of functional crosslinked membranes using poly(vinyl alcohol) as macromolecular crosslinker for fuel cells, *RSC Adv.*, 6 (2016) 41428
  201. W. H. Philipp, L. C. Hsu, Three Methods for In Situ Cross-Linking of Polyvinyl Alcohol Films for Application, as Ion-Conducting Membranes in Potassium Hydroxide Electrolyte, *NASA Technical Paper 1407* (1979)
  202. K. C. S. Figueiredo, T. L. M. Alves, C. P. Borges, Poly(vinyl alcohol) Films Crosslinked by Glutaraldehyde Under Mild Conditions, *J. Appli. Poly. Sci.*, 111 (2009) 3074–3080
  203. A. K. Sonker, H. D. Wagner, R. Bajpai, R. Tenne, X. M. Sui, Effects of tungsten disulphide nanotubes and glutaric acid on the thermal and mechanical properties of polyvinyl alcohol, *Compos. Sci. Techno.*, 127 (2016) 47-53
  204. D. Rong, K. Usui, T. Morohoshi, N. Kato, M. Zhou, T. Ikeda, Symbiotic degradation of polyvinyl alcohol by *Novosphingobium* sp. and *Xanthobacter flavus*, *J. Environ. Biotechnol.*, 9 (2) (2009) 131–134.
  205. C. C. Thong, D. C. L. Teo, C. K. Ng, Application of polyvinyl alcohol (PVA) in cement-based composite materials: A review of its engineering properties and microstructure behaviour, *Constr. Build. Mater.*, 107 (2016) 172–180
  206. S. Gu, G. He, X. Wu, Y. Guo, H. Liu, L. Peng, G. Xiao, Preparation and characteristics of crosslinked sulfonated poly(phthalazinone ether

- 
- sulfone ketone) with poly(vinyl alcohol) for proton exchange membrane. *J. Mem. Sci.*, 312 (2008) 48–58.
207. C. Sullivan, B. Rounsefell, P. J. Halley, R. Truss, W. P. Clarke, The anaerobic degradability of thermoplastic starch: Polyvinyl alcohol blends: Potential biodegradable food packaging materials, *Bioresour. Tech.*, 100 (2009) 1705–1710
208. N. Georgieva, R. Bryaskova, R. Tzoneva, New Polyvinyl alcohol-based hybrid materials for biomedical application, *Mat. Lett.*, 88 (2012) 19–2
209. S. Moulay, Review: poly(vinyl alcohol) functionalizations and applications, *Poly. Plasti, Tech. Eng.*, 54 (2015) 1289–1319,
210. Polyvinyl Alcohol (PVA) Market Analysis, By End-use (Paper, Food Packaging, Construction, Electronics), By Region (North America, Europe, Asia Pacific, Central & South America, MEA), And Segment Forecasts, 2018 – 2025), GVR-1-68038-837-4 (2017)
211. C. D. Armit, P. Wheeler, POSS keeps high temperature plastics flowing, *Plasti. Additiv. Compound.*, 10 (2008) 36–39
212. D. B. Cordes, P. D. Lickiss, F. Rataboul, Recent developments in the chemistry of cubic polyhedral oligosilsesquioxanes, *Chem. Rev.*, 110 (2010) 2081–2173.
213. J. M. Mabry, A. Vij, S. T. Iacono, B. D. Viers, Fluorinated Polyhedral Oligomeric Silsesquioxanes (F-POSS), *Angew. Chem. Int. Ed.*, 47 (2008) 4137–4140
214. G. Pan, Polyhedral Oligomeric Silsesquioxane (POSS), *Physical Properties of Polymers Handbook*, Springer, New York., (2007) 577–584
215. S. K. Kumar, B. C. Benicewicz, R. A. Vaia, K. I. Winey, 50th Anniversary Perspective: Are Polymer Nanocomposites Practical for Applications?, *Macromolecules* 50 (3) (2017) 714–731
216. S. H. Phillips, T. S. Haddad, S. J. Tomczak, Developments in nanoscience: polyhedral oligomeric silsesquioxane (POSS)-polymers, *Curr. Opin. Solid State. Mater. Sci.*, 8 (2004) 21–29
217. G. Guerrero, M. B. Hägg, G. Kignelman, C. Simon, T. Peters, N. Rival, C. Denonville, Investigation of amino and amidino

- 
- functionalized polyhedral oligomeric silsesquioxanes (poss<sup>®</sup>) nanoparticles in PVA-based hybrid membranes for CO<sub>2</sub>/N<sub>2</sub> separation, *J. Mem. Sci.*, 544 (2017) 161-173
218. Y. Y. Yang, X. Wang, Y. Hu, H. Hu, D. C. Wu, F. J. Xu, Bioreducible POSS-Cored Star-Shaped Polycation for Efficient Gene Delivery, *ACS Appl. Mater. Interf.*, 6 (2) (2014) 1044–1052
219. Kowalewska, Anna, Self-Assembling Polyhedral Silsesquioxanes - Structure and Properties, *Curr. Org. Chem.*, 21 (2017) 1243-1264(22)
220. W. Zhang, A. H.E. Müller, Architecture, self-assembly and properties of well-defined hybrid polymers based on polyhedral oligomeric silsesquioxane (POSS), *Prog. Polym. Sci.*, 38 (2013) 1121-1162
221. K. Tanaka, Y. Chujo. Advanced functional materials based on polyhedral oligomeric silsesquioxane (POSS), *J. Mater. Chem.*, 22 (2012) 1733-1746
222. M. Z. Asuncion, R. M. Laine, Silsesquioxane barrier materials, *Macromolecules* 40 (2007) 555-562
223. L. Peponi, D. Puglia, L. Torre, L. Valentini, J. M. Kenny, Processing of nanostructured polymers and advanced polymeric based nanocomposites, *Mater. Sci. Eng. R: Reports*, 85 (2014) 1-46
224. J. Zhao, Y. Fu, S. Liu, Polyhedral oligomeric silsesquioxane (POSS)-modified thermoplastic and thermosetting nanocomposites: a review, *Polym. Polym. Compos.*, 16(8) (2008) 483-500
225. G. Li, L. Wang, H. Ni, C. U. Pittman, Polyhedral oligomeric silsesquioxane (POSS) polymers and copolymers: a review, *J. Inorg. Organomet. Polym.*, 11 (2001) 123-154, <https://doi.org/10.1023/A:1015287910502>
226. Y. Kawakami, Y. Kakihana, A. Miyazato, S. Tateyama, M.A Hoque, Polyhedral oligomeric silsesquioxanes with controlled structure: formation and application in new Si-based polymer systems, *Silicon Polymers. Advances in Polymer Science*, Springer, Berlin, Heidelberg., 235(2010)185-228, ISBN: 978-3-642-16048-6
227. E. Amerio, M. Sangermano, G. Colucci, G. Malucelli, M. Messori, R. Taurino, P. Fabbri, UV curing of organic-inorganic hybrid

- 
- coatings containing polyhedral oligomeric silsesquioxane blocks, *Macromole. Mater. Eng.*, 293 (2008)700-707
228. Z. Li, J. Kong, F. Wang, C. He, Polyhedral oligomeric silsesquioxanes (POSSs): an important building block for organic optoelectronic materials, *J. Mater. Chem. C.*, 5 (2017) 5283-5298
229. K. Pu, Q. Fan, L. Wang, W. Huang, Advances in POSS-containing polymers, *Prog.Chem.*, 18(5) (2006) 609-615
230. E. L. Heeley, D. J. Hughes, Y.E. Aziz, I. Williamson, P. G. Taylor, A. R. Bassindale, Properties and self-assembled packing morphology of long alkyl-chained substituted polyhedral oligomeric silsesquioxanes (POSS) cages, *Phys. Chem.Chem. Phys.*, 15 (2013) 5518-5529
231. J. Wu, P. T. Mather, POSS polymers: physical properties and biomaterials applications, *Polym.Rev.*, 49 (2009)25-63
232. K. Imai, Y. Kaneko, Preparation of ammonium-functionalized polyhedral oligomeric silsesquioxanes with high proportions of cage-like decamer and their facile separation, *Inorg. Chem.*, 56 (7) (2017) 4133-4140
233. X. You, T. Ma, Y. Su, H. Wu, M. Wu, H. Cai, G. Sun, Z. Jiang, Enhancing the permeation flux and antifouling performance of polyamide nanofiltration membrane by incorporation of PEG-POSS nanoparticles, *J. Mem. Sci.*, 540 (2017) 454-463
234. E. Ayandele, B. Sarkar, P. Alexandridis, Polyhedral oligomeric silsesquioxane (POSS)-containing polymer nanocomposites, *Nanomaterials* 2 (2012)445-475.
235. W. Zhang, X. Li, X. Guo, R. Yang, Mechanical and thermal properties and flame retardancy of phosphorus-containing polyhedral oligomeric silsesquioxane (DOPO-POSS)/polycarbonate composites, *Poly. Degrad.Stab.*, 95(12) (2010)2541-2546
236. H. Zhou, Q. Yea, J. Xu, Polyhedral oligomeric silsesquioxane-based hybrid materials and their applications, *Mater. Chem. Front.*, 1(2017) 212-230
237. S.W. Kuo, F.C. Chang, POSS related polymer nanocomposites, *Prog.Polym.Sci.*, 36 (2011) 1649-1696

- 
238. K. Pielichowski, J. Njuguna, B. Janowski, J. Pielichowski, Polyhedral oligomeric silsesquioxanes (POSS)-containing nanohybrid polymers, *Supramole. Polym. Polymer. Beta. Oligo.*, ISBN:978-3-540-31924-5 (2006) 225-296
239. J. H. Moon, A. R. Katha, S. Pandian, S. M. Kolake, S. Han, Polyamide–POSS hybrid membranes for sea water desalination: Effect of POSS inclusion on membrane properties, *J. Mem. Sci.*, 461 (2014) 89–95
240. A. Fina, O. Monticelli, G. Camino, POSS-based hybrids by melt/reactive blending, *J. Mater. Chem.*, 20(2010) 9297-9305
241. Z. Li, J. Kong, F. Wang, C. He, Polyhedral oligomeric silsesquioxanes (POSSs): an important building block for organic optoelectronic materials, *J. Mater. Chem. C.*, 5 (2017) 5283-5298
242. F. Wang, X. Lu, C. He, Some Recent Developments of Polyhedral Oligomeric Silsesquioxane (POSS)-Based Polymeric Materials, *J. Mater. Chem.*, 21(2011) 2775-2782
243. Q. Ye, H. Zhou, Dr. J. Xu, Cubic Polyhedral oligomeric silsesquioxane based functional materials: synthesis, assembly, and applications, 11(2016)1322–1337
244. K. J. Shea, D. A. Loy, Bridged polysilsesquioxanes. Molecular-engineered hybrid organic-inorganic materials, *Chem. Mater.*, 13(2001)3306-3319
245. P.T. Knight, K.M Lee, H.Qin, P.T. Mather, Biodegradable thermoplastic polyurethanes incorporating polyhedral oligosilsesquioxane, *Biomacromolecules* 9 (9) (2008) 2458–2467
246. X. Wang, Q. Ye, J. Song, C. Mui Cho, C. He, J. Xu, Fluorinated polyhedral oligomeric silsesquioxane, *RSC Adv.*, 5 (2015)4547-4553
247. V. K. Daga, E. R. Anderson, S. P. Gido, J. J. Watkins, Hydrogen bond assisted assembly of well-ordered polyhedral oligomeric silsesquioxane block copolymer composites, *Macromolecules* 44 (17) (2011)6793–6799
248. H. W. Milliman, D. Boris, D. A. Schiraldi, Experimental determination of hansen solubility parameters for select POSS and polymer compounds as a guide to POSS–polymer interaction potentials, *Macromolecules* 45 (4) (2012) 1931–1936

249. T. Tokunaga, S. Koge, T. Mizumo, J. Ohshita, Y. Kaneko, Facile preparation of a soluble polymer containing polyhedral oligomeric silsesquioxane units in its main chain, *Polym. Chem.*, 6(2015) 3039-3045
250. S. Kanehashi, Y. Tomita, K. Obokata, T. Kidesaki, S. Sato, T. Miyakoshi, K. Nagai, Effect of substituted groups on characterization and water vapor sorption property of polyhedral oligomeric silsesquioxane (POSS)-containing methacryl polymer membranes, *Polymer* 54 (2013) 2315-2323
251. H. S. Liu, S. C. Jeng, Liquid crystal alignment by polyhedral oligomeric silsesquioxane (POSS)-polyimide nanocomposites, *Optical Materials* 35 (2013) 1418-1421
252. D. M. Fox, M. Novy, K. Brown, M. Zammarano, R. H. Harris Jr, M. Murariu, E. D. McCarthy, J. E. Seppala, J. W. Gilman, Flame retarded poly(lactic acid) using POSS-modified cellulose. Effects of intumescent flame retardant formulations on polymer degradation and composite physical properties, *Polym. Degrad. Stab.*, 106 (2014) 54-62
253. F. Wang, X. Lu, C. He, Some recent developments of polyhedral oligomeric silsesquioxane (POSS)-based polymeric materials, *J. Mater. Chem.*, 21 (2011) 2775-2782
254. R. H. Baney, M. Itoh, A. Sakakibara, T. Suzuki, Silsesquioxane, *Chem. Rev.*, 95 (1995) 1409-1430
255. S. Chimjarn, R. Kunthom, P. Chancharone, R. Sodkhomkhum, P. Sangtrirutnugul, V. Ervithayasuporn, Synthesis of aromatic functionalized cage-rearranged silsesquioxanes ( $T_8$ ,  $T_{10}$ , and  $T_{12}$ ) via nucleophilic substitution reactions, *Dalton Trans.*, 44 (2015) 916-919
256. Novel organic-inorganic hybrids based on  $T_8$  and  $T_{10}$  silsesquioxanes: synthesis, cage-rearrangement and properties *RSC Adv.*, 5 (2015) 72340-72351
257. V. Ervithayasuporn, S. Chimjarn, Synthesis and Isolation of Methacrylate- and Acrylate-Functionalized Polyhedral Oligomeric Silsesquioxanes ( $T_8$ ,  $T_{10}$ , and  $T_{12}$ ) and Characterization of the Relationship between Their Chemical Structures and Physical Properties, *Inorgan. Chem.*, 52 (22) (2013) 13108-13112

- 
258. P. D Lickiss, F. Rataboul, fully condensed polyhedral oligosilsesquioxanes (POSS): from synthesis to application. *Advan. Organometallic Chem.*, (2008) 1–116.
259. S. Randriamahefa, C. Lorthioir, P. Guegan, J. Penelle, Synthesis and bulk organization of polymer nanocomposites based on hemi/ditelechelic poly (propylene oxide) end-functionalized with POSS cages, *Polymer* 50 (2009) 3887-3894
260. A. Voigt, Stannasiloxanes with Acyclic, Bicyclic, and Cubic Core Structures: X-ray Crystal Structure of the Bicyclic Compound [RSi(OSnPh<sub>2</sub>O)<sub>3</sub>SiR] (R = (2,6-Me<sub>2</sub>C<sub>6</sub>H<sub>3</sub>)NSiMe<sub>3</sub>), *Organometallics* 15 (1996) 5097
261. J. D. Lichtenhan, J. J Schwab, F. J. Feher, D. Soulivong, Method of functionalizing polycyclic silicones and the compounds so formed, U. S. Patent 5942638, (1999)
262. J. D. Lichtenhan, J. J Schwab, nanostructured™ chemicals: a new era in chemical technology., 32<sup>nd</sup> International SAMPE Technical Conference (2000)
263. G. Li, L. C. Wang, H. Toghiani, T. L. Daulton, K. Koyama, C. U. Pittman, Viscoelastic and mechanical properties of epoxy/multifunctional polyhedral oligomeric silsesquioxane nanocomposites and epoxy/ladder like polyphenylsilsesquioxane blends, *Macromolecules* 34(25) (2001)8686-8693
264. F. J. Feher, R. Torroba, R. Z. Jin, S. Lucke, F. Nguyen, R. Brutchey, K. O. Wyndham, Major advances in the synthesis of POSS monomers, Symposium CC – Hybrid Organic/Inorganic Materials., 628 (2000)CC2.1.1-CC2.1.6
265. W. Zhang, A.H.E Muller, Synthesis of tadpole-shaped POSS-containing hybrid polymers via click chemistry, *Polymer* 51 (2010) 2133.
266. J. H. Choi, C.H. JunG, D. K. Kim, D. H. Suh, Y.C. Nho, P.H. Kang, R. Ganesan, Preparation of polymer/POSS nanocomposites by radiation processing, *Radi.Phys. Chem.*,78 (2009) 517–520
267. K. Pielichowski, J. Njuguna, B. Janowski, J. Pielichowski, Polyhedral oligomeric silsesquioxanes (POSS)-containing nanohybrid polymers, *Adv. Poly.Sci.*, 201 (2006) 225-296



- 
268. B. W. Mason, J. J. Morrison, P. I. Coupar, P. Jaffres, R. E. Morris, Synthesis of aldehyde functionalised polyhedral oligomeric silsesquioxanes, *J. Chem. Soci, Dalton Transact.*, 0(2001)1123
269. H. Mori, Design and synthesis of functional silsesquioxane-based hybrids by hydrolytic condensation of bulky triethoxysilanes, *Internat. J. Polym. Sci.*, 173624 (2012)17
270. Y. Xue, Y. Liu, F. Lu, J. Qu, H. Chen, L. Dai, Functionalization of graphene oxide with polyhedral oligomeric silsesquioxane (POSS) for multifunctional applications, *J. Phys. Chem. Lett.*, 3 (12) (2012) 1607–1612
271. J. Wu, T. S. Haddad, P. T. Mather, Vertex Group Effects in entangled polystyrene-polyhedral oligosilsesquioxane (POSS) copolymers, *Macromolecules* 42 (2009)1142-1152
272. A. Fina, H. C. L. Abbenhuis, D. Tabuani, A. Frache, G. Camino, Polypropylene metal functionalised POSS-nanocomposites: a study by thermogravimetric analysis, *Poly. Degra. Stab.*, 91(5) (2006)1064
273. A. Ullah, S. Ullah, G. S. Khan , S. M. Shah , Z. Hussain, S. Muhammada, M. Siddiq , H. Hussain, Water soluble polyhedral oligomeric silsesquioxane based amphiphilic hybrid polymers: Synthesis, self-assembly and applications, *Europ. Polym. J.*, 75 (2016) 67–92
274. F. A. Sheikh,N. A. M. Barakat,B. S.S. Aryal,M. S. Khil,H. Y. Kim, Self-assembled amphiphilic polyhedral oligosilsesquioxane (POSS) grafted poly(vinyl alcohol) (PVA) nanoparticles, *Mater. Sci. Eng. C.*, 29 (2009) 869-876
275. C. K. Kim,B. S. Kim, F. A. Sheikh, U. S. Lee, M. S. Khil, H. Y. Kim, Amphiphilic poly(vinyl alcohol) hybrids and electrospun nanofibers incorporating polyhedral oligosilsesquioxane, *Macromolecules*40 (14) (2007)4823–4828
276. Q. Zhou, K. P. Pramoda, J. M. Lee, K. Wang, L. S. Loo, Role of interface in dispersion and surface energetics of polymer nanocomposites containing hydrophilic POSS and layered silicates, *J. Collo. Interf. Sci.*, 355 (2011) 222–230
277. X. You, T. Ma, Y. Su, H. Wu, M. Wu, H. Cai, G. Sun, Z. Jiang, Enhancing the permeation flux and antifouling performance of

- 
- polyamide nanofiltration membrane by incorporation of PEG-POSS nanoparticles, *J. Mem. Sci.*, 540 (2017) 454-463
278. H. Ghanbari, A. Mel, A. M. Seifalian, Cardiovascular application of polyhedral oligomeric silsesquioxane nanomaterials: a glimpse into prospective horizons, *Inter. J. Nanomed.*, 6(2011) 775-786
279. J. Engstrand, A. Lopez, H. Engqvist, C. Persson, Polyhedral oligomeric silsesquioxane (POSS)-poly(ethylene glycol) (PEG) hybrids as injectable biomaterials, *Biomed. Mater.*, 7 (2012) 035013
280. H. Ghanbari, B. G. Cousins, A. M. Seifalian, A Nanocage for Nanomedicine: Polyhedral Oligomeric Silsesquioxane (POSS), *Macromol. Rapid Commun.*, 32 (2011) 1032-1046
281. P. Fadaiea, M. Ataib, M. Imanib, A. Karkhaneha, S. Ghasaban, Cyanoacrylate-POSS nanocomposites: Novel adhesives with improved properties for dental applications, *Dent. Mater.*, 29 (2013) 61-69
282. S. K. Kim, S. J. Heo, J. Y. Koak, J. H. Lee, Y. M. Lee, D. J. Chung, J. I. Lee, S. D. Hong, A biocompatibility study of a reinforced acrylic-based hybrid denture composite resin with polyhedral oligomeric silsesquioxane, *J. Oral. Rehabil.*, 34 (2007) 389-395.
283. A. N. Frone, F. X. Perrin, C. Radovici, D. M. Panaitescu, Influence of branched or un-branched alkyl substituents of POSS on morphology, thermal and mechanical properties of polyethylene, *Compos. Part B.*, 50 (2013) 98-106
284. R. Y. Kannan, H. J. Salacinski, M. Odlyha, P. E. Butler, A. M. Seifalian, The degradative resistance of polyhedral oligomeric silsesquioxane nanocore integrated polyurethanes: An invitro study, *Biomaterials* 27(2006) 1971-1979.
285. Q. C. Zou, Q. J. Yan, G. W. Song, S. L. Zhang, L. M. Wu, Detection of DNA using cationic polyhedral oligomeric silsesquioxane nanoparticles as the probe by resonance light scattering technique, *Biosens. Bioelec.*, 22 (2007) 1461-1465
286. C. J. Wohl, M. A. Belcher, S. Ghose, J. W. Connell, Modification of the surface properties of polyimide films using polyhedral oligomeric silsesquioxane deposition and oxygen plasma exposure, *Appl. Surf. Sci.*, 255 (2009) 8135-8144

- 
287. B. Augustine, W. C. Hughes, K. Zimmermann, A. Figueiredo, X. Guo, C. Chusuei, J. Maidment, Plasma surface modification and characterization of POSS-based nanocomposite polymeric thin films, *Langmuir* 23 (2007) 4346-4350
288. W. J. Lin, W. C. Chen, W. C. Wu, Y. H. Niu, A. K. Y. Jen, Synthesis and optoelectronic properties of starlike polyfluorenes with a silsesquioxane core, *Macromolecules* 37 (2004) 2335-2341
289. S. Xiong, J. Ma, X. Lu, A complementary electrochromic device based on polyaniline tethered polyhedral oligomeric silsesquioxane and poly(3,4-ethylenedioxythiophene)/poly(4-styrene sulfonic acid), *Sola. Ener. Mater. Sol. Cell.*, 93 (2009) 2113-2117
290. R. I. Gonzalez, S. J. Tomczak, T. K. Minton, A. L. Brunsvold, G. B. Hoflund, synthesis and atomic oxygen erosion testing of space-survivable POSS (polyhedral oligomeric silsesquioxane) polyimides, In: *Proc. 9th International Symposium on Materials in a Space Environment*, ESA Publications Division, Noordwijk, The Netherlands, ESA-540, (2003) 113-120

# Materials, Methods and Characterisation Techniques

---

---

## *Summary*

*This chapter provides comprehensive information of the materials used and the experimental methods employed for the preparation of membranes. It also covers different characterisation techniques used to analyse the properties of membranes.*

---

## 2.1 Materials

### 2.1.1 Poly (vinyl alcohol) (PVA)

Poly (vinyl alcohol) (PVA) with molecular weight 1,25,000 g/mol, hydrolysis degree 98-100 mol% and polymerisation degree  $\sim 2800$  was purchased from Hi-media Laboratories Pvt. Ltd, India. PVA is an odourless, tasteless, hydrophilic, semicrystalline, biocompatible, nontoxic, ecofriendly synthetic polymer with remarkable hot water solubility, H-bonding capability with different additives and insolubility in majority of organic solvents. The polymer possesses good tensile strength, flexibility, thermal characteristics and gas barrier property.

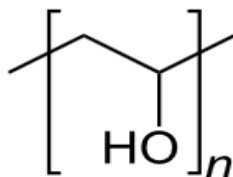


**Figure 2.1:** Structure of PVA

### 2.1.2 Poly (ethylene oxide) (PEO)

Poly (ethylene oxide) (PEO) with molecular weight 1,00,000 was supplied by Alfa Aesar. PEO is a linear polymer, which is an odourless, tasteless and free-flowing white powder that exhibits hot water solubility, biodegradability and nontoxic characteristics. It is also soluble in organic solvents such as toluene, THF, chloroform and dimethyl formamide.

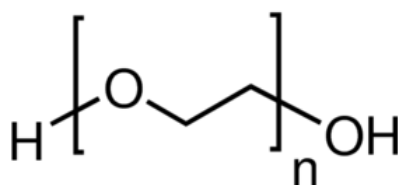


**Figure 2.2:** Structure of PEO

### 2.1.3 Glutaraldehyde (GLA)

Glutaraldehyde (GLA) with molecular weight 100.117g/mol and density 1.06 g/mL is generally used as crosslinking agent for polymers in presence of acid catalyst such as sulphuric acid and acetic acid. It is a pale yellow liquid with pungent rotten apple odour. The boiling point and melting point of GLA are 187 and -14°C respectively.

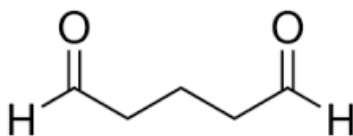


**Figure 2.3:** Structure of GLA

### 2.1.4 Amphiphilic POSS

Polyhedral oligomeric silsesquioxane (POSS) is a cage-shaped hybrid organic-inorganic molecule with the chemical formula  $(\text{RSiO}_{1.5})_n$ , consisting of well-defined rigid siloxane core made up of tetravalent silicon and oxygen, and the peripheral organic groups (R). The overall diameter of POSS molecule is in the range of 1-3 nm, the Si-Si diameter is 0.53nm and the ratio of Si:O is 2:3. The siloxane core of POSS molecule is found to be very rigid and inert due to the strong overlapping of two lone pair electrons on the oxygen with vacant d orbital of Si (Si-O bond energy is  $444 \text{ kJmol}^{-1}$ ).

Recently, water soluble POSS molecules functionalised with polar groups have been synthesised. It has been widely applied in biomedical materials such as in sensors and probes. Poly ethylene glycol-polyhedral oligomeric silsesquioxane (PEG-POSS) and Octatetra methyl ammonium-polyhedral oligomeric silsesquioxane (Octa-TMA-POSS) are two important amphiphilic POSS, which are employed in the present study.<sup>1</sup>

#### 2.1.4.1 Poly ethylene glycol-polyhedral oligomeric silsesquioxane (PEG-POSS)

Poly ethylene glycol functionalised polyhedral oligomeric silsesquioxane (PEG-POSS) material was procured from Hybrid Plastics, Inc, USA.

PEG-POSS is a hybrid molecule with poly ethylene glycol groups attached at the corners of the inorganic silsesquioxane core (**Figure 2.4**). The molecule has the general formulae  $(\text{C}_{2m+3}\text{H}_{4m+7}\text{O}_{m+1})_n(\text{SiO}_{1.5})_n$  where  $n=8,10,12$  and  $m=13.3$ . It is found to be thermally stable upto  $250^\circ\text{C}$ . PEG-POSS is widely employed in biomaterials, lithium batteries, cosmetics, dispersion of carbon particles and oxides.<sup>2-8</sup> Tang and Qiu studied the effect of poly (ethylene glycol)-polyhedral oligomeric silsesquioxane (PEG-POSS) on the

crystallisation characteristics of poly(ethylene succinate) (PES). It was found that PEG-POSS improves the crystallisation behaviour of PES through its plasticizing action. The basic crystal structure of PES remained unchanged even in the presence of POSS.<sup>9</sup>

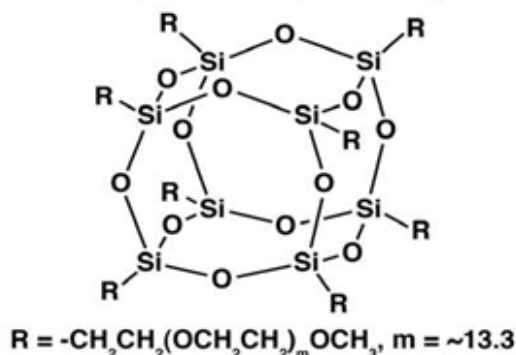


**Figure 2.4:** Structure of PEG-POSS

#### 2.1.4.2 Octa tetra methyl ammonium- polyhedral oligomeric silsesquioxane (Octa- TMA-POSS)

Cage structured anionic-octa(tetramethylammonium)-polyhedral oligomeric silsesquioxane (Octa-TMA-POSS) was procured from Hybrid Plastics, Inc, USA.

In Octa-TMA-POSS, the centre inorganic silsesquioxane core corners are functionalised with anionic oxygen and tetra methyl ammonium ion (**Figure 2.5**). It is widely employed as glassification aid, for luminescence of quantum dots and as dispersion agent for metal oxides and nanocarbon. Based on the molecular weight and structure, it is found that Octa-TMA-POSS is composed of 52 wt% octa(tetramethylammonium).<sup>10-12</sup>

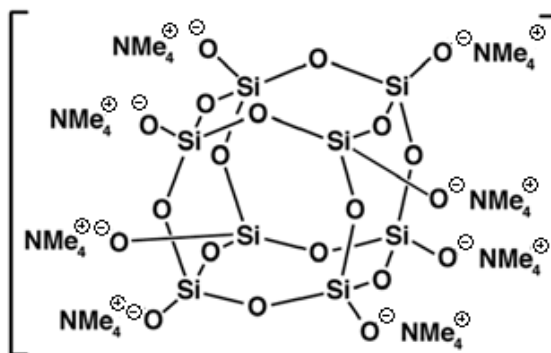


**Figure 2.5:** Structure of Octa-TMA-POSS

### 2.1.5 Cetyltrimethylammonium bromide ( $C_{16}H_{33}N(CH_3)_3Br$ , CTAB)

Cetyltrimethylammonium bromide (CTAB( $C_{16}H_{33}N(CH_3)_3Br$ , CTAB) a quaternary ammonium cationic surfactant with molecular weight 364.45g/mol was purchased from Sigma Aldrich.

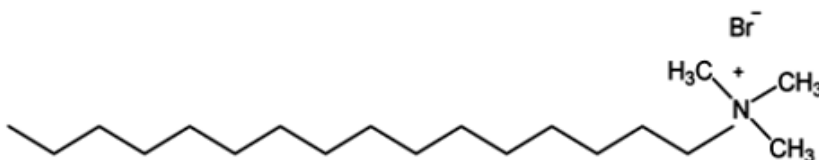


**Figure 2.6:** Structure of CTAB

### 2.1.6 Carboxy methyl cellulose sodium salt (CMC)

Sodium Salt of carboxy methyl cellulose was procured from Merck, Germany. CMC is soluble in water. CMC is widely used as a stabiliser for emulsions and chemical dispersants. About 1% of CMC solution in water has 1500-3000 centipoise (cps) viscosity at 25°C.



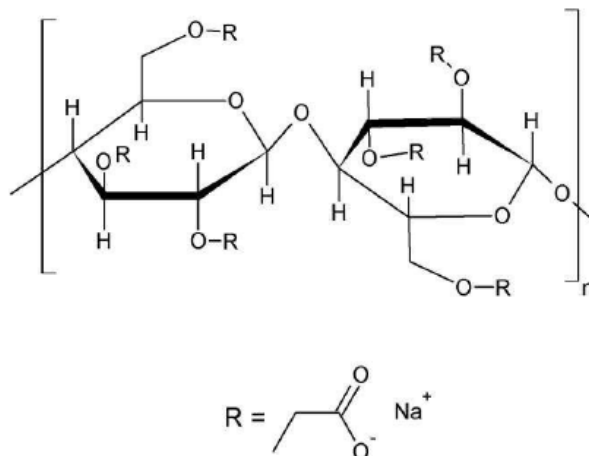


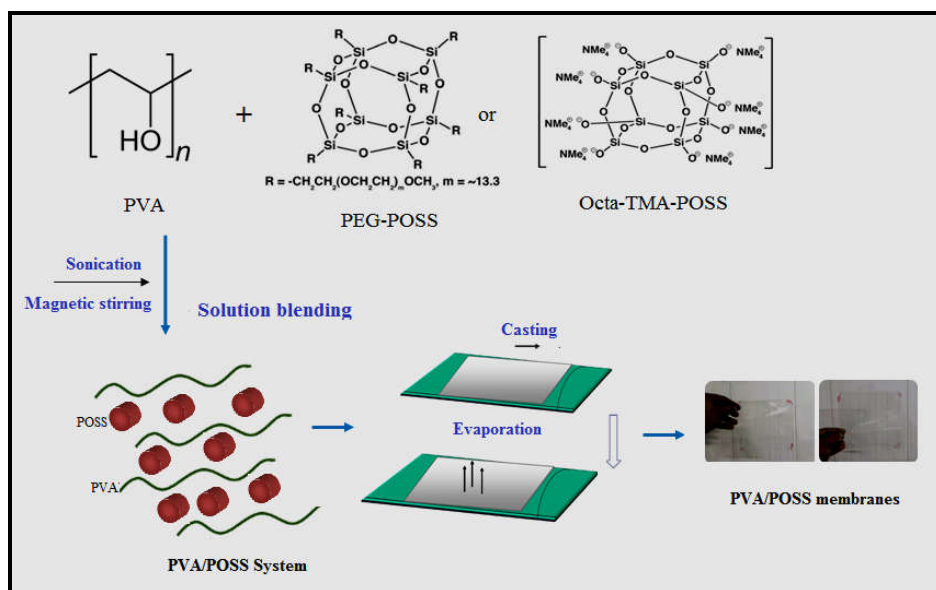
**Figure 2.7:** Carboxy methyl cellulose sodium salt

## 2.2 Methods

### 2.2.1 Preparation of poly(vinyl alcohol) (PVA)-polyhedral oligomeric silsesquioxane (POSS) membranes

Solution blending method was employed to prepare PVA/POSS membranes (**Scheme 2.1**). PVA/POSS hybrid membranes with different weight percentage of filler loadings (0, 1, 3 & 5 wt% POSS) were prepared with respect to the weight % of PVA. 0.1g of POSS was uniformly dispersed in 10 ml of deionized water using probe sonicator for 15 minutes and 10 g of PVA was kept under stirring in deionized water at 75°C for 3 hrs. POSS dispersion was added to the PVA with constant stirring for 2 hrs followed by sonication for 15 minutes to obtain homogeneous solution. Membranes were prepared by casting on a glass plate at ambient temperature. Then the membranes were dried at 40°C for 48 hrs in an air oven and 24 hrs in vacuum oven. After drying, the samples were kept in a desiccator. The samples were coded as P0, PPP1, PPP3, PPP5, POTP1, POTP3 and POTP5, where P stands for poly(vinyl alcohol), PP for PEG-POSS and OTP for Octa-TMA-POSS, the

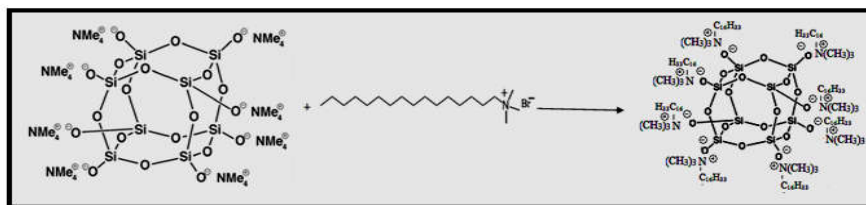
numbers 1, 3 and 5 indicate the weight percentage of POSS and P0 stands for neat PVA.



**Scheme 2.1:** Schematic diagram for the preparation of PVA/POSS membrane

### 2.2.2 Modification of Octa-TMA-POSS using cetyltrimethylammonium bromide ( $C_{16}H_{33}N(CH_3)_3Br$ , CTAB)

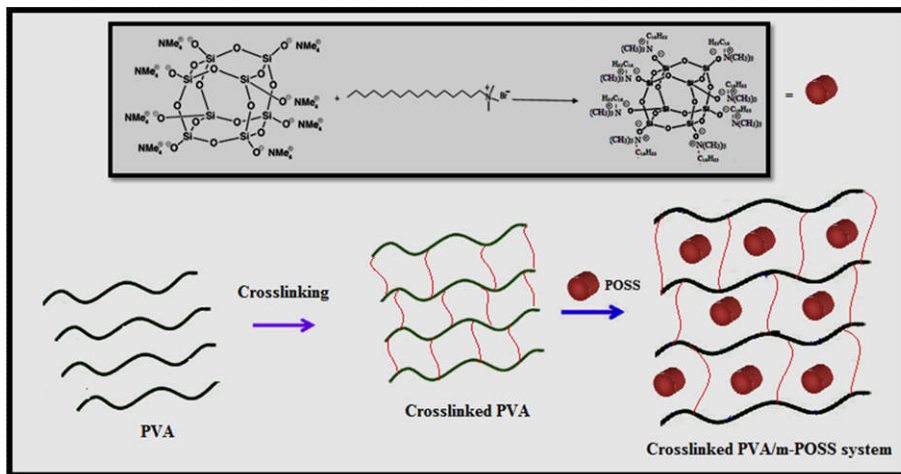
Octa-TMA-POSS is modified with CTAB (m-POSS) by adopting the method reported in the literature.<sup>10</sup> It is presented in **Scheme 2.2**. 982 mg (2.7 mmol) of CTAB was dissolved in 35ml of deionised water and 3.994g (1.8mmol) of Octa-TMA-POSS was dissolved in 170 ml deionized water at room temperature. CTAB solution was added dropwise into the Octa-TMA-POSS at room temperature using magnetic stirring. The initial fresh precipitate was isolated by filtration and washed many times with hot water. The reaction continued for 2 h at a temperature of 50°C with the remaining CTAB solution which was added dropwise. The resulting precipitate was separated by a centrifugation, washed with abundant hot water and dried under vacuum (500 Pa, 50°C).



**Scheme 2.2:** Preparation of m-POSS

### 2.2.3 Fabrication of crosslinked PVA/m-POSS Membranes

PVA/m-POSS membranes with different weight percentages of POSS (0, 1, 3 & 5 wt%) were fabricated by solution blending method. The CTAB modified POSS (m-POSS) was ultrasonically dispersed in deionized (DI) water for 25 min. PVA was dissolved in DI water by subjecting continuous magnetic stirring for 3 hrs at 75°C. The m-POSS dispersion was slowly transferred into PVA solution with constant magnetic stirring for 4 h followed by sonication for 15 min. The resultant solution was cooled down to room temperature and crosslinked using 5 vol% glutaraldehyde (GLA) and 1 vol% HCl by adding slowly. It was further stirred for 1 h. Membranes were fabricated by casting the solution on a glass plate at room temperature and then dried in an air oven at 40°C for 48 hrs and further kept in an vacuum oven for 24 hrs. The membranes were coded as P0, PG, POCPG1, POCPG3 and POCPG5 where P stands for PVA, OCP for CTAB modified Octa-TMA-POSS and G for glutaraldehyde. The numbers 1, 3 and 5 represents the weight percentages of m-POSS. P0 and PG indicate pristine PVA and crosslinked PVA respectively (**Scheme 2.3**). Glutaraldehyde crosslinked PEG-POSS and Octa-TMA-POSS incorporated PVA membranes were coded as PGP and PGO respectively.

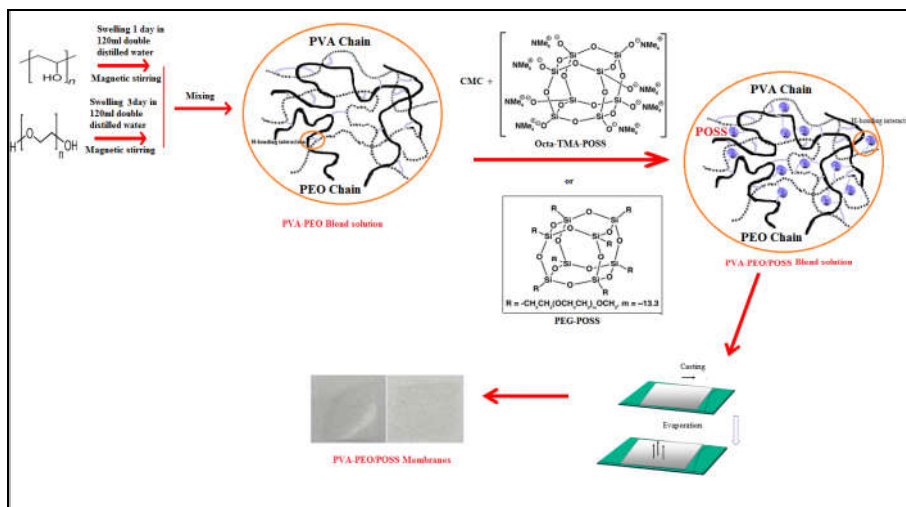


**Scheme 2.3:** Fabrication of crosslinked PVA/m-POSS membranes

#### 2.2.4 Fabrication of PVA-PEO/POSS membranes

In order to fabricate PVA-PEO/POSS membrane through solution blending method, 9g of PVA and 1g of PEO kept separately in double distilled (DD) water (120ml) for 1 and 3 days respectively for swelling. A homogeneous solution of PVA and PEO were prepared by magnetic stirring at 75°C and 40°C separately for 3 hrs. PEO and 4% CMC solution were transferred slowly to PVA solution kept at 60°C with constant stirring for 13 hrs. POSS (3wt%, with respect to PVA-PEO) was ultrasonically dispersed in DD water for 20 min and added dropwise to the solution and stirred for 24 hrs at 60°C. Membranes were fabricated by pouring the solution on a glass plate at room temperature, and then allowed to dry in an air oven at 40°C for four days and finally dried under vacuum for 24 hrs. The samples were coded as P0, PPCPP3 and PPCOP3, where P0 represents pristine PVA, PP for PVA-PEO blend, C stands for carboxy methyl cellulose, PP3 and OP3 stands for 3wt% PEG-POSS and Octa-TMA-POSS respectively. PVA-PEO blend membranes without POSS molecules were found to be less stable. The system exhibited good film forming property at 3wt% POSS loading. However, in the presence of POSS molecules PVA-PEO membranes shows excellent properties, which

indicates strong interfacial interactions between PEO and PVA as presented in **Scheme 2.4**.



**Scheme 2.4:** Preparation of PVA-PEO/POSS membranes

## 2.3 Characterisation

### 2.3.1 Spectroscopic Analysis

#### 2.3.1.1 Fourier transform infrared (FTIR) spectroscopy

FT-IR is a powerful technique for the qualitative identification of substances or functional groups such as C-H, O-H, N-H, C=O etc present in the sample. Transmission and ATR are the major mode of analysis for FT-IR.

In the present work, fourier transform infrared (FTIR) study was carried out using Nicolet iS5 (Thermo Fisher Scientific) spectrometer with a spectral range from 4000–400 cm<sup>-1</sup> and a resolution of 4cm<sup>-1</sup>. FTIR spectra of CTAB, Octa-TMA-POSS and m-POSS particles were taken in transmission mode whereas PVA/POSS and PVA-PEO/POSS membranes were carried out in attenuated total reflection (ATR) mode.

H- Bonding interaction between PVA and nanoparticles are obtained from the FT-IR measurements. Khoonsap *et al.* prepared a nanocomposite of PVA by introducing poly(2-hydroxyethyl methacrylate)-grafted silica nanospheres (PHEMA grafted SNSs). The peak characteristic of PVA at  $3300\text{cm}^{-1}$  get shifted to lower wavenumber by the introduction of PHEMA grafted SNSs in PVA matrix suggesting H-bonding between PVA and PHEMA grafted SNSs.<sup>13</sup> Huang *et al.* found that the OH stretching peak of PVA at  $3302\text{cm}^{-1}$  get broadened and shifted to lower wave number by the incorporation of graphene oxide nanosheet (GONS), indicating H-bonding interaction between PVA and GONS.<sup>14</sup>

### 2.3.1.2 <sup>1</sup>H NMR spectroscopy

<sup>1</sup>H NMR measurement of m-POSS particle was recorded on a Bruker Avance III, 400 MH FT NMR spectrometer operated at 400MHz using tetramethylsilane (TMS) as a reference. The m-POSS particle was dissolved in D-chloroform ( $\text{CDCl}_3$ ).

### 2.3.1.3 Positron annihilation lifetime spectroscopy (PALS)

Positron annihilation lifetime spectroscopy (PALS) is the most acceptable technique to probe free volume parameters such as size, size distribution and concentration of fractional free volume present in the polymer membrane by measuring the lifetime of positrons implanted into the few tenths of mm interior of polymer. They either annihilated directly as free positron or migrate to cavities (free volume space) in the polymer where they interact with electrons in polymer and form hydrogen-like positronium (Ps) particle. Ps can be formed two possible spin states: para-positronium (p-Ps having positron-electron antiparallel spin) and ortho-positronium (o-Ps having parallel spin) with 1:3 is the formation rate. So the materials generally give

three life time components ( $\tau_1$ ,  $\tau_2$  and  $\tau_3$ ). The fourth component ( $\tau_4$ ) also achieved in certain polymers. The first component ( $\tau_1$ ) is an admixture of annihilation of p-Ps lifetime (125 ps) and the annihilation of positron life time. The second component is characteristic for the annihilation of free positrons ( $\tau_2 \approx 4$  ps) entrapped in polymer holes. o-Ps component entrapped in a free volume cavity exhibit longest pick-off annihilation lifetimes  $\tau_3$  (o-Ps  $\approx 142$  ns). In some membranes o-Ps have longer life time  $\tau_3$  and  $\tau_4$  are present due to the presence of both smaller and larger sized free volume defects.  $\tau_3$  and  $\tau_4$  are proportional to the size of free volume cavity in the membrane and the intensities  $I_3$  and  $I_4$  are corresponding to the concentration of free void with radius  $R_3$  and  $R_4$  in the membrane respectively. Tao and Eldrup designed a model correlated Ps (quantum particle) lifetime  $\tau_3$  with radius of free volume  $R_3$  using simple quantum mechanical model (equation (2.1)).<sup>15-16</sup> Assumed that Ps resides in a spherical potential well (free volume cavities) of radius  $R$  with infinite depth. The Ps interacts with electrons in a thin layer  $\Delta R$  at the spherical wall

$$\tau_3 = 0.5ns \left[ 1 - \frac{R_3}{R_0} + \frac{1}{2\pi} \text{Sin} \left( \frac{2\pi r_3}{r_0} \right) \right]^{-1} \quad (2.1)$$

where  $R_0$  is  $R_3 + \Delta R$ .  $\Delta r$  is derived to be  $1.66 \text{ \AA}$ . Fractional free volume  $f_v$  present in the membrane could be calculated by,

$$f_v = \frac{4\pi}{3} R_3^3 I_3 \quad (2.2)$$

PALS has been performed in EG&G ORTEC fast-slow coincidence spectrometer under high vacuum condition, with quartz window as detector which is shaped conically to achieve improved resolution. All samples were cut to the dimensions of  $1.0 \times 1.0$  cm area pieces with 1.0 mm thickness for

the test and  $^{22}\text{Na}$  positron source stacked in between the samples, to make sure that the Ps is annihilated in the membrane. The spectra were measured using a finite-term lifetime analysis method with PATFIT program and by a continuous lifetime distribution with the MELT program.

Choudalakis and Gotsis widely reviewed free volume and transport properties of polymer nanocomposites. The presence of nanoparticle in the polymer greatly influences the diffusion of molecule across the polymer because of the tortuosity of the diffusion path and changes in the free volume. In clay incorporated polymer systems tortuosity effect is the dominating factor, while in spherical particle incorporated polymers free volume properties are the controlling factor for the diffusion of molecules.<sup>17</sup>

### **2.3.2 Microscopic analysis**

Morphology as well as distribution of nanoparticle on the polymer matrix can be analysed through microscopic studies such as scanning electron microscopy (SEM), transmission electron microscopy (TEM) and atomic force microscopy (AFM). These imaging techniques can provide information about composition, agglomeration and phase separation of nanoscale additives in the polymer matrix.

#### **2.3.2.1 Transmission electron microscopy (TEM)**

TEM is a very powerful technique to produce highly magnified and more detailed image of samples and can be used to measure nanoparticle size, crystallite size and to detect internal composition of samples. Zhang *et al.* synthesised amphiphilic aminoisobutyl-POSS incorporated poly(acrylic acid) (PAA) hybrid by RAFT polymerization of *tert*-butyl acrylate. From the TEM image they found the self assembling behaviour of POSS embedded PAA in water.<sup>18</sup>



The distribution of POSS particles in the PVA matrix was analysed through transmission electron microscopy (TEM) using JEOL-JEM 2100, Japan, and operated at 200 kV. The ultra-microtome (Leica, Ultracut UCT) employed to cryocutting of specimens into ultrathin sections and sited on a 300 mesh Cu grids at room temperature.

### **2.3.2.2 Scanning electron microscopy (SEM)**

SEM is another technique used to study the surface morphology of materials. SEM image of cryogenically fractured surface of PVA/POSS, PVA/m-POSS and PVA-PEO/POSS membranes were examined using scanning electron microscope (SEM), SU6600 (Hitachi, Japan) device. The specimens were fractured in liquid nitrogen and coated with gold before examination. Morphology of all tensile fractured specimens were observed using JEOL Model JSM-6390 LV.

SEM image of all tensile fractured samples at hydrated state were taken under the Tescan Vega 3 SBH at 1-30 KV. The samples were coated with Quorum SC7620 (Au-Pd) by sputtering to avoid charging.

### **2.3.2.3 Atomic force microscopy (AFM)**

Atomic force microscopy (AFM) is another powerful high-resolution imaging technique for understanding the morphology of composite membranes from the micron to atomic scale. It provides 1000 times better resolution than an optical diffraction limit.

The morphology analyses of the PVA/POSS, PVA/m-POSS and PVA-PEO/POSS membranes were performed in the tapping mode Alpha 300RA atomic force microscope (AFM). Height, phase and 3D images of membranes were taken at 25°C under ambient air condition with a silicon nitride

cantilever at 256 X 256 pixels resolution. Phase image provides the information about membrane surface structure and height image records surface roughness along with morphological information. The root-mean-square surface roughness ( $R_q$ ) was determined-using the equation,

$$R_q = R(F \sum(Z_i - Z_{ave}), N) \quad (2.3)$$

$R_q$  investigate the value of standard deviation of height ( $Z$ ) in the given area of the membrane.  $N$ ,  $Z_i$  and  $Z_{ave}$  corresponds to number of points in the given area, current and average  $Z$  values respectively within the given area of the membrane.

### 2.3.3 X-ray diffraction (XRD)

XRD is a widely used characterisation technique in materials science. It is a key tool to characterise structural information of material such as phase transitions, crystallinity, interatomic distances, bond angles and size. An X-ray beam falls over the crystal, atoms in the crystal scatters the X-rays by constructive interference and produce a diffraction pattern that is characteristic to its structure or the arrangement of atoms in the crystal. Diffractogram of the material is plotted by taking  $2\theta$  (angle of diffraction) against intensity. The correlation between angle of incidence of the beam, the spacing between the crystal lattice planes of atoms and incident X-rays wavelength are shown by Bragg's law.

$$n\lambda = 2d \sin \theta \quad (2.4)$$

Crystallinity is an important factor that affects the mass transport performance of polymer membranes due to the highly impermeable nature of the crystalline phase of the polymers. Amorphous polymer membranes exhibit good transport performance due to the presence of free volume

available for diffusion. Semicrystalline polymers have lesser free volume than the amorphous polymer hence the transport occurring in such membranes are around the crystallites in a tortuous path.

X-ray diffraction (XRD) experiments were performed on X'pert diffractometer, Philips using Ni- filtered Cu-K $\alpha$  radiation with  $\lambda=0.154$  nm and operated at 40 keV and 30 mA. The samples were scanned in step mode by 1.5 $^\circ$ /min scan rate in the range of  $2\theta < 12^\circ$ . The specimens of 1x1cm dimension were used for the analysis.

### **2.3.4 Water contact angle ( $\theta$ ) measurement**

Water contact angle measurements were conducted on membrane surface at 27 $^\circ$ C using Tanteq machine, model CAM-Micro. Using the micro syringe 5  $\mu$ l volume is kept up in the sessile drop and the contact angle was determined within 50–60 s of the addition of the water drop on the membrane surface. The measurements were repeated using the five samples of the same membrane and the images were saved as snap shots.

Wettability of membrane surface is an important parameter in material and surface science. It ascribes the extent of liquid spread on a solid surface and is analysed using water contact angle ( $\theta$ , it is the angle between the solid and liquid surface) measurements. Depending on the nature of the surface such as geometrical structure and surface chemistry, the contact angle,  $\theta$  changes significantly. If  $\theta \ll 90^\circ$ , indicates higher affinity of membrane towards water or fast spreading of water (hydrophilic surface). Those membranes with  $\theta \gg 90^\circ$  indicates hydrophobic surface.<sup>19</sup>

The contact angle study is very important to examine all solid–liquid interfacial phenomena. Fundamental wetting features are work of adhesion ( $W_A$ ), surface free energy ( $\gamma_s$ ) and interfacial free energy ( $\gamma_{sl}$ )

(1)  $W_A$  calculated as follows,

$$W_A = (1 + \cos \theta) \gamma_l \quad (2.5)$$

where  $\gamma_l$  is the surface tension of the liquid used for the contact angle measurement.

(2) Owens–Wendt theory is employed to calculate  $\gamma_s$  and is given below,

$$\gamma_s = \gamma_s^d + \gamma_s^p \quad (2.6)$$

(3) The following Dupres equation applied to calculate  $\gamma_{sl}$

$$\gamma_{sl} = \gamma_s + \gamma_l - W_A \quad (2.7)$$

Contact angle between liquid drop and solid surface can be illustrated using the Young's equation shown below

$$\gamma_{sg} = \gamma_{sl} + \gamma_{lg} \cos \theta_Y \quad (2.8)$$

Where  $\theta_Y$  is the Young's contact angle,  $s$ ,  $l$  and  $g$  represents solid, liquid and gas respectively.  $\gamma_{sg}$ ,  $\gamma_{sl}$ ,  $\gamma_{lg}$  correspond to the interfacial surface tensions.

Relation between contact angle of a solid surface with surface roughness for homogeneous and heterogeneous surfaces can be explained by Wenzel and Cassie–Baxter models respectively.

Wenzel equation is,

$$\cos\theta_w = r \cos\theta_Y \quad (2.9)$$

Cassie-Baxter equation is given below,

$$\cos\theta_c = f \cos\theta + f - 1 \quad (2.10)$$

In Wenzel equation,  $r$  is the surface roughness factor and  $\theta_w$  the apparent contact angle. Based on this model, increased surface roughness leads to the increase in the wetting characteristic of the membrane.

In Cassie-Baxter equation,  $f$  is the fractional area of solid in contact with liquid drop having contact angle of  $\theta$ .  $\theta_c$  is the contact angle in the Cassie-Baxter model. If  $f$  increases surface roughness also increases.

### 2.3.5 Differential scanning calorimetry (DSC)

Differential scanning calorimetric (DSC) studies of PVA/POSS membranes were performed using DSC 8500-Perkin Elmer, Waltham, Massachusetts, U.S., calorimeter at a scan rate of 10°C/min during the temperature range of 30-240°C under N<sub>2</sub> atmosphere.

DSC analysis of PVA/m-POSS and PVA-PEO/POSS membranes were conducted using DSC-Q1000, Universal V4.2E TA instruments under nitrogen gas flow in the temperature range of 0 to 250°C at a heating rate of 10°C/ min. The first cooling and second heating curves were identified and analysed in a nitrogen atmosphere to find out the crystalline behaviour of the composites. The degree of crystallinity ( $X_c$ ) of all membranes were determined using the equation,

$$X_c = \left( \frac{\Delta H_f}{\Delta H_f^o} \right) \times 100 \quad (2.11)$$

Where  $\Delta H_f$  is the measured enthalpy of fusion and  $\Delta H_f^0$  is the theoretical value for enthalpy of fusion of the 100 % crystalline PVA.  $\Delta H_f^0$  of PVA is 138.6 J/g.<sup>20</sup>

### 2.3.6 Water uptake study

Dry membranes with thickness 0.5mm were cut into circular shapes with 1.3 cm diameter and weighed ( $W_{dry}$ ). It was then dipped into a diffusion bottle containing distilled water at room temperature. The membranes were drawn out periodically and wiped with a filter paper and weighed ( $W_{wet}$ ) in an electronic balance. The weights were noted periodically. The average values were obtained with 4 pieces of membranes. The water absorption capacity (WAC %) were calculated using the equation below.

$$\text{Water uptake (\%)} = \frac{W_{wet} - W_{dry}}{W_{dry}} \times 100 \quad (2.12)$$

### 2.3.7 Swelling study

Dry membranes with a known weight ( $W_0$ ) were immersed in azeotropic THF-water (for PVA/POSS and PVA-PEO/POSS membranes) and isopropanol (IPA)-water mixture (for PVA/m-POSS membranes) for 3 days at room temperature to allow them to reach their equilibrium swelling. The swollen membranes ( $W_1$ ) were wiped with a filter paper and weighed ( $W_1$ ). The degree of swelling (DS) was calculated using the equation below.

$$DS(\%) = \frac{W_1 - W_0}{W_0} \times 100 \quad (2.13)$$

### 2.3.8 Mechanical properties

Mechanical properties of polymer composites are highly influenced by the structure and properties of interphase between matrix and filler because the

stress transfer between nanofillers and the polymer matrix is controlled by the interphase between them. The addition and fine dispersion of fillers in polymer matrix is found to be an effective method to enhance the polymer properties.<sup>21-22</sup> The interfacial interaction between polymer matrix and filler is the key factor in controlling the stress transfer from host matrix to reinforcing agents. The tensile properties of all fabricated membranes were performed using INSTRON-3365 at room temperature with tensile force of 5 kN and crosshead speed of 50 mm/ min. Rectangular samples with 10 X 1 cm dimension and 0.5mm thickness were used for the analysis. In order to demonstrate reproducibility, five samples of each membrane were analysed. The mechanical strength of the samples in wet condition were also analysed with INSTRON-3365 at 50 mm/min crosshead speed. All specimens of each sample were kept in water containing dessicator for two weeks prior to the tensile test at ambient temperature.

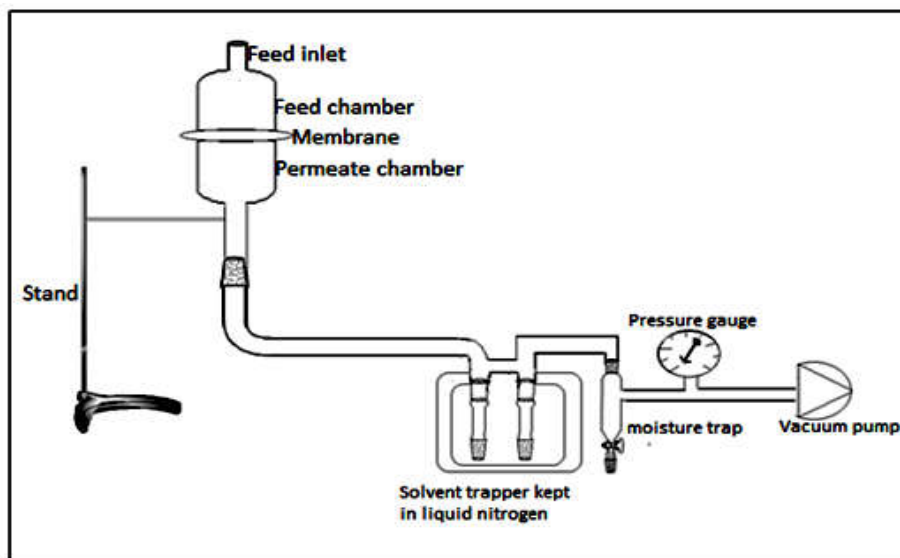
### **2.3.9 Dynamic mechanical analysis (DMA)**

Dynamic mechanical analysis is used to measure the viscoelastic properties of the material by the application of oscillatory deformation as a function of temperature. Dynamic mechanical analysis (DMA) of PVA/POSS membranes were performed using Metravib instrument under tensile mode at a fixed frequency of 1 Hz and in a temperature range from 25 to 150°C at a heating rate of 3°C min<sup>-1</sup>. Storage modulus (E'), loss modulus (E'') and damping behaviour of PVA/POSS membranes were computed from the data.

### **2.3.10 Pervaporation studies**

Apparatus used for pervaporation experiments is schematically illustrated in **Scheme 2.5**. For the pervaporation process, mass transfer through the membrane occurs according to the solution diffusion mechanism. The pervaporation separation of azeotropic mixture of THF-water (ie, 94.7 wt% THF and 5.3 wt% water) and IPA-water (ie, 87.5 wt% IPA and 12.5 wt%

water) system were performed using circular membrane with an effective membrane area of  $16.6 \text{ cm}^2$ . The feed mixture at azeotropic composition was poured into the upstream side of the membrane. Concentration gradient between upper and downstream side of the membrane is the basic driving force for separation, which is created by maintaining the pressure on the permeate side at 1 mm of Hg by a vacuum pump. The permeate vapour was collected and condensed in a cold solvent trapper kept in liquid nitrogen. The collected permeate was weighed using a digital microbalance (Mettler Toledo- JB1603-C/FACT) with an accuracy of  $10^{-4} \text{ g}$  to evaluate the flux. Permeates were analysed by gas chromatography (GC) (Agilent GC7894 equipped with a DB624 column with length 30 m and 0.32 mm thickness and a FID detector) as well as Abbe's refractometer to calculate the membrane selectivity. The obtained refractive index value was compared with a standard graph of refractive index versus feed mixture composition curve. The experiment was repeated for all membranes at the same condition until reproducible data were obtained.



**Scheme 2.5:** Schematic illustrations of the pervaporation apparatus



There are number of well known equations in the field of transport studies, which are presented here.

### 2.3.10.1 Flux and separation factor

Separation performance of polymer membranes can be described on the basis of total flux ( $J$ ) and separation factor ( $\alpha$ ) and pervaporation separation index (PSI), that can be calculated from the following equations.<sup>23</sup>

$$J = \frac{Q}{At} \quad (2.14)$$

Here  $J$  is the molar flux ( $\text{Kg}/\text{m}^2\text{h}$ ),  $Q$  is the total mass of the permeate ( $\text{Kg}$ ),  $A$  is the membrane area in contact with feed ( $\text{m}^2$ ) and  $t$  is the permeation time.

The component flux of each component of a liquid mixture (for example: THF-water system) was calculated using equation (2.15). It is the product of the total permeation flux with the weight fraction of each component in the permeate.

$$J_{THF} = J * X_{THF} \quad \text{and} \quad J_{H_2O} = J * X_{H_2O} \quad (2.15)$$

$J_{H_2O}$  and  $J_{THF}$  indicating the component flux of water and THF respectively.  $X_{H_2O}$  and  $X_{THF}$  are the permeate composition of water and THF in THF-water mixture.

The permselectivity of composite membrane is defined by separation factor ( $\alpha$ ):

$$\alpha = \frac{X_w / X_T}{Y_w / Y_T} \quad (2.16)$$

where  $X_w$ ,  $X_T$ ,  $Y_w$  and  $Y_T$  are the weight fraction of water and THF in the permeate and feed respectively.

Enrichment factor ( $\beta$ ) is another parameter to assess membrane separation performance, which can be expressed as

$$\beta = \frac{X_w}{Y_w} \quad (2.17)$$

Generally, pervaporation separation index (PSI) is applied to summarize the overall permeance of the membrane for a selected feed mixture as a product of flux and selectivity.

$$PSI = J(\alpha - 1) \quad (2.18)$$

In the absence of separation, PSI becomes zero.

### 2.3.10.2 Permeance and Selectivity

Recently Baker *et al.*, developed a more accurate and better expression for PV data in terms of permeability or permeance and selectivity instead of flux and separation factor.<sup>24</sup> Membrane permeability ( $P_i$ ) of each component in the feed can get from the expression,

$$P_i = J_i \left( \frac{l}{P_{i0} - P_{il}} \right) \quad (2.19)$$

Where  $J_i$  is the molar flux of the component  $i$  in the feed,  $l$  is the membrane thickness and  $P_{i0}$  and  $P_{il}$  vapour pressure of the component  $i$  over feed and permeate side of the membrane, which is the driving force for the separation.

The membrane permeance ( $P_i/l$ ) is defined as the molar fluxes divided by the difference of partial vapour pressures at the feed and permeate side of the membrane. This is expressed in gas permeation unit (gpu) and one gpu is  $3.349 \times 10^{-10}$  mol per  $m^2 \cdot s \cdot Pa$ .

$$P_i/l = \frac{J_i}{P_{i0} - P_{i1}} \quad (2.20)$$

The membrane water selectivity ( $\alpha_{wt}$ ) is defined as the ratio of permeability coefficients or permeance ( $P_W$ ) of water over the THF ( $P_T$ ) through the membrane.

$$\alpha_{wt} = \frac{P_W}{P_T} \quad (2.21)$$

### 2.3.10.3 Diffusion coefficient measurement

Diffusion coefficient ( $D$ ) is a kinetic parameter, which is greatly influenced by factors such as molecular diameter of the penetrant and segmental mobility of the polymer.  $D$  can be obtained from the following equations.<sup>25-26</sup>

$$\frac{Q_t}{Q_\infty} = 1 - \left( \frac{8}{\pi^2} \right) \sum_{n=0}^{n=\infty} \left[ \frac{1}{(2n+1)^2} \exp \left[ -D(2n+1)^2 \pi^2 t/h^2 \right] \right] \quad (2.22)$$

$$Q_t(\%) = \frac{M_s / MM_s}{M_p} \times 100 \quad (2.23)$$

where  $n$  is an integer and  $h$  is the thickness of the membrane.  $Q_t$  and  $Q_\infty$  refers to the solvent uptake at time 't' and equilibrium mole percentage of solvent uptake of the samples respectively.

$MM_s$ ,  $M_s$  and  $M_p$  are the molar mass of solvent, mass of the solvent absorbed and mass of polymer respectively.

$D$  can be calculated from the initial slope ( $\theta$ ) of the linear portion of  $Q_t$  Vs  $t^{1/2}$  graph

$$\frac{Q_t}{Q_\infty} = \frac{4}{h} \left( \frac{D}{\pi} \right)^{1/2} t^{1/2} \quad (2.24)$$

$$D = \pi \left( \frac{h\theta}{4Q_\infty} \right)^2 \quad (2.25)$$

#### 2.3.10.4 Swelled membranes density measurements

The density of swelled membrane was determined using specific gravity bottle and calculated using the following expression.<sup>27</sup>

$$\rho_w = \frac{W_w}{V_{sp} - \overline{V}_{sp}} \quad (2.26)$$

where  $W_w$  is the weight of swollen membrane,  $V_{sp}$  and  $\overline{V}_{sp}$  are the volume of the bottle and the volume of the filled water in the bottle.

$V_{sp}$  is calculated by:

$$V_{sp} = \frac{W_{sp.w} - W_{sp.d}}{\rho_w} \quad (2.27)$$

Where  $W_{sp.d}$  and  $W_{sp.w}$  are the weight of dry bottle and the bottle filled with distilled water.  $\rho_w$  is the density of water at room temperature.

Each swelled membranes were weighed and immediately transferred into the specific gravity bottle filled with distilled water and its weight ( $W_{sp.m}$ ) was taken. From this,  $\bar{V}_{sp}$  was calculated using the equation (2.28),

$$\bar{V}_{sp} = \frac{W_{sp.m} - W_w - W_{sp.d}}{\rho_w} \quad (2.28)$$

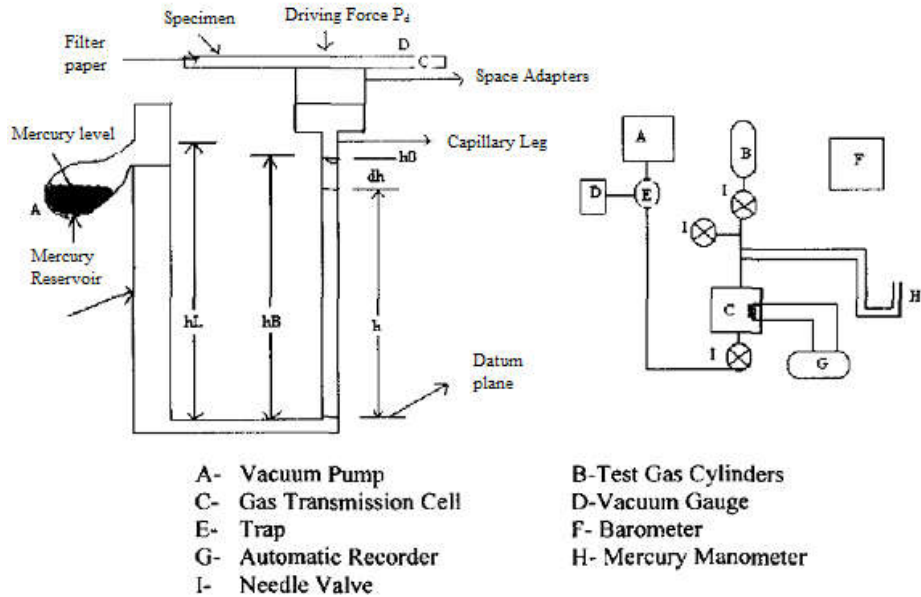
### 2.3.11 Gas permeability analysis

The LYSSY AG L 100–5000 gas permeability tester employed to analyse gas permeability of N<sub>2</sub>, O<sub>2</sub> and CO<sub>2</sub> of membranes in manometric method at room temperature and 1 atm pressure according to ASTM standard D1434. All measurements were repeated three times for all samples. Samples of 9 cm diameter were employed for the analysis. Schematic representation of experimental set up is presented in **Scheme 2.6**.

Permeability ( $P_x$ ) and selectivity ( $\alpha_{x/y}$ ) are the intrinsic gas transport properties of the particular membrane-gas permeate system.  $P_x$  and  $\alpha_{x/y}$  are expressed as ,

$$P_x = \frac{J l}{f_2 - f_1} \quad \text{or}$$

$$P_x = \frac{(\text{quantity of the permeant}) X (\text{thickness of the membrane})}{(\text{pressure drop across the membrane}) X (\text{time}) X (\text{area})} \quad (2.29)$$



**Scheme 2.6:** Set up for gas permeability tester

$$\alpha_{x/y} = \frac{P_x}{P_y} = \frac{S_x}{S_y} X \frac{D_x}{D_y} \quad (2.30)$$

where  $P_x$  and  $P_y$  refers to permeability of polymer towards the gases  $x$  and  $y$ ,  $J$  is the flux of the gas achieved with the membrane.

Permeability is expressed in Barrer ( $1 \text{ Barrer} = 10^{-10} \text{ cm}^3 \text{ (STP) cm cm}^{-2}\text{s}^{-1} \text{ cmHg}^{-1}$ ). Gas Permeance Unit (GPU) is employed instead of Barrer if the thickness of the membrane is not provided ( $1 \text{ GPU} = 10^{-6} \text{ cm}^3 \text{ (STP) cm}^{-1}\text{s}^{-1} \text{ cmHg}^{-1}$ ).

‘P’ can also be expressed in different units such as ‘ $\text{cm}^3 \cdot \text{cm} / \text{cm}^2 \cdot \text{s} \cdot \text{Pa}$ ’, ‘ $\text{cm}^3 \cdot \text{cm} / \text{cm}^2 \cdot \text{s} \cdot \text{cmHg}$ ’ and ‘ $\text{cm}^3 \cdot \text{cm} / \text{m}^2 \cdot \text{day} \cdot \text{atm}$ ’

**2.3.12 Thermo gravimetric analysis (TGA)**

An insight into the thermal stability is important to control the processing conditions of the polymer. Thermal degradation studies of membranes were analysed using Pyris 7 TGA, of M/s Perkin Elmer, California. Samples were scanned from room temperature to 700°C at a heating rate of 10°C/minute under nitrogen atmosphere.

## 2.4 References

1. <http://hybridplastics.com/>
2. E. Markovic, J. Matisons, M. Hussain, G. P Simon, Poly (ethylene glycol) octafunctionalized polyhedral oligomeric silsesquioxane: WAXD and rheological studies, *Macromolecules* 40 (2007) 4530-4534
3. E. Markovic, M. G. Markovic, S. Clarke, J. Matisons, M. Hussain, G. P. Simon, Poly (ethylene glycol)-octafunctionalized polyhedral oligomeric silsesquioxane: synthesis and thermal analysis, *Macromolecules* 40 (2007) 2694-2701
4. S. Randriamahefa, C. Lorthioir, P. Guegan, J. Penelle, Synthesis and bulk organization of polymer nanocomposites based on hemi/ditelechelic poly(propylene oxide) end-functionalized with POSS cages, *Polymer* 50 (2009) 3887-3894
5. Y. Bian, J. Mijovi, Molecular Dynamics of PEGylated Multifunctional Polyhedral Oligomeric Silsesquioxane, *Macromolecules* 42 (2009) 4181-4190
6. J. Wu, Q. Ge, P. T. Mather, PEG-POSS Multiblock Polyurethanes: Synthesis, Characterization, and Hydrogel Formation, *Macromolecules* 43 (2010) 7637-7649
7. P. Maitra, S. L. Wunder, Oligomeric Poly(ethylene oxide)-Functionalized Silsesquioxanes: Interfacial Effects on  $T_g$ ,  $T_m$ , and  $\phi H_m$ , *Chem. Mater.*, 14 (2002) 4494-4497
8. C. H. Jung, I. T. Hwang, C. H. Jung, J. H. Choi, Preparation of flexible PLA/PEG-POSS nanocomposites by melt blending and radiation crosslinking, *Rad. Phys. Chem.*, 102 (2014) 23-28
9. L. Tang, Z. Qiu, Effect of poly (ethylene glycol)-polyhedral oligomeric silsesquioxanes on the crystallization kinetics and morphology of biodegradable poly (ethylene succinate), *Poly. Degra. Stab.*, 134 (2016) 97-104
10. L. Liu, Y. Hu, L. Song, X. Z. Gu, Z. Ni, Fabrication of lamellar nanostructure from cage-like poly-anion silicate and surfactant by template-directed synthesis, *J. Compos. Mater.*, 45 (2011) 307-319



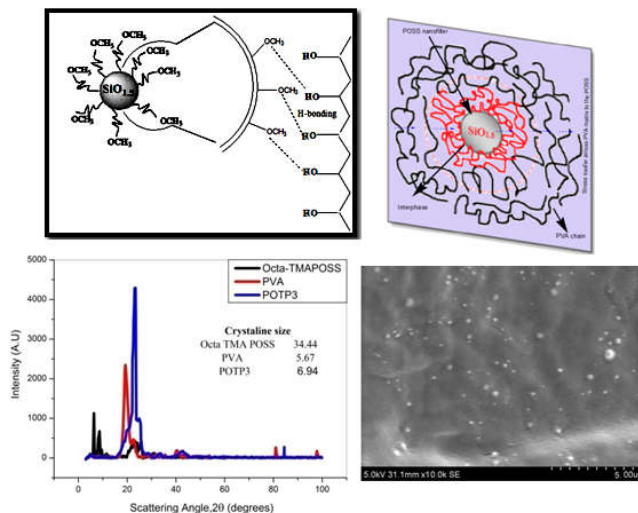
11. S. Manickam, P. Cardiano, P. Mineo, S. L. Schiavo, Star-shaped quaternary alkylammonium polyhedral oligomeric silsesquioxane ionic liquids, *Europ. J. Inorg. Chem.*, 2014 (**2014**) 2704-2710
12. B. L. Frankamp, N. O. Fischer, R. Hong, S. Srivastava, Vincent M. Rotello, Surface modification using cubic silsesquioxane ligands. facile synthesis of water-soluble metal oxide nanoparticles, *Chem. Mater.*, 18 (**2006**) 956-959
13. S. Khoonsap, S. Rugmai, W.S. Hung, K. R. Lee, S. Klinsrisuk, S. Amnuaypanich, Promoting permeability-selectivity anti-trade-off behavior in polyvinyl alcohol (PVA) nanocomposite membranes, *J. Mem. Sci.*, 544 (**2017**) 287-296
14. H. D. Huang, P. G. Ren, J. Chen, W. Q. Zhang, X. Ji, Z. M. Li, High barrier graphene oxide nanosheet/poly(vinyl alcohol) nanocomposite films, *J. Mem. Sci.*, 409– 410 (**2012**) 156-163
15. S. J. Tao, Positronium annihilation in molecular substances (liquids and solids), *J. Chem. Phys.*, 56 (**1972**) 5499-5510
16. M. Eldrup, D. Lightbody, N.J. Sherwood, The temperature dependence of positron lifetimes in solid pivalic acid, *Chem. Phys.*, 63 (**1981**) 51
17. G. Choudalakis, A. D. Gotsis, Free volume and mass transport in polymer nanocomposites, *Curr. Opin. Collo. Interf. Sci.*, 17 (**2012**) 132-140
18. W. Zhang, B. Fang, A. Walther, A. H. E. Muller, Synthesis via RAFT polymerization of tadpole-shaped organic/ inorganic hybrid Poly(acrylic acid) containing polyhedral oligomeric silsesquioxane (POSS) and their self-assembly in water, *Macromolecules* 42 (7) (**2009**) 2563-2569
19. K. Liu, M. Cao, A. Fujishima, L. Jiang, Bio-Inspired Titanium Dioxide Materials with Special Wettability and Their Applications, *Chem. Rev.*, 114 (**2014**) 10044-10094
20. S. S Ray, K. Yamada, M. Okamoto, K. Ueda, Polylactide-layered silicate nanocomposite: a novel biodegradable material, *Nano. Lett.*, 2 (**2002**) 1093-1096
21. M. Fang, K. Wang, H. Lu, Y. Yang, S. Nutt, Covalent polymer functionalization of graphene nanosheets and

- mechanical properties of composites, *J. Mater. Chem.*, 19 (2009) 7098-7105
22. S. Y. Fu, X. Q. Feng, B. Lauke, Y. W. Mai, Effects of particle size, particle/matrix interface adhesion and particle loading on mechanical properties of particulate–polymer composites, *Compos. Part B. Eng.*, 39 (2008) 933-961
23. T. Jose, S. C. George, M. G. Maya, H. J. Maria, R. Wilson, S. Thomas, Effect of bentonite clay on the mechanical, thermal, and pervaporation performance of the poly(vinyl alcohol) nanocomposite membranes. *Ind. Eng. Chem. Res.*, 53 (2014) 16820-16831
24. R. W. Baker, J. G. Wijmans, Y. Huang, Permeability, permance and selectivity: a preferred way of reporting pervaporation performance data. *J. Mem. Sci.*, 348 (2010) 346-352
25. E. Southern, A. G. Thomas, Diffusion of liquids in crosslinked rubbers. Part 1, *Trans. Farad. Soc.*, 63 (1967) 1913.
26. R. Stephen, K. Joseph, Z. Oommen and S. Thomas, Molecular transport of aromatic solvents through microcomposites of natural rubber (NR), carboxylated styrene butadiene rubber (XSBR) and their blends, *Compos. Sci. Technol.*, 67 (2007) 1187-1194.
27. U. K. Ghosh, N. C. Pradhan, B. Adhikari, separation of water and o-chlorophenol by pervaporation using HTPB-based polyurethaneurea membranes and application of modified maxwell-stefan equation, *J. Mem. Sci.*, 272 (2006) 93-102

## Characterisation, Mechanical and Viscoelastic Behaviour of PVA/POSS System

### Summary

Polyhedral oligomeric silsesquioxane (POSS) embedded poly(vinyl alcohol) (PVA) hybrid membrane was successfully fabricated by solution blending method. The membranes were characterised using FTIR, XRD, SEM, TEM, AFM and contact angle measurements. The melting and crystallisation behaviour of PVA/POSS system was studied from differential scanning calorimetric (DSC) analysis. The effect of POSS on the mechanical and dynamic mechanical properties of PVA has been analysed and discussed in detail with respect to the weight percentage of POSS. The relaxation corresponding to the crystal-crystal slippage, characteristic of semicrystalline polymers were observed in storage modulus curves of PVA/POSS system, which is an indication of the crystalline nature of matrix even in the presence of POSS.



This chapter has been published in *Journal of Applied Polymer Science*, Wiley, 2017,134, 45447

### 3.1 Introduction

In recent years, organic-inorganic hybrid materials have received wide research interest because of their outstanding comprehensive property arising from the synergizing effect of both components. Polyhedral oligomeric silsesquioxane (POSS) is a potential hybrid organic-inorganic reinforcing nanofiller. The most significant feature of POSS is its molecular scale equivalence to organically modified particles. The chemical composition of POSS is in between silica ( $\text{SiO}_2$ ) and silicones ( $\text{R}_2\text{SiO}$ ). This versatile filler possesses three-dimensional rigid Si-O frame forming core with the formula  $\text{Si}_8\text{O}_{12}$  (the ratio of Si:O is 2:3) with Si-Si diameter of 0.53 nm surrounded by eight different functionalised organic groups represented by R. Unlike other nanofillers, POSS molecules have perfectly defined chemical structure and good functionalisation flexibility. It is possible to generate large number of different characteristic POSS-based molecules by changing the size and nature of functional side groups on the POSS and that will improve compatibility of POSS with many polymer systems. The rigid POSS molecules incorporated polymers have drawn as a new chemical technology and acquired great attention due to the simplicity in processing and superior performance for polymer systems in terms of viscoelastic behaviour, mechanical properties, rheological properties, flame retardance and thermal behaviour.<sup>1-9</sup>

Poly(vinyl alcohol) (PVA) is a water soluble, non-toxic, biodegradable and biocompatible polymer that has been studied intensively in many research industries for the application in drug-delivery systems and artificial biomedical devices. However, hydrophilic nature and insufficient mechanical properties of PVA seriously limit its wider application.<sup>10-14</sup> In the present study, PVA/POSS membranes were prepared by solution casting method. Two types of POSS were used for the present study, anionic-octa(tetramethylammonium) (Octa-TMA) and poly(ethylene glycol) (PEG)

functionalized POSS. Rahman *et al.* reported the effect of amphiphilic PEG-POSS on the thermal and gas permeation properties of some polymeric systems.<sup>15-16</sup> The present chapter deals with the effect of different functionalised POSS on the mechanical and dynamic mechanical properties of PVA.

## 3.2 Results and discussion

### 3.2.1 Characterisation

FTIR studies are carried out in order to determine the interaction in PVA and PVA/POSS systems. As shown in **Figure 3.1(a)** PVA exhibits a band at  $3260\text{ cm}^{-1}$  characteristic of O–H group. However, with the introduction of PEG-POSS broadening and shifting of the O–H peak of PVA to lower wavenumber is observed due to the weak H-bonding interaction between PVA and PEG-POSS.<sup>17</sup> Schematic representation of expected interactions between PVA and PEG-POSS is presented in **Scheme 3.1**.

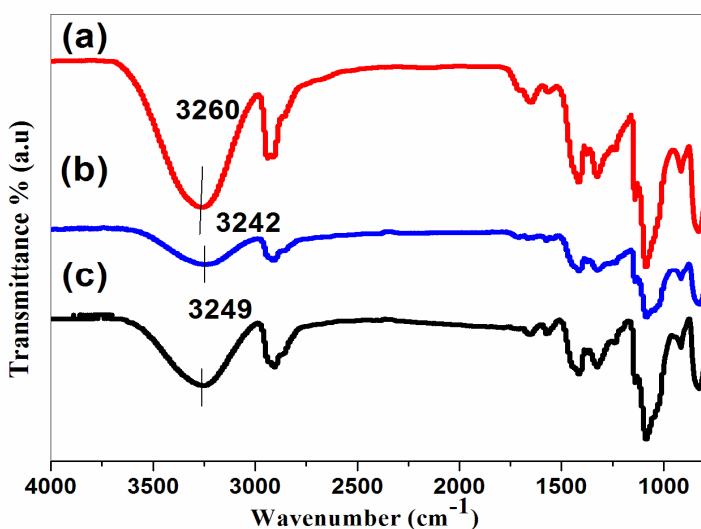
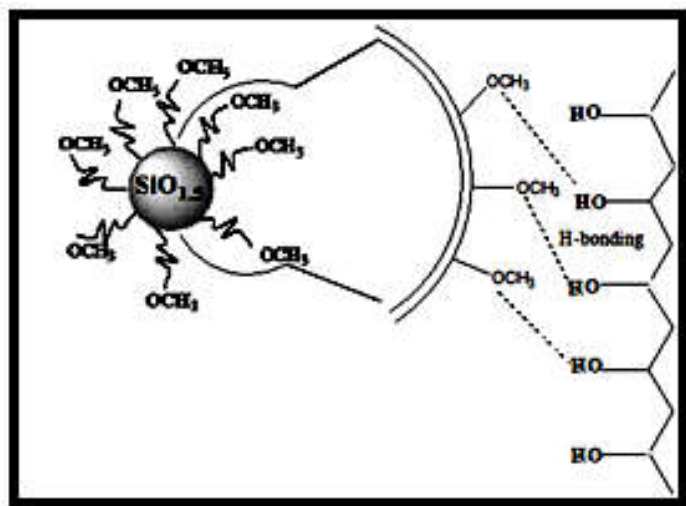


**Figure 3.1:** FTIR spectra of (a) PVA (b) PPP1 and (c) PPP3

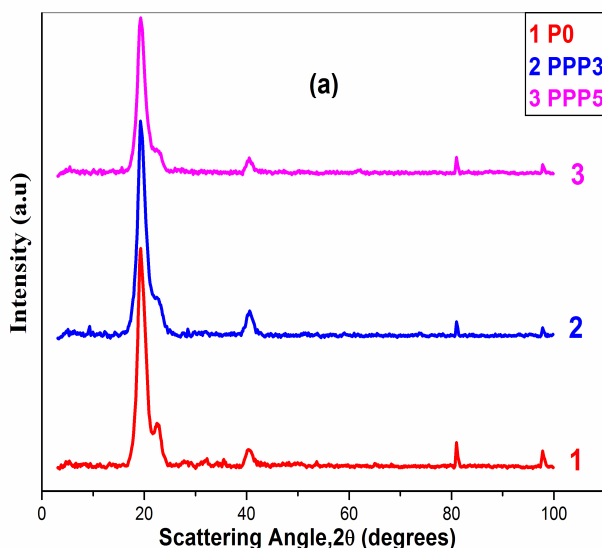


**Scheme 3.1:** Schematic representation of hydrogen bonding interaction between PEG-POSS and PVA

XRD measurements are used to investigate the effect of amphiphilic POSS on the semicrystalline nature of PVA matrix due to its tendency to form hydrogen bonds. Neat PVA shows a strong intense diffraction peak at  $19.3^\circ$  which is assigned to (200)/(100) planes. The obtained data is in agreement with the value reported by Zhao *et al.* for PVA.<sup>18</sup> It also shows less intense peaks at  $2\theta$ ,  $22.4^\circ$ ,  $40.3^\circ$ ,  $81.0^\circ$  and  $94.8^\circ$ , which are characteristic of semicrystalline PVA.

**Figure 3.2(a)** shows the XRD pattern of pristine PVA and PVA/PEG-POSS systems. In the PEG-POSS embedded PVA system the intensity of diffraction peak at  $19.3^\circ$  get reduced with increasing the weight percentage of PEG-POSS, corresponding to the decrease in the chain packing of PVA in the presence of PEG-POSS particles. The decrease in diffraction intensity with the weight percentage of PEG-POSS indicates the difficulty in PVA crystallite formation due to the intercalation of PEG-POSS molecules between the PVA chains. The observation is in well-agreement with the crystallinity computed from DSC which is discussed in the later part of this

chapter. **Figure 3.2(b)** shows strong diffraction peaks at  $2\theta$ 's of  $6.3^\circ$  ( $d=13.8$   $\text{\AA}$ ),  $8.6^\circ$  ( $10.2$   $\text{\AA}$ ),  $25.7^\circ$  ( $3.4$   $\text{\AA}$ ),  $27.4^\circ$  ( $3.2$   $\text{\AA}$ ),  $80.9^\circ$  ( $1.1$   $\text{\AA}$ ) and  $97.8^\circ$  ( $1.0$   $\text{\AA}$ ) for Octa-TMA-POSS, which is an indication of the high crystallinity of the material. But the sharp diffraction peaks derived from Octa-TMA-POSS disappear when it is dispersed in PVA matrix due to the uniform dispersion of silsesquioxane in PVA matrix. However, the intensity of peak at  $2\theta=19.3^\circ$ , which is characteristic of semicrystalline PVA increases significantly upon the introduction of Octa-TMA-POSS, indicating the Octa-TMA-POSS induced change in the crystalline phase of PVA chain. It may be due to the electrostatic interaction (ion-dipole) which exist between PVA and Octa-TMA-POSS resulting in the positional orientation, and is schematically illustrated in **Scheme 3.2**. Octa-TMA-POSS can act as a nucleating agent and there is a remarkable increase in the crystallinity of composites.



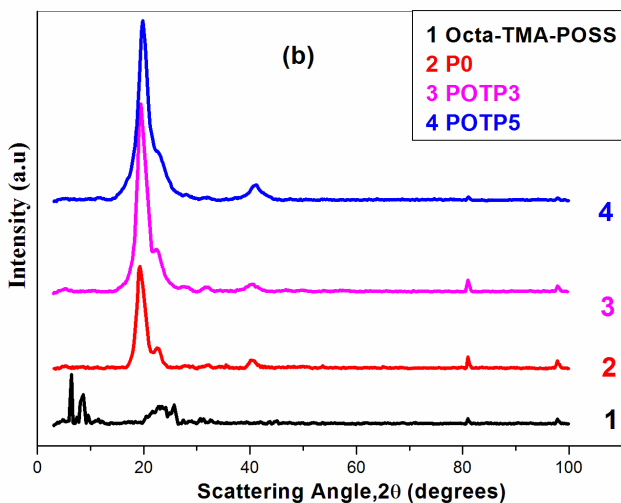
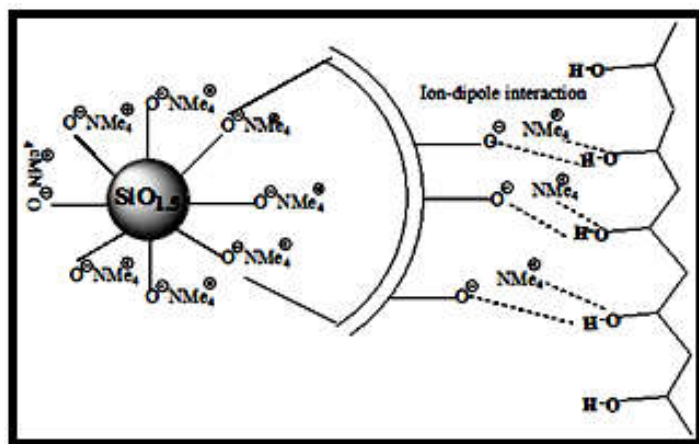


Figure 3.2: XRD patterns of (a) PVA and (b) PVA/POSS systems

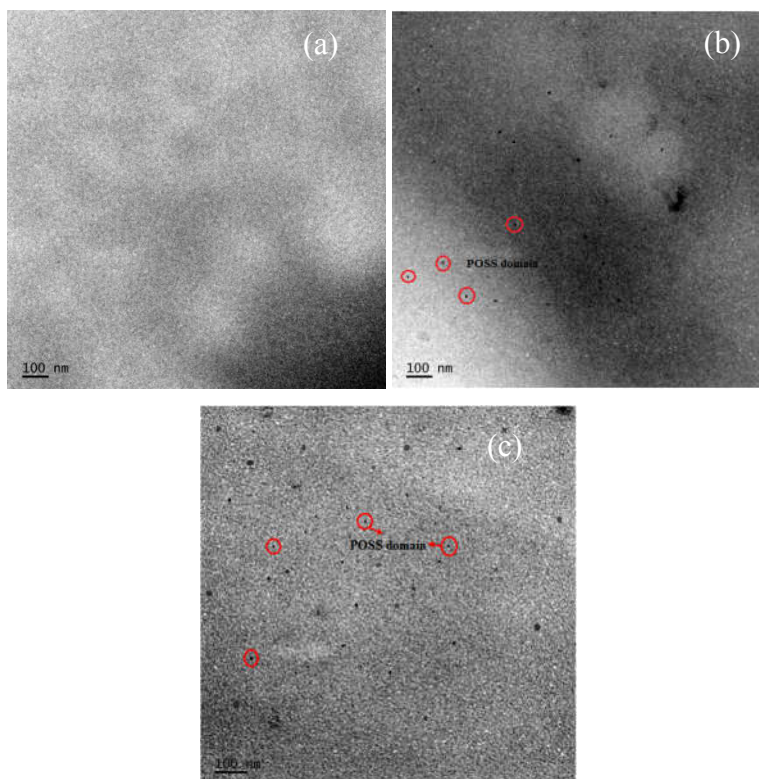


Scheme 3.2: Schematic representation of ion-dipole interaction between Octa-TMA-POSS and PVA

Morphology and distribution of particles in the matrix has great influence on the properties of the polymer membrane. The homogeneous dispersion of POSS particles in PVA matrix is observed from transmission electron



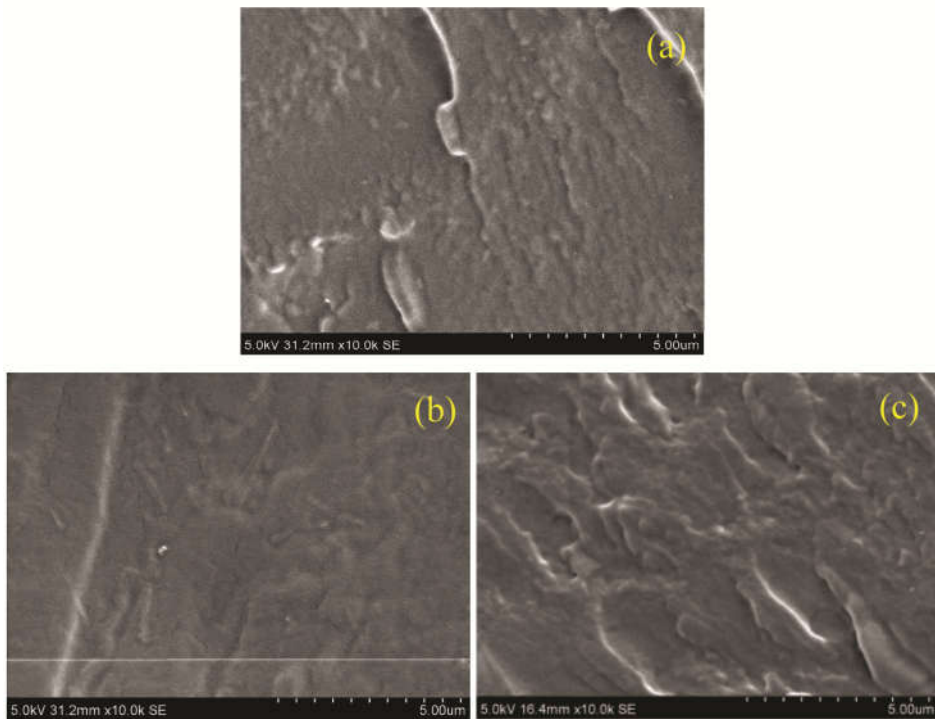
micrographs and is presented in **Figure 3.3**. The dark and bright portions in TEM indicate the POSS and polymer matrix respectively. It is seen that the POSS particles are rather well dispersed in the polymer matrix. This can be explained in terms of good interaction of organic constituents of POSS with PVA matrix. The functional groups in the PEG-POSS and Octa-TMA-POSS are chemically interacted with PVA by hydrogen bonding and ion-dipole interactions respectively.



**Figure 3.3:** TEM image of (a) PVA (b) PPP3 (c) POTP3

The evaluation of field emission scanning electron micrographs (FESEM) of cryogenically fractured membranes gives information about domain morphology with varying functional group on the POSS and it is displayed in

**Figure 3.4.** PEG-POSS embedded PVA membrane (**Figure 3.4 (b&c)**) shows a smooth and dense structure as in pure PVA without forming any bulky agglomeration due to the good interfacial bonding between polymer and POSS without any noticeable defect at the PVA–POSS interface. However, spherically shaped Octa-TMA-POSS particles are observed in the PVA matrix as seen in **Figure 3.4 (e-f)**.



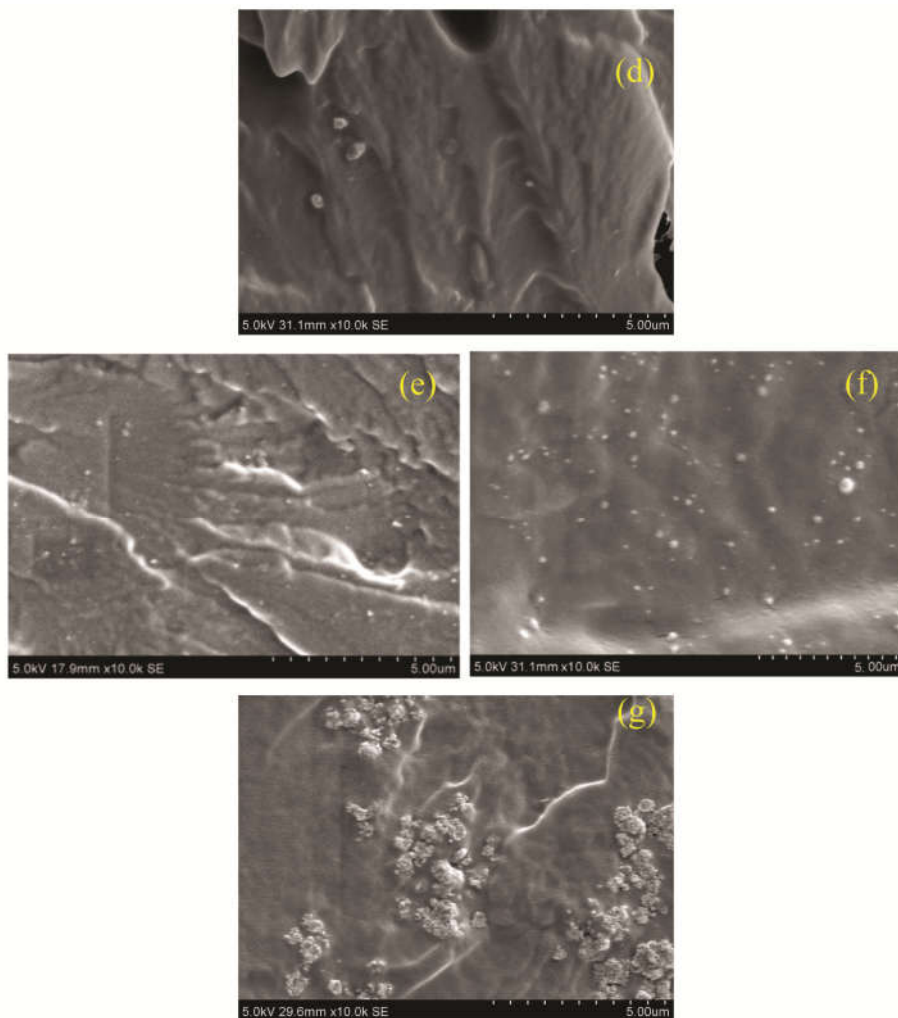


**Figure 3.4 (a-g):** SEM images of (a) P0 (b) PPP1 (c) PPP3 (d) PPP5 (e) POTP1 (f) POTP3 (g) POTP5

In POTP system, the silsesquioxane core effect is more prominent over side chain effect. The clustering of POSS particles are seen at higher weight percentage (5wt%) due to its nanostructure, as it has tendency to reduce its surface energy (**Figure 3.4 (d & g)**). Therefore, at higher wt% of POSS,

POSS-POSS network formation is considered to be predominant over PVA-POSS network. As a result, the surface area and surface activity of the filler get reduced followed by the reduction in the interfacial interaction between the filler and matrix. It reduces the crystallinity and general properties of the membrane like the separation of solvent and gas mixtures.

The SEM micrographs of tensile fractured surfaces of PVA/POSS are presented in **Figure 3.5**. In the micrographs, it is very hard to observe nanoparticles, which indicate the homogeneous dispersion of filler in the matrix. The arrows shown in the images represent the crack initiation front, as well as the crack propagation direction. The SEM image of PVA exhibits nonlinear deformation of the surface and branched crack propagation. The fibrillar-like structure can be seen throughout the fracture surface of 3wt% PEG-POSS incorporated PVA, suggesting a collective contribution of nanofiller to the fracture toughness. PEG chain on the surface of POSS molecule is responsible for the crack bifurcation in PPP system. The rigid core of POSS particle can act as an obstacle for the growing crack and leading to the deviation from the initial path thereby creating secondary cracks. However, for the 3wt% POTP system, a linear-like propagation can be observed indicating the least expenditure of energy for the fracture. The uniform dispersion and the strong interaction of Octa-TMA-POSS enhance the crystallinity as well as the mechanical properties of the composite.

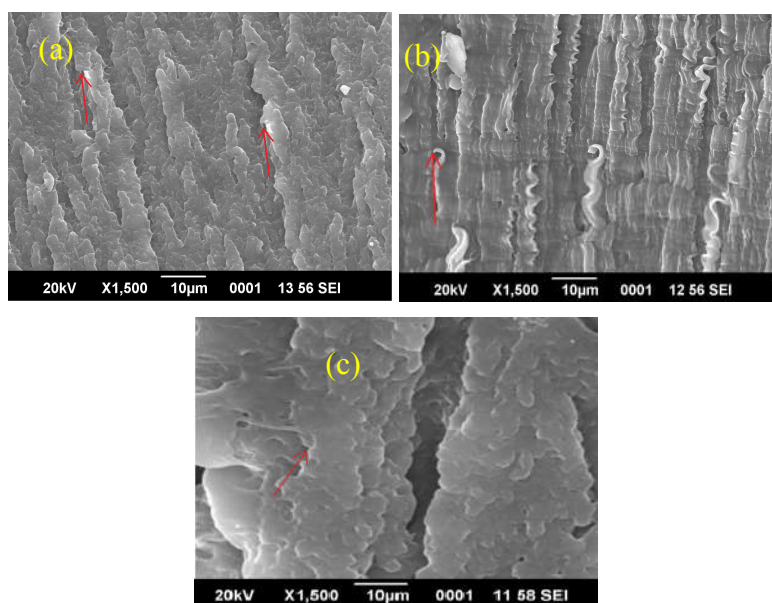


**Figure 3.5:** SEM images of tensile fractured surfaces of (a) PVA (b) PPP3 (c) POTP3 systems

The wettability of the membrane surface is an important aspect of material science and surface chemistry because it can be used to ascribe the extent to which a liquid spread on a solid surface and is usually expressed by contact angle  $\theta$ . It provides a primary data on the surface wetting behaviour of a polymer when it is in contact with a liquid. If  $\theta \ll 90^\circ$  the surface is hydrophilic and  $\theta \gg 90^\circ$  surface is hydrophobic. The surface roughness plays a significant role in the determination of surface wettability.

When a drop of water is in contact with a surface, depending on the nature of the surface the shape of the droplet get changed. As illustrated in **Figure 3.6**, the water contact angle for pristine PVA is in the wetting range ( $61^\circ$ ). With the introduction of the hydrophilic POSS to PVA matrix, a significant change in contact angle value is observed due to the presence of peripheral side chain

and rigid siloxane core of POSS. This can be attributed to the good interaction between hydrophilic POSS and PVA chains. The contact angle of PPP system is found to be  $< 40^\circ$  due to the adhesive interaction of the liquid drop on the solid surface. The Wenzel model is considered to be more appropriate for explaining the behaviour of PPP system.<sup>19</sup> The equation is,  $\cos \theta_w = r \cos \theta_Y$ , where  $\theta_w$  the apparent contact angle,  $\theta_Y$  is Young contact angle and  $r$  is the surface roughness factor. According to this equation, the increase in surface roughness results in enhancement of the wetting property. If  $r > 1$ , the hydrophilicity ( $\theta_Y < 90^\circ$ ) of the surface increases ( $\theta_w < \theta_Y$ ). In the present case, the hydrophilic PVA surface becomes more hydrophilic and rougher (shown in AFM studies) by the incorporation of the PEG-POSS due to the compatibility of the hydrophilic PEG tails in the PVA matrix. In the case of PVA/Octa-TMA-POSS system, the contact angle is found to be higher at lower loading as compared to PVA while at higher loading it decreases due to the presence of polar functional group on the membrane surface. Based on the molecular weight and structure of POSS, PEG-POSS and Octa-TMA-POSS composed of approximately 92 and 52 wt% of hydrophilic functional groups respectively. As seen in **Figure 3.6**, the hydrophilicity of PPP systems are higher than POTP systems.

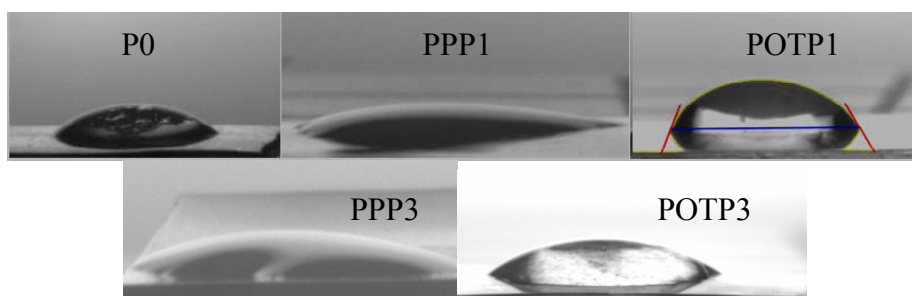


**Figure 3.6:** Water contact angle images on the surface of PVA and PVA/POSS membranes.

Atomic force micrographs of neat PVA and PVA/POSS systems of surface area  $5 \times 5 \mu\text{m}$  are presented in **Figure 3.7** and **Figure 3.8**. The bright and dark spots observed in the AFM image of the membranes represents the highest and lowest points in the membrane surface.<sup>15</sup> The roughness parameters such as average deviation of height ( $R_a$ ) and root mean square deviation of height ( $R_q$ ) of all membranes are included in the AFM images. It is evident that PVA membrane exhibits higher surface roughness and substantial changes in surface topography by the introduction of PEG-POSS particles and at higher Octa-TMA-POSS loading. However, 1wt% Octa-TMA-POSS introduction in PVA matrix reduced the surface roughness significantly. The variation in the surface roughness by varying functional group and concentration of POSS molecule in PVA matrix is probably due to the variation in the polar functional group accumulation on the membrane surface and variation in the nature of interaction between the functional group on the POSS and PVA chains which led to surface reorganisation of chains of PVA. Generally, rough surface materials have higher hydrophilicity.<sup>20</sup> Surface roughness and hydrophilicity enhance the sorption sites in the membrane, which results in large flux for PEG-POSS incorporated PVA systems. In the case of POTP system, a new surface morphology developed due to ion-dipole interaction and later studies revealed that it enhances the selectivity of the membrane.



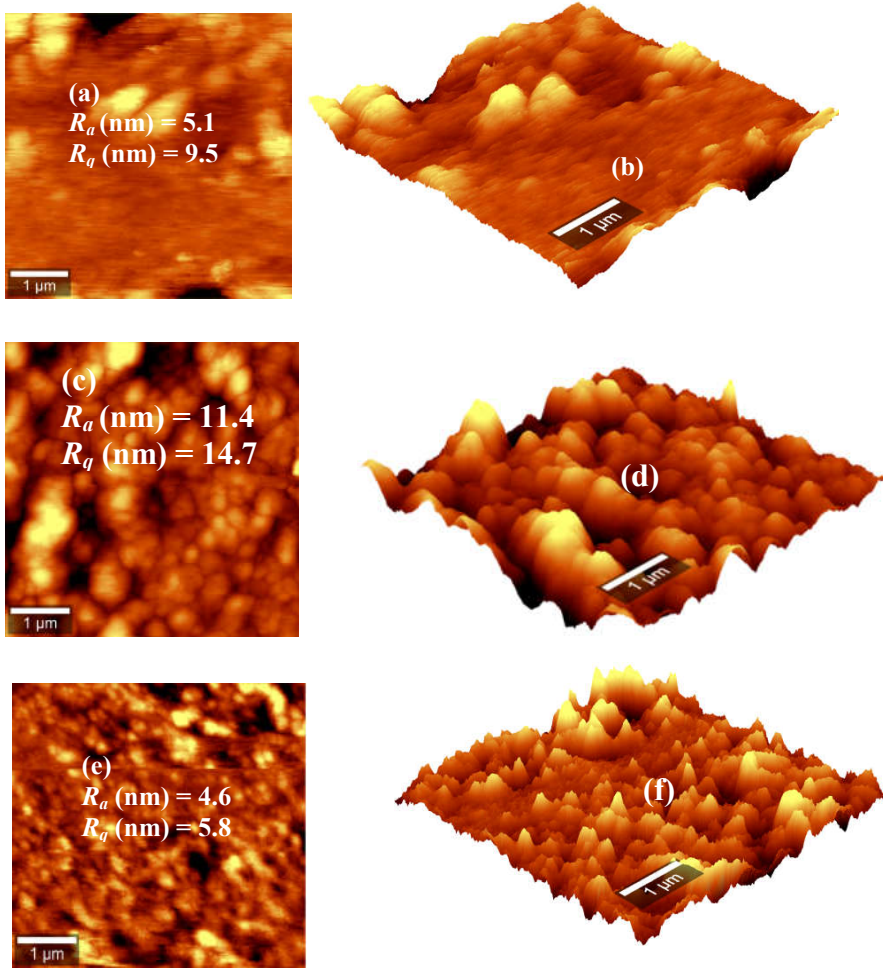


**Figure 3.7:** Height image and corresponding 3-D AFM images of (a-b) pure PVA, (c-d) PPP1 and (e-f) POTP1



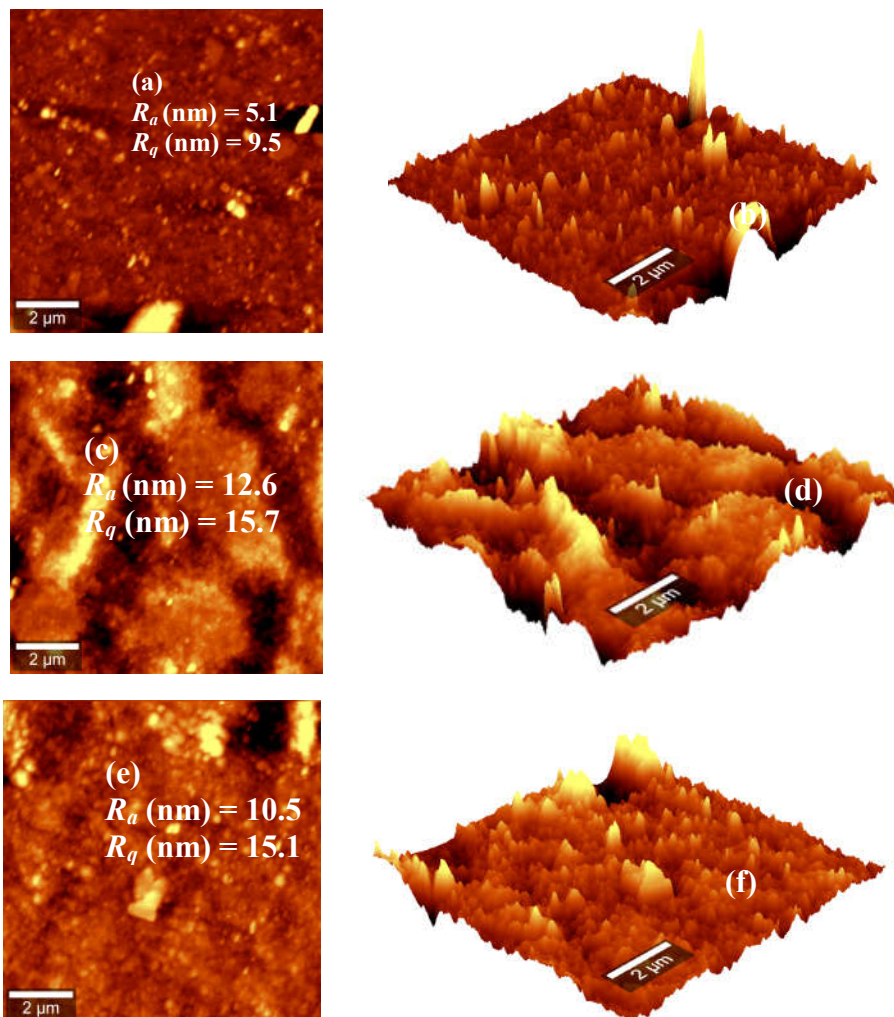


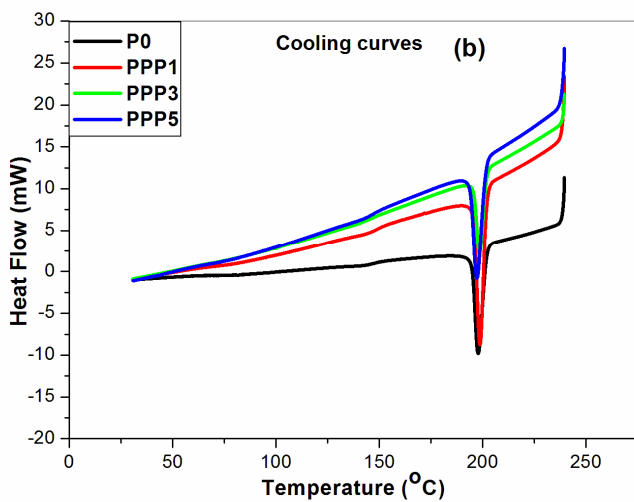
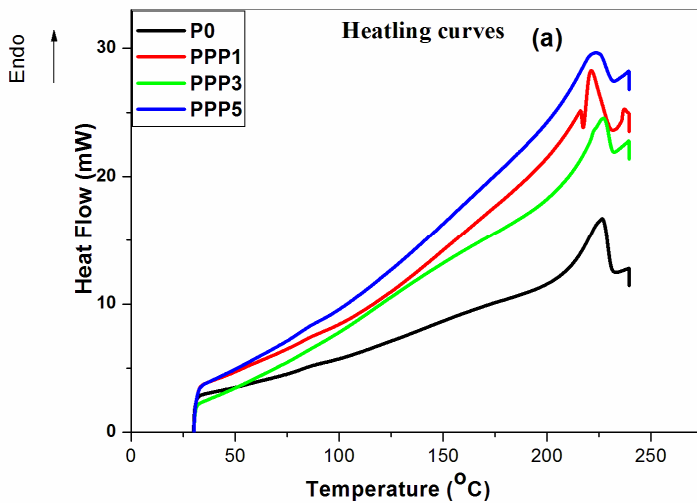
**Figure 3.8:** Phase image and corresponding 3-D AFM images of (a-b) pure PVA, (c-d) PPP3 and (e-f) POTP3

DSC analysis provide information about various parameters such as melting temperature ( $T_m$ ), crystallisation temperature ( $T_c$ ), heat of fusion ( $\Delta H_f$ ) and heat of crystallisation ( $\Delta H_c$ ) of PVA/POSS system. **Figure 3.9** shows the DSC curves of neat PVA and PVA/POSS systems in heating and cooling

mode. The melting peak corresponding to POSS molecule is absent in the heating scan indicates the good dispersion of POSS molecules in the PVA matrix. PVA shows the melting endotherm with an onset and end set temperature of 209 and 231°C, respectively. A summary of melting and crystallisation data corresponding to the heating and cooling curves are presented in **Table 3.1**. A alteration in melting and crystallisation behaviour of PVA can be observed upon the addition of functionalised POSS.

PEG-POSS reduces the  $T_m$  and  $\Delta H_f$  of PVA, since the low molecular weight PEG side groups on POSS hinders crystallisation process in PVA and it gets melted at a lower temperature than PVA. In POTP system, there is a significant increase in  $T_m$  of PVA at lower weight percentage of POSS due to the increased crystalline behaviour of PVA in the presence of Octa-TMA-POSS. The crystallisation exotherm of PVA is slightly shifted to higher temperature in the presence of PEG-POSS and Octa-TMA-POSS due to the nucleating action of PEG-POSS and Octa-TMA-POSS on PVA matrix.

The degree of relative crystallinity ( $X_c$ ) in all samples can be calculated using the equation (2.11) given in chapter 2.<sup>21</sup> The principle of polymer physics establishes that the polymer with greater crystallinity also possesses greater heat of fusion and melting point. The presence of eight flexible oligomeric PEG units on the siloxane core of POSS destroyed the crystalline area of the PVA after the addition of PEG-POSS. The POTP system exhibits enhanced crystallinity at minimum loading of Octa-TMA-POSS due to the presence of highly rigid three dimensional inorganic core of POSS. At higher loading, there is a marginal decrease in crystallinity due to the clustering behaviour of Octa-TMA-POSS.



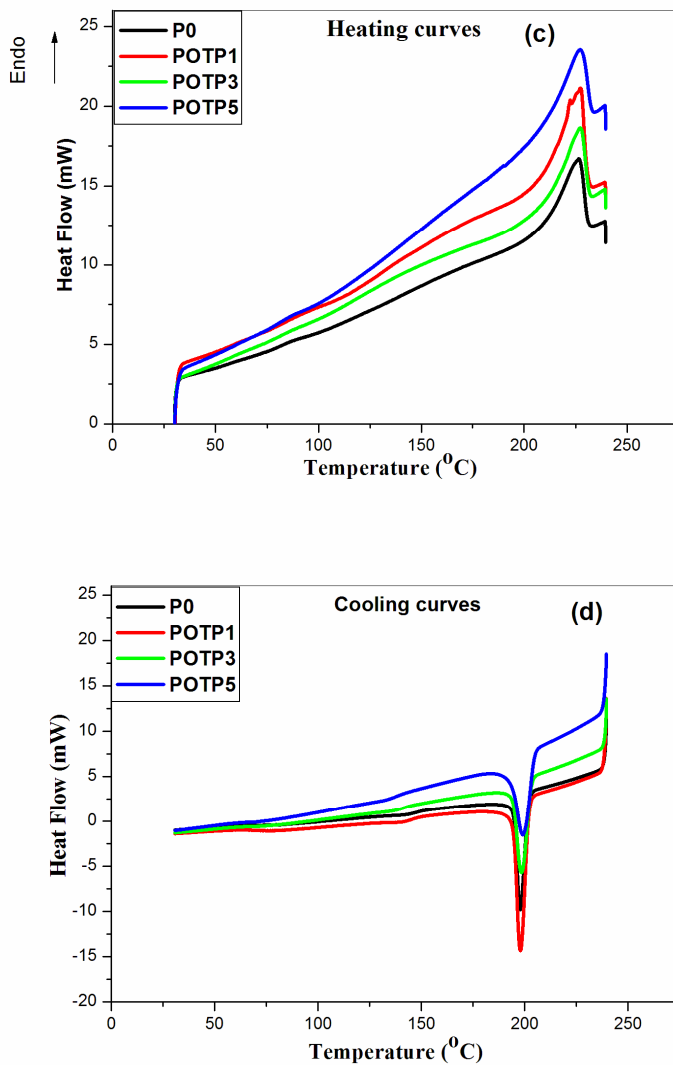


**Figure 3.9:** DSC heating and cooling curves of PVA/PEG-POSS (a&b) and PVA/Octa-TMA-POSS (c&d)

**Table 3.1:** The Effect of POSS loading on the melting and crystallisation parameters of PVA

Samples	T <sub>m</sub> (°C)	ΔH <sub>f</sub> (J/g)	T <sub>c</sub> (°C)	ΔH <sub>c</sub> (J/g)	Crystallinity %
P0	226	56	197	65	40
PPP1	221	46	198	59	39
PPP3	226	49	199	57	38
PPP5	221	54	197	55	36
POTP1	228	59	198	65	43
POTP3	227	56	198	65	41
POTP5	226	50	199	64	36

### 3.2.2 Properties

#### 3.2.2.1 Mechanical properties

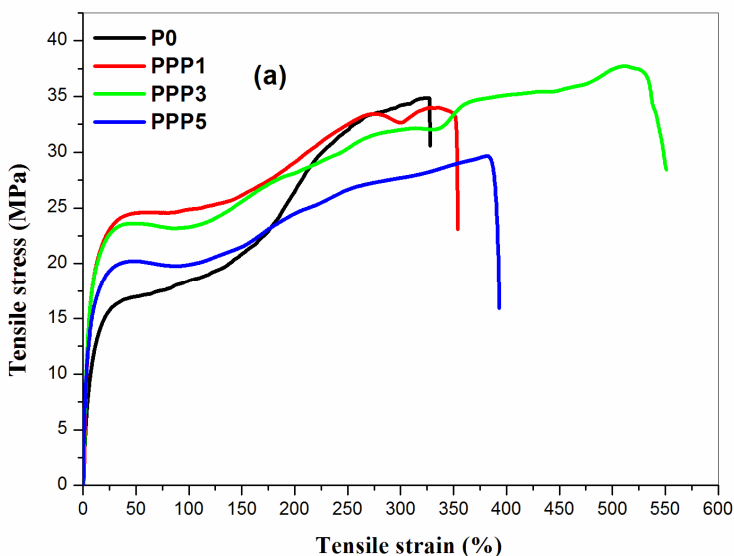
The mechanical properties of PVA-POSS system depend on the structure and functional groups present in the POSS as well as the interfacial characteristics of the components.<sup>22</sup> Interfacial interaction depends on the area at the interfacial region and the extent of interaction between filler and matrix. Tensile testing results are tabulated in **Table 3.2**. **Figure 3.10** depicts the stress-strain graph of PVA and PVA/POSS films with 1,3 and 5wt % POSS loading. It can be seen that PVA attained a maximum strain of 327% before fracture while the POSS-incorporated PVA exhibits remarkable changes in fracture strain. It is interesting to note in the **Figure 3.10 (a)** that the PPP3 system exhibits sharp enhancement in fracture strain from 327 to 536% due to the presence of eight flexible PEG tails on the siloxane core of POSS.<sup>23-24</sup> The mechanical performance of POSS filled systems is highly influenced by soft and ductile organic shell, as well as hard and rigid inorganic silica core

of POSS. PPP system possesses excellent ductility as evidenced by the very high elongation at break. The soft and flexible PEG moiety in the functionalised POSS is the reason behind the enhancement in ductile nature and toughness of PVA. Similar behaviour is reported for poly(methyl methacrylate)/POSS system.<sup>25</sup> On the other hand, in the **Figure 3.10 (b)** POTP3 system exhibited reduction in fracture strain from 327 to 280% due to the dominating rigid core effect of POSS over anionic Octa-TMA functional side group. The elongation at break of POTP system decreases with increase in Octa-TMA-POSS loading, which indicate that the system becomes more brittle when compared with pure PVA.

The introduction of oligomeric PEG functionalised POSS on PVA reduces the tensile strength of PVA membrane from  $35\pm 4$  to  $33\pm 3$  MPa at 3wt % PEG-POSS and is presented in **Table 3.2**. This can be attributed in terms of the flexible nature of PEG functional groups in PEG-POSS, which dominates over rigid core effect of POSS; moreover, PEG has plasticizing effect on PVA matrix. However, the tensile strength of POTP3 nanocomposite membrane increases significantly from  $35\pm 4$  to  $41\pm 2$  MPa as compared to neat PVA due to the strong interfacial interaction between PVA and Octa-TMA-POSS, which promotes the homogeneous dispersion of POSS in PVA matrix. Nanostructured POSS particles act as stress transferring agents in the PVA matrix and as a result the stress experienced by the matrix is comparatively less. **Scheme 3.3** shows the interfacial interaction between PVA and POSS. PVA chains are absorbed on the POSS surface by good attractive interaction between organic side group on POSS and hydroxyl group of PVA, which results in the enhancement of contact surface area between polymer chains and the rigid filler surface.

Another interesting observation is the remarkable enhancement in Young's modulus of PVA even at low weight percentage of POSS. This can be attributed to the presence of rigid three-dimensional inorganic core of POSS, which is made up of high bond energy possessing Si-O linkage (451 kJ/mol). At higher loading of POSS, there is a reduction in the mechanical properties of PVA/POSS system due to the clustering behaviour of these amphiphilic POSS.

The filler–matrix interaction can be evaluated from the fracture surface morphologies. For weakly bonded particles, there exist a separation between particles and the matrix. However, in the case of strongly bonded systems, particles are held tightly by the matrix and are acting as stress transferring agents during deformation. The fracture toughness of a polymeric matrix can be affected by the filler size, shape, volume fraction and filler-matrix adhesion strength.



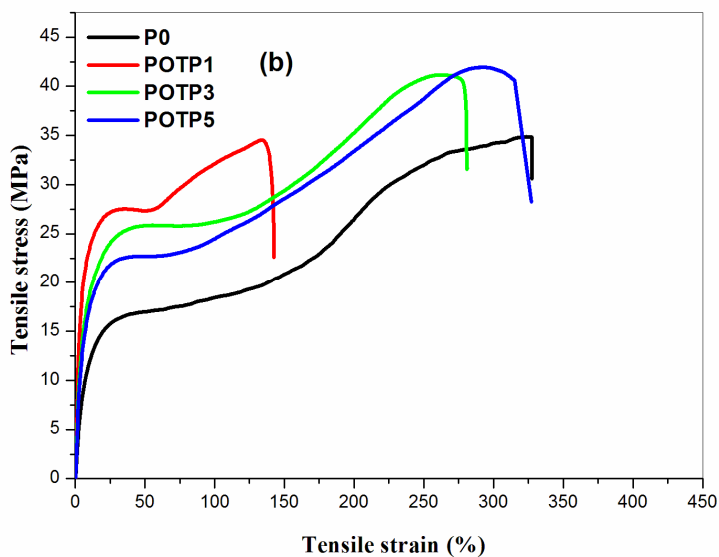
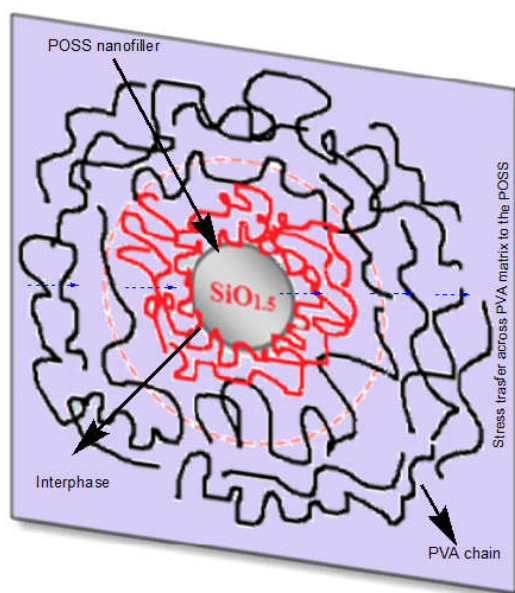


**Figure 3.10:** Stress-strain graphs of PVA/PEG-POSS (a) and PVA/Octa-TMA-POSS (b)

**Table 3. 2:** Tensile Properties of PVA and PVA/POSS systems

Sample	Tensile Strength (MPa)	Elongation @Break (%)	Young's Modulus (MPa)
P0	35±4	327±6.2	198±5.8
PPP1	34±4	354±7.1	486±6.2
PPP3	33±2	536±7.2	472±6.1
PPP5	30±2	393±6.5	442±5.1
POTP1	43±1	192±7.7	637±5.3
POTP3	41±2	280±6.1	491±5.6
POTP5	40±4	320±6.5	343±4.9





**Scheme 3.3:** Interfacial interaction between PVA and POSS

### Theoretical modeling of tensile properties of PVA/POSS systems

Several theoretical predictions have been developed to relate the influence of different parameters of filler on the deformation performance of polymer composites. The physical property of the polymer composites depends on various factors of filler such as particle geometry, size, surface area, and dispersion within the matrix. Therefore, the filler property has to be considered during the theoretical calculation of properties of composites. The ultimate properties of composites vary significantly with the nature of filler. In the present work, three composite theories are exercised to evaluate the Young's modulus of PVA and PVA/POSS systems. The effect of volume fraction of filler, particle morphology, and packing fraction on the properties of PVA-POSS systems have been evaluated theoretically and compared with the experimental findings.

Guth model is extensively applied to compare the modulus of polymer composites and is given by,<sup>26</sup>

$$E_c = E_m (1 + K_E \phi + 14.1 \phi^2) \quad (3.2)$$

where  $K_E$  is the Einstein coefficient or intrinsic viscosity its value is 1.0 for dispersed spheres with slippage at the interface. If no interface slippage occurs,  $K_E$  turns to 2.50.  $E_c$  is the modulus of composite,  $E_m$  is the modulus of pure PVA matrix, and  $\phi$  is the volume fraction of filler.

Kerner equation has been applied for composites with spherical fillers. The greatly simplified form of Kerner equation is applied in composite systems if the filler is extremely rigid than pure polymer matrix.<sup>27</sup> The equation is,

$$E_c = E_m \left[ 1 + \left( \frac{\phi}{1 - \phi} \right) \left\{ \frac{15(1 - \nu)}{8 - 10\nu} \right\} \right] \quad (3.3)$$

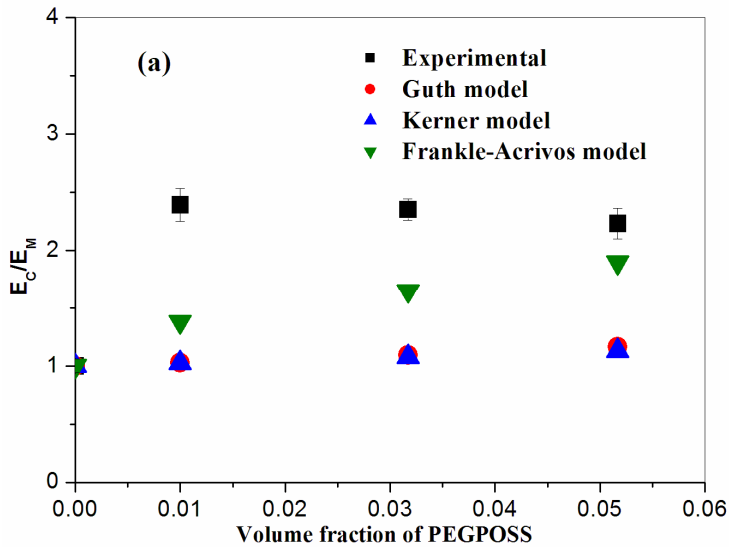
$\nu$  is an another elastic constant called Poisson's ratio and its value is in between 0.35 and 0.50 for most polymers. For PVA, Poisson's ratio is between 0.42 and 0.48.

Frankle-Acrivos model considered the maximum packing fraction of the filler ( $\phi_{\max}$ ).  $\phi_{\max}$  changes with particle shape and state of agglomeration.<sup>28</sup>

$\phi_{\max} = 0.632$  for nonagglomerated random close packed particles. The model can be expressed as follows,

$$E_c = E_m \left[ 1 + \frac{9}{8} \frac{\left( \frac{\phi}{\phi_{\max}} \right)^{\frac{2}{3}}}{1 - \left( \frac{\phi}{\phi_{\max}} \right)^{\frac{2}{3}}} \right] \quad (3.4)$$

The experimental data of composites are evaluated with different theoretical models and are shown in **Figure 3.11**. It is observed that theoretically predicted values are lower than the experimental values due to the presence of rigid siloxane core of the POSS.



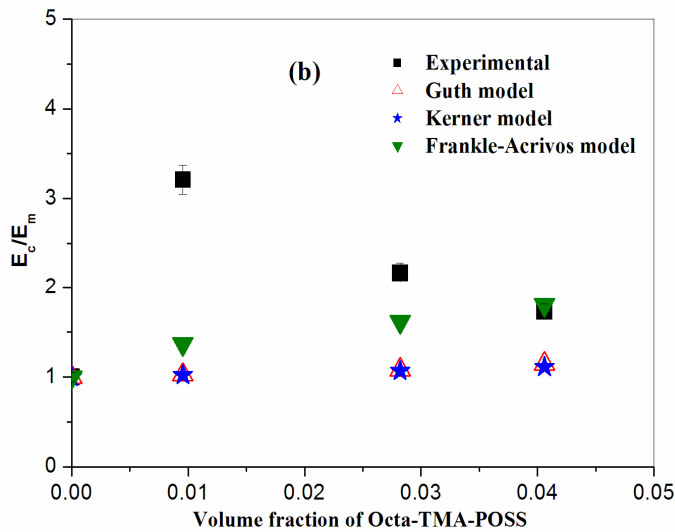


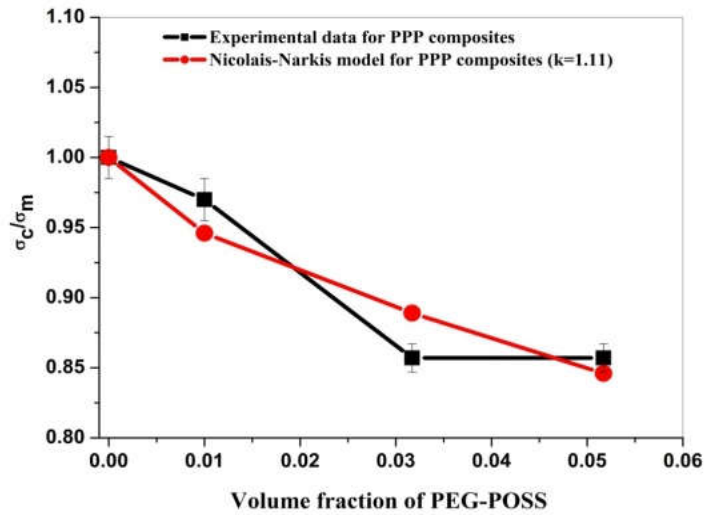
**Figure 3.11:** Theoretical comparison of modulus as a function of volume fraction of POSS.

Tensile strengths of spherical POSS embedded PVA systems have been estimated using the well-known Nicolais-Narkis model.<sup>29-30</sup> The equation is given by,

$$\sigma_c = \sigma_m \left( 1 - k\phi^{\frac{2}{3}} \right) \quad (3.5)$$

where  $\sigma_m$  symbolises tensile strength of material and  $k$  is a stress concentration factor. When the  $k$  value is less than 1.21, strong adhesion occurs between spherical particle and the polymer matrix. Hence, the filler reduces the stress concentration effect and deformation behaviour of the polymer matrix. In **Figure 3.12**, the experimental records for tensile strength of pure PVA and the PVA/POSS system are compared with Nicolais–Narkis model using a least square method to establish the suitable  $k$  values.<sup>31-32</sup> The

k values for PEG-POSS and Octa-TMA-POSS added PVA are established to be 1.11 and 0.39, respectively, indicating that Octa-TMA-POSS exhibits good adhesion with PVA but PEG-POSS shows weaker adhesion to the matrix. It is mainly due to the plasticizing action of oligomeric PEG on PVA matrix that reduces the strength of PVA matrix.



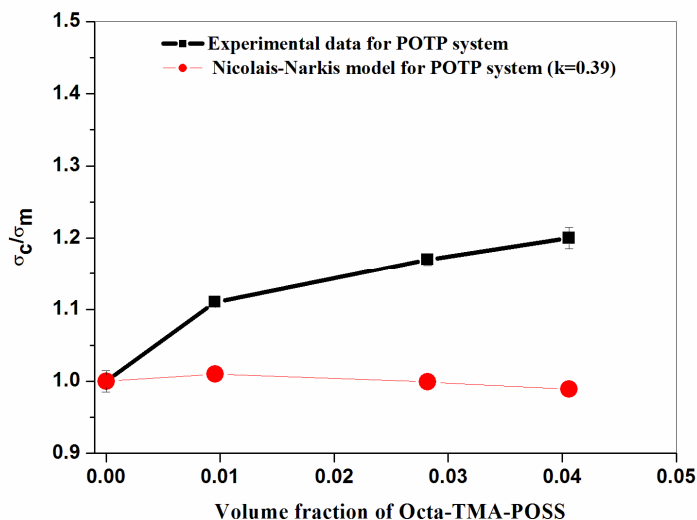


**Figure 3.12:** Theoretical comparison of tensile strength as a function of volume fraction of POSS.

### 3.2.2.2 Dynamic mechanical analysis

Polymers are viscoelastic materials and exhibit both solid and liquid characteristics in its mechanical behaviour as a function of temperature. DMA is used to characterise the viscoelastic behaviour of polymers. It provides information about the glass transition temperature, relaxation modulus, damping behaviour, molecular orientation and morphology of polymer systems.<sup>33</sup> The effect of cage structured POSS on the viscoelastic properties of the PVA has been analyzed with respect to the weight percentages of POSS. The interaction of the macromolecular chain of the PVA and spherical POSS results in significant variation in modulus and damping behaviour. The dynamic storage modulus ( $E'$ ) as a function of temperature plots of PVA as well as PVA/POSS systems are presented in

**Figure 3.13.** Transitions corresponding to  $\alpha$  and  $\beta$  characteristics of PVA matrix can be observed in the storage modulus curves. It is interesting to note that in the glassy region, at lower weight percentage of POSS, PVA shows increase in storage modulus. This enhancement in the modulus or rigidity of PVA by the addition of POSS can be interpreted in terms of the efficient nanoreinforcement contribution of rigid silicon-oxygen-based POSS core matrix. It means that the incorporation of cage-structured silsesquioxane core into the PVA matrix restricts the segmental mobility of the polymer chain. Comparing the two types of functionalised POSS, POTP system exhibits slightly higher storage modulus than PPP system. In the glassy region, PVA/POSS systems exhibit highest storage modulus than neat PVA due to the strong interfacial interaction between PVA and POSS. In the rubbery region, PVA shows more storage modulus owing to its crystalline nature, and it resists the intermolecular slippage. In rubbery state, PVA chains initiate the thermal motion resulting in the detachment of PVA/POSS network. Consequently, the POSS molecule offers steric hindrance and decrement in storage modulus in the rubbery region.

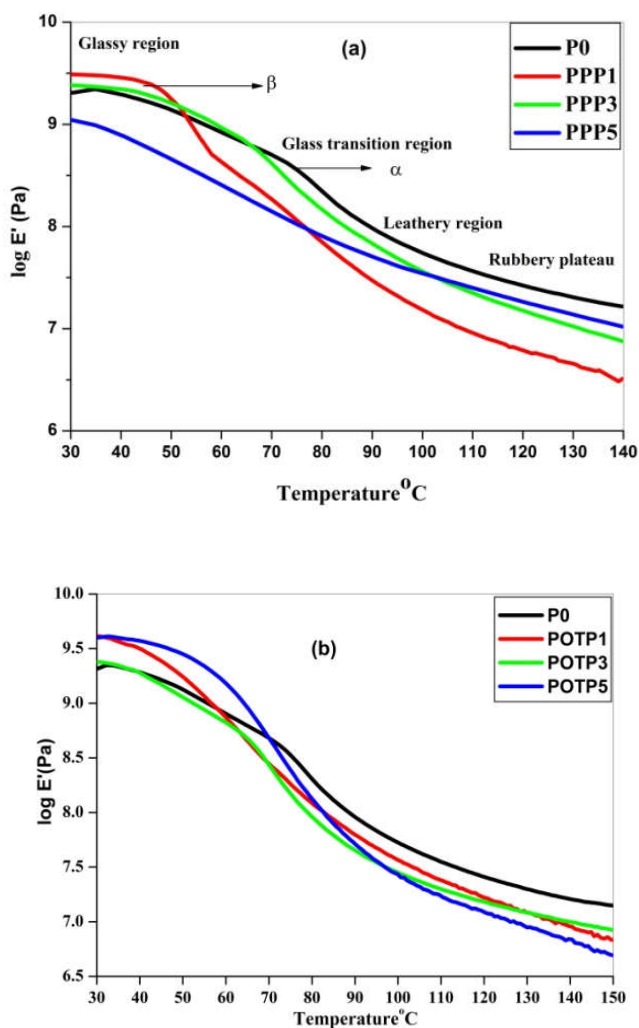
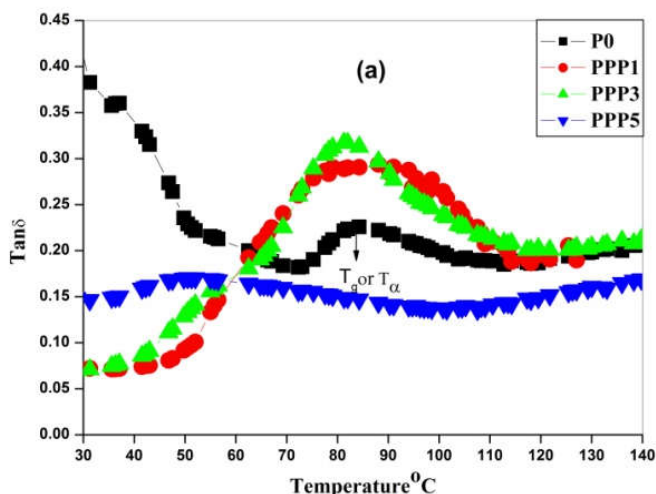


**Figure 3.13 (a-b):** Storage modulus versus temperature curve of PVA and PVA/POSS systems

DMA can be used to analyse the mobility of polymer chains at glass transition regions. The mechanical loss factor  $\tan\delta$ , mathematically expressed as the ratio of loss modulus to the storage modulus, is very sensitive to the structural changes of the material.  $\tan\delta$  versus temperature spectra for PEG-POSS and Octa-TMA-POSS filled PVA systems at the frequency of 1 Hz are



shown in **Figure 3.14(a-b)**. The temperature at which maximum  $\tan \delta$  observed corresponds to the glass transition temperature ( $T_g$ ) of the matrix. The  $\alpha$ -peak (major transition) corresponds to the  $T_g$  of PVA (**Table 3.3**). The formation of H-bond between PEG side group of POSS and PVA restricts the segmental mobility of PVA chain, consequently,  $T_g$  of PEG-POSS system increases at lower concentration of POSS. The decrement in  $T_g$ 's and broadening of peak at higher concentration of PEG-POSS could be attributed in terms of the more pronounced plasticization effect of higher percentage of low-molecular weight side groups. The depression in  $T_g$  at lower loading of Octa-TMA-POSS implies lower stability of Octa-TMA functional organic side groups of the POSS. The increment in  $T_g$  at higher loading of the Octa-TMA-POSS could be explained in terms of good interfacial interaction between PVA and Octa-TMA-POSS and thereby reduction in the mobility of polymer chain.



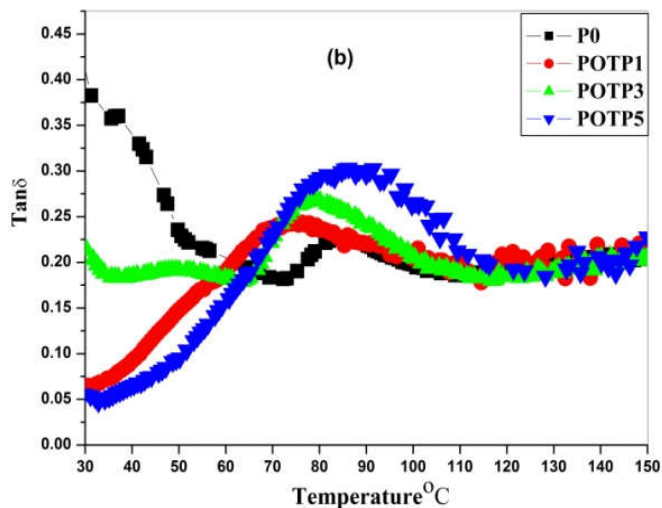


**Figure 3.14 (a-b):**  $\text{Tan}\delta$  versus temperature curve of PVA and PVA/POSS systems

**Table 3.3:** Glass transition temperature of PVA/POSS systems

Samples	P0	PPP1	PPP3	PPP5	POTP1	POTP3	POTP5
$T_g(^{\circ}\text{C})$	$82\pm 4$	$90\pm 3$	$80\pm 3$	$51\pm 5$	$73\pm 3$	$79\pm 4$	$86\pm 3$

Damping behaviour of polymeric systems is highly sensitive to all types of molecular motions, transitions, relaxation process, structural and the morphological changes. Damping or absorption performance of material is crucial to design material structure and to determine life span and safety of a structure.<sup>34</sup> Polymers at the glass transition region have a high possibility for vibration damping since the macromolecular chains of polymers achieve mobility and this dissipates a large amount of energy through viscous movement. High damping materials possess high rate of energy dissipation. **Figure 3.15** presents the  $\text{tan}\delta_{\text{max}}$  versus weight percentage of POSS for PVA/POSS systems. The  $\text{tan}\delta_{\text{max}}$  value of PVA is shifted to higher value

upon the incorporation of POSS. In the case of PPP system,  $\tan\delta_{\max}$  increases with weight percentage of POSS up to 3 wt% and after that  $\tan\delta_{\max}$  decreases. The reason behind this observation is the presence of low-molecular-weight PEG side groups on the POSS, which decreases the internal friction of the composites through polymer-filler and filler-filler interaction.<sup>35</sup> POTP system exhibits good damping property at higher Octa-TMA-POSS loading due to the increase in the available surface area per unit volume of the POSS resulting in higher internal friction between polymer-filler and filler-filler networks. This will increase the rate of dissipation of energy and the damping property. The interaction between polymer and filler could be find out by calculating the percentage reduction in  $\tan \delta_{\max}$  using the following equation<sup>36</sup>,

$$\% \text{ Reduction} = \frac{(\tan\delta_{\max})_{PVA} - (\tan\delta_{\max})_{PVA/POSS}}{(\tan\delta_{\max})_{PVA}} \times 100 \quad (3.6)$$

The values are tabulated in **Table 3.4**. The percentage of reduction is found to be higher for PVA/PEG-POSS system at lower weight percentage of POSS owing to the better interaction between filler and polymer. PVA/Octa-TMA-POSS membrane shows gradual increase in  $\tan \delta_{\max}$  as a function of the weight percentage of filler due to the presence of more polar functional groups in the POSS molecule.

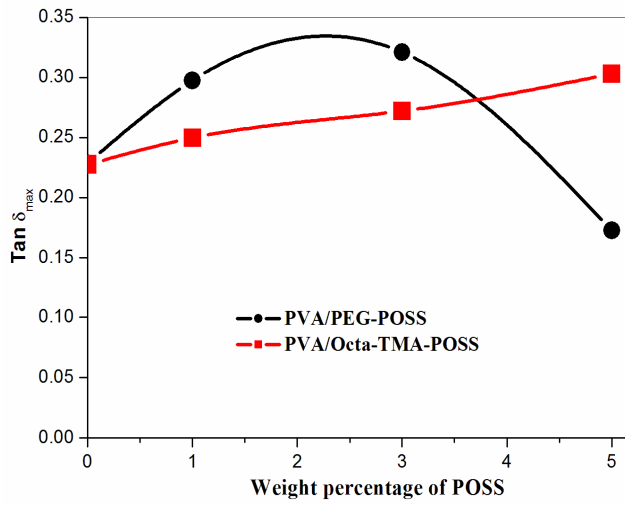


**Figure 3.15:** Effect of weight percentage of POSS on the  $\tan \delta_{\max}$  values of PVA/POSS systems

**Table 3.4:** Percentage reduction in  $\tan \delta_{\max}$  of PVA/POSS systems

Sample	% Reduction
PPP1	30
PPP3	40
PPP5	24
POTP1	10
POTP3	20
POTP5	33

### **3.3 Conclusions**

PVA-POSS hybrid membranes using two kinds of POSS, namely Octa-TMA-POSS and PEG-POSS, were prepared successfully by solution casting method. FTIR revealed the hydrogen bonding interaction between PVA and PEG-POSS. Distribution of filler particles in the matrix were analysed from SEM and TEM. The hydrophilic POSS introduced PVA membrane had excellent hydrophilicity and was confirmed from contact angle studies. Surface roughness of the systems were analysed from AFM images and was found to be higher for PPP system. Crystalline structure of the systems were estimated from the XRD pattern, due to ion-dipole interaction POTP system showed excellent crystalline nature when compared to neat PVA. PEG-POSS incorporated PVA system exhibited good ductility and toughness due to the presence of eight flexible PEG tails on the siloxane core of POSS. However, Octa-TMA-POSS incorporated PVA system showed excellent tensile strength and modulus due to the presence of dominant rigid three-dimensional inorganic core in the POSS. The viscoelastic property of POTP system at higher concentration of Octa-TMA-POSS was significant, which exhibited higher storage modulus and glass transition temperature. This can be explained in terms of the good interfacial interaction between PVA and Octa-TMA-POSS, and the presence of rigid inorganic silsesquioxane core in the PVA matrix. The damping behaviour of PVA membrane increased in the presence of POSS particles. PEG-POSS suppressed the crystallinity of PVA due to the plasticizing nature of low-molecular-weight PEG group, while Octa-TMA-POSS enhanced the PVA crystallinity.

### 3.4 References

1. W. Zhang, A. H. E. Müller, Architecture, self-assembly and properties of well-defined hybrid polymers based on polyhedral oligomeric silsesquioxane (POSS), *Prog. Polym. Sci.*, 38 (2013) 1121-1162
2. D. B. Cordes, P. D. Lickiss, F. Rataboul, Recent developments in the Chemistry of cubic polyhedral oligosilsesquioxanes, *Chem. Rev.*, 110 (2010) 2081-2173
3. Q. Zhang, H. He, K. Xi, X. Huang, X. Yu, X. Jia, Synthesis of *N*-Phenylaminomethyl POSS and its utilization in polyurethane, *Macromolecules* 44 (2011) 550-557
4. P. Chen, X. Huang, Q. Zhang, K. Xi, X. Jia, Hybrid networks based on poly (styrene-co-maleic anhydride) and *N*-phenylaminomethyl POSS, *Polymer* 54 (2013) 1091-1097
5. H. W. Milliman, D. Boris, D. A. Schiraldi, Experimental determination of hansen solubility parameters for select POSS and polymer compounds as a guide to POSS–polymer interaction potentials, *Macromolecules* 45 (2012) 1931-1936
6. K. N. Raftopoulos, S. Koutsoumpis, M. Jancia, J. P. Lewicki, K. Kyriakos, H. E. Mason, S. J. Harley, E. Hebda, C. M. Papadakis, K. Pielichowski, P. Pissis, Reduced phase separation and slowing of dynamics in polyurethanes with three-dimensional POSS-based cross-linking moieties, *Macromolecules* 48 (2015) 1429 -1441
7. S. D. Jiang, G. Tang, Z. M. Bai, Y. Y. Wang, Y. Hu, L. Song, Surface functionalization of MoS<sub>2</sub> with POSS for enhancing thermal, flame-retardant and mechanical properties in PVA composites, *RSC Adv.*, 4 (2014) 3253-3262
8. M. L. Chua, L. Shao, B. T. Low, Y. Xiao, T. S. Chung, Polyetheramine–polyhedral oligomeric silsesquioxane organic–inorganic hybrid membranes for CO<sub>2</sub>/H<sub>2</sub> and CO<sub>2</sub>/N<sub>2</sub> separation, *J. Mem. Sci.*, 385 (2011) 40-48
9. N. L. Le, Y. Wang, T. S. Chung, Pebax/POSS mixed matrix membranes for ethanol recovery from aqueous solutions via pervaporation, *J. Mem. Sci.*, 379 (2011) 174-183

10. F. A. Sheikh, N. A. M. Barakat, B. S. Kim, S. Aryal, M. S. Khil, H. Y. Kim, Self-assembled amphiphilic polyhedral oligosilsesquioxane (POSS) grafted poly (vinyl alcohol)(PVA) nanoparticles, *Mat. Sci. Eng:c.*, 29 (2009) 869-876
11. S. Huang, X. Cen, H. Zhu, Z. Yang, Y. Yang, W. W. Tjiu, T. Liu, Facile preparation of poly (vinyl alcohol) nanocomposites with pristine layered double hydroxides, *Mat.Chem.Phys.*, 130 (2011) 890-896
12. H. N. Chandrakala, B. Ramaraj, Shivakumaraiah, G. M. Madhu, Siddaramaiah, Preparation of polyvinyl alcohol–lithium zirconate nanocomposite films and analysis of transmission, absorption, emission features, and electrical properties, *J. Phys. Chem. C.*, 117 (2013) 4771-4781
13. X. Zhao, Q. Zhang, D. Chen, Enhanced mechanical properties of graphene-based poly (vinyl alcohol) composites, *Macromolecules* 43 (2010) 2357-2363
14. S. Virtanen, J. Vartanen, H. Setälä, T. Tammelin, S. Vuoti, Modified nanofibrillated cellulose–polyvinyl alcohol films with improved mechanical performance, *RSC Adv.*, 4 (2014) 11343-11350
15. Md. M. Rahman, V. Filiz, S. Shishatskiy, C. Abetz, S. Neumann, S. Bolmer, M. M. Khan, V. Abetz, PEBAX® with PEG functionalized POSS as nanocomposite membranes for CO<sub>2</sub> separation, *J. Mem. Sci.*, 437(2013) 286-297
16. Md. M. Rahman, V. Filiz, S. Shishatskiy, C. Abetz, P. Georgopoulos, M. M. Khan, S. Neumann, V. Abetz, Influence of Poly(ethylene glycol) Segment Length on CO<sub>2</sub> Permeation and Stability of PolyActive Membranes and Their Nanocomposites with PEG POSS, *Appl. Mater. Interf.*, 7 (2015) 12289-12298
17. H. D. Huang, P. G. Ren, J. Chen, W. Q. Zhang, X. Ji, Z. M. Li, High barrier graphene oxide nanosheet/poly (vinyl alcohol) nanocomposite films. *J. Mem. Sci.*, 409–410 (2012) 156-163.
18. X. Zhao, Q. Zhang, D. Chen, Enhanced Mechanical Properties of Graphene-Based Poly(vinyl alcohol) Composites, *Macromolecules* 43 (2010) 2357–2363.

19. K. Liu, M. Cao, A. Fujishima, L. Jiang, Bio-inspired titanium dioxide materials with special wettability and their applications. *Chem. Rev.*, 114 (2014) 10044-10094.
20. H. M. Shang, Y. Wang, S. J. Limmer, T. P. Chou, K. Takahashi, G. Z. Cao, Optically transparent superhydrophobic silica-based films, *Thin Solid Films* 472 (2005) 37-43
21. V. P. Swapna, P. Selvin Thomas, K.I. Suresh, V. Saranya, M. P. Rahana, R. Stephen, Thermal properties of poly (vinyl alcohol) (PVA)/halloysite nanotubes reinforced nanocomposites, *Int. J. Plast. Technol.*, 19 (2015) 124-136
22. J. N. Coleman, U. Khan, W. J. Blau, Y. K. Gunko, Small but strong: a review of the mechanical properties of carbon nanotube-polymer composites, *Carbon* 44 (2006) 1624-1652
23. Q. G. Zhang, Q. L. Liu, F. F. Shi, Y. Xiong, Structure and permeation of organic-inorganic hybrid membranes composed of poly (vinyl alcohol) and polysilisesquioxane, *J. Mater. Chem.*, 18 (2008) 4646-4653
24. J. Zhang, J. Wang, T. Lin, C. H. Wang, K. Ghorbani, Magnetic and mechanical properties of polyvinyl alcohol (PVA) nanocomposites with hybrid nanofillers-Graphene oxide tethered with magnetic Fe<sub>3</sub>O<sub>4</sub> nanoparticles, *Chem. Eng. J.*, 237 (2014) 462-468
25. E. T. Kopesky, G. H. McKinley, R. E. Cohen, Toughened poly (methyl methacrylate) nanocomposites by incorporating polyhedral oligomeric silsesquioxanes, *Polymer* 47 (2006) 299-309
26. E. Guth, Theory of Filler Reinforcement, *J. Appl. Phys.*, 16 (1945) 20
27. Y. Dong, D. Chaudhary, C. Ploumis, K. T. Lau, Correlation of mechanical performance and morphological structures of epoxy micro/nanoparticulate composites, *Composites: Part A* 42 (2011) 1483-1492
28. Y. Zare, A. Daraei, M. Vatani, P. Aghasafari, An analysis of interfacial adhesion in nanocomposites from recycled polymers, *Comput. Mat.Sci.*, 81 (2014) 612-616
29. Y. Dong, A. Ghataura, H. Takagi, H. J. Haroosh, A.N. Nakagaito, K.T. Lau, Polylactic acid (PLA) biocomposites reinforced with coir



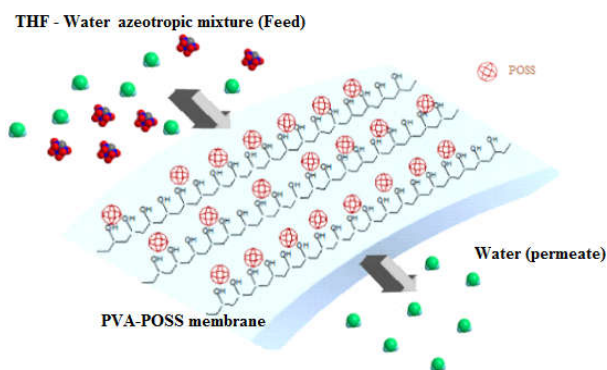
- fibres: Evaluation of mechanical performance and multifunctional properties, *Composites: Part A* 63 (2014) 76-84
30. Y. J. Zare, Modeling approach for tensile strength of interphase layers in polymer nanocomposites, *Collo. Inter. Sci.*, 471 (2016) 89-93
31. D. W. Marquardt, An algorithm for least-squares estimation of nonlinear parameters, *J. Soc. Indust. Appl. Math.*, 11 (1963) 43-441
32. Y. Dong, R. Lin, D Bhattacharyya, Determination of critical material parameters for numerical simulation of acrylic sheet forming, *J. Mater. Sci.*, 40 (2005) 399-410
33. P. Bindu, S. Thomas, Viscoelastic behavior and reinforcement mechanism in rubber nanocomposites in the vicinity of spherical nanoparticles, *J. Phys. Chem. B.*, 117 (2013) 12632-12648
34. J. L. Tsai, N. R. Chang, Investigating damping properties of nanocomposites and sandwich structures with nanocomposites as core materials, *J. Compos. Mater.*, 45 (2011) 2157-2164
35. T. Wang, S. Chen, Q. Wang, X. Pei, Damping analysis of polyurethane/epoxy graft interpenetrating polymer network composites filled with short carbon fiber and micro hollow glass bead, *Mater & Desig.*, 31 (2010) 3810-3815
36. S. Pattanawanidchai, P. Saeoui, C. Sirisinha, Influence of precipitated silica on dynamic mechanical properties and resistance to oil and thermal aging in CPE/NR blends, *J. Appl. Polym. Sci.*, 96 (2005) 2218-2224

# Pervaporation Separation of Azeotropic Mixture of Tetrahydrofuran-Water System Using PVA/POSS membrane

---

## Summary

Chapter 4 deals with the pervaporation separation of azeotropic mixture of tetrahydrofuran (THF)-water system using PVA/POSS membrane. The membranes exhibited excellent water selectivity and permeance due to the preferential interaction of membrane towards water molecule in the azeotropic THF-water mixture. In the presence of PEG-POSS and Octa-TMA-POSS, PVA membrane exhibited a significant increase in selectivity. Swelling study and density measurements also supported the pervaporation performance of the membranes. Modified Maxwell-Stefan equation was used for the computation of theoretical flux and was compared with the experimental values.



## **4.1 Introduction**

Tetrahydrofuran (THF) is an extensively used highly volatile polar aprotic solvent. It is widely employed in chemical industry for the manufacture of pharmaceutical products, as reagent for drug synthesis, adhesives, paints and inks. Moreover, highly pure THF is required for the production of various polymers like poly (tetramethylene oxide) and its copolymers.<sup>1</sup> THF and water can easily form azeotrope at 94.7% of THF in mole fraction. It is difficult to obtain commercially important highly pure (99.9 mol%) THF from THF-water azeotropic mixture by conventional separation methods like distillation, liquid-liquid extraction and absorption. In industry, columns filled with molecular sieves are used to remove water from THF.<sup>2</sup> The distillation process creates many environmental, economical and technical challenges as well as a risk of explosion due to the reaction of THF with atmospheric oxygen.<sup>3</sup> The complex separation problem of the azeotrope can be solved by polymer membrane based pervaporation (PV) technology. It is an efficient, ecofriendly and easily performed separation method as compared to conventional separation process. The success of a pervaporation process depends on the morphology of membrane and its properties. Membranes with good selectivity and high permeability are desirable for the better separation of solvent mixtures.<sup>4-5</sup> Recently, silica-polymer hybrid membranes are found to be useful in drug release and separation of azeotropic liquid mixture due to its unique transport properties, which are not present in the individual components.<sup>6-8</sup>

Poly(vinyl alcohol) (PVA) is a water soluble, semicrystalline glassy polymer. PVA is used for the manufacture of membranes for separation process, artificial biomedical devices and drug delivery systems due to its good film

forming nature, chemical stability, hydrophilicity, biocompatibility and biodegradability. PVA membranes have the problem of swelling in certain solvents that leads to its reduced chemical, mechanical and separation properties. PVA modified with inorganic nanofillers are found to exhibit enhanced mechanical, thermal and separation properties even in the presence of aqueous solution. The hybrid systems exhibit some unique properties which are not present in individual components.<sup>9-14</sup> Nevertheless, there are still some other major drawbacks such as poor dispersion and incompatibility of fillers in the polymer matrix as well as weak interaction between inorganic fillers and polymers resulting in a trade-off between permeability and selectivity.

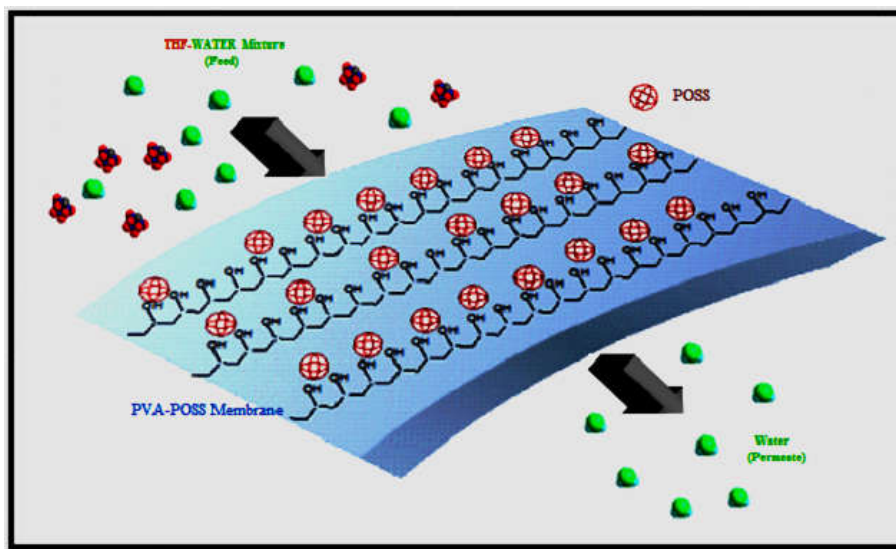
Polyhedral oligomeric silsesquioxane (POSS) is a potential three-dimensional nanofiller with unique inorganic/organic hybrid chemistry. Mostly studied POSS have cubic or cage shaped  $\text{Si}_8\text{O}_{12}$  core with a variety of eight substituent organic groups at the apex of silicon atom. The appropriate organically functionalised POSS can be easily incorporated into the polymer matrix at the molecular level.<sup>15-18</sup> The aim of the present study is to investigate the effect of varying amount of different organically functionalised POSS on the pervaporation performance of PVA membrane for the separation of THF-water azeotropic mixture. Le *et al.* developed Pebax/POSS mixed matrix membranes and they studied the ethanol dehydration performance of the membrane through pervaporation method. The presence of POSS in pebax improved the pervaporation performance of the membrane by the enhancement of both the separation factor and total flux.<sup>19</sup> Recently, Sairam *et al.* obtained a remarkable improvement in water selectivity during the pervaporation dehydration of tetrahydrofuran using poly(vinyl alcohol)-iron oxide nanocomposite membranes.<sup>20</sup> In the present

work, we demonstrated the successful fabrication of new class of PVA-POSS hybrid nanocomposite membranes by solution casting method. Two kinds of amphiphilic POSS namely anionic-octa(tetramethylammonium)-polyhedral oligomeric silsesquioxane (Octa-TMA-POSS) and polyethylene glycol-polyhedral oligomeric silsesquioxane (PEG-POSS) were employed for the preparation of membranes. As compared to reported system<sup>20</sup>, the present PVA/POSS system exhibited approximately four times higher water selectivity during the separation of azeotropic THF- water mixture.

## **4.2 Results and discussion**

### **4.2.1 Effect of POSS on pervaporation performance of PVA membrane**

The fabrication of membranes with high permeability and selectivity is a challenging problem for material scientists. In pervaporation process, permeation of solvent molecules across the polymer membrane occurs according to solution diffusion mechanism. The process carried out under reduced pressure consists of three steps: (1) dissolution of feed solvent mixture into the membrane (2) diffusion of permeate on upper and downstream side of the membrane and (3) desorption of permeate vapour. Permeability of the liquid molecule is the product of its solubility and diffusivity. The size of solvent molecule, affinity of membrane towards solvent molecule and mobility of polymer chain are the major factors that determine the penetrant diffusivity. A significant pervaporation performance such as high permeability and selectivity are observed in PVA/POSS membranes. A schematic representation for the pervaporation separation of azeotropic composition of THF-water system through the PVA/POSS membrane is presented in **Scheme 4.1**.



**Scheme 4.1:** Schematic illustration of the pervaporation separation of THF-water azeotropic mixture through PVA-POSS membrane.

The effect of POSS loading on the separation of THF-water azeotropic mixture through PVA membrane are evaluated from the permeation flux, separation factor and component flux. From **Figure 4.1** and **Table 4.1**, it is observed that the highest flux as well as permeance for PPP and POTP membranes are achieved at 3wt% of POSS. Compared with pure PVA membranes, PEG-POSS and Octa-TMA-POSS incorporated PVA membranes display 7.5 and 2.7 fold increase in permeance respectively. PVA membranes containing 3wt% of PEG-POSS exhibited maximum permeance when compared to other PVA/POSS membranes. This can be attributed to the functionalisation of cage structured silsesquioxane with low molecular weight poly(ethylene glycol) soft segment, which enhances the flexibility of the membrane and the diffusion of solvent molecules. DSC results reported in chapter 3 also supported the flexibility of PPP system. As shown in **Figure 4.2** and **Table 4.1** the maximum separation factor and selectivity towards water molecule are found to be maximum at 1 and 3 wt% of POSS for PPP

and POTP respectively. In comparison with pristine PVA membrane, the addition of PEG-POSS and Octa-TMA-POSS shows remarkable increase in selectivity. The experimentally observed result supported the high water selectivity of POTP membrane due to the preferential interaction of membrane towards water molecule. Anionic Octa-TMA-POSS has electrostatic (ion-dipole) interaction with water and PVA along with hydrogen bond formation between PVA and water molecule. The preferential interaction between water- Octa-TMA-POSS nanoparticles and improved crystallinity of POTP membrane leads to high selectivity of the membrane towards water over pristine PVA and PPP membranes. However, at higher concentration of Octa-TMA-POSS the interstitial space between polymer chains are occupied by the bulk POSS molecules and thereby the crystallinity as well as selectivity of the membrane decreases.<sup>21-22</sup> The remarkable separation performance of PVA/POSS membranes can be attributed to the good interaction of the membrane with water molecules, which promotes preferential transportation of water from THF-water azeotropic feed. At lower weight percentage of POSS, microcavities are formed at the particle-polymer interface to facilitate the solvent transport. Water molecule transport occurs easily when compared to THF molecule due to the lower molecular size of water than THF.<sup>18</sup> Although the dipole moment of THF and water are closer, the permittivity of THF are found to be lower due to the weaker THF-water interaction than water-water interaction.

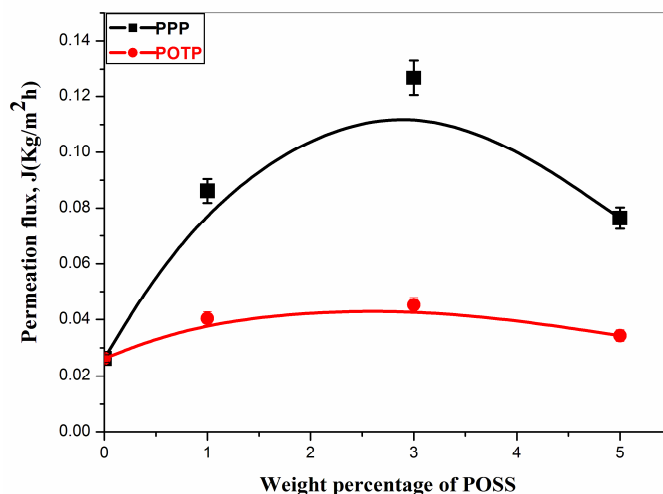


**Figure 4.1:** Effect of different weight percentage of POSS on permeation flux of PVA/POSS system for the separation of azeotropic composition of THF-water mixture

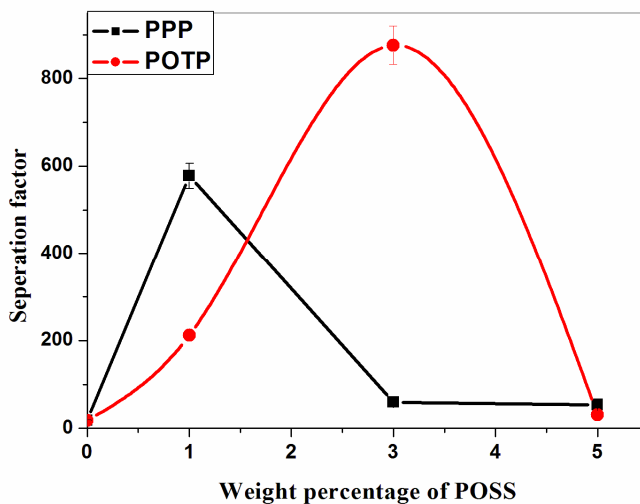


**Figure 4.2:** Effect of different weight percentage of POSS on separation factor of PVA/POSS system for the separation of azeotropic composition of THF-water mixture



**Table 4.1:** Variation of enrichment factor, pervaporation separation index, selectivity and permeance of PVA membrane with different weight percentage of POSS

Sample	Enrichment factor ( $\beta$ )	Pervaporation separation index (PSI)	Selectivity	Permeance (gpu)
P0	9.43	0.27	15	629
PPP1	18.30	57.60	917	3647
PPP3	14.52	7.45	81	4701
PPP5	14.15	4.01	73	2838
POTP1	15.66	8.51	119	1488
POTP3	18.49	41.07	1246	1714
POTP5	11.88	1.00	41	1294

Separation efficiency parameter of a membrane is most generally expressed in a term known as enrichment factor ( $\beta$ ), which is the ratio of weight fraction of water in permeate to the feed side and the values are presented in **Table 4.1**. Separation efficiency is found to be higher for PPP1 and POTP3 systems. Pervaporation separation index (PSI) includes both flux and separation factor variables and hence a single factor can assess the performance of the membrane. It is observed that PPP1 and POTP3 systems show better pervaporation performance when compared to pristine PVA and other PVA/POSS systems due to good compatibility of PEG-POSS and Octa-TMA-POSS in PVA matrix at lower concentration. The component flux for THF and water is found to be almost equal for neat PVA, which is shown in **Figure 4.3 (a-b)**. It is interesting to note that the incorporation of hydrophilic POSS enhances the water selectivity of the membrane. The total flux and flux values of water are found to be almost equal in PVA, while the THF flux is

dramatically reduced in PVA/POSS due to its large size, which restrict the diffusion through the membrane.

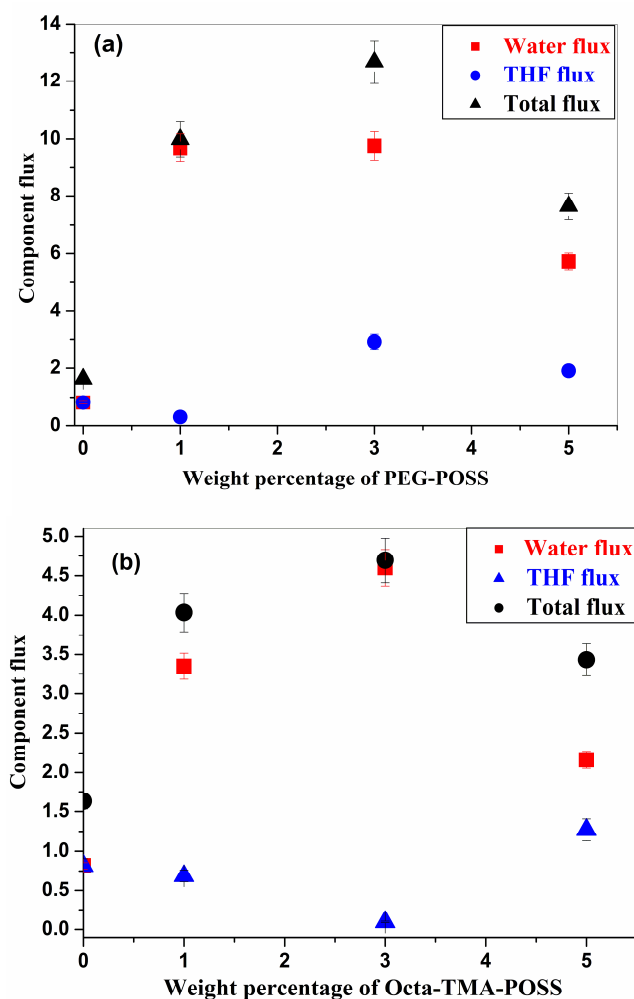


**Figure 4.3 (a-b):** Effect of different weight percentages of (a) PEG- POSS and (b) Octa-TMA-POSS on component flux.

Degree of swelling ( $DS$ ) and diffusion coefficient of the membranes are presented in **Table 4.2**. The PVA-POSS membranes show higher  $DS$  and diffusion coefficient for water ( $D_{water}$ ) compared with the pristine PVA

membrane because of the high affinity of PVA/POSS system towards water molecule as compared with PVA. These observations also supported the pervaporation performance of PVA/POSS membranes during the separation of THF-water azeotropic mixture.

**Table 4.2:** Degree of swelling and diffusion parameters of azeotropic composition of THF-water mixture in PVA/POSS membrane

Membrane	Degree of swelling (%)	$D_{\text{water}} \times 10^5 (\text{cm}^2/\text{s})$	$D_{\text{THF}} \times 10^5 (\text{cm}^2/\text{s})$
P0	20	6.00	5.88
PPP1	26	18.89	4.55
PPP3	29	19.63	9.00
PPP5	26	11.19	2.55
POTP1	23	9.12	3.00
POTP3	24	8.12	4.82
POTP5	21	6.11	5.23

#### 4.2.2 Application of modified Maxwell-Stefan equation for pervaporation separation of THF-water azeotropic mixture

An appropriate transport model can predict the success of a membrane to be used in pervaporation process. This help to fabricate excellent membranes and scale up the pervaporation separation of liquid mixtures. The transport of multicomponents in a feed through a membrane during pervaporation (PV) has been modeled by Maxwell-Stefan in support of solution diffusion model. Mason and Viehland further modified this model based on the principles of statistical mechanics and the classical mechanical Liouville equation. The modified Maxwell-Stefan equation takes into account the relationship between chemical potential driving force and friction resistance in multi-component mixture. This equation can be written as follows

$$\frac{d\mu_i}{dz} = \sum_{j=1}^n x_j (v_j - v_i) \frac{RT}{D_{ji}^0} \quad (4.1)$$

where  $\mu_i$  and  $\frac{d\mu_i}{dz}$  are the chemical potential and chemical potential gradient of component i respectively.  $x_j$  are the mole fraction of j components where  $j = 0, 1, 2, \dots, n$ .  $v$  are the local velocities of the components and  $\frac{RT}{D_{ji}^0}$  correspond to frictional coefficient, which represents the frictional effect exerted by component j on component i.

The modified Maxwell-Stefan model described the flux equations for the three component system, ie., a binary mixture and membrane in pervaporation process. It is expressed in equations (4.2) and (4.3).<sup>23-24</sup>

$$J_1 = \overline{D_{1M}} \left( \frac{\overline{D_{2M}} \overline{w_1}' + D_{12}}{D_{12} + \overline{D_{2M}} \overline{w_1}' + \overline{D_{1M}} \overline{w_2}'} \right) \overline{\rho}_M \frac{\Delta w_1'}{\delta_M} + \overline{D_{1M}} \left( \frac{\overline{D_{2M}} \overline{w_1}'}{D_{12} + \overline{D_{2M}} \overline{w_1}' + \overline{D_{1M}} \overline{w_2}'} \right) \overline{\rho}_M \frac{\Delta w_2'}{\delta_M} \quad (4.2)$$

$$J_2 = \overline{D_{2M}} \left( \frac{\overline{D_{1M}} \overline{w_2}' + D_{12}}{D_{12} + \overline{D_{1M}} \overline{w_2}' + \overline{D_{2M}} \overline{w_1}'} \right) \overline{\rho}_M \frac{\Delta w_2'}{\delta_M} + \overline{D_{2M}} \left( \frac{\overline{D_{1M}} \overline{w_2}'}{D_{12} + \overline{D_{1M}} \overline{w_2}' + \overline{D_{2M}} \overline{w_1}'} \right) \overline{\rho}_M \frac{\Delta w_1'}{\delta_M} \quad (4.3)$$

where  $\overline{w}_i' = (w_{iF}' + w_{iP}') / 2$ ,  $\Delta w_i' = w_{iF}' - w_{iP}'$ ,  $w_{iF}'$  and  $w_{iP}'$  represents the weight fraction of component i in the feed and in the permeate respectively,

$\delta_M$  denotes the thickness of the membrane,  $\bar{\rho}_M$  is the average density of the swollen polymer membrane,  $D_{iM}$  is diffusion coefficient of pure components ie, THF and water in the active layer of the membrane and  $\overline{D_{iM}}$  is the average diffusion coefficient.  $D_{12}$  lies between diffusion coefficient ( $D_1$  and  $D_2$ ) of pure components, which can be adjusted to the experimental partial fluxes.

$\overline{D_{iM}}$  and  $\bar{\rho}_M$  are defined as:

$$\overline{D_{iM}} = \frac{\int_{w'_{iP}}^{w'_{iF}} D_{iM}(w'_i) dw'_i}{w'_{iF} - w'_{iP}} \quad (4.4)$$

$$\bar{\rho}_M = \frac{\int_{w'_{iP}}^{w'_{iF}} \rho_M(w'_i) dw'_i}{w'_{iF} - w'_{iP}} \quad (4.5)$$

The above theoretical modeling is applied to PVA and PVA-POSS nanocomposite membrane for the pervaporation separation of THF-water azeotropic mixture. In **Figure 4.4 (a-b)**, experimentally achieved total permeate flux is compared with that obtained by applying the modified Maxwell-Stefan model. It is interesting to note that, at lower loading of POSS, theoretical flux is higher than experimental flux while at higher weight percentage of POSS the experimental value is in good agreement with theoretical flux owing to the interaction between the functionalised POSS and solvent molecules.

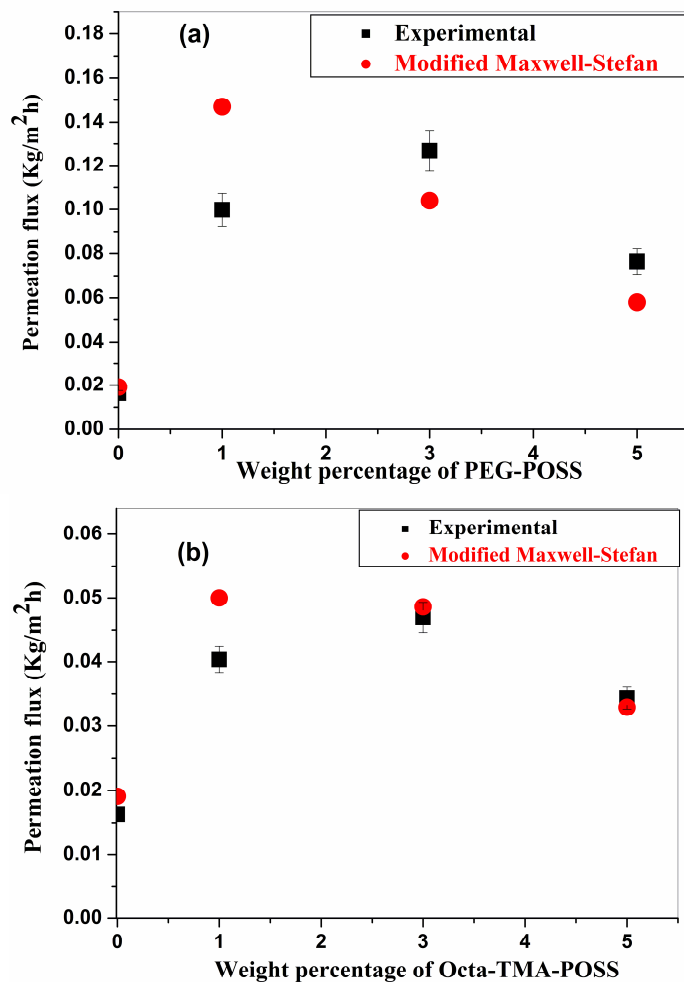


Figure 4.4 (a-b): Experimental and theoretical flux vs. weight percentage of (a) PEG-POSS and (b) Octa-TMA-POSS

### 4.3 Conclusions

We report an effective, ecofriendly and easy method for the separation of THF-water azeotropic mixture through membrane pervaporation technology. The amphiphilic POSS incorporated PVA membranes exhibited excellent pervaporation performance for the separation of THF-water azeotropic

mixture. The hydrophilic POSS introduced PVA membrane had exhibited excellent water selectivity and permeance due to the preferential interaction of membrane towards water molecule in the azeotropic THF-water mixture. Swelling study and density measurements also supported the pervaporation performance of the membranes. As compared with pure PVA, PEG-POSS and Octa-TMA-POSS introduced PVA showed 61 and 83 fold increase in selectivity as well as 7.5 and 2.7 fold increase in permeance respectively. From the results, it is revealed that PEG-POSS and Octa-TMA-POSS were found to be suitable nanostructured material to improve the permeability and selectivity of PVA membrane. Using modified Maxwell-Stefan equation, theoretical permeation flux values of composites were estimated and compared with experimental values. Better agreement between experimental and theoretical values at higher weight percentage of POSS was observed, suggesting good interaction between POSS and solvent molecules.

#### 4.4 References

1. C. Fodor, G. Kali, R Thomann, Y. Thomann, B. Ivan R. Mulhaupt, Nanophasic morphologies as a function of the composition and molecular weight of the macromolecular cross-linker in poly(*N*-vinylimidazole)-*l*-poly(tetrahydrofuran) amphiphilic conetworks: bicontinuous domain structure in broad composition ranges, *RSC Advan.*, 7 (2017) 6827-6834.
2. D. Bradley, G. Williams, M. Lawton, Drying of organic solvents: quantitative evaluation of the efficiency of several desiccants. *J. Org. Chem.*, 75 (2010) 8351-8354.
3. A. Urtiaga, P. F. Castro, P. Gómez, I. Ortiz, Remediation of wastewaters containing tetrahydrofuran. Study of the electrochemical mineralization on BDD electrodes, *Chem. Eng. J.*, 239 (2014) 341-350.
4. L. M. Vane, V. Namboodiri, G. Lin, M. Abar, F.R. Alvarez, Preparation of water-selective polybutadiene membranes and their use in drying alcohols by pervaporation and vapor permeation technologies, *ACS Sustainable Chem. Eng.*, 4 (8) (2016) 4442-4450.
5. Y. J. Han, W. C. Su, J. Y. Lai, Y. L. Liu, Hydrophilically surface-modified and crosslinked polybenzimidazole membranes for pervaporation dehydration on tetrahydrofuran aqueous solutions, *J. Mem. Sci.*, 475 (2015) 496-503.
6. L. L. Xia, C. L. Li, Y. Wang, In-situ crosslinked PVA/organosilica hybrid membranes for pervaporation separations, *J. Mem. Sci.*, 498 (2016) 263-275.
7. Z. Osvath, T. Toth, B. Ivan, Synthesis, characterization, LCST-type behavior and unprecedented heating-cooling hysteresis of poly(*N*-isopropylacrylamide-*co*-3-(trimethoxysilyl)propyl methacrylate) copolymers, *Polymer* 108 (2017) 395-399.
8. Z. Osvath, T. Toth, B. Ivan, Sustained Drug Release by Thermoresponsive sol-gel hybrid hydrogels of poly(*N*-isopropylacrylamide-*co*-3-(trimethoxysilyl) propyl methacrylate)



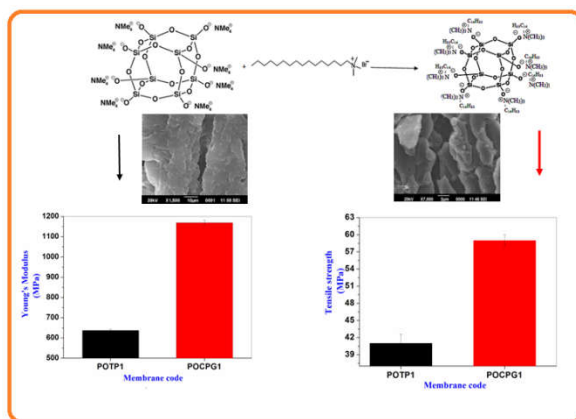
- copolymers, *Macromol. Rapid. Commun.*, 38 (2017)  
DOI:10.1002/marc.201600724
9. Z. Qiao, Y. Wu, X. Li, J. Zhou, Molecular simulation on the separation of water/ethanol azeotropic mixture by poly (vinyl alcohol) membrane, *Fluid Phase Equil.*, 302 (2011) 14-20.
  10. Q. G. Zhang, B. C. Fan, Q. L. Liu, A. M. Zhu, F. F. Shi, A novel poly(dimethyl siloxane)/poly(oligosilsesquioxanes) composite membrane for pervaporation desulfurization, *J. Mem. Sci.*, 366 (2011) 355-341.
  11. N. L. Le, Y. P. Tang, T. S. Chung, The development of high-performance 6FDA- NDA/DABA/POSS/Ultem<sup>®</sup> dual-layer hollow fibers for ethanol dehydration via pervaporation, *J. Mem. Sci.*, 447 (2013) 163-176.
  12. Y. Shirazi, M.A. Tofighy, T. Mohammadi, Synthesis and characterization of carbon nanotubes/poly vinyl alcohol nanocomposite membranes for dehydration of isopropanol, *J. Mem. Sci.* 378 (2011) 551-561
  13. Y. Zhu, S. Xia, G. Liu, W. Jin, Preparation of ceramic-supported poly(vinyl alcohol)-chitosan composite membranes and their applications in pervaporation dehydration of organic/water mixtures, *J. Mem. Sci.*, 349 (2010) 341-348.
  14. V. T. Magalad, G. S. Gokavi, K. V. S. N. Rajub, T. M. Aminabhavi, Mixed matrix blend membranes of poly(vinyl alcohol)-poly(vinyl pyrrolidone) loaded with phosphomolybdic acid used in pervaporation dehydration of ethanol, *J. Mem. Sci.*, 354 (2010) 150-161
  15. Q. Zhang, H. He, K. Xi, X. Huang, X. Yu, X. Jia, Synthesis of *N*-phenylaminomethyl POSS and its utilization in polyurethane, *Macromolecules* 44 (3) (2011) 550-557.
  16. P. Chen, X. Huang, Q. Zhang, K. Xi, X. Jia, Hybrid networks based on poly(styrene-co-maleic anhydride) and *N*-phenylaminomethyl POSS, *Polymer* 54 (2013) 1091-1097.
  17. K. N. Raftopoulos, S. Koutsoumpis, M. Jancia, J. P. Lewicki, K. Kyriakos, H. E. Mason, S.J. Harley, E. Hebda, C. M. Papadakis, K.

- Pielichowski, P. Pissis, Reduced phase separation and slowing of dynamics in polyurethanes with three-dimensional POSS-based cross-linking moieties, *Macromolecules* 48 (5) (2015) 1429-1441.
18. M. L. Chua, L. Shao, B. T. Low, Y. Xiao, T. S. Chung, M. L. Chua, L. Shao, B.T. Low, Y. Xiao, T. S. Chung, Polyetheramine-polyhedral oligomeric silsesquioxane organic-inorganic hybrid membranes for CO<sub>2</sub>/H<sub>2</sub> and CO<sub>2</sub>/N<sub>2</sub> separation, *J. Mem. Sci.*, 385-386 (2011) 40-48.
19. N. L. Le, Y. Wang, T. S. Chung, Pebax/POSS mixed matrix membranes for ethanol recovery from aqueous solutions via pervaporation, *J. Mem. Sci.*, 379 (2011) 174-183.
20. M. Sairam, B.V.K. Naidu, S. K. Nataraj, B. Sreedhar, T. M. Aminabhavi, Poly (vinyl alcohol)-iron oxide nanocomposite membranes for pervaporation dehydration of isopropanol, 1, 4-dioxane and tetrahydrofuran, *J. Mem. Sci.*, 283 (2006) 65-73
21. V. P. Swapna, D. Ponnamma, K. K. Sadasivuni, S. Thomas, R. Stephen, Effect of nanostructured polyhedral oligomeric silsesquioxane on the physical properties of poly (vinyl alcohol), *J. Appl. Polym. Sci.*, 134 (2017) 45447
22. N. L. Le, Y. Wang, T. S. Chung, High performance sulfonated polyimide/polyimide/polyhedraloligomeric silsesquioxane hybrid membranes for ethanol dehydration applications, *J. Mem. Sci.*, 45 (2014) 462-73.
23. U. K. Ghosh, N.C. Pradhan, B. Adhikari, Separation of water and o-chlorophenol by pervaporation using HTPB-based polyurethaneurea membranes and application of modified Maxwell-Stefan Equation, *J. Mem. Sci.*, 272 (2006) 93-102.
24. P. Izak, L. Bartovska, K. Friess, M. Sipek, P. Uchytíl, Description of binary liquid mixtures transport through non-porous membrane by modified Maxwell-Stefan equations, *J. Mem. Sci.*, 214 (2003) 293-309.

# Characterisation, Mechanical and Pervaporation Performance of Chemically Modified PVA/POSS Membranes

## Summary

Permselective polymeric membranes are important materials for the efficient separation of organic solvents and azeotropic mixtures. In this work, we address an effective strategy to the fabrication of novel high performance membranes of crosslinked poly(vinyl alcohol) (PVA) by incorporating chemically modified cage structured polyhedral oligomeric silsesquioxane (*m*-POSS) through solution casting method. The fabricated PVA/*m*-POSS system shows excellent mechanical stability as well as good pervaporation performance for the separation of isopropanol (IPA)-water azeotropic mixture. Moreover, the membranes exhibited excellent water selectivity, hydrophilicity and excellent anti-fouling properties compared to traditional hydrophilic membranes. The excellent mechanical properties and other comprehensive properties reveal the potential of the PVA/*m*-POSS system for the effective separation of azeotropic IPA-water mixture. Modified Maxwell-Stefan model applied for the theoretical estimation of permeation flux and it was in good agreement with the experimental findings.



This chapter has been published in *Journal of Materials Science*, Springer, 2019, 54, 8319-8331

## **5.1 Introduction**

The liquid-liquid mixture separation is considered to be one of the major challenges in chemical and pharmaceutical industries. Conventional separation methods like distillation is an energy-exhausting process, it produces many environmental, economical, technical issues and is ineffective to separate azeotropic mixtures. Currently, polymer membrane-based pervaporation (PV) technology is extensively used instead of the distillation process for the efficient separation of organic-water mixtures, organic-organic mixtures, purification of water by removing dilute organic species and separation of azeotropic mixtures.<sup>1</sup> Solution-diffusion model can be employed to demonstrate the liquid mixture separation based on PV technique across the nonporous dense polymeric membranes.<sup>2</sup> PV dehydration process of solvents utilizes relatively high water soluble and diffusible hydrophilic polymer membranes for effective outcomes. Generally, the membrane material would exhibit trade-off effect between permeability and selectivity during separation. There are many regulation methods to be adopted for membranes such as nanomaterial doping, blending, surface modifications etc. to improve PV performance by achieving high flux coupled with selectivity for desired permeate.<sup>3-6</sup>

The intrinsic PV performance of polymeric membranes vary significantly depending on the degree of hydrolysis, molecular weight of polymers, crosslinking degree, nature of crosslinks and membrane structure. Surface wettability of a polymer membrane has profound effect on solution-diffusion based pervaporation process. The wettability of membrane increases the water molecule dissolution on membrane surface and diffusion across the membranes during solvent dehydration process.<sup>7</sup> Poly(vinyl alcohol) (PVA) is widely utilized in the separation process due to its hydrophilicity, abundant availability, nontoxicity and barrier properties. However, its hydrophilic

nature reduces the mechanical stability of the membrane, which deteriorates the selectivity of these polymer membranes during PV process. Hence the hydrophilic polymers are not suitable for dehydration applications of high water containing solutions. It can be rectified by the modification of PVA through blending, crosslinking or grafting. Kursun and Isiklan developed poly(vinyl alcohol)-g-poly(N-isopropylacrylamide) membrane for the pervaporation separation of azeotropic composition of isopropyl alcohol/water mixtures.<sup>8</sup> The addition of nanofillers to the polymers enhance the thermal and mechanical stability as well as permeance and selectivity of the membranes.<sup>9-13</sup> However, several limitations exist in the membrane systems such as poor homogeneous dispersion and incompatibility of fillers in the polymer matrix as well as weak interaction between the filler and polymer resulting in a poor PV performance.

In the present study, we explored the introduction of modified polyhedral oligomeric silsesquioxane (m-POSS) moiety into the crosslinked poly(vinyl alcohol) architecture by solution casting method. The effect of m-POSS on the PV performance and mechanical property of crosslinked PVA were analysed. The possibility of fine-tuning of the functional groups of POSS not only brings the diversity but also provide good compatibility with the polymer matrix. The improved performance of polymer-POSS systems can be mainly attributed to the presence of strong siloxane core as well as the functional groups attached to it.<sup>14-18</sup>

## 5.2 Results and discussion

### 5.2.1 Characterisation

FT-IR spectra of Octa-TMA-POSS, CTAB and CTAB modified Octa-TMA-POSS (m-POSS) are shown in **Figure 5.1**. The replacement of  $(\text{CH}_3)_4\text{N}^+$  groups by  $(\text{C}_{16}\text{H}_{33})\text{N}^+(\text{CH}_3)_3$  by ion-exchange reaction is confirmed from the FTIR spectra. For Octa-TMA-POSS, the peaks at 1012, 1404, 1652 and 2917  $\text{cm}^{-1}$  denotes the characteristic Si-O,  $\text{CH}_3\text{N}$ ,  $\text{CH}_3\text{NO}$  and C-H stretching vibrations respectively. CTAB shows two intense bands at 2917 and 2849  $\text{cm}^{-1}$  corresponding to the asymmetric and symmetric stretching vibrations of C- $\text{CH}_2$  in the methylene chains of cetyltrimethylammonium. The strong peak at 1431 and 1472  $\text{cm}^{-1}$  is attributed to the deformation of  $-\text{CH}_3$  and  $-\text{CH}_2$  groups. The weak peak at 3016  $\text{cm}^{-1}$  in CTAB is characteristic of C- $\text{CH}_3$  asymmetric stretching and N- $\text{CH}_3$  symmetric stretching vibrations of cetyltrimethylammonium. All the characteristic peaks of cetyltrimethylammonium group are clearly observed in m-POSS, which suggest the replacement of  $(\text{CH}_3)_4\text{N}^+$  groups by  $(\text{C}_{16}\text{H}_{33})\text{N}^+(\text{CH}_3)_3$  by ion-exchange reaction. The peak at 1022  $\text{cm}^{-1}$  denotes the characteristic Si-O-Si stretching vibration, which indicates the occurrence of silsesquioxane core in m-POSS.<sup>19</sup>

The successful attachment of cetyltrimethylammonium group on silsesquioxane cage is further confirmed by  $^1\text{H}$  NMR spectra presented in **Figure 5.2**. Proton signal observed at 0.88, 1.25, 1.70 and 3.30 ppm are corresponding to groups in the m-POSS as marked in the structure given in nmr spectra.<sup>19</sup>

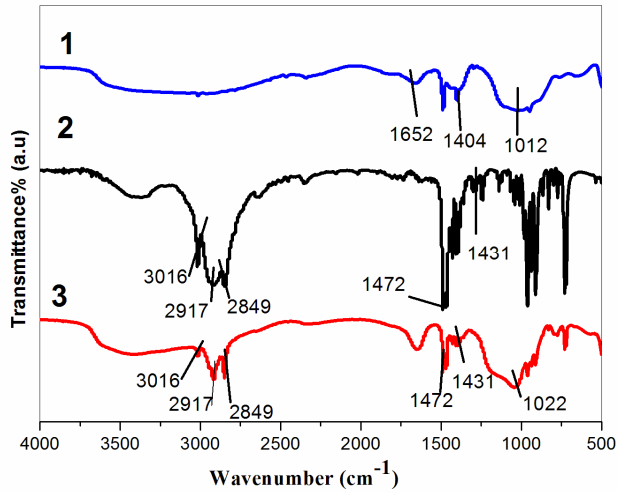


**Figure 5.1:** FT-IR spectra of (1) Octa-TMA-POSS, (2) CTAB and (3) CTAB modified Octa-TMA-POSS (m-POSS)

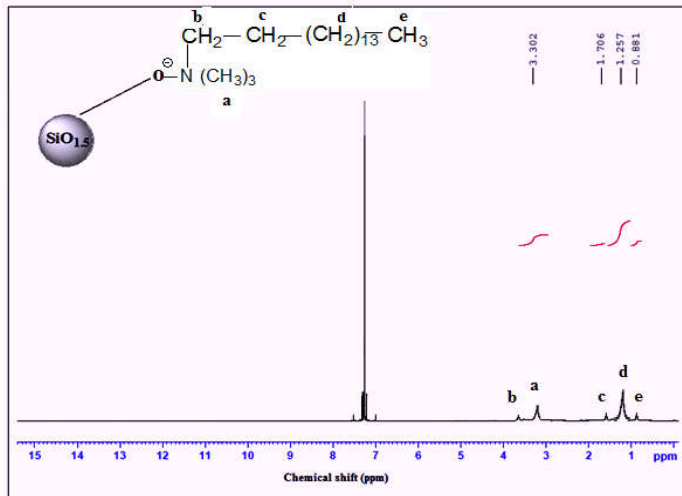


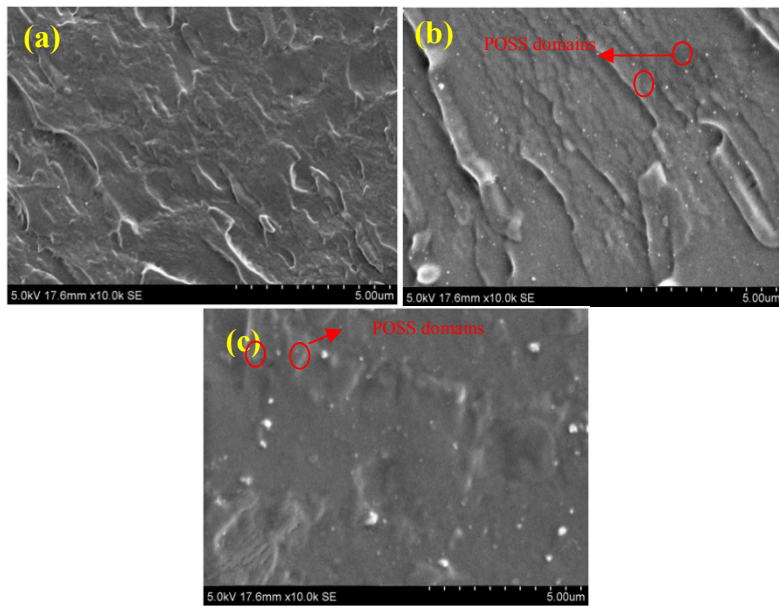
**Figure 5.2:**  $^1\text{H}$  NMR spectra for m-POSS

### 5.2.2 Morphology

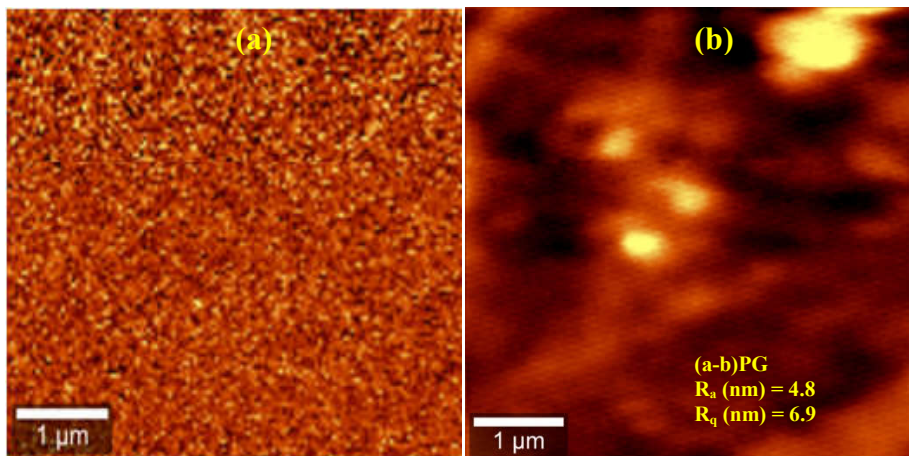
SEM and AFM analysis have been carried out to study the effect of m-POSS particles on the morphological features of crosslinked PVA. The main challenge in the fabrication of nanostructured materials incorporated polymer membrane is the homogeneous dispersion of nanosized material into the polymer matrix. **Figure 5.3** shows SEM image of crosslinked PVA (coded as PG) and PVA/m-POSS membranes. Spherical structured POSS particles can be seen in the surface of polymer matrix. This shows a homogeneous dispersion of m-POSS in the PVA matrix without forming any aggregation. While at higher loading, slight aggregations of m-POSS particles are observed in the PVA matrix owing to its tendency to reduce its surface area and surface activity by forming POSS-POSS network.

**Figure 5.4** is the phase and height AFM images of crosslinked PVA and PVA/m-POSS. Here morphology of 3wt% m-POSS introduced PVA membranes are compared with the PVA. The roughness parameter  $R_a$  and  $R_q$  represents the average and root mean square deviation of height respectively.  $R_q$  value for PVA is 6.9 whereas POC PG3 membrane exhibit higher roughness value. The increased surface roughness can be attributed to the surface reorganization of PVA chains by the incorporation of m-POSS. Increase in surface roughness leads to increase in sorption sites in the membrane which is further corroborated in the pervaporation studies.





**Figure 5.3:** SEM images of cryofractured cross section of (a) PG (b) POCPG1 (c) POCPG3



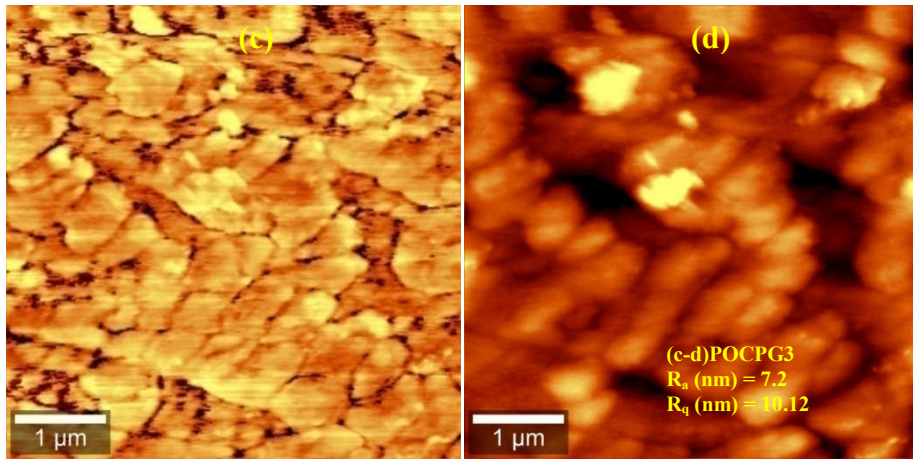


**Figure 5.4:** Phase (left picture) and height (right picture) AFM images of (a-b) PG (c-d) POCPG3

### 5.2.3 Water uptake and contact angle studies

Water uptake capacity of a polymer membrane has a profound effect on its both mechanical and pervaporation performances. The driving force for the water uptake of PVA is its hydrophilicity. The effect of introduction of modified POSS on the water uptake capacity of PVA membranes has been examined. It is found that the functional groups on the POSS has significant effect on the water absorption capacity of the membrane.

The water uptake capacity of the membranes are calculated using the equation (2.12) given in the chapter 2 and is depicted in **Figure 5.5**. All membranes show rapid initial water uptake followed by levelling off to an equilibrium value. It is interesting to observe that water uptake of PVA/m-POSS system is higher than that of PVA due to the presence of electrostatic interaction between anionic amphiphilic POSS and water.

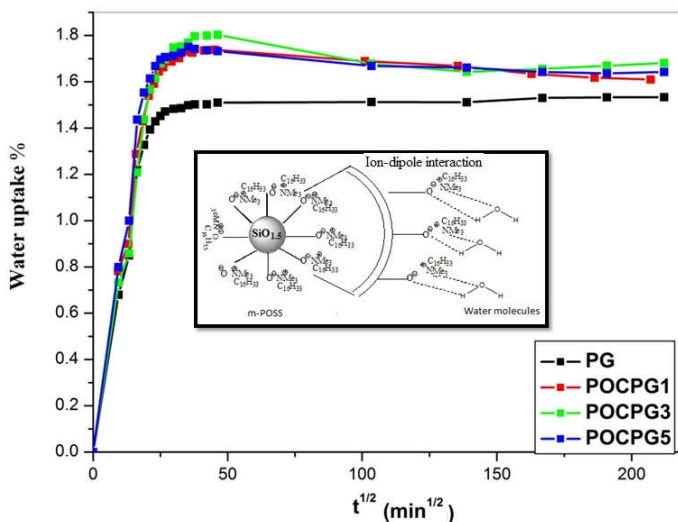


**Figure 5.5:** Water uptake of crosslinked PVA and PVA/m-POSS systems as a function of time

The wetting phenomenon is governed by geometrical structure as well as surface chemistry of the material, which is characterised by contact angle measurements. The water droplet on a hydrophilic films exhibit very fast spreading or absorption on the surface and exhibit water contact angle (CA) less than  $90^\circ$ , which is found to be an extensive practical application in industries, medicine, agriculture and daily life. The wetting characteristics such as work of adhesion, work of spreading and energy of hydration for a hydrophilic surface is 73, 0 and  $146 \text{ mJm}^{-2}$  respectively. As shown in **Figure 5.6** the PVA membrane exhibits a contact angle of  $80^\circ$ . However, the contact angle value of 1wt% m-POSS doped PVA system is  $46^\circ$  and  $\theta$  is further reduced upon increasing the weight fraction of POSS. The reason behind the increased wettability of PVA by the introduction of m-POSS is the good electrostatic (ion-dipole) interaction between high density hydroxyl group at the surface of the PVA with POSS as well as good affinity of POSS molecule with water. The newly introduced cetyltrimethylammonium side group on the POSS provides improved wetting characteristic for PVA membrane due to its

amphiphilic nature capable of interacting with water. The observation is in well agreement with AFM characterisation. Generally, wettable materials with rough surface have lower water contact angle.<sup>20-21</sup>

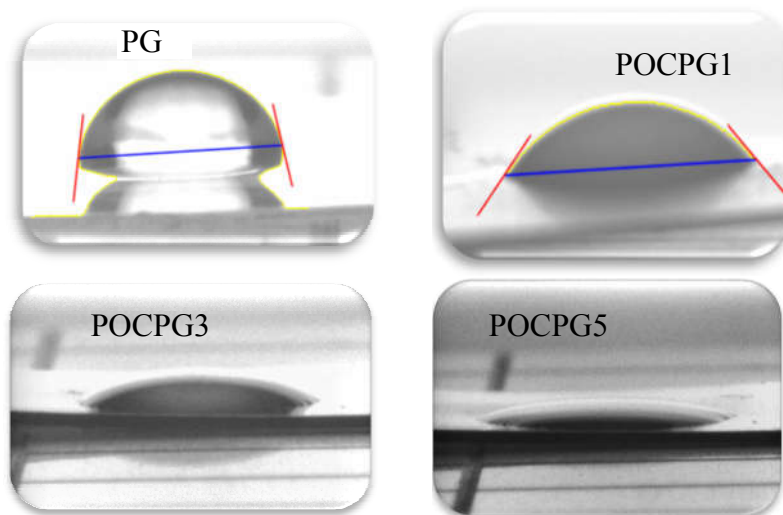


**Figure 5.6:** Water contact angle images on the surface of crosslinked PVA and PVA/m-POSS membranes

#### 5.2.4 Differential scanning calorimetry (DSC)

**Figure 5.7** presents the DSC curves of the PVA and PVA/m-POSS systems recorded during heating and cooling cycle. A significant improvement in melting and crystallisation parameters of PVA can be observed upon the introduction of m-POSS (1wt %). From the heating curve, the glass transition temperature ( $T_g$ ) of crosslinked PVA is found to be 79°C and is shifted to 81°C by embedding 1wt % of m-POSS molecule as presented in **Table 5.1**. This result demonstrates the restricted mobility of PVA chain in the presence of bulky and rigid POSS cages. The shift in melting temperature ( $T_m$ ) to higher temperature can be observed in PVA/m-POSS and is due to the influence of POSS moieties on the improved crystallinity of PVA. It is owing to the nucleation ability of m-POSS particles in PVA matrix. At higher weight percentage of POSS, there is a marginal decrease in melting and

crystallisation properties of PVA due to the slight agglomeration of m-POSS particles in the polymer chain, as seen in FE-SEM.

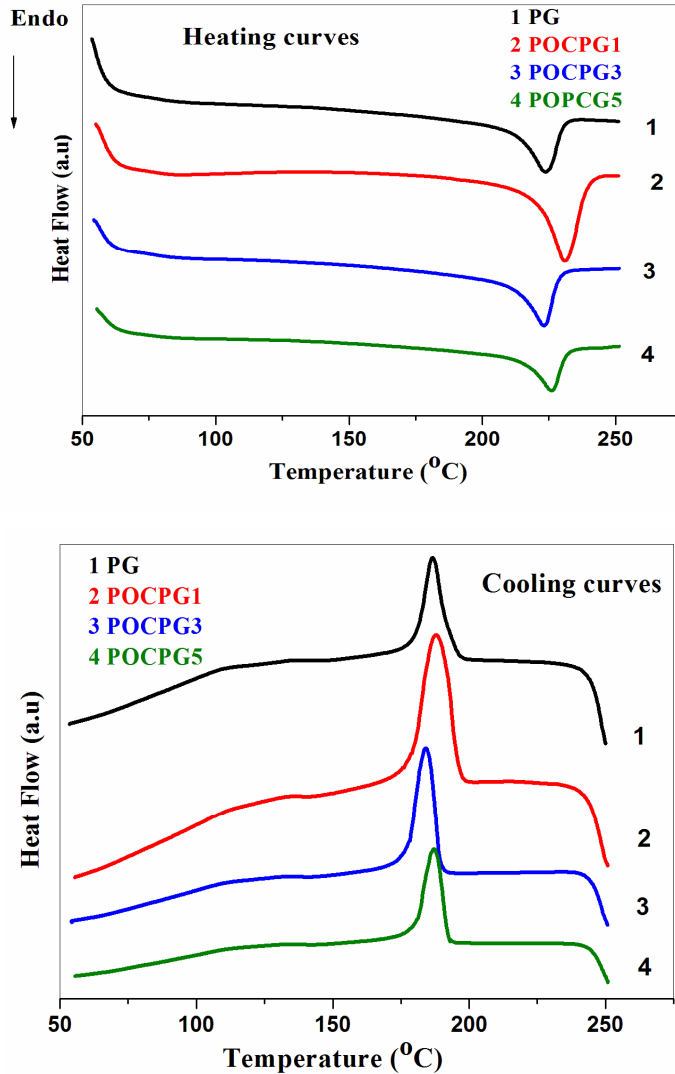
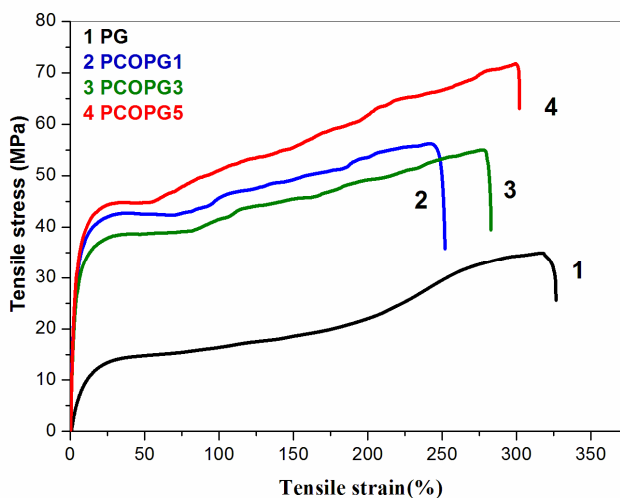


Figure 5.7: Heating and cooling curves of crosslinked PVA and PVA/m-POSS membranes.

### 5.2.5 Mechanical properties

The focus on introducing cetyltrimethylammonium group modified POSS to the PVA matrix is to improve its mechanical stability as well as transport properties. The mechanical properties of the PVA/m-POSS greatly depend on various factors such as properties of PVA, structure, dispersion, crosslinking, functional groups present on the m-POSS and the interfacial interaction between the PVA matrix and m-POSS nanoparticles. The mechanical strength of PVA/m-POSS system increases significantly due to the reinforcement effect of m-POSS, which acts as stress transferring agents. Typical stress-strain diagram of PVA and m-POSS incorporated PVA systems are depicted in **Figure 5.8** and tensile testing data are tabulated in **Table 5.1**. For PVA, its average Young modulus and tensile strength are 144 and 35 MPa respectively. It is interesting to observe that the introduction of CTAB modified POSS in PVA created a dramatic improvement in mechanical properties such as Young's modulus and tensile strength. 1wt% m-POSS introduced PVA membrane exhibits about 8-fold increase in Young's modulus (1169MPa) relative to the PVA matrix. The reason behind it is the better dispersion of POSS in a large interfacial area of the PVA matrix. Uniform dispersion and compatibility of m-POSS in PVA matrix is evident from SEM analysis. PVA/m-POSS exhibits maximum tensile strength at 5wt% of m-POSS loading; it is about 202% higher than that of PVA. This can be ascribed to the good interfacial interaction between PVA and m-POSS resulted in exceptional load transfer between PVA and rigid siloxane core. Jiang *et al.* recently reported that the tensile strength of PVA is increased by 57% upon the incorporation MoS<sub>2</sub> functionalised POSS.<sup>22</sup> PVA reinforced with melamine (MA) also showed improved tensile strength and Young's modulus, it increases to about 22 and 25% respectively.<sup>23</sup> About 181 and 198% increase in tensile strength and modulus is observed for PVA by the incorporation of aryl diazonium salt functionalised graphene (ADS-G).<sup>24</sup>

In chapter 3 the mechanical properties of Octa-TMA-POSS incorporated uncrosslinked PVA is presented and found that the tensile strength and Young's modulus of PVA improves to 122 and 321% respectively in the presence of POSS, which is much lower than the present system.<sup>25</sup> Hence the introduction of CTAB modified Octa-TMA-POSS in the crosslinked PVA is an effective method to achieve excellent mechanical performance of PVA membrane. As seen in **Figure 5.8**, a slight reduction in the ductility and toughness of crosslinked PVA/m-POSS observed in an acceptable range at lower loading of POSS due to the restricted free movement of PVA chains. The presence of long alkyl chain on m-POSS imparts CH<sub>2</sub>-CH<sub>2</sub> interaction within the crosslinked membrane, which boost up greater intermolecular forces between chains.



**Figure 5.8:** Stress-strain response of crosslinked PVA and PVA/m-POSS membranes

**Table 5.1:** Thermal and mechanical properties of the crosslinked PVA and PVA/m-POSS systems

Sample	Tensile Strength (MPa)	Young's Modulus (MPa)	Elongation @Break (%)	T <sub>m</sub> (°C)	ΔH <sub>f</sub> (J/g)	T <sub>g</sub> (°C)	T <sub>c</sub> (°C)	ΔH <sub>c</sub> (J/g)	% crystallinity
PG	35±2	144±4.7	303±3.9	224	52	79	190	60	37
POCPG1	57±3	1169±5.1	251±5.8	230	58	81	193	66	41
POCPG3	57±4	1156±4.6	283±4.9	224	52	80	188	61	37
POCPG5	71±4	1069±4.2	302±4.9	226	49	79	189	59	35

Guth, Kerner and Frankle–Acrivos models are exercised to assess the Young’s modulus of PVA/m-POSS membranes.<sup>26-28</sup> Equations are presented in chapter 3 of the thesis (Equations. 3.2, 3.3 and 3.4).

Theoretically computed values are depicted in **Figure 5.9**. Theoretical calculations are based on the assumption of spherical nature of POSS particles. Experimentally observed Young’s moduli are found to be higher than theoretical values. This can be attributed to the good interfacial interaction between PVA and m-POSS.

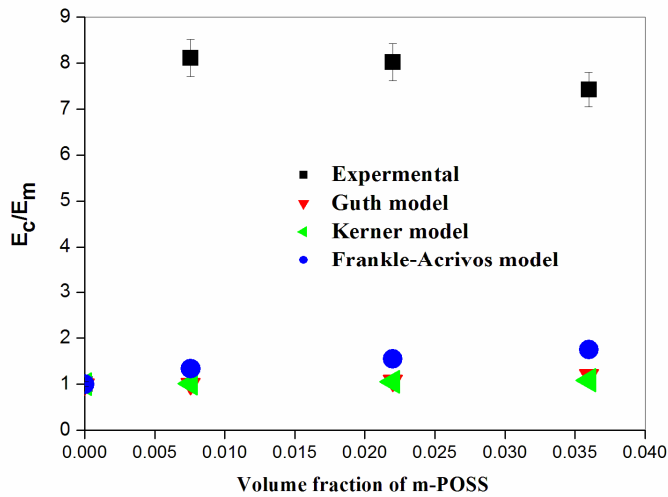


**Figure 5.9:** Comparison of experimental Youngs modulus with various theoretical models



PVA and m-POSS interaction and their mechanical behaviour can be correlated from the microscopic examination of the fracture surface. SEM micrograph of tensile fracture surface of 3wt% m-POSS embedded PVA membrane is presented in **Figure 5.10**. PVA/m-POSS system exhibit the crack bifurcation with the least expenditure of energy for the fracture. The good dispersion and the strong adhesion of PVA and m-POSS enhances the effective stress transfer between PVA and POSS.

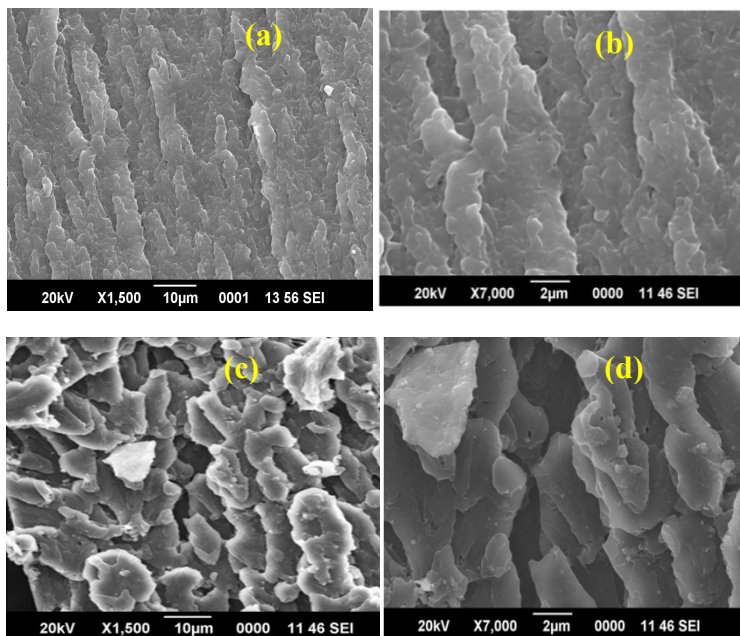
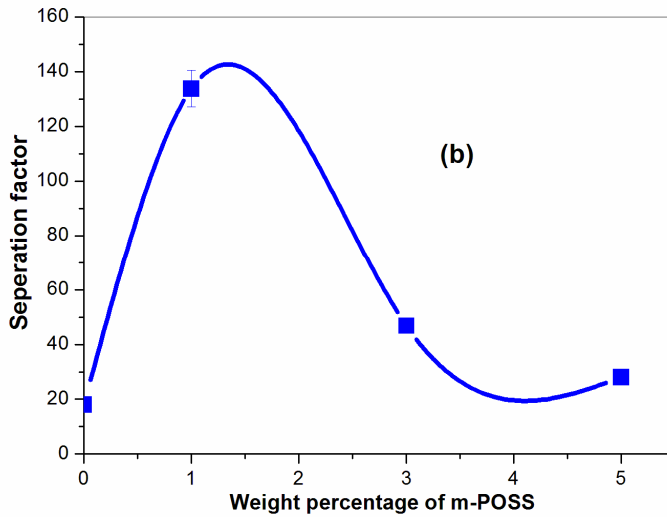
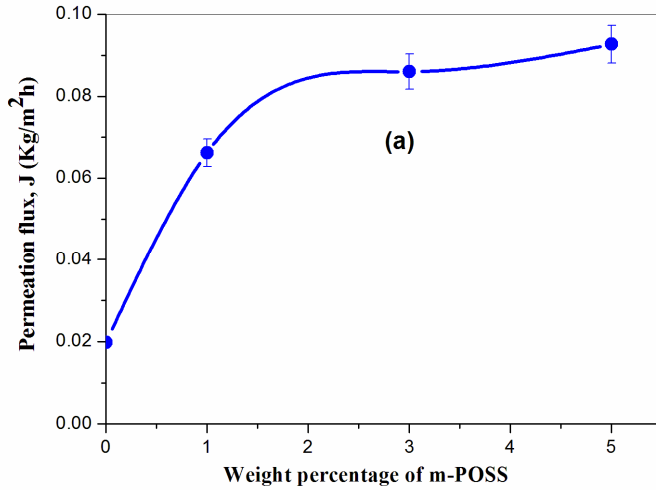


**Figure 5.10:** SEM images of tensile fractured cross section of (a-b) P0 (c-d) POCPG3

### 5.2.6 Pervaporation performance

Isopropanol (IPA) is an extensively used industrial solvent due to its non-toxic, easy to dissolve and quick evaporation ability. Industries produce large amount of IPA aqueous solution as waste and so it is important to separate water from IPA mixtures.<sup>29</sup> The pervaporation performance of the m-POSS incorporated PVA membrane was evaluated for the azeotropic IPA-water separation (ie, 87.5wt% IPA and 12.5wt% water). As demonstrated in **Figure**

**5.11(a-b)**, 1wt% m-POSS embedded PVA system shows 3-fold and 7-fold increase in the permeation flux and separation factor respectively with respect to crosslinked PVA.



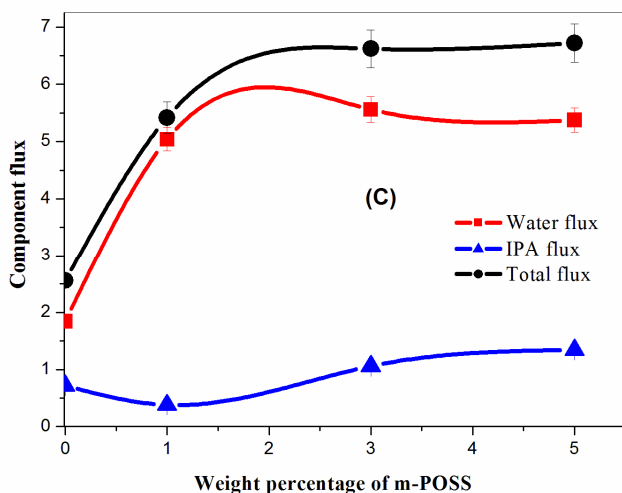


**Figure 5.11:** Effect of different weight percentage of POSS on the separation performance of PVA/m-POSS membranes

Component flux graph for PVA/m-POSS systems are presented in **Figure 5.11(c)**. Interestingly, total flux and flux values of water are almost equal in m- POSS embedded PVA membrane while IPA flux is negligible especially at 1wt% of m-POSS. It reflects the good affinity of PVA/m-POSS membrane towards water in the water-IPA azeotropic mixture. Separation efficiency and overall performance of the membrane can be assessed from enrichment factor ( $\beta$ ) and pervaporation separation index (PSI) respectively, and the data are presented in **Table 5.2**. It is observed that  $\beta$  and PSI values of PVA membranes get improved by 1.32 and 16 fold in the presence of 1wt% of m-POSS due to the good compatibility of m-POSS in PVA matrix.

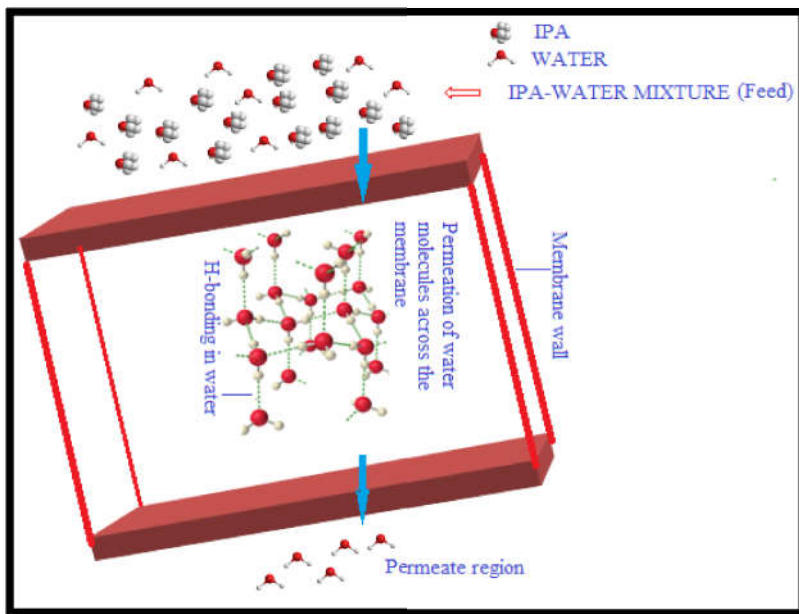
The intrinsic membrane properties are further illustrated from the permeance and selectivity of PVA and PVA/m-POSS system (**Table 5.2**). For PVA membrane, water selectivity and permeance is 30 and 2106 gpu respectively. As shown in **Table 5.2**, 1 wt% m-POSS introduced PVA membrane exhibits a 3-fold and 2-fold increase in water selectivity and permeance respectively

when compared with the PVA. It is noteworthy that the lower weight percentage of m-POSS addition combined with crosslinking generated a PVA membrane with excellent PV performance by achieving both permeance and selectivity together. The hydrophilic PVA/m-POSS membranes preferentially trap water from feed and easily transports across the membrane. As seen in contact angle measurements, the hydrophilicity of the PVA membrane increases in the presence of m-POSS, resulting in the high affinity of membrane towards water molecule. Thus the membrane offers good selectivity for the separation of azeotropic IPA-water mixture. At higher filler loading, PVA membrane exhibit reduced selectivity due to the increase in hydrophilicity as a function of weight percentage of POSS (contact angle measurements). Consequently, swelling (**Table 5.2**) and mobility of the polymer chain increases. Therefore, the transport of comparatively large IPA molecule takes place along with water molecules. Briefly, hydrophilicity increases the swelling and as a result the organic content diffuses through the membrane, which leads to high permeance and reduced selectivity. Thus, the membrane properties of PVA such as hydrophilicity, swelling and the pervaporation performance are effectively tuned by the introduction of m-POSS.

Selective permeation of water molecules through the hydrophilic PVA/m-POSS membrane is presented in **Scheme 5.1**. The application of concentration gradient between upper (feed region) and the downstream (permeate region) side of the membrane force the water molecule to diffuse out through the other side.<sup>30</sup> The pervaporation separation performance of PVA/m-POSS membrane is further confirmed from the diffusion coefficient of the membrane (**Table 5.2**). As compared with PVA membrane, PVA/m-POSS system shows improved diffusion coefficient for water ( $D_{\text{water}}$ ) because of the increase in hydrophilic nature of the PVA membrane by the introduction of m-POSS.

**Table 5.2:** Variation of transport properties of crosslinked PVA membrane with different weight percentage of m-POSS

Sample	Enrichment factor ( $\beta$ )	Pervaporation separation index (PSI)	Selectivity	Permeance (gpu)	Degree of swelling (%)	$D_{\text{water}} \times 10^5$ ( $\text{cm}^2/\text{s}$ )	$D_{\text{IPA}} \times 10^5$ ( $\text{cm}^2/\text{s}$ )
PG	5.76	0.435	30	2106	13	5.8	9.2
POCPG1	7.64	7.04	92	4256	16.2	18	5
POCPG3	6.72	2.97	43	5275	16.8	21	11
POCPG5	6.4	1.81	36	5411	17	19	12



**Scheme 5.1:** Schematic representation of hydrogen bond formation between water molecules in the membrane channel, partial pressure difference force the water molecule to diffuse out through the other side.

### 5.2.7 Modified Maxwell-Stefan model to assess the permeation flux during the IPA-water azeotropic mixture PV separation

Detailed description of modified Maxwell-Stefan equation is reported in many previous works.<sup>31-32</sup> Abridged description of the Maxwell-Stefan

equation is presented in chapter 4. **Figure 5.12** presents the experimentally determined and theoretically evaluated flux for IPA-water azeotropic mixture. As observed, theoretically predicted values are in considerable agreement with experimental results. This can be explained in terms of good affinity of the membrane towards water molecule in the presence of POSS molecules for the separation of azeotropic IPA-water mixture.

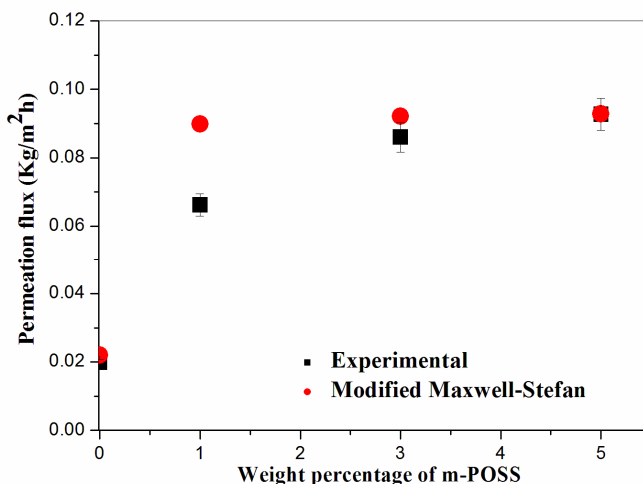


**Figure 5.14:** Theoretical comparison of flux with weight percentage of m-POSS

**Table 5.3** provides a comparative study of the PV separation of azeotropic IPA-water mixture using various polymer membranes. As observed, PVA/m-POSS membrane used in the present study exhibited excellent separation factor with satisfactory flux as compared with the reported data. This revealed the potential of PVA/m-POSS membrane for the effective separation of azeotropic IPA-water mixture.

**Table 5.3:** Comparative study of the PV separation of azeotropic IPA-water mixture using the present membrane with reported systems.

Membrane	Water flux (kg/m <sup>2</sup> h)	Separation factor	References
1. PVA-g PNIPAAm	0.01	95	8
2. PVA/clay	0.08	32	33
3. F2PVGLU6	4.72	72.70	34
4. <b>PVA/m-POSS</b>	<b>0.06</b>	<b>133</b>	<b>Present work</b>

### 5.3 Conclusions

PVA membrane with excellent mechanical and pervaporation performance was fabricated by introducing CTAB modified POSS in crosslinked PVA matrix. Hydrophilicity of the chemically crosslinked PVA membrane increased with increase in the weight percentage of m-POSS. Tensile strength and Young's modulus of PVA matrix were enhanced remarkably to 202 and 742% respectively at higher weight percentage of m-POSS. A significant improvement in water selectivity and permeance were observed at lower loading of POSS (1 wt % w.r.to PVA). The membranes showed remarkable separation factor with satisfactory flux as compared with reported data found in literature. The exceptional mechanical property and pervaporation performance observed revealed the potential of PVA/m-POSS membrane for the effective separation of azeotropic IPA-water mixture.

## 5.4 References

1. X. Cheng, F. Pan, M. Wang, W. Li, Y. Song, G. Liu, H. Yang, B. Gao, H. Wu, Z. Jiang, Hybrid membranes for pervaporation separations, *J.Mem.Sci.*, 541 (2017) 329-346
2. P. Salehian, T. S. Chung, Thermally treated ammonia functionalized graphene oxide/polyimide membranes for pervaporation dehydration of isopropanol, *J.Mem.Sci.*, 528 (2017) 231-242
3. H. Nagasawa, N. Matsuda, M. Kanezashi, T. Yoshioka, T. Tsuru, Pervaporation and vapor permeation characteristics of BTESE-derived organosilica membranes and their long-term stability in a high-water-content IPA/water mixture, *J.Mem.Sci.*, 498(2016)336-344
4. T. Narkkun, W. Jenwiriyakul, S. Amnuaypanich, Dehydration performance of double-network poly(vinyl alcohol) nanocomposite membranes (PVAs-DN), *J.Mem.Sci.*, 528 (2017) 284-295
5. L. L. Xia, C. L. Li, Y. Wang, In-situ crosslinked PVA/organosilica hybrid membranes for pervaporation separations, *J.Mem.Sci.*, 498(2016)263-275
6. G. Wu, M. Jiang, T. Zhang, Z. Jia, Tunable pervaporation performance of modified MIL-53(Al)-NH<sub>2</sub>/poly(vinyl alcohol) mixed matrix membranes, *J.Mem.Sci.*, 507(2016)72-80
7. L. Shan, L. Gong, H. Fan, S. Ji, G. Zhang, Spray-assisted biomineralization of a superhydrophilic water uptake layer for enhanced pervaporation dehydration, *J.Mem.Sci.*, 522 (2017) 183-191
8. F. Kurşun, N. Işıklan, Development of thermo-responsive poly(vinyl alcohol)-g-poly(N-isopropylacrylamide) copolymeric membranes for separation of isopropyl alcohol/water mixtures via pervaporation, *J.Indus. Eng.Chem.*, 41 (2016) 91-104
9. X. Zhao, Q. Zhang, D. Chen, Enhanced mechanical properties of graphene-based poly(vinyl alcohol) composites, *Macromolecules* 43(2010)2357-2363
10. J. Chen, Y. Gao, W. Liu, X. Shi, L. Li, Z. Wang, Y. Zhang, X. Guo, G. Liu, W. Li, B. D. Beake, The influence of dehydration on the interfacial bonding, microstructure and mechanical properties of poly(vinyl alcohol)/graphene oxide nanocomposites, *Carbon* 94 (2015)845-855



11. S. K. Sharma, J. Prakash, K. Sudarshan, D. Sen, S. Mazumder, P. K. Pujari, Structure at interphase of poly(vinyl alcohol)–SiC nanofibercomposite and its impact on mechanical properties: Positron annihilation and small-angle X-ray scattering studies, *Macromolecules* 48 (2015) 5706-5713
12. K. Tanaka, Y. Chujo, Advanced functional materials based on polyhedral oligomeric silsesquioxane (POSS), *J. Mater. Chem.*, 22 (2012)1733-1746
13. V. P. Swapna, P. S. Thomas, K. I. Suresh, V. Saranya, M. P. Rahana, R. Stephen, Thermal properties of poly (vinyl alcohol)(PVA)/halloysite nanotubes reinforced nanocomposites, *Int. J. Plast. Tech.*, 19(2015)124-136
14. Y. Fang, H. Ha, K. Shanmuganathan, C. J. Ellison, Polyhedral oligomeric silsesquioxane-containing thiol–ene fibers with tunable thermal and mechanical properties, *ACS Appli. Mater. Interface.*, 8 (2016) 11050-11059
15. W. H. Liao, S. Y. Yang, S.T. Hsiao, Y.S. Wang, S.M. Li, C. C.M. Ma, H. W. Tien, S. J. Zeng, Effect of octa(aminophenyl) polyhedral oligomeric silsesquioxane functionalized graphene oxide on the mechanical and dielectric properties of polyimide composites, *ACS Appli. Mater. Interface.*, 6(2014)15802-15812
16. E. Mc Mullin, H.T. Rebar, P. T. Mather, Biodegradable thermoplastic elastomers incorporating POSS: synthesis, microstructure, and mechanical properties, *Macromolecules* 49 (2016)3769-3779
17. H. Zhou, Q. Yea, J. Xu, Polyhedral oligomeric silsesquioxane-based hybrid materials and their applications, *Mat.Chem.Fronti.*,1 (2017) 212-230
18. W. Zhanga, A. H. E. Müller, Architecture, self-assembly and properties of well-defined hybrid polymers based on polyhedral oligomeric silsesquioxane (POSS), *Prog. Poly.Sci.*, 38 (2013) 1121-1162
19. L. Liu, Y. Hu, L. Song, X. Z. Gu, Z. Ni, Fabrication of lamellar nanostructure from cage-like poly-anion silicate and surfactant by template-directed synthesis, *J. Compos. Mater.*, 45(2011) 307-319
20. H. M. Shang, Y. Wang, S. J. Limmer, T. P. Chou, K. Takahashi, G. Z. Cao, Optically transparent superhydrophobic silica-based films, *Thin Solid Films* 472 (2005) 37-43.

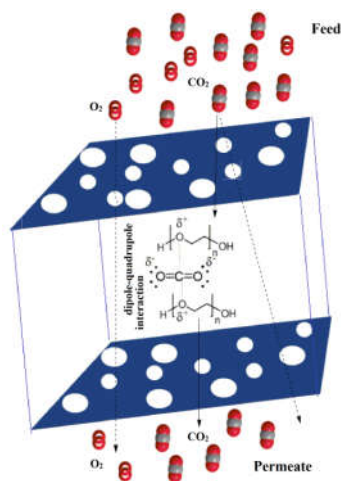
21. C. H. Tsou, Q. F. An, S. C. Lo, M. D. Guzman, W. S. Hung, C.C. Hu, K. R. Lee, J.Y. Lai, Effect of microstructure of graphene oxide fabricated through different self-assembly techniques on 1-butanol dehydration, *J. Mem.Sci.*, 477(2015)93-100
22. S. D. Jiang, G. Tang, Z. M. Bai, Y. Y. Wang, Y. Hu, L. Song, Surface functionalisation of MoS<sub>2</sub> with POSS for enhancing thermal, flame-retardant and mechanical properties in PVA composites, *RSC Adv.*, 4(2014) 3253-3262
23. P. Song, Z. Xu, Q. Guo, Bioinspired strategy to reinforce PVA with improved toughness and thermal properties via hydrogen-bond self-assembly, *ACS Macro Lett.*, 2 (12) (2013) 1100-1104
24. D. S. Yu, T. Kuila, N. H. Kim, J. H. Lee, Enhanced properties of aryl diazonium salt-functionalized graphene/poly (vinyl alcohol) composites, *Chem. Eng. J.*, 245 (2014) 311-322
25. V. P. Swapna, D. Ponnamma, K. K. Sadasivuni, S. Thomas, R. Stephen, Effect of nanostructured polyhedral oligomeric silsesquioxane on the physical properties of poly(vinyl alcohol), *J. Appl. Poly. Sci.*, 134(2017) 45447
26. E. Guth, Theory of Filler Reinforcement, *J. Appl. Phys.*, 16 (1945) 20.
27. Y. Dong, D. Chaudhary, C. Ploumis, K. T. Lau, Correlation of mechanical performance and morphological structures of epoxy micro/nanoparticulate composites, *Compos. Part A.*, 42 (2011) 1483-1492
28. Y. Zare, A. Daraei, M. Vatani, P. Aghasafari, An analysis of interfacial adhesion in nanocomposites from recycled polymers *Comput. Mater. Sci.*, 81(2014)612-616
29. Y. L. Liao, C. C. Hu, J. Y. Lai, Y. L. Liu, Crosslinked polybenzoxazine based membrane exhibiting in-situ self promoted separation performance for pervaporation dehydration on isopropanol aqueous solutions, *J. Mem. Sci.*, 531(2017)10-15
30. H. Takaba, Molecular simulation of pressure-driven fluid flow in nanoporous membranes, *The. J.Chemi. Phys.*, 127 (2007) 054703
31. U. K. Ghosh, N. C. Pradhan, B. Adhikari, Separation of water and o-chlorophenol by pervaporation using HTPB-based polyurethaneurea membranes and application of modified maxwell-stefan equation, *J.Mem.Sci.*, 272 (2006) 93-102

32. P. Izak, L. Bartovska, K. Friess, M. Sipek, P. Uchytíl, Description of binary liquid mixtures transport through non-porous membrane by modified Maxwell-Stefan equations, *J.Mem.Sci.*, 214(2003) 293-309.
33. T. Jose, S. C. George, M. G. Maya, H. J. Maria, R. Wilson, S. Thomas, Effect of bentonite clay on the mechanical, thermal, and pervaporation performance of the poly(vinyl alcohol) nanocomposite membranes, *Ind. Eng. Chem. Res.*, 53(2014)16820-16831
34. P. Das, S. K. Ray, S. B. Kuila, H.S. Samanta, N. R. Singha, Systematic choice of crosslinker and filler for pervaporation membrane: A case study with dehydration of isopropyl alcohol–water mixtures by polyvinyl alcohol membranes, *Sep. Puri. Tech.*, 81 (2011) 159-173

# Gas Transport Properties and Free volume Studies of PVA/POSS and PVA/m-POSS Membranes

## Summary

Gas transport properties of PVA/POSS and PVA/m-POSS membranes were studied and it was related to the free volumes. Free volume of the membranes were evaluated by positron annihilation lifetime spectroscopic (PALS) measurements. These membranes were found to be good for CO<sub>2</sub> separation, especially PEG-POSS filled PVA membrane due to the dipole-quadrupole interaction of CO<sub>2</sub> with ethylene oxide (polar ether oxygen) group on POSS. Finally, Maxwell-Wagner-Sillar and Higuchi models were applied for the theoretical prediction of permeability of fabricated membrane.



*This chapter has been communicated to Polymer Composites, Wiley*

## **6.1 Introduction**

Carbon dioxide emission from fossil fuels, automobiles and industry has become a major threat for environmental ecology and the sustainable growth of human society. Mitigation of CO<sub>2</sub> waste from various sources to the atmosphere is the only way to protect the delicate balance of the environmental system, at least in the present state.<sup>1-4</sup> An extensive work is going on to develop a green approach for the highly efficient, energy saving and cost effective technique for CO<sub>2</sub> separation. Polymer membranes based gas separation is one of the best method to be adopted in various fields for gas separation. In membranes very less area is enough for the separation of gas mixtures, hence from the economical and application point of view, polymer membranes are excellent material for gas separation. The major advantages of polymer membranes mediated gas separation strategy over other traditional separation processes like adsorption, absorption and thermal-driven cryogenic distillation is its offered energy efficiency, low operating costs, ease of application and moreover, it is a green approach.

CO<sub>2</sub> is found to be a common constituent in gas mixtures in industries such as natural gas, flue gas, in bio gas processing and hydrogen purification. So there is a substantial demand for energy-efficient, low cost polymer membrane tool for the CO<sub>2</sub> separation.<sup>5-8</sup> However, the trade off behaviour between permeability and selectivity recognized by the Robeson's upper bound in polymer membranes are the major disadvantage and leading to a compromise on the separation performance. Therefore, fabrication of high-performing polymer membranes with efficient separation performance and good physicochemical stability has fascinated high interest of the researchers. Addition of suitable inorganic fillers in polymer matrix is found to be a successful approach for the designing of membranes for good gas separation

performance.<sup>9-12</sup> Introduction of nanofillers to the polymer matrix often lead to reduction in the membrane transport property, in which the nanoparticle act as barrier to minimize the passage of gas molecules. In some cases addition of particulate fillers like silica and metal oxides, significantly improves gas permeance and selectivity of membranes even for the large penetrants. Xin *et al.* fabricated a mixed matrix membrane by incorporating different functionalised silica in poly(ether ether ketone) (SPEEK) and pyridine functionalised silica microspheres incorporated SPEEK. The membranes exhibited remarkable gas separation performance due to the presence of large number of CO<sub>2</sub> interacting sites (amine group) in the membrane and enhanced polymer chain rigidification.<sup>13</sup> There are a number of mechanisms proposed for the improvement in gas permeation and selectivity. Particularly, the incorporation of nanoparticle in polymer, which disrupt the polymer chain packing and form polymer-particle interfacial regions or free volume pockets, will improve the permeation of gas without sacrificing selectivity.<sup>14-16</sup> The additional free volume pockets produced upon the introduction of nanoparticle in the polymer membranes can be observed in PALS analysis.<sup>17-20</sup>

CO<sub>2</sub> gas has high solubility in polar membranes over light gases. Freeman *et al.* developed strategies to achieve high polar/non-polar selectivity. They have recognised ethylene oxide (EO) based materials to attain high permeability and CO<sub>2</sub>/light gas selectivity.<sup>21</sup> Poly(ethylene oxide)/poly(ethylene glycol) (PEG) is well recognised for its high CO<sub>2</sub>-philicity originated from the dipole-quadrupole interaction between ether groups of PEG and CO<sub>2</sub>.<sup>22-26</sup>

Polyhedral oligomeric silsesquioxane (POSS) nanomaterials are employed to modify polymeric membranes for improved gas transport performance. It is a

promising nanomaterial for modifying polymer membrane and developing membranes with good gas separation performance.<sup>27-28</sup> In a recent report, it was shown that 10 wt.% of PEG-POSS doped PIM-1 membrane exhibited 150% improvement in CO<sub>2</sub>/CH<sub>4</sub> selectivity with respect to pure PIM-1 and 1300 Barrer permeability.<sup>29</sup> PEBA<sup>X</sup>® 2533 membrane doped with 30wt% of PEG-POSS exhibit simultaneous improvement in selectivity and permeability at 30°C.<sup>30</sup>

In the present study, three types of functionalised polyhedral oligomeric silsesquioxane containing polyethylene glycol, anionic-octa-tetramethylammonium (PEG-POSS and Octa-TMA-POSS) and cetyltrimethyl ammonium (CTA) group modified Octa-TMA-POSS molecules were used to modify PVA membrane. CO<sub>2</sub>/O<sub>2</sub> and CO<sub>2</sub>/N<sub>2</sub> separation performance of these membranes were investigated. Free volume property of the membranes were analysed through positron annihilation lifetime spectroscopy (PALS). Chapter 6 focus on the correlation between free volume properties and gas transport performance of the membranes.

## 6.2 Results and discussion

### 6.2.1 Positron annihilation lifetime spectroscopic (PALS) analysis

According to the free volume theory, diffusion of permeant across the polymeric membrane is the outcome of random redistribution of free volume defects within a polymer membrane. PALS is a powerful and direct technique to probe free volumes within a polymer membrane. The effect of various functionalised POSS molecules on the free volume parameters such as radius ( $R$ ) of free volume hole, corresponding intensities ( $I$ ) and fractional free volume ( $f_v$ ) of PVA membrane have been analysed by PALS technique and the parameters are presented in **Table 6.1**. It can be seen from the PALS

results that, in pure PVA (denoted as P0 in Table 1), both smaller ( $R_3$ ) and larger sized ( $R_4$ ) free volume defects are present, as indicated by an additional free volume defect component of positronium lifetime  $\tau_4$  and intensity  $I_4$ . Moreover, no  $\tau_2$  and  $I_2$  are observed because all positrons are trapped, eventually formed positronium atoms and got annihilated from this bound state, a situation described as “saturation trapping” in positron literature. Upon the incorporation of POSS molecules (i.e., in samples PPP1 and PPP3), the radius and fractional free volume of the smaller free volume cavities ( $R_3$  and  $f_{v3}$  (%)) are observed to get enlarged in the PVA membrane. The POSS molecules enter in between the polymer chains and provide a viable pathway for the transport of gas molecules owing to its rigid and spherical structure. Large free volume cavities can be observed in the case of cetyltrimethyl ammonium functionalised POSS (m-POSS) introduced PVA membrane. It is noteworthy that in PCOPG1, all free volume defects are evenly distributed and shows only  $\tau_3$ . But in PCOPG3,  $\tau_3$  and  $\tau_4$  are present, which means that the free volume defects are drifting to smaller and larger sizes. This can be attributed to the inefficient chain packing at higher loading and the dominant nanoparticle-nanoparticle interaction over nanoparticle-polymer interaction, resulting in new voids at interfacial regions. While the intensity  $I_3$  decreased for all POSS doped PVA, which is an indication of the number of permeating path ways in the membrane. It gets reduced in the presence of nanoparticles in the PVA matrix.

**Table 6.1:** PALS data of PVA and PVA/POSS membranes

Sample	$\tau_1$ (ns)	$\tau_2$ (ns)	$\tau_3$ (ns)	$\tau_4$ (ns)	$I_1$ (%)	$I_2$ (%)	$I_3$ (%)	$I_4$ (%)	$R_3$ (Å)	$R_4$ (Å)	$f_{v3}$ (%)	$f_{v4}$ (%)
P0	0.15	Nil	1.20	2.02	78.53	Nil	18.77	2.70	1.97	2.88	1.00	0.45
PPP1	0.15	0.45	1.45	-	54.88	27.64	17.48	-	2.29	-	1.46	-
PPP3	0.17	0.50	1.54	-	59.41	23.56	17.03	-	2.41	-	1.66	-



POTP1	0.18	0.41	1.46	-	46.44	34.65	18.91	-	2.30	-	1.54	-
POTP3	0.18	0.42	1.45	-	49.89	31.12	18.99	-	2.29	-	1.53	-
POCPG1	0.12	0.45	1.48	-	58.36	24.72	16.92	-	2.32	-	1.47	-
POCPG3	0.15	0.40	1.34	2.73	49.09	31.55	17.38	1.98	2.15	3.45	1.20	0.57

### 6.2.2 Gas separation performance of PVA/POSS membranes

Permeability  $P$  is the most frequently used basic parameter to characterise gas barrier properties of the membrane and it is the product of solubility coefficient ( $S$ ) and diffusion coefficient ( $D$ ) ie,  $P = D \times S$ . The solution-diffusion mechanism describes the permeation of a gas molecule across the dense polymeric membranes. In this mechanism, gas molecules dissolve on the upper face of the membrane (high pressure side) and then diffuses through the membrane driven by concentration gradient.<sup>31-32</sup> Finally, desorption of the gas molecules occur at the low pressure downstream face of the membrane. Assumed that gas penetrant's upstream fugacity ( $f_2$ ) is much higher than downstream fugacities ( $f_1$ ) ie,  $f_2 \gg f_1$  and Fick's law of gas diffusion is prevalent.

Permeability ( $P_x$ ) and selectivity ( $\alpha_{x/y}$ ) are the intrinsic gas transport properties of the particular membrane-gas permeate system.  $P_x$  and  $\alpha_{x/y}$  is expressed as,

$$P_x = \frac{J l}{f_2 - f_1} \quad \text{or}$$

$$P_x = \frac{(\text{quantity of the permeant}) \times (\text{thickness of the membrane})}{(\text{pressure drop across the membrane}) \times (\text{time}) \times (\text{area})} \quad (6.1)$$

$$\alpha_{x/y} = \frac{P_x}{P_y} = \frac{S_x}{S_y} \times \frac{D_x}{D_y} \quad (6.2)$$

where  $P_x$  and  $P_y$  refers to the permeability of polymer towards the gases x and y, and  $J$  is the flux of the gas achieved with the membrane.

The solubility and diffusivity of the penetrants in the membrane are affected by various factors such as the physical or chemical interactions between the penetrant and membrane (hydrogen bonds, polar group interactions), morphology or chemical structure of the membrane and environmental parameters (such as pressure and temperature). The effect of different functionalised POSS molecules on the gas transport property of PVA membrane have been analysed using nitrogen, oxygen and carbon dioxide single gases. As seen in **Figure 6.1**, PEG-POSS doped PVA shows remarkable improvement in  $N_2$ ,  $O_2$  and  $CO_2$  gas permeability when compared with pure PVA due to the plasticizing action of flexible low molecular weight PEG group on POSS situated between the PVA chains. The hydrogen-bonding interaction between PVA and PEG-POSS decrease the crystallinity of the membrane and thereby construct a PVA/PEG-POSS system with high intermolecular space. Consequently, the gas transport through the membranes gets improved. The improved free volume characteristics of the PVA/PEG-POSS membranes are confirmed from PALS studies. The high degree of roughness on the surface of the PVA/PEG-POSS membrane (clear from AFM images presented in chapter 3) provides more surface area and offer large adsorption sites to the membrane than pure PVA. It is very interesting to observe that  $CO_2$  transport across the PVA/PEG-POSS membrane is found to be higher than  $O_2$  and  $N_2$  gases due to the strong dipole-quadrupolar interaction between low molecular weight polar ethyl glycol functional group on the POSS with  $CO_2$  molecule and is schematically shown in **Scheme 6.1**.

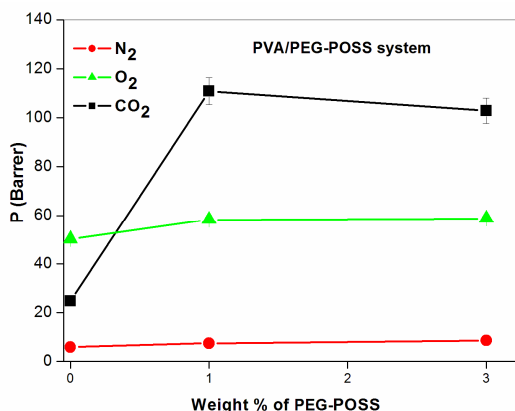
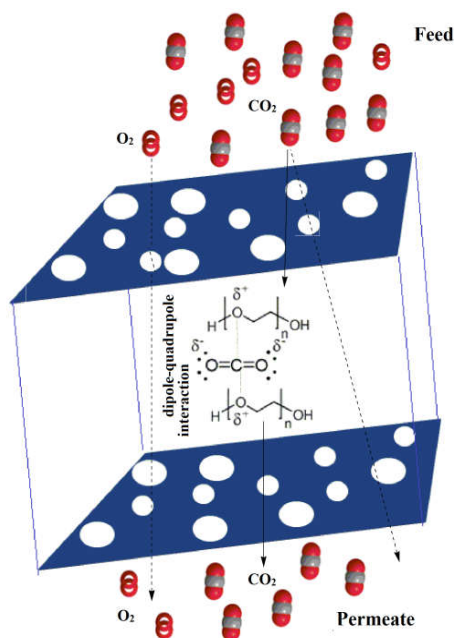


**Figure 6.1:** Variation in N<sub>2</sub>, O<sub>2</sub> and CO<sub>2</sub> permeability of PVA/PEG-POSS system as a function of weight % of PEG-POSS



**Scheme 6.1:** Schematic representation of the mechanism of transport of CO<sub>2</sub> and O<sub>2</sub> gas mixtures across the PVA/PEG-POSS membranes. Dashed arrows represent the transport of gas molecules through solution-diffusion mechanism and solid arrows represent CO<sub>2</sub> transport due to dipole–quadrupole interaction

As shown in **Figure 6.2** and **Figure 6.3**, PVA/Octa-TMA-POSS and PVA/m-POSS (at 1wt%) systems exhibit reduced O<sub>2</sub> and N<sub>2</sub> transport due to the reduction in the number of permeating pathways and improved crystallinity as compared to pure PVA. The presence of dominant rigid crystalline siloxane core framework in Octa-TMA-POSS restricts the segmental mobility of PVA chains. As a result, the permeate has to travel through more tortuous path in the membrane. A schematic representation of the diffusion path of gas molecules in pure PVA and tortuous path model in POTP1 and POCPG1 membranes are presented in **Scheme 6.2**. Interestingly the membrane shows exceptionally high CO<sub>2</sub> permeance than the pure PVA owing to the high affinity of anionic POSS towards polar CO<sub>2</sub> molecule. Another interesting observation is the high gas permeability of 3wt% m-POSS incorporated PVA membrane owing to the significant increase in the free volume defects in the membrane.

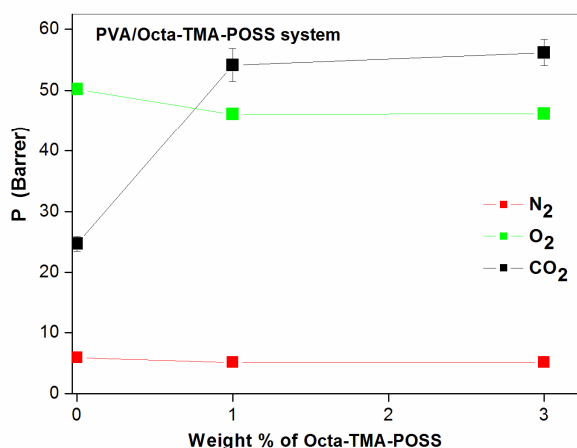


**Figure 6.2:** Variation in N<sub>2</sub>, O<sub>2</sub> and CO<sub>2</sub> permeability of PVA/Octa-TMA-POSS system as a function of weight % of POSS

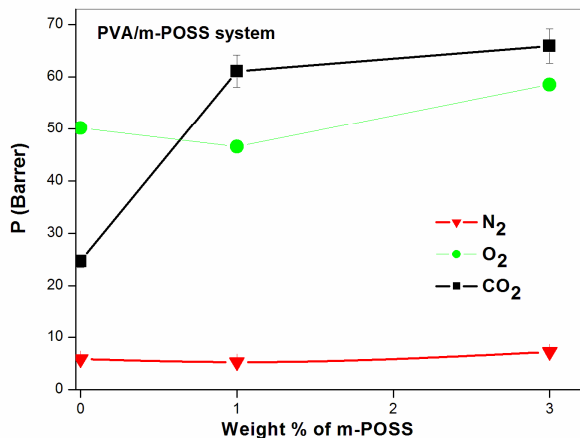
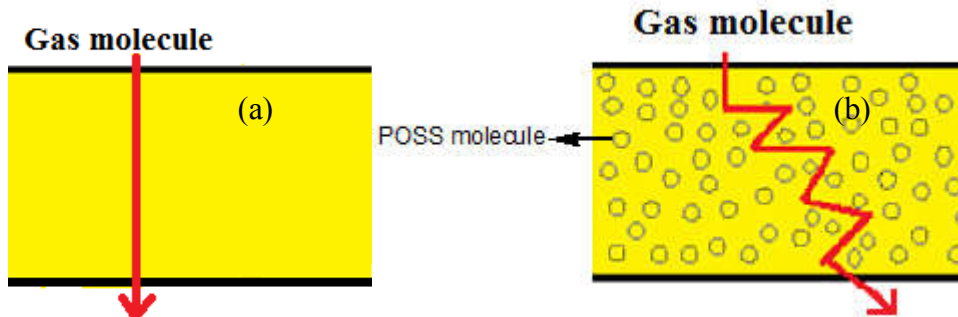


**Figure 6.3:** Variation in N<sub>2</sub>, O<sub>2</sub> and CO<sub>2</sub> permeability of PVA/m-POSS membrane as a function of weight % of POSS



**Scheme 6.2:** (a) Permeation path of gas molecules in pure PVA (b) Tortuous path model in POSS incorporated PVA membranes

Membranes with both high permeability and selectivity to the preferred gas is required for efficient gas separation. The permselectivity ( $\alpha$ ) of a membrane towards CO<sub>2</sub>, O<sub>2</sub> and N<sub>2</sub> gases are computed from the expressions

$$\alpha(\text{CO}_2, \text{O}_2) = \frac{P(\text{CO}_2)}{P(\text{O}_2)} \quad (6.3)$$

$$\alpha(\text{CO}_2, \text{N}_2) = \frac{P(\text{CO}_2)}{P(\text{N}_2)} \quad (6.4)$$

where  $P(\text{CO}_2)$ ,  $P(\text{O}_2)$  and  $P(\text{N}_2)$  are the permeability coefficients of  $\text{CO}_2$ ,  $\text{O}_2$  and  $\text{N}_2$  gases respectively.

**Table 6.2** shows the permselectivity values of PVA/POSS membranes towards  $\text{O}_2$ ,  $\text{N}_2$  and  $\text{CO}_2$ . It is noteworthy that all membranes exhibited higher  $\text{CO}_2$  selectivity when compared with pure PVA. It is due to the high affinity of membrane towards  $\text{CO}_2$  over nonpolar  $\text{O}_2$  and  $\text{N}_2$  gases.

**Table 6.2:**  $\text{CO}_2/\text{O}_2(\text{N}_2)$  permselectivity values of all PVA/POSS membranes,

Sample	Permselectivity ( $P(\text{CO}_2)/P(\text{N}_2)$ )	Permselectivity ( $P(\text{CO}_2)/P(\text{O}_2)$ )
P0	4.64	0.49
PPP1	14.82	1.97
PPP3	12.75	1.86
POTP1	10.57	1.17
POTP3	10.65	1.20
POCPG1	11.54	1.31
POCPG3	9.15	1.11

### Theoretical predictions of gas permeation

The gas permeability through membranes are further explored by applying modified Higuchi and Maxwell-Wagner-Sillars models<sup>33-36</sup> The modified Higuchi model is given by

$$P = P_c \left( 1 - \frac{6\varphi_f}{4 + 2\varphi_f - K_H(1 - \varphi_f)} \right) \quad (6.5)$$

where  $P_c$  is the permeability of continuous PVA phase,  $P$  is the permeability of PVA/POSS system,  $\varphi_f$  is the volume fraction of POSS and  $K_H$  is the Higuchi constant. Higuchi selected  $K_H$  values as 0.78 for spherical particles on the basis of experimental data.<sup>33</sup> According to his observations the  $K_H$  value varies with the change in particle size. In the present work, no good agreement in gas permeability between experimental data and Higuchi model could be found when  $K_H = 0.78$  because of the nanosize effect of POSS particles. Therefore, for the best fit of Higuchi model with experimental data, appropriate values of  $K_H$  values are identified through least square method and it is presented in **Table 6.3**. **Figures 6.4, 6.5 and 6.6** depict the correlation between the experimental results and the Higuchi model based on the selected  $K_H$  parameter. It can be seen that  $K_H$  increases with increase in gas permeability through PVA/POSS membrane. Similar observations are reported for C-MOF-5 incorporated polyetherimide (PEI) mixed matrix membranes.<sup>37</sup> The order of decreasing permeability and  $K_H$  are  $PCO_2 > PO_2 > PN_2$  and  $K_H CO_2 > K_H O_2 > K_H N_2$  respectively.

**Table 6.3:** The best fitted  $K_H$  parameters obtained for different gases in PVA/POSS membranes according to the Higuchi model.

Gas	PVA/PEG-POSS	PVA/Octa-TMA-POSS	PVA/m-POSS
N <sub>2</sub>	4.5	3.2	3.1
O <sub>2</sub>	4.6	3.21	3.5
CO <sub>2</sub>	4.64	4.49	4.09

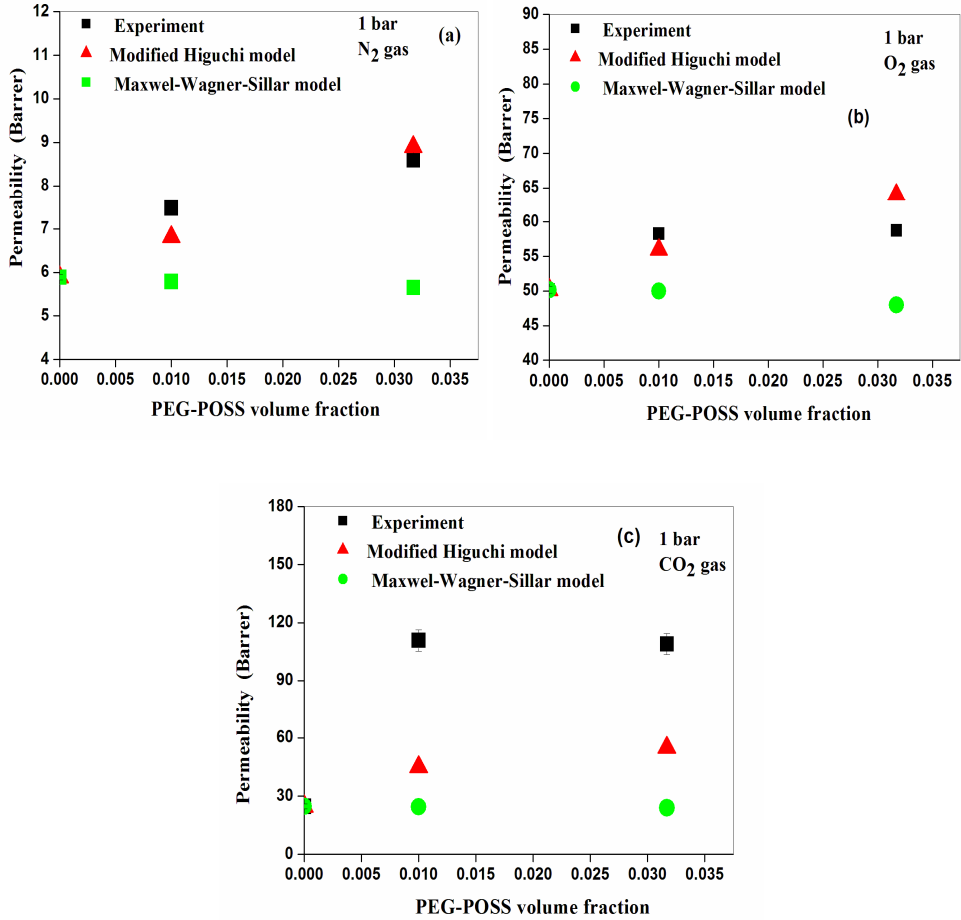


**Figure 6.4:** Comparison of experimental and theoretical permeability of PVA/PEG-POSS membranes for (a)  $N_2$ , (b)  $O_2$  and (c)  $CO_2$  gases.

The other model, known as Maxwell-Wagner-Sillar model, is given by the expression

$$P = P_C \frac{nP_F + (1-n)P_C - (1-n)\phi_f(P_C - P_F)}{nP_F + (1-n)P_C + n\phi_f(P_C - P_F)} \quad (6.6)$$



In the case of non-porous impermeable spherical particle ( $n = 1/3$  and  $P_F = 0$ ) dispersed polymer membranes, the Maxwell-Wagner-Sillar model becomes

$$P = P_C \frac{(1 - \varphi_f)}{(1 + 0.5\varphi_f)} \quad (6.7)$$

As seen in **Figure 6.4 (a-b)**,  $N_2$  and  $O_2$  permeability of PEG-POSS dispersed PVA systems calculated from Higuchi model exhibited good agreement with the experimental data. However, the experimental  $CO_2$  permeability is found to be higher than that predicted by the Higuchi model due to the high dipole-quadrupolar interaction of  $CO_2$  molecules with polar ethylene oxide groups (**Figure 6.4(c)**). Similar results are observed in the case of Octa-TMA-POSS and m-POSS dispersed PVA systems (**Figure 6.5** and **Figure 6.6**). However, for 3wt% of m-POSS loaded PVA system, experimental results show high permeability to all gases than the theoretical values owing to the significant change in the PVA-POSS interfaces and the presence of both smaller and larger free volume holes as seen from PALS results. Maxwell-Wagner-Sillar model is not in agreement with the experimental results because of the fact that the model is only considering the effect of volume fraction of POSS particle on the matrix. The interaction of gas molecules with the membrane and the influence of size and shape of POSS particles are not included in this model.

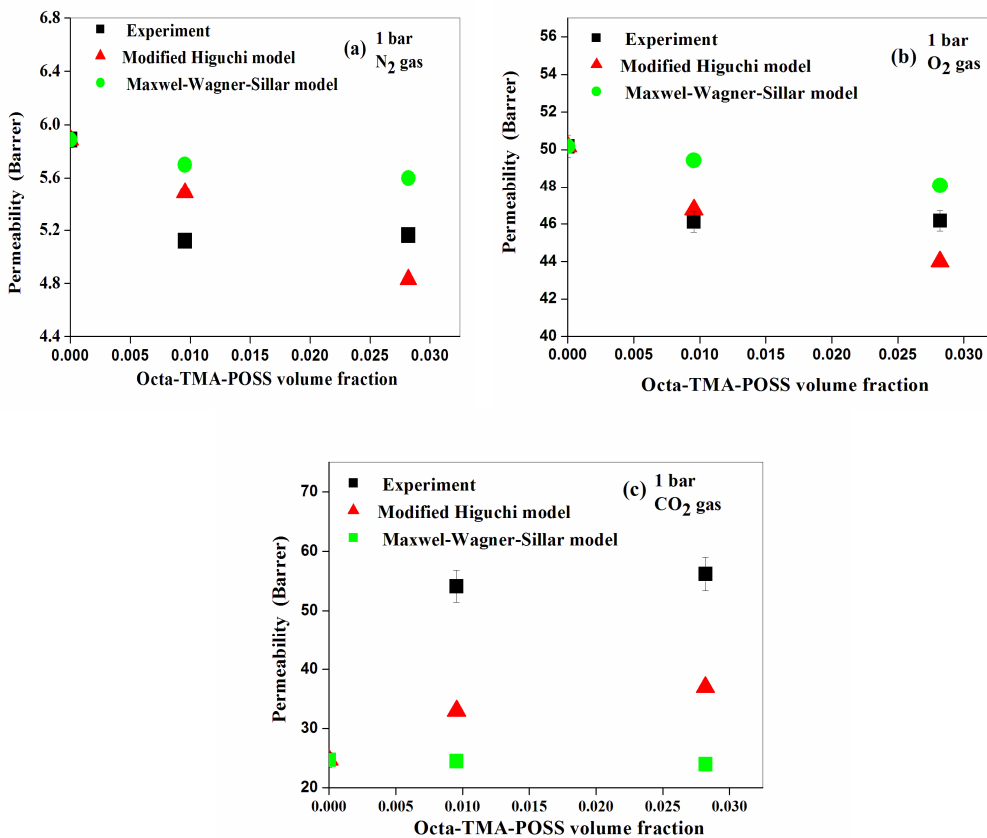


**Figure 6.5:** Comparison of experimental and theoretical permeability of PVA/Octa-TMA-POSS membranes for (a) N<sub>2</sub>, (b) O<sub>2</sub> and (c) CO<sub>2</sub> gases.

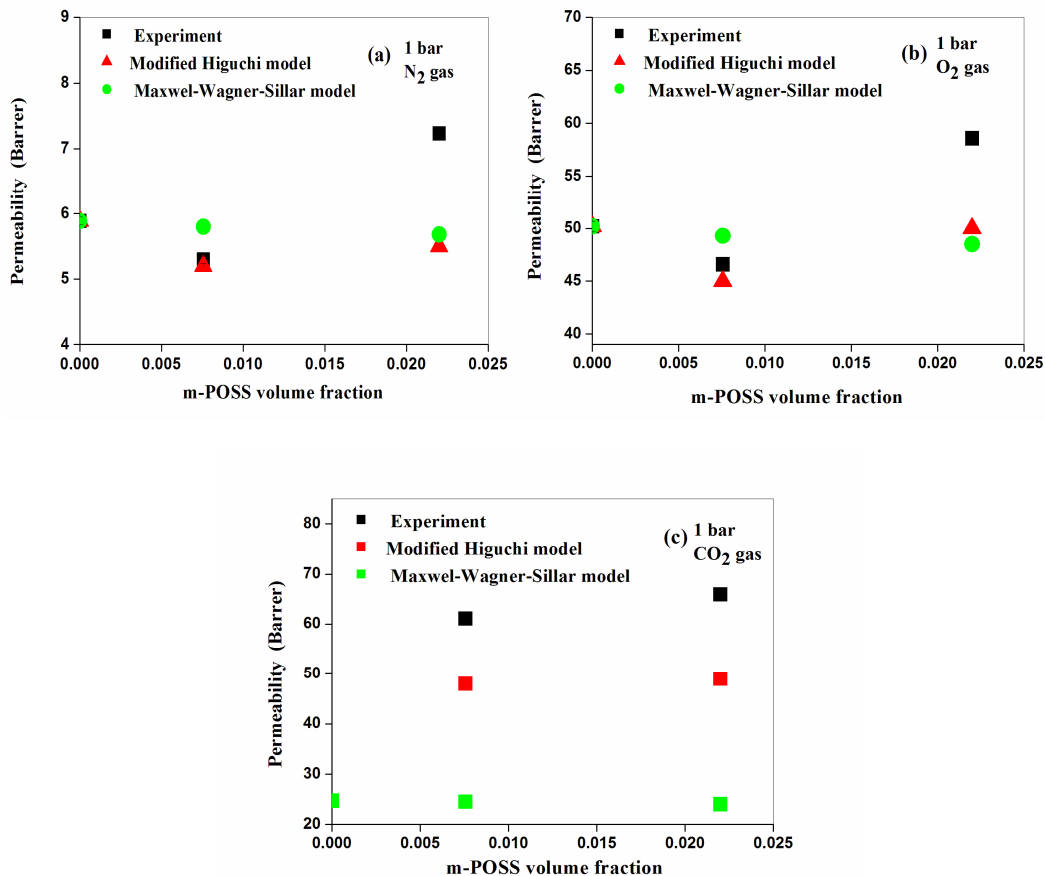


**Figure 6.6:** Comparison of experimental and theoretical permeability of PVA/m-POSS membranes for (a) N<sub>2</sub>, (b) O<sub>2</sub> and (c) CO<sub>2</sub> gases.

### 6.3 Conclusions

In summary, the effect of different functionalised POSS particles on the permeability of N<sub>2</sub>, O<sub>2</sub> and CO<sub>2</sub> molecules in PVA membrane were examined. The diffusion of gas molecules through the membrane was correlated to the free volume of the system evaluated by PALS measurements. Free volume as well as gas diffusion observed in PVA/POSS

system was higher as compared to pristine PVA. PVA/PEG-POSS membranes showed remarkable improvement in CO<sub>2</sub> permeability and selectivity because of the plasticizing action of flexible low molecular weight PEG group on the POSS situated between PVA chains and high dipole-quadrupolar interaction of CO<sub>2</sub> molecules with ethylene oxide groups present in the membrane. The introduction of Octa-TMA-POSS reduced the O<sub>2</sub> and N<sub>2</sub> permeability of the PVA membrane due to the improved crystallinity of PVA/Octa-TMA-POSS system as compared to pure PVA. The Higuchi model of permeability provided good agreement for the experimental data in the case of N<sub>2</sub> and O<sub>2</sub>, whereas the experimental values were found to be significantly higher than the theoretical values for the permeability of CO<sub>2</sub> molecule due to dipole-quadrupolar interaction of CO<sub>2</sub> molecules with polar ethylene oxide groups.

## 6.4 References

1. S. Hasebe, S. Aoyama, M. Tanaka, H. Kawakami, CO<sub>2</sub> separation of polymer membranes containing silica nanoparticles with gas permeable nano-space, *J. Mem. Sci.*, 536 (2017) 148-155
2. M. Galizia, W. S. Chi, Z. P. Smith, T. C. Merkel, R. W. Baker, Benny D. Freeman, 50th anniversary perspective: polymers and mixed matrix membranes for gas and vapor separation: a review and prospective opportunities, *Macromolecules* 50 (20) (2017) 7809-7843
3. S. Wang, X. Li, H. Wu, Z. Tian, Q. Xin, G. He, D. Peng, S. Chen, Y. Yin, Z. Jiang, M. D. Guiver, Advances in high permeability polymer-based membrane materials for CO<sub>2</sub> separations, *Energ. Environ. Sci.*, 9 (2016) 1863-1890
4. V. S. Abhisha, V. P Swapna, R. Stephen, Modern trends and applications of gas transport through various polymers, Elsevier (2017) ISBN:9780128098851
5. D. Zhao, J. Ren, Y. Wang, Y. Qiu, H. Li, K. Hua, X. Li, J. Ji, M. Deng, High CO<sub>2</sub> separation performance of Pebax<sup>®</sup>/CNTs/GTA mixed matrix membranes, *J. Mem. Sci.*, 521 (2017) 104-113
6. D. Wu, C. Sun, P. K. Dutta, W.S.W. Ho, SO<sub>2</sub> interference on separation performance of amine-containing facilitated transport membranes for CO<sub>2</sub> capture from flue gas, *J. Mem. Sci.*, 534 (2017) 33-45
7. A. Mondal, B. Mandal, CO<sub>2</sub> separation using thermally stable crosslinked poly(vinyl alcohol) membrane blended with polyvinylpyrrolidone/polyethyleneimine/tetraethylenepentamine, *J. Mem. Sci.*, 460 (2014) 126-138
8. Y. Chen, L. Zhao, B. Wang, P. Dutta, W.S. W. Ho, Amine-containing polymer/zeolite Y composite membranes for CO<sub>2</sub>/N<sub>2</sub> separation, *J. Mem. Sci.*, 497 (2016) 21-28
9. S. Khoonsap, S. Rugmai, W. S. Hung, K.R. Lee, S. Klinsrisuk, S. Amnuaypanich, Promoting permeability-selectivity anti-trade-off behavior in polyvinyl alcohol (PVA) nanocomposite membranes, *J. Mem. Sci.*, 544 (2017) 287-296

10. Q. Xin, Y. Zhang, Y. Shi, H. Ye, L. Lin, X. Ding, Y. Zhang, H. Wu, Z. Jiang, Tuning the performance of CO<sub>2</sub> separation membranes by incorporating multifunctional modified silica microspheres into polymer matrix, *J. Mem. Sci.*, 514 (2016) 73-85
11. D. Peng, S. Wang, Z. Tian, X. Wu, Y. Wu, H. Wu, Q. Xin, J. Chen, X. Cao, Z. Jiang, Facilitated transport membranes by incorporating graphenenanosheets with high zinc ion loading for enhanced CO<sub>2</sub> separation, *J. Mem. Sci.*, 522 (2017) 351-362
12. F. Huang, C.J. Cornelius, Polyimide-SiO<sub>2</sub>-TiO<sub>2</sub> nanocomposite structural study probing free volume, physical properties, and gas transport, *J. Mem. Sci.*, 542 (2017) 110-122
13. Q. Xin, Y. Zhang, Y. Shi, H. Ye, L. Lin, X. Ding, Y. Zhang, H. Wu, Z. Jiang, Tuning the performance of CO<sub>2</sub> separation membranes by incorporating multifunctional modified silica microspheres into polymer matrix, *J. Mem.Sci.*, 514 (2016) 73-85
14. M. Wang, Z. Wang, N. Li, J. Liao, S. Zhao, J. Wang, S. Wang, Relationship between polymer-filler interfaces in separation layers and gas transport properties of mixed matrix composite membranes, *J. Mem. Sci.*, 495 (2015) 252-268
15. E. Chehrazi, A. Sharif, M. Omidkhah, M. Karimi, Modeling the effects of interfacial characteristics on gas permeation behavior of nanotube-mixed matrix membranes, *ACS Appl. Mater. Interfa.*, 9 (42) (2017) 37321-37331
16. S. Hassanajili, M. Khademi, P. Keshavarz, Influence of various types of silica nanoparticles on permeation properties of polyurethane/silica mixed matrix membranes, *J. Mem. Sci.*, 453 (2014) 369-383
17. S. Zekriardehani, S. A. Jabarin, D. R. Gidley, M. R. Coleman, Effect of chain dynamics, crystallinity, and free volume on the barrier properties of poly(ethylene terephthalate) biaxially oriented films, *Macromolecules* 50 (7) (2017) 2845-2855
18. S. Awad, H. M. Chen, B. P. Grady, Abhijit Paul, W. T. Ford, L. James Lee, Y. C. Jean, Positron annihilation spectroscopy of polystyrene filled with carbon nanomaterials, *Macromolecules* 45 (2012) 933-940

19. S. Khoonsap, S. Rugmai, W. S. Hung, S. Klinsrisuk, S. Amnuaypanich, Promoting permeability-selectivity anti-trade-off behavior in polyvinyl alcohol (PVA) nanocomposite membranes, *J. Mem. Sci.*, 544 (2017) 287-296
20. C. R. Bilchak, E. Buenning, M. Asai, K. Zhang, C. J. Durning, S. K. Kumar, Y. Huang, B. C. Benicewicz, D. W. Gidley, S. Cheng, A. P. Sokolov, M. Minelli, F. Doghieri, Polymer-grafted nanoparticle membranes with controllable free volume, *Macromolecules* 50 (18) (2017) 7111-7120
21. H. Lin, B.D. Freeman, Materials selection guidelines for membranes that remove CO<sub>2</sub> from gas mixtures, *J. Mol. Struct.*, 739 (1-3) (2005) 57-74
22. M. Galizia, M. G. D. Angelis, M. Messori, G. C. Sarti, Mass transport in hybrid PTMSP/Silica membranes, *Ind. Eng. Chem. Res.*, 53 (2014) 9243-9255
23. Md. M. Rahman, V. Filiz, S. Shishatskiy, C. Abetz, P. Georgopoulos, M. M. Khan, S. Neumann, V. Abetz, Influence of poly(ethylene glycol) segment length on CO<sub>2</sub> permeation and stability of poly active membranes and their nanocomposites with PEG POSS, *ACS Appl. Mater. Interfa.*, 7 (23) (2015) 12289-12298
24. V. Pryamitsyn, B. Hanson, V. Ganesan, Coarse-grained simulations of penetrant transport in polymer nanocomposites, *Macromolecules* 44 (2011) 9839-9851
25. L. Khounlavong, V. Pryamitsyn, V. Ganesan, Many-body interactions and coarse-grained simulations of structure of nanoparticle-polymer melt mixtures, *The. J. Chem. Phys.*, 133 (2010) 144904.
26. J. M. Kropka, V. Pryamitsyn, V. Ganesan, Relation between glass transition temperatures in polymer nanocomposites and polymer thin films, *Phys. Rev. Lett.*, 101 (2008) 075702.
27. Y. Kinoshita, K. Wakimoto, A. H. Gibbons, A.P. Isfahani, H. Kusuda, E. Sivaniah, B. Ghalei, Enhanced PIM-1 membrane gas separation selectivity through efficient dispersion of functionalized POSS fillers, *J. Mem. Sci.*, 539 (2017) 178-186

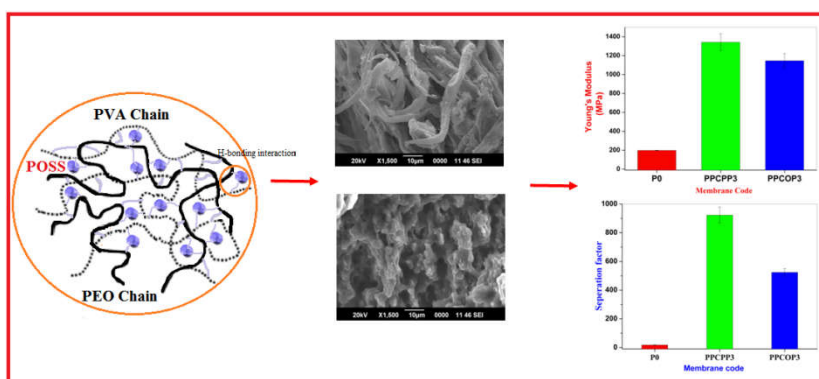
28. N. Konnertz, Y. Ding, W. J. Harrison, P. M. Budd, A. Schönhals, M. Böhning, Molecular mobility and gas transport properties of nanocomposites based on PIM-1 and polyhedral oligomeric phenethyl-silsesquioxanes (POSS), *J. Mem. Sci.*, 529 (2017) 274-285
29. L. Yang, Z. Tian, X. Zhang, X. Wu, Y. Wu, Y. Wang, D. Peng, S. Wang, H. Wu, Z. Jiang, Enhanced CO<sub>2</sub> selectivities by incorporating CO<sub>2</sub>-philic PEG-POSS into polymers of intrinsic microporosity membrane, *J. Mem. Sci.*, 543 (2017) 69-78
30. Md. M. Rahman, V. Filiz, S. Shishatskiy, C. Abetz, S. Neumann, S. Bolmer, M. M. Khan, V. Abetz, PEBAX® with PEG functionalized POSS as nanocomposite membranes for CO<sub>2</sub> separation, *J. Mem. Sci.*, 437 (2013) 286-297
31. M. Li, X. Zhang, S. Zeng, L. Bai, H. Gao, J. Deng, Q. Yang, S. Zhang, Pebax-based composite membranes with high gas transport properties enhanced by ionic liquids for CO<sub>2</sub> separation., *RSC Adv.*, 7 (2017) 6422-6431
32. C. H. Lau, T. S. Chung, Effects of Si-O-Si agglomerations on CO<sub>2</sub> transport and separation properties of sol-derived nanohybrid membranes, *Macromolecules* 44 (15) (2011) 6057-6066
33. W. I. Higuchi, A new relationship for the dielectric properties of two phase mixtures, *J. Phys. Chem.*, 62 (1958) 649-653
34. M. Sadeghia, M. A. Semsarzadehb, M. Barikanic, M. P. Chenar, Gas separation properties of polyether-based polyurethane-silica nanocomposite membranes, *J. Mem. Sci.*, 376 (2011) 188-195
35. H. V. Thang, S. Kaliaguine, Predictive models for mixed-matrix membrane performance: a review, *chem. Rev.*, 113 (7) (2013) 4980-5028
36. A. Idris, Z. Man, A.S. Maulud, F. Uddin, Modified bruggeman models for prediction of CO<sub>2</sub> permeance in polycarbonate/silica nanocomposite membranes, *The. Canadi. J. Chem. Eng.*, 95 (2017) 2398-2409
37. M. Arjmandi, M. Pakizeh, Mixed matrix membranes incorporated with cubic-MOF-5 for improved polyetherimide gas separation membranes: Theory and experiment, *J. Indus. Eng. Chem.*, 20 (2014) 3857-3868



# Mechanical Properties and Permeation Performance of PVA-PEO/POSS Membranes

## Summary

Mechanically stable novel POSS embedded poly(vinyl alcohol) (PVA)/poly(ethylene oxide)(PEO) blend membranes were prepared by solution blending followed by casting. Addition of carboxy methyl cellulose (CMC) enhanced the interfacial activities of PVA and PEO blends. This chapter deals with the characterisation, mechanical and separation properties of PVA-PEO/POSS membranes. As compared to PVA membrane, PEG-POSS and Octa-TMA-POSS embedded PVA-PEO membranes exhibit 678 and 579% enhancement in Young's modulus as well as 134 and 137% improvement in tensile strength respectively. The presence of ethylene oxide tail on POSS as well as PEO in the blend membrane enhances the CO<sub>2</sub> affinity of the membrane. The presence of hydrophilic functional group on the POSS improves the hydrophilicity of the membrane and produces more binding sites for water molecule in the membrane during the pervaporation separation of THF-water azeotropic mixture.



## 7.1 Introduction

In the last decades, polymer membrane-based separation technologies have generated considerable industrial and research attention as a prominent paradigm for gas and liquid mixture separation. Polymer membranes have great interest for separation applications because of its ease of availability, processability, low operation cost and good mechanical properties.<sup>1-3</sup> The separation technologies achieve outstanding advantages and overcome the limitations of traditional separation processes such as distillation, which involve many complicated operations as well as economical, environmental and technical challenges.

Separation process through membranes are driven by the gradient in chemical potential or gradient in concentration between the upstream and downstream sides of the membrane, which is created by the application of partial pressure difference to the diffusing species across the membrane. Chemical and physical interaction between permeating molecule and polymer can enhance the penetrant solubility. The diffusivity of penetrants are affected by the presence of free volume occupied between the chains of polymers, where diffusing molecules can be situated.<sup>4-7</sup> The interaction between polymer chains with nanofillers may interrupt polymer chain packing and improves free volume and diffusivity of penetrants. Yave *et al.* synthesised Pebax®/PEG blend membranes, which exhibited high gas permeability and selectivity with enhanced CO<sub>2</sub> solubility. It is due to the presence of ethylene oxide unit and availability of free volume within the membrane by the plasticization action of PEG.<sup>8</sup> The constituents with higher affinity with the membrane could favorably absorb and diffuses across the membrane than its counterpart. Separation using polymer membranes can be extensively applied in oxygen enrichment in combustion processes, CO<sub>2</sub>/N<sub>2</sub> and CO<sub>2</sub>/CH<sub>4</sub> separation during flue gas and bio gas treatment, natural gas drying and roofing membranes.<sup>9-11</sup> Among these potential applications, CO<sub>2</sub> capture and

storage is very essential since it plays a vital role in global warming. Polar/non-polar selective membranes are largely applied for the separation of quadrupolar CO<sub>2</sub> from light nonpolar gases such as H<sub>2</sub>, N<sub>2</sub> and CH<sub>4</sub> based on the difference in solubility. Lin and Freeman have recognized that ethylene oxide based materials are suitable to achieve efficient CO<sub>2</sub>/light gas selectivity along with excellent permeance.<sup>12</sup> The high affinity of poly(ethylene glycol) (PEG) group towards CO<sub>2</sub> molecule is achieved through Lewis acid-base interaction between CO<sub>2</sub> molecule and ether unit.<sup>13</sup>

Morphology, molecular structure, mobility of polymer chains, free volume, hydrophilicity, orientation of additives and the penetrant-polymer interaction are the critical factors that greatly influence the diffusion and permeation properties of the membranes. Robenson *et al.* reported the strong correlation between transport properties and morphology of the miscible and phase separated polymer blends.<sup>14</sup> Unique hierarchical morphologies are usually observed in nanofillers compatibilised polymer blends, which will improve the electrical, magnetic and mechanical properties of the membrane.<sup>15</sup> Wang *et al.* studied the morphology of polymer-filler interface and its effect on gas transport performance of mixed-matrix composite membranes.<sup>16</sup> Scientists have developed innovative methods such as polymer blending, incorporation of nanoparticles to polymer systems with tailored properties like high permeance and selectivity together to overcome the usual trade-off behaviour of pure polymers. Both poly(vinyl alcohol) (PVA) and poly(ethyleneoxide) (PEO) are of particular interest because of their water solubility, biodegradability, nontoxicity, gas permeability, thermal properties and ability to form strong H-bonds with various additives.<sup>17-20</sup> Sengwa *et al.* fabricated MMT clay embedded PVA-PEO blend system and studied its dielectric properties and polymer chain dynamics.<sup>21</sup> Wang *et al.* reported the properties of nanosilica-compatibilised immiscible (poly(vinylidene fluoride)/ poly(L-lactide)) blend.<sup>22</sup> Recently Dilshad *et al.* fabricated highly CO<sub>2</sub> selective

2wt% zinc oxide filled PVA-PEG (60wt% PEG with Mw = 570-630 g/mol) blend membrane. The membrane is cross-linked using 60 mol% formaldehyde. The membrane exhibited 423 Barrers CO<sub>2</sub> permeability and 112.8 CO<sub>2</sub>/N<sub>2</sub> selectivity.<sup>23</sup> The major challenge in the fabrication of PVA based membrane for separation process is to reduce its swelling behaviour in water and to enhance the separation performance. Inorganic moieties incorporated organic polymer membranes have been found to be a highly successful strategy to produce advanced material with remarkable mechanical and transport properties.<sup>24-26</sup> The H-bonding ability of hydrophilic polymers such as PVA (hydrogen bond donor) and PEO (ether groups are hydrogen bond acceptor) with various nanofillers can provide an adequate compatibility of nanoparticle in the polymer matrix. Lee *et al.* developed POSS incorporated poly(vinyl alcohol)/poly(acrylic acid) cross-linked nanofibrous hybrid composites with excellent mechanical properties.<sup>27</sup>

Chapter 7 discuss the synthesis of mechanically stable, CO<sub>2</sub> and water selective POSS embedded PVA-PEO blend membrane, which can be used for the CO<sub>2</sub> separation from CO<sub>2</sub>/N<sub>2</sub> and CO<sub>2</sub>/O<sub>2</sub> gas mixtures and pervaporation separation of water from THF-water azeotropic mixture. The presence of ethylene glycol unit in the PVA membrane enhances the affinity of membrane towards CO<sub>2</sub> and water molecules. Permeation properties of the synthesised membranes have been correlated with available free volume within the system.

## 7.2 Results and discussion

### 7.2.1 FT-IR analysis

ATR-FTIR characterization can provide an insight into the specific interaction in PVA-PEO blend system incorporated with functionalised cage structured POSS nanomaterial. Carboxy methyl cellulose (CMC) is added to modify the interface of PVA-PEO. ATR-FTIR spectra are depicted in **Figure**

7.1. Pristine PEO exhibits peak for C–H stretching, CH<sub>2</sub> scissoring, CH<sub>2</sub>, C–O–C, C–O bending and C–O–C stretching vibration at 2880, 1456, 1340, 1276, 1240 and 1094cm<sup>-1</sup> respectively. Pristine PVA shows two intense peaks at 3260 and 2939cm<sup>-1</sup>, which is characteristic of O–H and CH<sub>2</sub> stretching vibrations. The peak at 1416cm<sup>-1</sup> corresponds to bending of O–H and wagging of CH<sub>2</sub> and peak at 1073cm<sup>-1</sup> is for C–O stretching and O–H bending from amorphous chain of PVA. The O–H peak of PVA membrane at 3260cm<sup>-1</sup> is found to be broadened and shifted to lower wavenumber upon blending with PEO and on the introduction of POSS and CMC. This could be attributed to the formation of intermolecular H-bonding interaction between PVA and PEO promoted by POSS and CMC at the interface.<sup>28</sup>

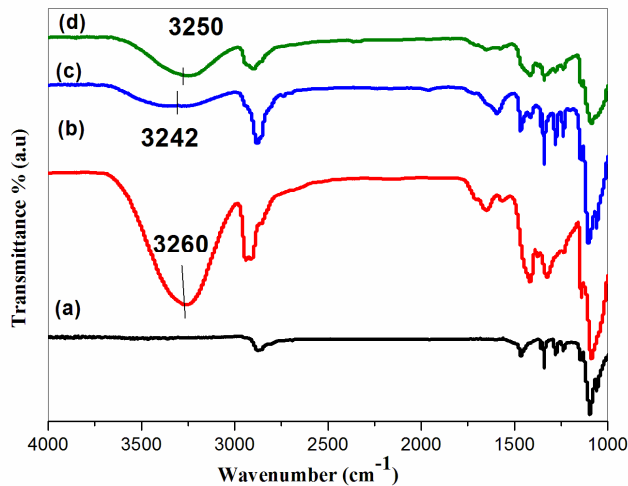


**Figure 7.1:** ATR-FTIR spectra of (a) PEO (b) PVA (c) PVA-PEO/PEG-POSS and (d) PVA-PEO/Octa-TMA-POSS

### 7.2.2 Morphology

In order to investigate the topography of fabricated PVA-PEO/POSS membranes AFM and SEM characterisations are performed. The phase, 3D and height AFM images and measured roughness parameter,  $R_q$  are displayed

in **Figure 7.2**. Biphasic morphology is seen in the AFM height image of the blend membranes. The surface roughness value ( $R_q$  (nm) = 9.5) of pristine PVA is reported in chapter 3. As compared with pristine PVA, PEG-POSS embedded PVA-PEO blend exhibits reduced surface roughness ( $R_q$  (nm) = 7.3). This decrease in surface roughness suggests good compatibility of POSS in PVA-PEO blend system. In contrast, Octa-TMA-POSS embedded PVA-PEO blend exhibit more rougher surface topography ( $R_q$  (nm) = 11) due to POSS-POSS interaction in the polymer matrix.

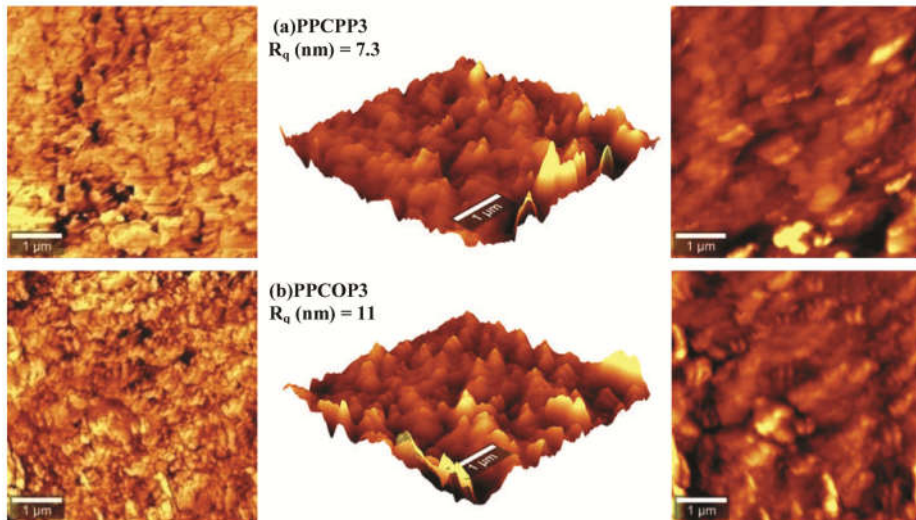


**Figure 7.2:** Phase (left picture), 3D (centre) and height AFM images of (a) PPCPP3 (b) PPCOP3

**Figure 7.3** shows the SEM images of cryofractured surface of pristine PVA and PVA-PEO/POSS systems. Micrographs of blend systems clearly disclose the dispersed droplet type morphology, PEO the minor component (10%) forms the dispersed phase. The system exhibits heterogeneous blend morphology, which is more visible in the case of PEG-POSS incorporated system owing to the higher content of PEO (**Figure 7.3(d-f)**). In the SEM micrographs of blend system phase separated morphology is observed, where

PEO phase is well dispersed within the major PVA continuous phase. In the case of Octa-TMA-POSS incorporated PVA-PEO system smaller dispersed particles of PEO is observed (**Figure 7.3(g-i)**) due to the restricted diffusion effects on the coalescence of particles due to the presence of POSS. The presence of CMC stabilise the PVA-PEO interface by forming hydrogen bond with PVA and the two systems become more compatible, which is evident from the spherical morphology observed in SEM.

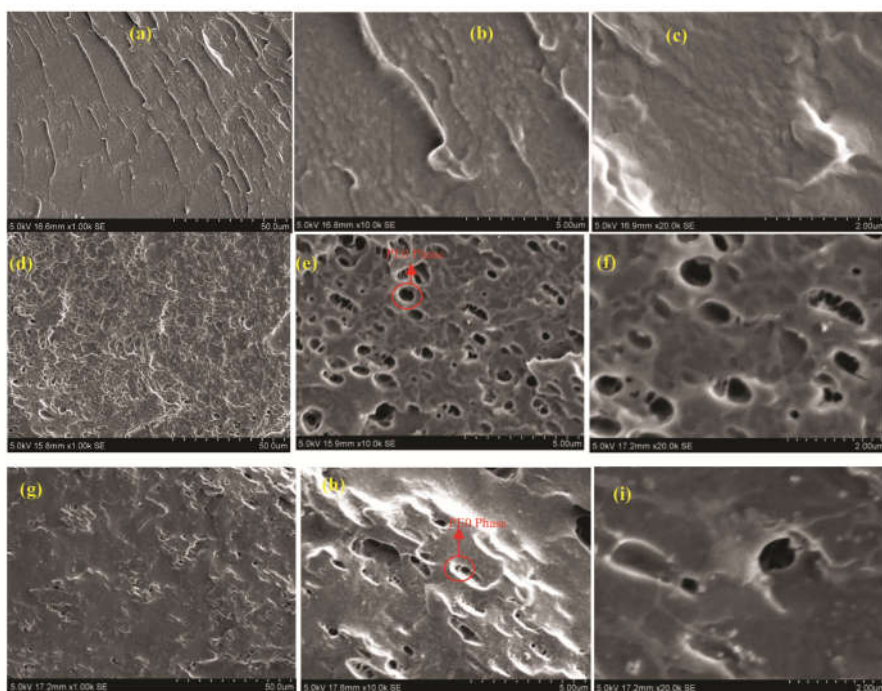


**Figure 7.3:** SEM images of (a-c) P0, (d-f) PPCPP3 and (g-i) PPCOP3 membranes at different magnifications.

### 7.2.3 Hydrophilicity

Hydrophilicity of the membrane surface is a critical parameter to examine the water-selectivity of the synthesised membrane. The hydrophilic nature of the membranes are examined by water contact angle analysis and is demonstrated in **Figure 7.4**. Pure PVA possess water contact angle of  $61^\circ$ , and the water droplets are found to be spread and run off very rapidly in the POSS embedded blend membrane surface than that of pristine PVA, which indicates the improved hydrophilicity of the blend membranes. PPCPP3 and PPCOP3 systems exhibited lower contact angles of  $44^\circ$  and  $50^\circ$  respectively, suggesting the improved hydrophilic nature with filler loading. This result could be reasonable since the presence of hydrophilic organic side groups on the POSS as well as hydrophilic polymer phases in the blend membrane offered high affinity towards water molecule.

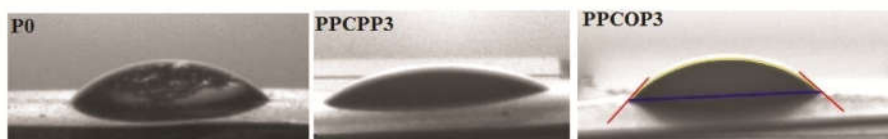


**Figure 7.4:** Water contact angle images on the surface of PVA, PEG-POSS incorporated PVA-PEO and Octa-TMA-POSS incorporated PVA-PEO blend membranes.

### 7.2.4 Differential scanning calorimetry (DSC)

**Figure 7.5** demonstrated the heating and cooling curves of blend systems and the details of the analysis are tabulated in **Table 7.1**. For pristine PVA, its melting peak temperature ( $T_m$ ) and crystallisation peak temperature ( $T_c$ ) are  $226^\circ\text{C}$  and  $197^\circ\text{C}$  respectively. PEG-POSS incorporated PVA-PEO system shows the crystallisation properties analogous to that of PVA due to the good



interaction between PVA and PEO in the presence of POSS and CMC molecule. However, for Octa-TMA-POSS incorporated blend system the crystallisation properties slightly reduced with respect to PVA, which could be explained by the network formation between POSS molecules to reduce the surface energy in the polymer matrices observed from SEM studies. The functional groups present on the POSS have a pronounced influence on the  $\Delta H_f$  and  $\Delta H_c$  values of blend system. The degree of crystallinity of PVA is computed from the  $\Delta H_f$  as given in equation (2.11) in chapter 2. Interestingly, PEG-POSS introduction in the blend retain the crystallinity of PVA, it indicates the miscibility of PVA and PEO in the presence of PEG-POSS and CMC.

**Table 7.1:** Thermal and mechanical properties of PVA and PVA-PEO/POSS membranes

Sample	T <sub>m</sub> (°C)	$\Delta H_f$ (J/g)	T <sub>c</sub> (°C)	$\Delta H_c$ (J/g)	% crystallinity	Tensile Strength (MPa)	Young's Modulus (MPa)	Elongation @Break (%)
P0	226	56	197	64	40	35±4	198±5	327±6
PPCPP3	225	54	197	56	39	47±4	1342±6	175±10
PPCOP3	220	51	196	53	36	48±4	1146±5	283±9

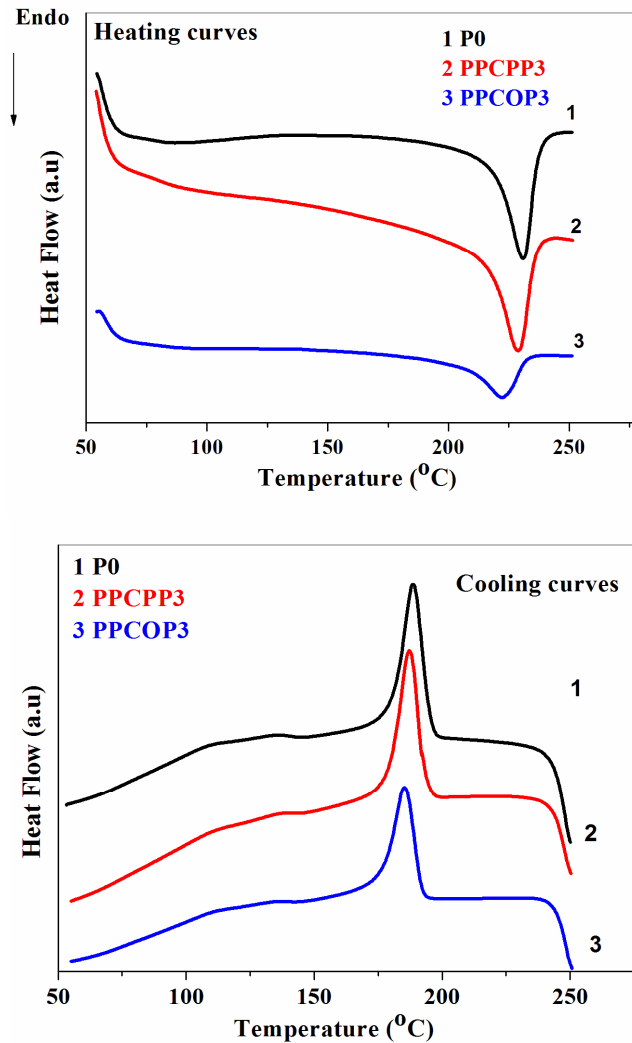


**Figure 7.5:** Heating and cooling curves of PVA and PVA-PEO/POSS membranes

### 7.2.5 Mechanical properties

**Figure 7.6** illustrated the typical stress vs strain curves of pure PVA and PVA-PEO/POSS membranes. The data of tensile studies are demonstrated in **Table 7.1**. As compared with pristine PVA, 678 and 579% enhancement in

Young's modulus as well as 134 and 137% improvement in tensile strength has been observed for PPCPP3 and PPCOP3 system respectively. It is worth mentioning that spherical shaped POSS nanofiller can efficiently transfer external load between the polymer blend matrix to its rigid siloxane core due to the strong interfacial interaction. Both PEG-POSS and Octa-TMA-POSS can acts as excellent mechanical reinforcing agents for PVA-PEO membrane and CMC enhances the miscibility of PVA-PEO. In chapter 3 the mechanical properties of PEG-POSS and Octa-TMA-POSS incorporated PVA is presented and it is observed that the mechanical stability of PVA membrane increased in the presence of POSS molecules, which is further increased on blending with PEO. The blend membrane exhibits reduced elongation at break and improved stiffness due to good miscibility of PVA and PEO polymers in the presence of CMC, CMC act as a stabiliser of the PVA-PEO blend.<sup>29</sup>

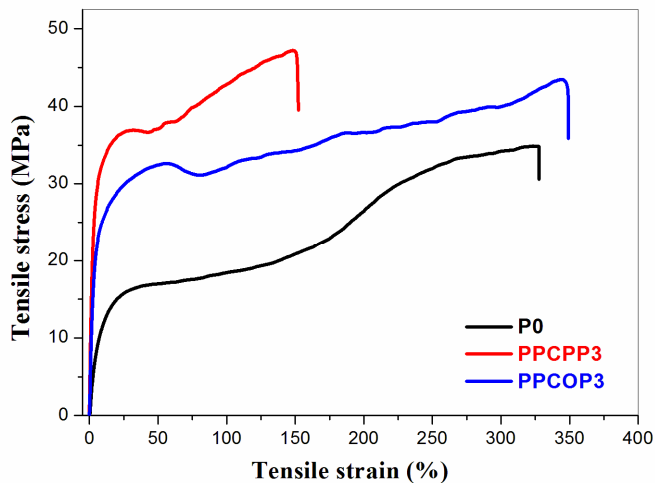


**Figure 7.6:** Stress-strain graphs of pure PVA and PVA-PEO/POSS membranes

Einstein (eq.7.1), Kerner and Frankle–Acrivos models (Equations 3.3 and 3.4 given in chapter 3) have been used to explain the Young's modulus properties of PVA-PEO/POSS systems.<sup>30-34</sup> As presented in **Figure 7.7**, for PPCPP3 and PPCOP3 system experimental Young's modulus are found to be higher than the theoretical values because of the action of CMC and POSS, which enhance the interfacial activity of PVA and PEO.

Einstein equation,

$$E_c = E_m (1 + 2.5\phi) \quad (7.1)$$

Where  $E_c$  and  $E_m$  are Young's modulus of composite and polymer matrix respectively,  $\phi$  is the volume fraction of filler.

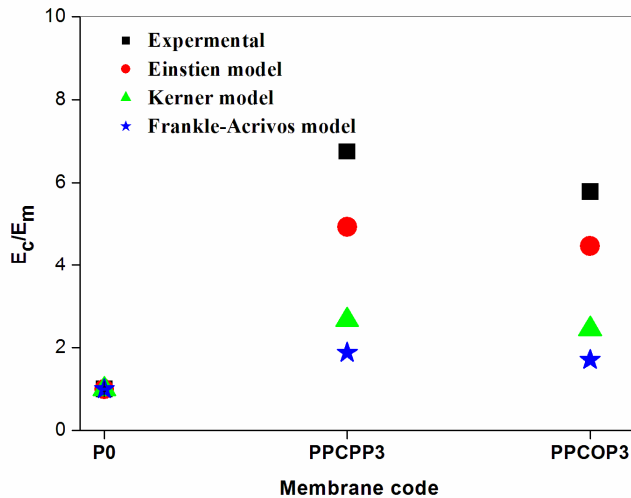


**Figure 7.7:** Theoretical modeling of Young's modulus of PVA-PEO/POSS Membranes

**Figure 7.8** illustrates the SEM micrograph of tensile fractured surface of POSS incorporated PVA-PEO blend membranes. SEM image of tensile fractured surface of pristine PVA shows branched crack propagation and non-linear deformation of the surface.<sup>40</sup> Here, as illustrated in the **Figure 7.8**, PEG-POSS embedded PVA-PEO exhibit a fibrillar like structure, suggesting high strength and modulus while, PPCOP3 system has many interface voids. During tensile breaking the system leaves many holes at the interface and as a result nonlinear cracks produce without any preferential orientation as seen in SEM.

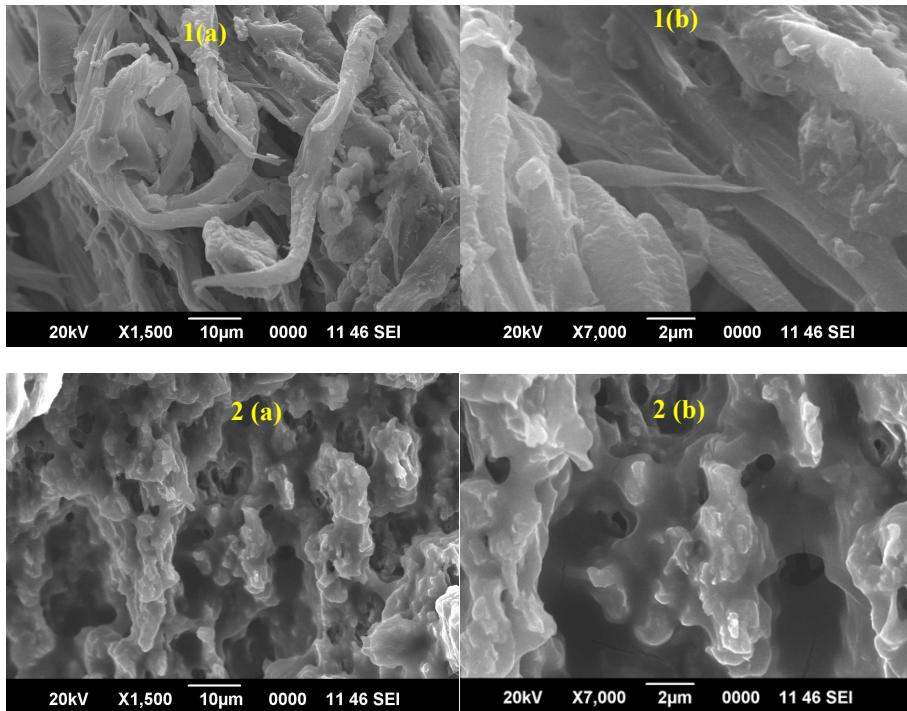


**Figure 7.8:** SEM micrographs of tensile fractured (1) PPCPP3 (2) PPCOP3 blend surfaces at (a) 10 μm and (b) 2 μm magnifications

### 7.2.6 Free volume studies

The diffusion of molecule in the polymer membrane occurs by the permeation of molecules from one void to another present in the polymer chains. The voids are termed as free volume elements (FVE)/holes. The PALS data of PVA and PVA-PEO/POSS membranes are tabulated in **Table 7.2**.  $\tau_2$  is the lifetime of free positrons trapped within the free volume defects. They are getting annihilated as free positrons, i.e., without forming the bound state positronium (Ps) and its corresponding intensity is  $I_2$ . The pure poly (vinyl alcohol) membrane does not exhibit  $\tau_2$  and  $I_2$ . This strange behaviour is called saturation trapping and all positrons so trapped eventually form Ps and then get annihilated. There is no free positron annihilation within the defects. Two kinds of smaller and larger sized free volume defects (holes) in both pure PVA and PVA-PEO/POSS membranes are observed. There is no distinct demarcation of the size limits of the holes. Depending upon the respective weight percentages, smaller ones get averaged around a certain value and so the larger ones to a different value. Radius of free volume defects ( $R_3$  and  $R_4$ ) and  $f_{v3}$  are found to be improved in blend with respect to pure PVA. This observation can be attributed to the intervention of filler particle in polymer blend matrix, which in turn disturb the polymer chain packing resulting in increase in free volume of the membrane. Meanwhile, H-bonding interaction between POSS especially PEG-POSS and polymer chain restrict the chain mobility, leading to decrease in  $I_3$  and  $I_4$ .  $f_{v4}$  are found to be higher in Octa-TMA-POSS incorporated PVA-PEO blend membrane. This result could be attributed to the high POSS-POSS interaction in the blend membrane, which creates large number of enlarged interstitial free void or o-Ps annihilation sites.

**Table 7.2:** PALS result of PVA and POSS incorporated PVA-PEO membranes

Sample	$\tau_1$ (ns)	$\tau_2$ (ns)	$\tau_3$ (ns)	$I_3$ (%)	$I_4$ (%)	$R_3$ (Å)	$R_4$ (Å)	$fv_3$ (%)	$fv_4$ (%)
P0	Nil	1.208	2.026	18.77	2.70	1.97	2.88	1.00	0.45
PPCPP3	0.390	1.349	2.315	15.98	0.90	2.16	3.13	1.12	0.36
PPCOP3	0.397	1.463	3.361	18.00	3.52	2.31	3.87	1.55	0.75

### 7.2.7 Gas transport properties

**Figure 7.9** depicted the gas permeability coefficient of nitrogen, oxygen and carbon dioxide gases and **Table 7.3** summarised the CO<sub>2</sub>/O<sub>2</sub> and CO<sub>2</sub>/N<sub>2</sub> selectivity of P0, PPCPP3 and PPCOP3 membranes. The free volume properties of the membranes and interaction between membrane and gas molecule are the key factors that affect the transport of gas molecule across the membrane. It is interesting to observe that the rigid POSS incorporated PVA-PEO membrane exhibited improved permeability to all gas molecule (O<sub>2</sub>, N<sub>2</sub> and CO<sub>2</sub>) across the membrane. This improvement can be attributed to the increased radius of free volume defects of POSS doped PVA-PEO membranes. PVA-PEO/POSS membrane exhibits significant improvement in CO<sub>2</sub> permeability and selectivity as compared with PVA. The PPCPP3 and PPCOP3 membrane exhibit permeability of 270 and 168 Barrer respectively, which is 1093 and 680% higher than the neat PVA. CO<sub>2</sub>/N<sub>2</sub> selectivity for those membranes is improved significantly when compared to neat PVA, which is found to be 37.12 and 21 respectively. The reason behind the enhancement in permeability is attributed to the strong quadrupole-dipole interaction between ethylene oxide unit in the membrane and CO<sub>2</sub> molecule (**Scheme 7.1**). The increased CO<sub>2</sub> interaction sites of the membrane promote

increased permeance and selectivity for the blend system. It can be concluded that not only the variation in free volume but also the interaction or affinity of material towards gas molecule is also a factor that determines the transport of gas molecule across the membrane.

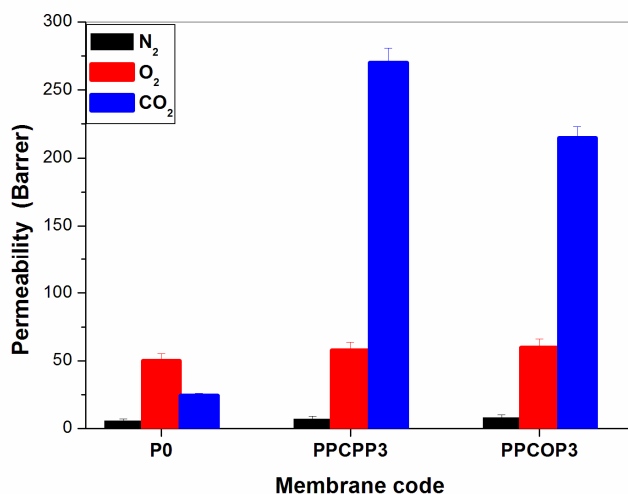
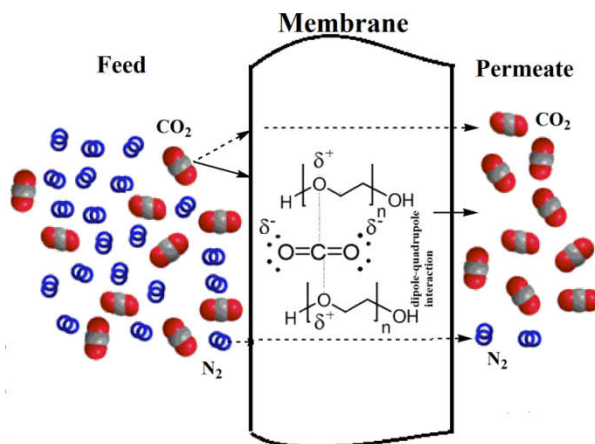


**Figure 7.9:** Permeability coefficient of (a) nitrogen, (b) oxygen and (c) carbon dioxide gases through PVA and PVA-PEO/POSS membranes

**Table 7.3:** Carbon dioxide to oxygen and carbon dioxide to nitrogen selectivity of PVA and POSS incorporated PVA-PEO membranes

Sample	Permselectivity, $P(\text{CO}_2)/P(\text{O}_2)$	Permselectivity, $P(\text{CO}_2)/P(\text{N}_2)$
P0	0.49	4.19
PPCPP3	4.74	38.60
PPCOP3	3.64	26.87





**Scheme 7.1:** The mechanism of transport of CO<sub>2</sub> and N<sub>2</sub> across the membrane. Solution-diffusion mechanism indicated by dashed arrow line and CO<sub>2</sub> transport due to dipole-quadrupole interaction represented by the solid arrow line.

### 7.2.8 Pervaporation separation of THF-water azeotropic mixture

THF form azeotrope with water at 94.7 wt%. **Figure 7.10 (a & b)** presented the permeation flux and separation factor of the THF-water azeotrope using PEG-POSS and Octa-TMA-POSS incorporated poly (vinyl alcohol) (PVA)-poly (ethylene oxide) (PEO) blend membrane. **Table 7.4** summarised the intrinsic properties such as permeance and selectivity of the POSS incorporated blend membranes. Compared with PVA, PPCPP3 system exhibits significant increase in water flux/permeance (2 fold) as well as separation factor/selectivity (52 fold) over pristine PVA. Similarly, PPCOP3 system also exhibit promising flux/permeance (3.5 fold) and separation factor/selectivity (30 fold). The enhanced pervaporation performance of the PVA-PEO/POSS membrane is mainly derived from the coupled effect of improved hydrophilicity and free volume properties of the membrane. The good interaction of POSS molecule as well as hydrophilic PVA and PEO chains with water molecule leads to preferential sorption and diffusion of

water molecule across the membrane. In the membrane channel water molecules form hydrogen bonds. Gradient in chemical potential between upper and downstream side of the membrane is the basic driving force for these separation. It is created by the application of partial pressure difference between upper and lower region and is the driving force for the desorption of water molecule to the permeate region (Scheme 7.2).<sup>35</sup>

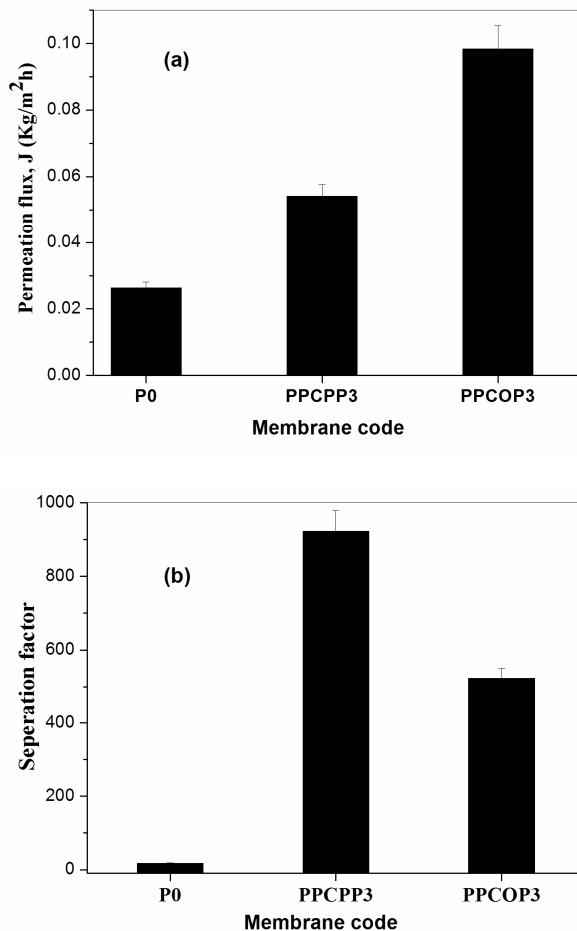
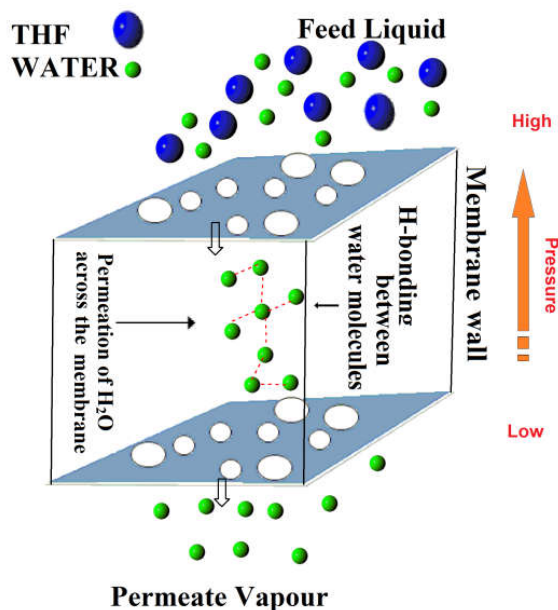


**Figure 7.10:** (a) Permeation flux and (b) separation factor of PVA and POSS incorporated PVA-PEO membranes for the separation of THF-water azeotropic mixture.



**Scheme 7.2:** The formation of H-bond between  $\text{H}_2\text{O}$  molecule in the membrane channel and desorption of water molecule towards permeate side by applying partial pressure difference between upper and lower region.

As demonstrated in the PALS result, the improved free volume radius in the PVA-PEO/POSS membrane provided enhanced water permeance. The presence of crystalline region in the membrane results in reduced fractional free volume and number of free volume defects in the membrane ( $I_3$  and  $I_4$ ), which has a major role to enhance the selectivity. As compared with PPCPP3, PPCOP3 system exhibits a marginal decrease in selectivity due to the reduced crystalline region and POSS aggregation in the membrane. As seen in **Figure 7.11**, for pure PVA, water and THF flux are found to be the same. But for PVA-PEO/POSS membrane water flux and total flux are in well agreement, which means the THF flux is negligible. It is due to the high affinity of the amphiphilic POSS embedded blend membrane towards water. In chapter 4, the PV separation of THF-water azeotropic mixture using PEG-POSS and

Octa-TMA-POSS incorporated PVA system is presented and maximum water selectivity of 1246 is observed for PVA/Octa-TMA-POSS system. However, for PVA-PEO/PEG-POSS membrane water selectivity is increased to 1264. This can be attributed to the presence of large number of hydrophilic ethylene oxide groups on the membrane.

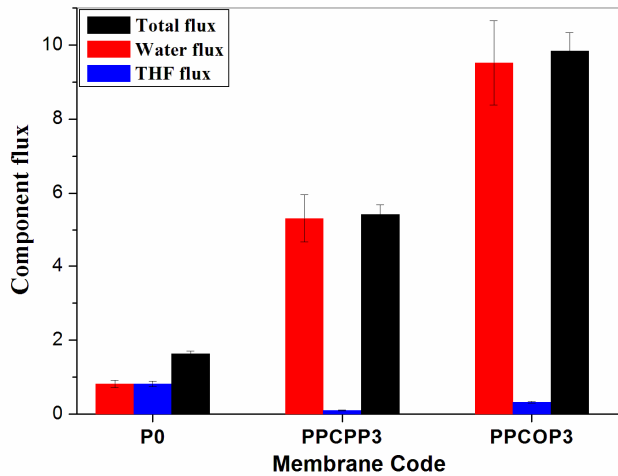


**Figure 7.11:** Component flux data of PVA and POSS incorporated PVA-PEO membranes

**Table 7.4:** Various PV separation parameters, degree of swelling and diffusion coefficient values of PVA-PEO/POSS membranes for the separation of THF–water azeotropic mixture

Sample	Enrichment factor ( $\beta$ )	Pervaporation separation index (PSI)	Selectivity	Permeance (gpu)	Degree of swelling (%)	$D_{\text{water}} \times 10^5$ ( $\text{cm}^2/\text{s}$ )	$D_{\text{THF}} \times 10^5$ ( $\text{cm}^2/\text{s}$ )
P0	9.43	0.27	24	1015	20	6.00	5.88
PPCPP3	18.50	49	1264	1978	26	20.82	5.28
PPCOP3	18.24	47.22	718	3595	29	20.96	9.00

**Table 7.4** demonstrated the enrichment factor ( $\beta$ ), which express separation efficiency of the membrane.  $\beta$  value increased significantly in PVA-PEO/POSS system as compared to PVA. Pervaporation separation index (PSI) is obtained by combining separation factor and flux, hence it reflects overall performance of the membrane. The improved  $\beta$  and PSI could be reasonably ascribed to the high hydrophilicity of the membrane and good compatibility of POSS nanoparticle in the blend matrix. To assess the membrane affinity towards water molecule, diffusion coefficient and degree of swelling (DS) studies have been carried out and data are summarised in **Table 7.4**. The POSS doped blend membrane exhibited higher DS and water diffusion coefficient with respect to pristine PVA. This indicates the high affinity of the PVA-PEO/POSS membrane towards water molecule.

### 7.3 Conclusion

This chapter discussed the successful fabrication of two types of mechanically stable, water and CO<sub>2</sub> selective POSS incorporated PVA-PEO blend membranes. As compared with pristine PVA, PEG-POSS and Octa-TMA-POSS embedded PVA-PEO membranes exhibited 678 and 579% enhancement in Young's modulus as well as 134 and 137% improvement in tensile strength respectively. The presence of ethylene oxide functional group on POSS as well as PEO polymer chain in the membrane offered enhanced CO<sub>2</sub> affinity to the membrane. The permeation behaviour of the synthesised membrane is related to the available free volume. Present study revealed the potential of PVA-PEO/POSS materials for the effective separation of CO<sub>2</sub> from CO<sub>2</sub>/N<sub>2</sub>(O<sub>2</sub>) gas mixtures. The high hydrophilicity, unique membrane morphology, improved free volume properties and sustained crystallinity of the PVA-PEO/POSS membrane provided high pervaporation separation of the THF-water azeotropic mixture. Thus, PVA-PEO/POSS blend membrane can be used as a promising material for separation process.

---

## 7.4 References

1. R. W. Baker, B. T. Low, Gas separation membrane materials: A perspective, *Macromolecules* 47 (20) (2014) 6999-7013
2. V. S. Abhisha, V. P. Swapna, R. Stephen, *Modern Trends and Applications of Gas Transport Through Various Polymers*, Elsevier (2017) ISBN:9780128098851
3. K. Nath, *Membrane separation processes*, (2017) Prentice Hall of India Private Limited, New Delhi, ISBN : 978-81-203-5291-9
4. H. Nagasawa, N. Matsuda, M. Kanezashi, T. Yoshioka, T.T. Suru, Pervaporation and vapor permeation characteristics of BTESE-derived organosilica membranes and their long-term stability in a high-water-content IPA/water mixture, *J. Mem. Sci.*, 498 (2016) 336-344
5. S. Zekriardehani, S. A. Jabarin, D. R. Gidley, M. R. Coleman, Effect of chain dynamics, crystallinity, and free volume on the barrier properties of poly(ethylene terephthalate) biaxially oriented films, *Macromolecules*, 50 (7) (2017) 2845-2855
6. C. Rizzuto, A. Brunetti, A. Caravella, C. H. Park, Y. M. Lee, E. Drioli, G. Barbieri, E. Tocci, Sorption and Diffusion of CO<sub>2</sub>/N<sub>2</sub> in gas mixture in thermally-rearranged polymeric membranes: A molecular investigation, 528 (2017) 135-146
7. L. Vanel, V. Namboodiri, G. Lin, M. Abar, F. Alvarez, Preparation of water-selective polybutadiene membranes and their use in drying alcohols by pervaporation and vapor permeation technologies, *ACS Sus. Chem. Eng.*, 4 (8) (2016) 4442-4450
8. W. Yave, A. Car, K. V. Peinemann, M. Q. Shaikh, K. Rätzke, F. Faupel, Gas permeability and free volume in poly(amide-b-ethylene oxide)/polyethylene glycol blend membranes, *J. Mem. Sci.*, 339 (2009) 177-183
9. V. Giel, Z. Morávková, J. Peter, M. Trchová, Thermally treated polyaniline/polybenzimidazole blend membranes: Structural changes and gas transport properties, *J. Mem. Sci.*, 537 (2017) 315-322
10. S. Li, X. Jiang, Q. Yang, L. Shao, Effects of amino functionalized polyhedral oligomeric silsesquioxanes on cross-linked poly (ethylene

- oxide) membranes for highly-efficient CO<sub>2</sub> separation, *Chem. Eng. Resea. Desig.*, 122 (2017) 280-288
11. D. Wu, C. Sun, P. K. Dutta, W.S. W. Ho, SO<sub>2</sub> interference on separation performance of amine-containing facilitated transport membranes for CO<sub>2</sub> capture from flue gas, *J. Mem. Sci.*, 534 (2017) 33-45
  12. H. Lin, B.D. Freeman, Materials selection guidelines for membranes that remove CO<sub>2</sub> from gas mixtures, *J. Mol. Stru.*, 739 (1-3) (2005) 57-74.
  13. M. Kawakami, Y. Yamashita, M. Yamasaki, M. Iwamoto, S. Kagawa, Effects of dissolved inorganic salts on gas permeabilities of immobilized liquid polyethylene glycol membranes, *J. Polym. Sci., Polym. Lett. Ed.*, 20 (1982) 251-257
  14. L. M. Robeson, Polymer blends in membrane transport processes, *Ind. Eng. Chem.Res.*, 49 (23) (2010) 11859-11865
  15. Y. H. Wang, K. L. Chen, C. H Xu, Y. K. Chen, Super toughened biobased poly(lactic acid)-epoxidized natural rubber thermoplastic vulcanizates: fabrication, co-continuous phase structure, interfacial in situ compatibilization, and toughening mechanism. *J. Phys. Chem. B.*, 119 (2015)12138-12146.
  16. M. Wang, Z. Wang, N. Li, J. Liao, S. Zhao, J. Wang, S.Wang, Relationship between polymer-filler interfaces in separation layers and gas transport properties of mixed matrix composite membranes, *J. Mem. Sci.*, 495 (2015) 252-268
  17. J. Lee, D. Bhattacharyya, A. J. Easteal, J. B. Metson, Properties of nano-ZnO/poly(vinyl alcohol)/poly(ethylene oxide) composite thin films, *Curr. Appli. Phy.*, 8 (2008) 42-47
  18. S. Y. Hu, Y. Zhang, D. Lawless, X. Feng, Composite membranes comprising of polyvinylamine-poly(vinyl alcohol) incorporated with carbon nanotubes for dehydration of ethylene glycol by pervaporation, *J. Mem. Sci.*, 417-418(2012) 34-44
  19. S. Li, X. Jiang, Q. Yang, L. Shao, Effects of amino functionalized polyhedral oligomeric silsesquioxanes on cross-linked poly (ethylene oxide) membranes for highly-efficient CO<sub>2</sub> separation, *Chem. Eng. Resea. Design.*, 122 (2017) 280-288

20. V. P. Swapna, P. Selvin Thomas, K. I Suresh, V. Saranya, M. P Rahana, R. Stephen, Thermal properties of poly (vinyl alcohol) (PVA)/halloysite nanotubes reinforced nanocomposites, *Int. J. Plast. Technol.*,19 (2015) 124-136
21. R. J. Sengwa, S. Choudhary, S. Sankhila, dielectric properties of clay filled poly(vinyl alcohol)/poly(ethylene oxide) blend composites, *Compos.Sci.Tech.*,70 (2010)1621-1627
22. H. Wang, X. Yang, Z. Fu, X. Zhao, Y. Li, J. Li, Rheology of nanosilica-compatible immiscible polymer blends: formation of a“heterogeneous network” facilitated by interfacially anchored hybrid nanosilica, *Macromolecules* 50 (2017) (23) 9494-9506
23. M. R. Dilshad, A. Islam, A. Sabir, M. Shafiq, M.T. Z. Butt, A. Ijaz, T. Jamil, Fabrication and performance characterization of novel zinc oxide filled cross-linked PVA/PEG 600 blended membranes for CO<sub>2</sub>/N<sub>2</sub> separation, *J. Ind. Eng. Chem.*, 55 (2017) 65-73
24. F. Clegg, C. Breen, Khairuddin, Synergistic and competitive aspects of the adsorption of poly(ethylene glycol) and poly(vinyl alcohol) onto NA-bentonite, *J. Phys. Chem. B.*, 118 (46) (2014)13268-13278
25. X. You, T. Ma, Y. Su, H. Wu, M. Wu, H. Cai, G. Sun, Z. Jiang, Enhancing the permeation flux and antifouling performance of polyamide nanofiltration membrane by incorporation of PEG-POSS nanoparticles, *J. Mem. Sci.*, 540 (2017) 454-463
26. V.P. Swapna, R. Stephen, T. Greeshma, C.S. Dev, M.S. Sreekala, Mechanical and swelling behavior of green nanocomposites of natural rubber latex and tubular halloysite nano clay, *Poly. Compos.*, 37 (2016) 602-611
27. E.S. Lee, D. Lei, K. Devarayan, B. S. Kim, High strength poly(vinyl alcohol)/poly(acrylic acid) cross-linked nanofibrous hybrid composites incorporating nanohybrid POSS, *Compos. Sci. Tech.*, 110 (2015) 111-117
28. H. D. Huang, P.G. Ren, J. Chen, W. Q. Zhang, X. Ji, Z. M. Li, High barrier graphene oxide nanosheet/poly(vinyl alcohol) nanocomposite films, *J. Mem. Sci.*, 409-410 (2012)156-163
29. B. Gupta, R. Agarwal, M. S. Alam, Preparation and characterization of polyvinyl alcohol-polyethylene oxide-carboxy methyl cellulose blend membranes, *J. App. Poly. Sci.*,127 (2012) 1301-1308

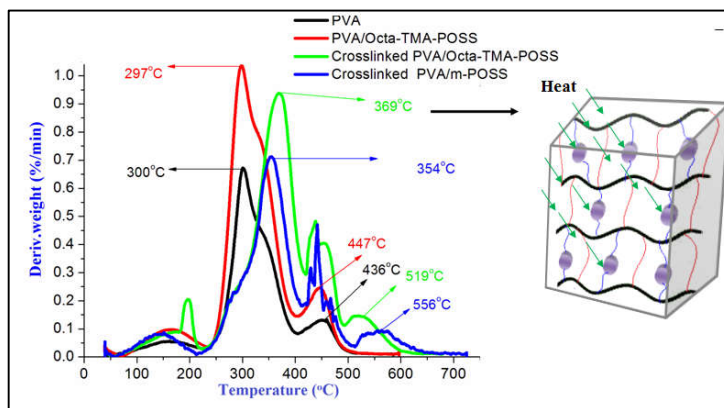


30. A. Einstein, Eine neue Bestimmung der Moleküldimensionen, *Ann. d. Physik* 19, 289-34 (1906) 591(1911)
31. S. Ahmed, F.R Jones. A review of particulate reinforcement theories for polymer Composites. *J. Mater Sci.*, 25(12) (1990) 4933-4942.
32. N. A. Frankel, A. Acrivos. On the viscosity of a concentrated suspension of solid spheres. *Chem. Eng. Sci.*, 22(6)(1967)847-853
33. Y. Dong, D. Chaudhary, C. Ploumis, K. T.Lau, Correlation of mechanical performance and morphological structures of epoxy micro/nanoparticulate composites, *Compos. Part A.*, 42 (2011) 1483-1492
34. Y. Zare, A. Daraei, M. Vatani, P. Aghasafari, An analysis of interfacial adhesion in nanocomposites from recycled polymers. *Comput. Mater. Sci.*, 81 (2014) 612-616
35. H. Takaba, Molecular simulation of pressure-driven fluid flow in nanoporous membranes, *J. Chem. Phys.*, 127 (2007) 054703

## Thermal and Water Stability of PVA/POSS, PVA/m-POSS and PVA-PEO/POSS Systems

### Summary

Thermal and water stability of the fabricated PVA/POSS, PVA/m-POSS and PVA-PEO/POSS membranes were investigated. Among the different membranes, PVA-PEO/POSS and crosslinked PVA/POSS systems exhibited excellent improvement in thermal stability at lower loading of POSS as compared to pure PVA and uncrosslinked PVA/POSS systems. Uncrosslinked PVA and PVA/POSS systems exhibited mainly two degradation steps. But in the crosslinked PVA/POSS system more degradation steps were observed, due to the formation of 3-dimensional network structure in the polymer. Activation energy for degradation was calculated from Horowitz–Metzger plot. The mechanical stability of PVA/POSS and PVA-PEO/POSS systems at hydrated state were analysed and observed a remarkable stability even in the wet condition.



This chapter has been communicated in *Journal of Thermal Analysis and Calorimetry*, Springer

## 8.1 Introduction

Hybrid organic-inorganic materials show remarkable properties such as ease in processability, improved mechanical properties as well as enhanced chemical and thermal stability.<sup>1-3</sup> Polyhedral oligomeric silsesquioxane (POSS) is one of the most versatile examples for inorganic nanobuilding block for the preparation of high performance hybrid polymers. POSS itself possess hybrid nanomaterial architecture containing robust siliceous inorganic core surrounded by large variety of peripheral organic groups at the Si vertices. The molecule possesses many advantages such as excellent thermal, mechanical, optical and electrical properties due to its rigid silicon-oxygen cores and nanoscopic dimension. The versatile functional groups in the POSS can promote miscibility with organic hosts and solubility in solvents.<sup>4-10</sup> The POSS nanofiller has three dimensional cage like structure with the chemical formula  $(\text{RSiO}_{1.5})_n$  and is approximately 1-3 nm in diameter. Octahedral POSS with formula  $(\text{RSiO}_{1.5})_8$  is investigated as the most common variety of POSS. The possibility for the fine tuning of the functional groups and the presence of organic components makes the material more compatible and dispersible in the polymer matrix. The nanosized POSS molecules can be incorporated into common polymeric architecture either thorough physical blending or by chemical copolymerisation. The POSS reinforcement have often show a remarkable improvement in properties of polymers such as thermal stability, flammability resistance, oxidation resistance, mechanical and gas barrier properties.<sup>11-17</sup> Recently, Yang *et al.* obtained excellent thermal stability for poly(dimethyl siloxane) by incorporating octa-vinyl POSS.<sup>18</sup>

Poly(vinyl alcohol) (PVA) and poly(ethylene oxide) (PEO) are water soluble, biodegradable, biocompatible and nontoxic synthetic polymers.<sup>19-21</sup> The

thermal stability of PVA play a vital role in processing of PVA based products since it undergoes degradation at high temperature.<sup>22-23</sup> Considering the wide applications of PVA due to its non-toxic nature, many researchers carried out various modifications to achieve high thermal stability for PVA.<sup>24-26</sup> From the reported literature, it is found that mechanical and thermal stability as well as hydrophilicity of PVA can be modified by the addition of rigid nanofillers.<sup>27-28</sup> Dong *et al.* reported that the thermal stability of PVA enhanced significantly by the incorporation of graphene nanofiller and poly (1-vinyl-3-ethyl-imidazolium bromide) compatibiliser.<sup>29</sup>

This chapter deals with the thermal degradation studies of POSS incorporated PVA and PVA-PEO membranes. The effect of crosslinking, nature of functional groups on POSS molecule and cetyltrimethylammonium modification of POSS (CTA modified Octa-TMA) on the thermal degradation of PVA and PVA-PEO membranes are investigated and presented in detail.

## **8.2 Results and discussion**

### **8.2.1 Thermo gravimetric analysis (TGA)**

#### **8.2.1.1 POSS molecules**

Thermogravimetric analysis of organically modified POSS systems provide information about the quantity of organic groups attached to the POSS core. In POSS molecule, the inner cage is fabricated by intrinsically strong siloxane linkages (Si-O bond energy = 444 kJmol<sup>-1</sup>), which is very stiff and inert because of the strong overlapping of two lone pair electrons on the oxygen and vacant d orbital of Si. The siloxane cages exhibit superior hydrophobic behaviour and does not participate in any interactions with other molecules because of the absence of free O-H groups on the core. According

to the molecular weight (5576.6 g/mol) and structure of PEG-POSS (**Figure 8.1**), approximately 92wt% of PEG-POSS consist of poly(ethyleneglycol). As shown in **Figure 8.2**, PEG-POSS undergoes 92% mass loss in the temperature range 100-500°C and 8% weight retention at 700°C. These thermal decomposition data revealed that PEG-POSS is functionalised with approx. 92wt% poly(ethylene glycol), which degraded between 100-700°C. The rigid and inert centre core of the POSS as well as some carbonaceous materials are responsible for the residual mass, which is in accordance with the calculated value based on the structure. In the case of anionic Octa-TMA-POSS, the weight percentage of octa(tetramethylammonium) surrounding the POSS was approx. 60wt%. As presented in **Figure 8.2**, 39% of weight retention can be observed for Octa-TMA-POSS at 450°C. Octa-TMA around the POSS core has been completely decomposed at 450°C, which is also in accordance with the calculation made from the structure (**Figure 8.1**). Thermogram of CTAB modified Octa-TMA-POSS (m-POSS, **Figure 8.1**) presented in **Figure 8.2**, which shows that the degradation begins at higher temperature and the yield of residue observed to be higher as compared with Octa-TMA-POSS. It indicates the high thermal stability of m-POSS as compared with Octa-TMA POSS, which is caused by the strong attachment of cetyltrimethylammonium (CTA) group to the siloxane core by electrostatic interaction.

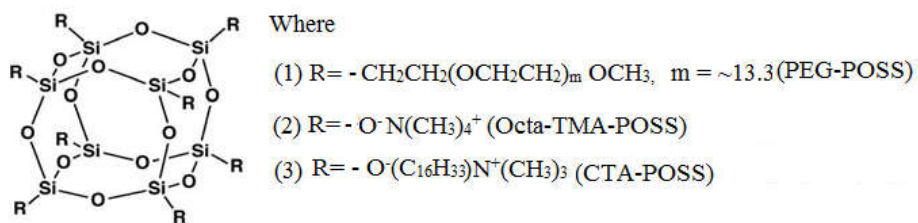


**Figure 8.1:** Structure of POSS with different functional group on the siloxane core

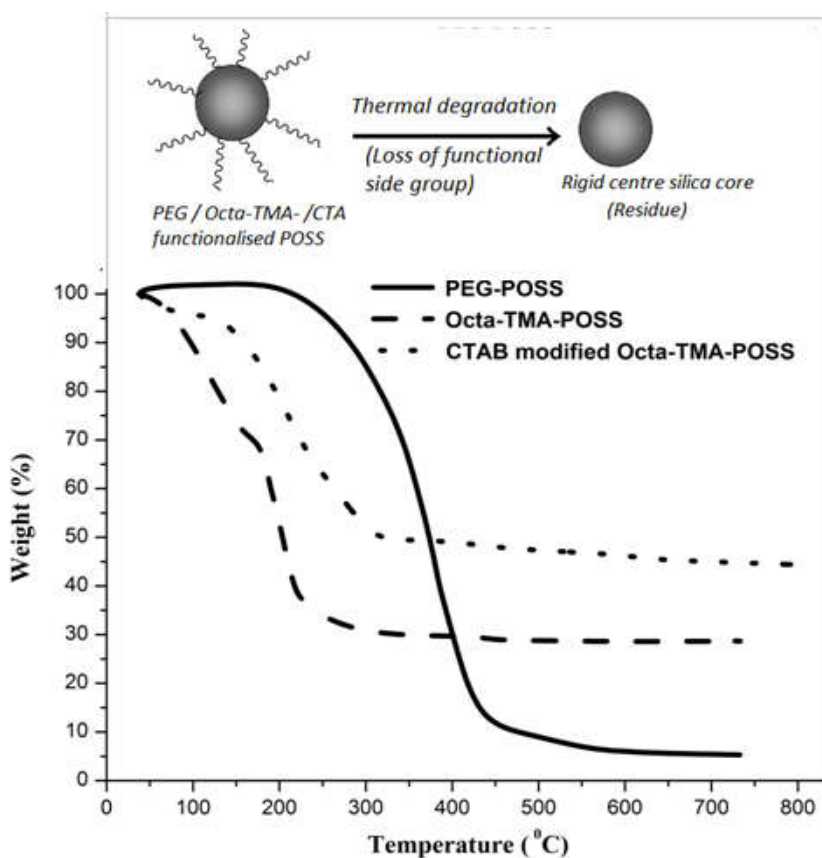


**Figure 8.2:** Thermogram of PEG-POSS, Octa-TMA-POSS and m-POSS

### 8.2.1.2 PVA/POSS systems

An insight into the thermal stability of polymers has an important role in regulating the processing conditions and applications. The thermal degradation mechanism of PVA is presented in **Figure 8.3**.<sup>30</sup> As seen in **Figure 8.3**, two major decomposition stages for pure PVA, which is represented by the two distinct mass changes with temperature is seen in the thermogram. In the temperature range 140-170°C a slight change in weight can be seen, which is associated with the evaporation of some low molecular weight components in the PVA. The weight loss in this region is nearly 4%

and is not regarded as the degradation reaction of the polymer chain. The temperature at which a minimum of 10% of mass loss take place is considered to be the onset of degradation in macromolecules.<sup>31</sup> The first stage principal thermal degradation of PVA takes place in the temperature range 215-350°C corresponding to the elimination reaction of the acetate group residue persist in the PVA chain due to incomplete hydrolysis. The second stage weight loss is observed in the temperature range 380-460°C, which mainly involves the degradation of carbonaceous materials such as polyene formed in first degradation step to yield carbon and hydrocarbon mixture.

**Figure 8.4 (a-d)** presented the TGA-DTG plots of PVA/PEG-POSS and PVA/Octa-TMA-POSS systems and the data for major weight loss regions are shown in **Table 8.1**. It is evident in **Figure 8.4 (a-b)**, the first and second stage degradation temperature of PVA/PEG-POSS systems are shifted to higher temperatures as compared with neat PVA, indicating increased degradation resistance of PVA system in the presence of low molecular weight PEG functionalised POSS. This suppression of thermal decomposition is due to the good interaction including H-bonding between organic PEG part of POSS and PVA chain. Moreover, the inorganic core of POSS possess high thermal stability, which can act as barrier for quick transmittance of heat and thereby minimise the continuous degradation of the PVA/PEG-POSS system. Schematic representation for the barrier effect of rigid core of POSS is shown in **Scheme 8.1**. As shown in **Figure 8.4 (c-d)**, PVA/Octa-TMA-POSS system exhibits lower thermal degradation stability as compared to PVA. It is caused by the lower degradation temperature of Octa-TMA group on the POSS. The surfactant nature of Octa-TMA-POSS leads to clustering of molecules at higher loading which inturn reduces the thermal stability of the membrane (**Scheme 8.2**).

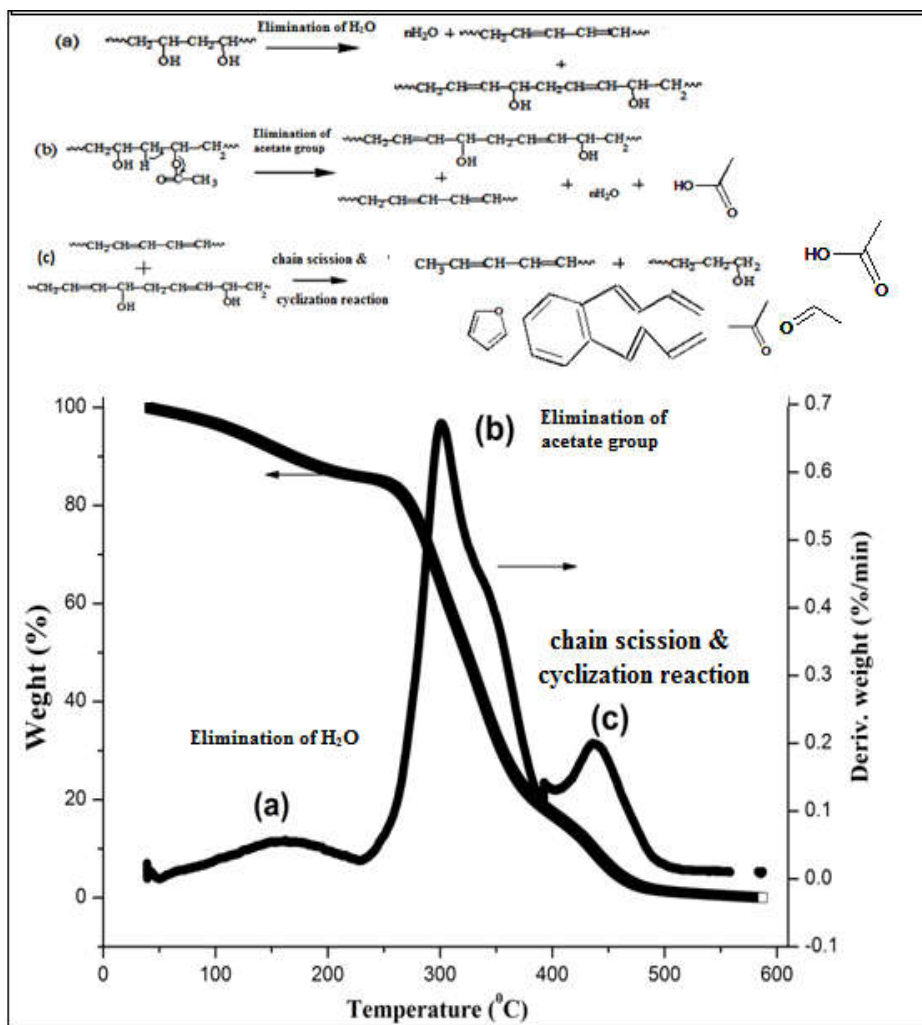


**Figure 8.3:** Thermograms (TGA) and differential thermograms (DTG) of PVA



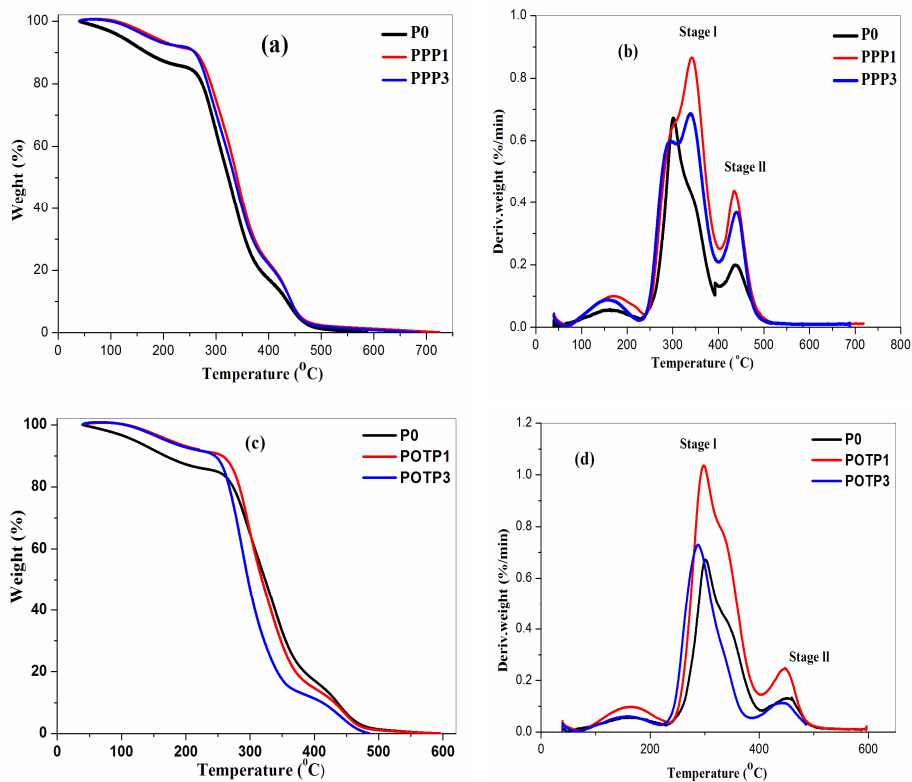
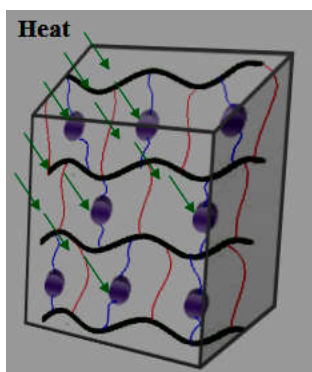


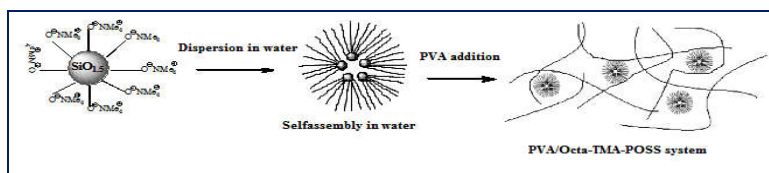
**Figure 8.4:** Thermograms and differential thermograms of PVA/POSS systems

**Table 8.1:** Effect of filler loading on the thermal degradation of PVA/POSS systems

Sample	$T_{4\%}$ (°C)	$T_{\max 1}$ (°C)	$T_{\max 2}$ (°C)
P0	154	300	436
PPP1	167	343	437
PPP3	155	340	437
POTP1	162	297	435
POTP3	157	287	434



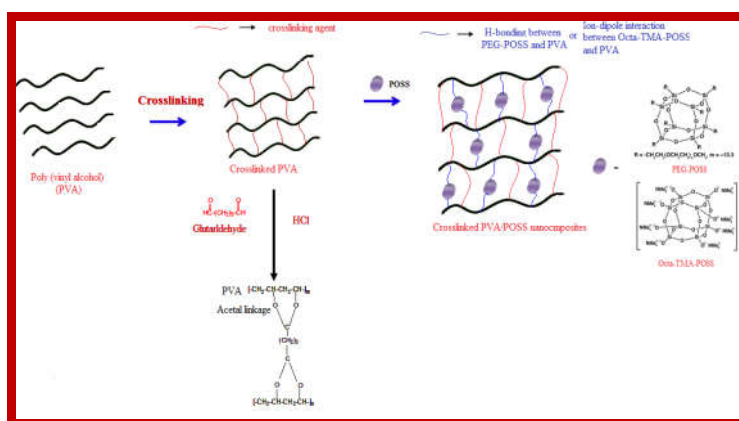
**Scheme 8.1:** Schematic representation showing the barrier effect of rigid siloxane core of the POSS



**Scheme 8.2:** Clustering behaviour of Octa-TMA-POSS in PVA/Octa-TMA-POSS system

### 8.2.1.3 Crosslinked PVA/POSS systems

**Figure 8.5** and **Table 8.2** demonstrates the effect of POSS on the thermal degradation property of the crosslinked PVA system. Schematic representation of the fabrication of crosslinked PVA/POSS membranes are presented in **Scheme 8.3**. The crosslinking of PVA with glutaraldehyde shows no significant changes in its characteristic degradation temperature (**Figure 8.5 (a)**). However, a significant change in degradation mechanism can be observed when POSS is incorporated in the crosslinked PVA. Presence of crosslinking in the PVA/POSS system reduce the mobility of PVA chains significantly. Consequently, high thermal energy is required for the cleavage of strongly crosslinked network. Crosslinked system exhibited considerably different multi-stage degradation process with new degradation steps as compared with pure PVA. This can be attributed to the presence of new interfacial interactions as well as the construction of 3-dimensional network structure in the polymer.



**Scheme 8.3:** Schematic diagram of crosslinked PVA/POSS system

It is interesting to observe that in the DTG plot of PEG-POSS embedded crosslinked PVA system (**Figure 8.5(b)**), a new minor peak is located at 289°C ( $T_{7\%}$ ) and which is absent in pure PVA or PGP1 system. Moreover, the first major degradation temperature of PGP1 sharply increased from 300 to 356°C, which is about 56°C higher than that of pure PVA. This improvement in degradation resistance and presence of new degradation step can be attributed to the presence of highly crosslinked network in the PVA matrix and improved interfacial interaction between crosslinked PVA with PEG-POSS. The second stage degradation temperature of PGP1 is increased by 83°C. This degradation is associated with the breakage of the PVA chain to carbon and hydrocarbons as well as acetal crosslinked network fraction present in the membrane.

**Table 8.2:** Effect of filler loading on the thermal degradation of crosslinked PVA/POSS systems

Sample	$T_{4\%}$ (°C)	$T_{\text{max}1}$ (°C)	$T_{\text{max}2}$ (°C)
PG	156	287	435
PGP1	148	356	443
PGO1	161	369	519

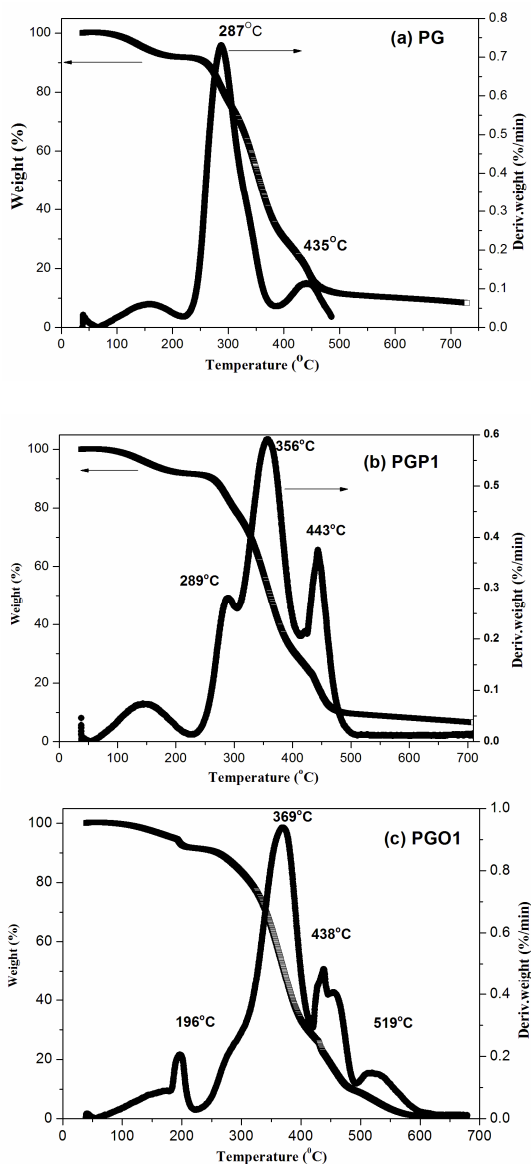


**Figure 8.5 (a-c):** Thermograms and differential thermograms of crosslinked PVA and crosslinked PVA/POSS systems

Crosslinked PVA/Octa-TMA-POSS system shows different thermal degradation behaviour as compared to PG and PGP1, which is presented in

**Figure 8.5 (c).** It can be attributed to the formation of high heat resistant three dimensional crosslinked network structure in polymer, which enhances the interfacial interaction between the chains and decreases the flexibility of the chains. Additional peaks observed for PGO1 at 196 and 438°C are associated with the breakage of crosslinked small network fragments confined in POSS particle surface and between the PVA chains. As evident from the thermogram, the first and second principal decomposition peak of PGO1 increased significantly (300 to 369°C and 436 to 519°C) due to the presence of highly crosslinked chains and the rigid inert core of POSS.

#### 8.2.1.4 PVA/m-POSS systems

The influence of m-POSS on the thermal degradation of glutaraldehyde crosslinked PVA are investigated through TGA analysis. TGA-DTG curves of PVA/m-POSS are presented in **Figure 8.6** and the data for relevant weight loss regions are shown in **Table 8.3**. It is interesting to observe that the introduction of m-POSS and GLA crosslinking enhance the thermal degradation stability of PVA matrix significantly, which indicates the existence of new interfacial interaction such as ion-dipole interaction. As compared with pure PVA, PVA/m-POSS system shows a new peak at 442°C with 9.5wt% weight loss, which is assigned to the thermal degradation of cetyltrimethylammonium group of POSS and the crosslinking networks present in the membrane. The first and second stage principal degradation temperature of POCPG1 is found to be increased by 67 and 128°C respectively as compared to that of crosslinked PVA, which is probably associated with the presence of strong crosslinking networks and good interfacial adhesion of m-POSS within the PVA matrix, which restrict the mobility of PVA chains. The long and high molecular weight alkyl chains in

the m-POSS provide  $\text{CH}_2\text{-CH}_2$  interaction that enhances greater intermolecular forces between chains.

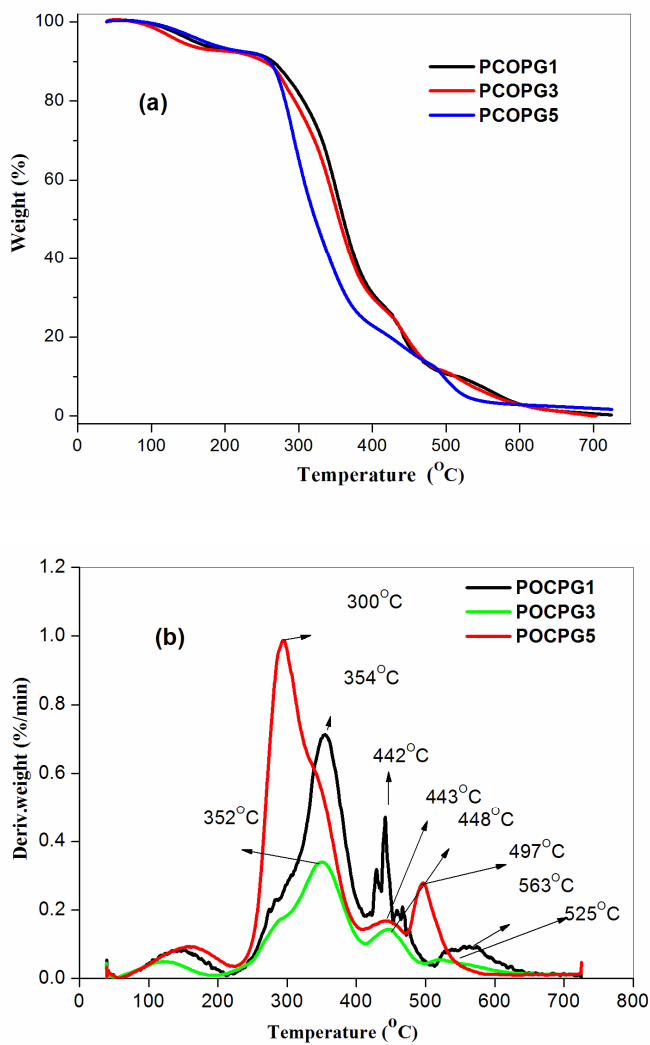


**Figure 8.6:** (a) Thermograms and (b) differential thermograms of PVA/m-POSS systems

**Table 8.3:** Effect of filler loading on the thermal degradation of PVA/m-POSS systems

Sample	T <sub>4%</sub> (°C)	T <sub>max1</sub> (°C)	T <sub>9.5%</sub> (°C)	T <sub>max2</sub> (°C)
PCOPG1	144	354	442	563
PCOPG3	124	352	448	525
PCOPG5	156	298	443	497

### 8.2.1.5 PVA-PEO/POSS systems

The effect of PEG-POSS and Octa-TMA-POSS on the thermal degradation of PVA-PEO blend systems are analysed and presented in **Figure 8.7** and **Table 8.4**. A single-stage decomposition can be observed for PEO through random scission of the chain links.<sup>32</sup> The degradation behaviour of PVA-PEO/POSS system is found to be very different from the PVA and PEO due to the H-bonding interaction between PVA and PEO promoted by POSS at the interface. The role of CMC in the blend system is to improve the interfacial interaction between PVA and PEO. As compared with PVA, PVA-PEO/POSS system exhibits one new decomposition step at 419°C which could be attributed to the good interfacial interaction between PVA and PEO with the help of POSS and CMC. T<sub>max1</sub> and T<sub>max2</sub> of PPCPP3 is increased by 29 and 45°C and that of PPCOP3 by 27 and 79°C respectively, suggesting the interaction of PVA-PEO at the interface in the presence of CMC and POSS molecule.

**Table 8.4:** Effect of filler loading on the thermal degradation of PVA and PVA-PEO/POSS systems

Sample	T <sub>4%</sub> (°C)	T <sub>max1</sub> (°C)	T <sub>14%</sub> (°C)	T <sub>max2</sub> (°C)
P0	154	300	-	437
PPCPP3	156	329	419	482
PPCOP3	156	327	426	516

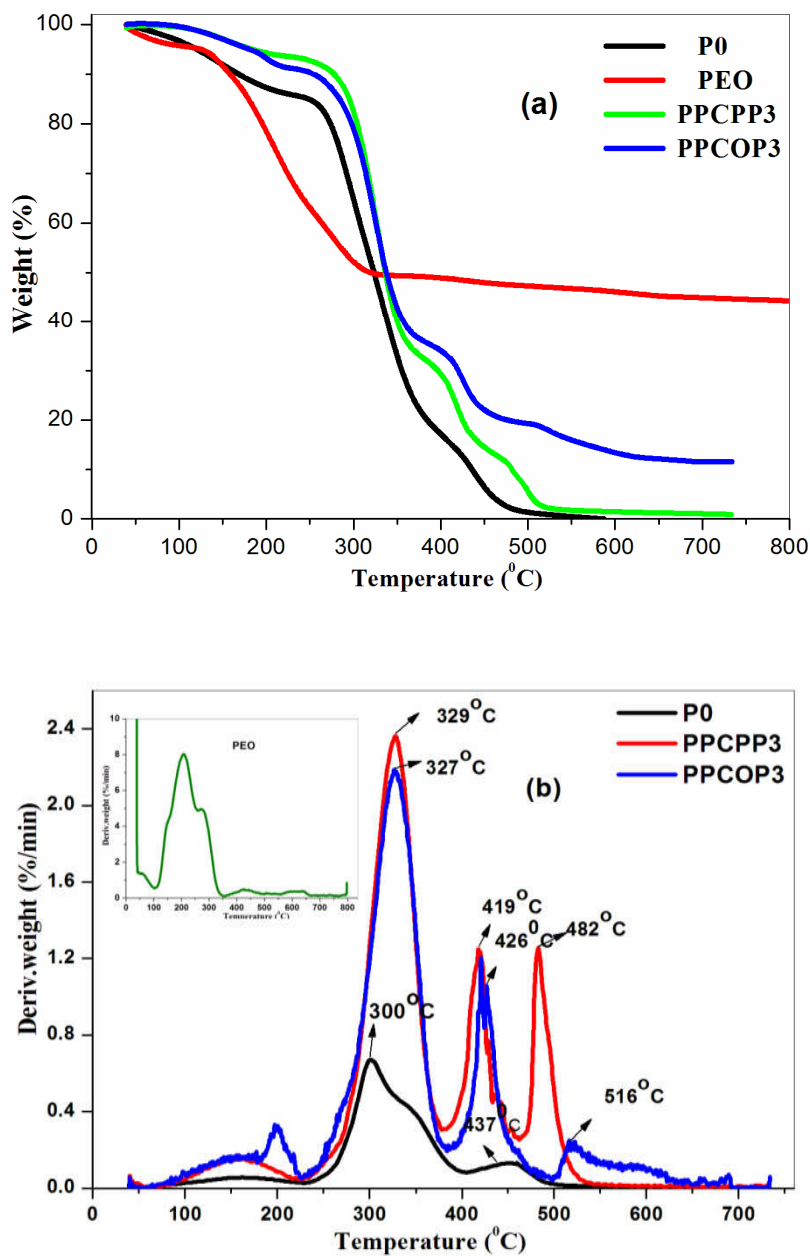


**Figure 8.7:** (a) Thermograms and (b) differential thermograms (DTG) of PVA, PEO (inset) and PVA-PEO/POSS systems



### 8.2.6 Analysis of residue of all systems

The residue remaining after degradation process of the POSS incorporated crosslinked PVA system at 550°C are found to be higher than PVA and are shown in **Figure 8.8**. For pure PVA only 0.879% weight of residue is remaining at 550°C. PEG-POSS and Octa-TMA-POSS incorporated PVA system shows almost similar weight loss as of pure PVA. But on crosslinking, pure PVA and PVA/POSS system show a significant enhancement in residue, which is due to the presence of acetal crosslinking network in the membrane, which reduces the flexibility and degradation of PVA chains. The mass of residue of Octa-TMA-POSS doped PVA-PEO system is found to be maximum (18.58%) as compared with all other systems due to the modification of interface of PVA-PEO with rigid POSS and CMC molecules.

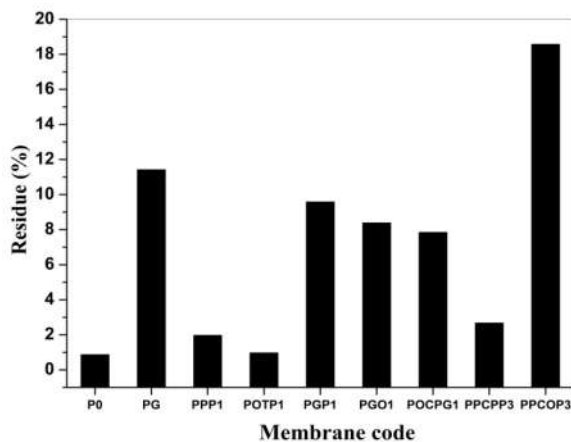


**Figure 8.8:** Residue (%) of all the membranes at 550°C

### 8.2.7 Activation energy for thermal degradation

Activation energy for the first stage principal degradation of all POSS incorporated PVA and PVA-PEO systems are analyzed by the Horowitz and Metzger (HM) integral method and its equation is given below.<sup>33</sup>

$$\ln\left[\ln\left(\frac{1}{1-\alpha}\right)\right] = \left[E_a \theta / RT_{\max}^2\right] \quad (8.1)$$

where  $\alpha$  is the degraded weight fraction ie,  $\alpha = w_i - w_T / w_i - w_f$ , where  $w_i$  is the weight at initial temperature,  $w_f$  is the weight at final temperature and  $w_T$  the weight at temperature chosen,  $E_a$  is the activation energy, R is the universal gas constant, T is the temperature at maximum rate of weight loss and is taken as  $T_{\max}$  and  $\theta$  is  $T - T_{\max}$ . Activation energy,  $E_a$  can be

calculated from the slope of the plot of  $\ln\left[\ln\left(\frac{1}{1-\alpha}\right)\right]$  versus  $\theta$ , where slope  $= E_a / RT_{\max}^2$ .

Horowitz–Metzger plots of PVA/POSS systems and their activation energy for degradation is calculated from the slope of the plot and are displayed in **Figure 8.9 (a-b)**. The PVA/PEG-POSS system showed higher activation energy than pure PVA. This can be attributed to the good interfacial interaction and homogeneous distribution of POSS, which restrict the mobility of PVA chains which leads to the increase in the degradation stability. The increase in  $E_a$  implies that more energy is required for the stage 1 degradation, which in turn indicates an enhancement in thermal stability of the composite. In the case of Octa-TMA-POSS incorporated PVA,  $E_a$  is less than pure PVA due to the lower thermal stability of anionic octa(tetramethylammonium)-side group on POSS.

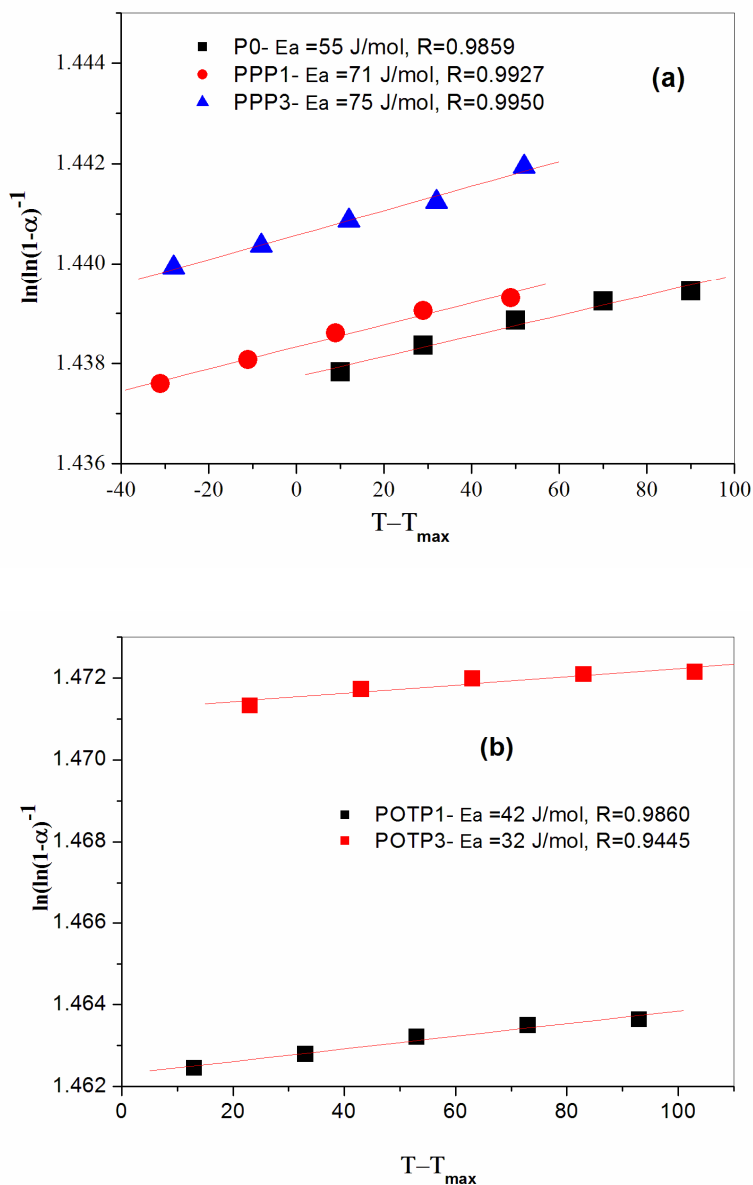


**Figure 8.9(a-b):** Kinetic plots of activation energy ( $E_a$ ) for degradation of PVA/POSS system.  $R$  in the inset of the graph indicates the regression of the linear plot.

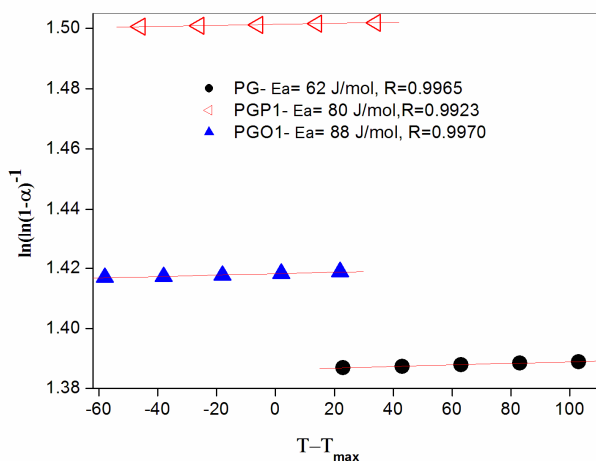


**Figure 8.10:** Kinetic plots of activation energy for degradation of crosslinked PVA/POSS system

Activation energy increased significantly upon the introduction of PEG-POSS and Octa-TMA-POSS molecules in crosslinked PVA matrix, which is illustrated in **Figure 8.10**. This can be attributed in terms of the formation of highly stable new 3-dimensional network structure in the polymer.

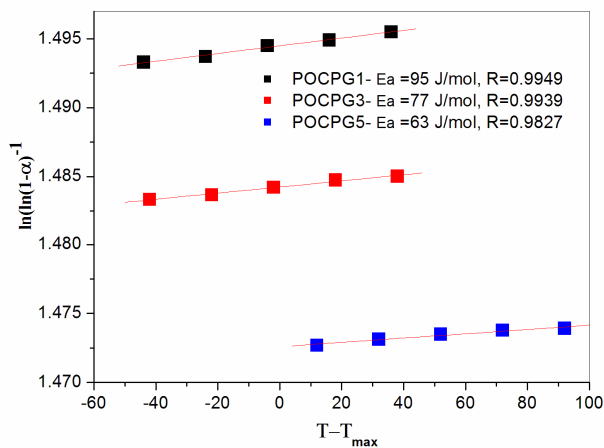


**Figure 8.11:** Kinetic plots of activation energy for degradation of PVA/m-POSS system

Interesting results are obtained upon the introduction of m-POSS in the crosslinked PVA. Among the various PVA/POSS systems presented, the 1wt% m-POSS embedded crosslinked PVA system shows the maximum activation energy for the degradation, it is evident from **Figure 8.11**. This can be explained in terms of the good interfacial interaction of m-POSS and PVA chains.

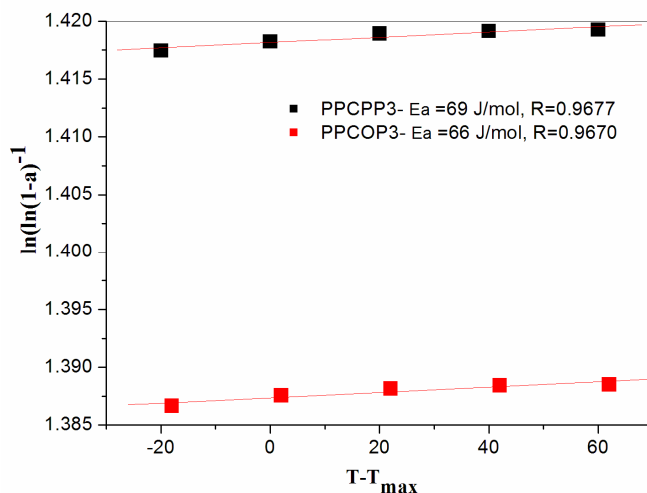


**Figure 8.12:** Kinetic plots of activation energy for degradation of PVA-PEO/POSS system

**Figure 8.12** illustrated the activation energy for degradation of PVA-PEO/POSS system. The significant improvement in activation energy is observed in the PVA-PEO/POSS systems as compared with pure PVA, which could be attributed to the modified interface of PVA by blending with PEO through H-bonding interaction supported by the CMC and POSS molecule.

### 8.2.8 Mechanical properties in the hydrated state

The mechanical properties of pristine PVA and PVA-POSS systems in the hydrated state are investigated and presented in the **Figure 8.13**. In the hydrated state, PVA can strongly interact with water molecule through H-

bonding. Thus PVA undergoes swelling and plasticization resulting in very poor tensile strength. Interestingly, the introduction of POSS molecule in PVA matrix made significant improvement in its wet tensile strength. Water content on the sample has large effect not only on the dispersibility of POSS but also on the interaction of POSS with the PVA matrix. The reason for the good mechanical performance of PVA/POSS systems might be the dominant matrix-filler interaction over the composite-water interaction. Moreover, in POSS molecule the inner cage is fabricated by intrinsically strong and hydrophobic siloxane linkages, which also contribute significantly to the strength of the PVA membranes. CTAB modified POSS introduced PVA membrane exhibit maximum improvement (2.5 times higher than neat PVA) in tensile strength due to its well dispersion in the PVA matrix and the CH<sub>2</sub>-CH<sub>2</sub> interaction of long alkyl tail of the m-POSS molecule with the PVA chains. From the results, it is revealed that the PVA/POSS membranes possess mechanical stability in an appreciable level even in the hydrated state.

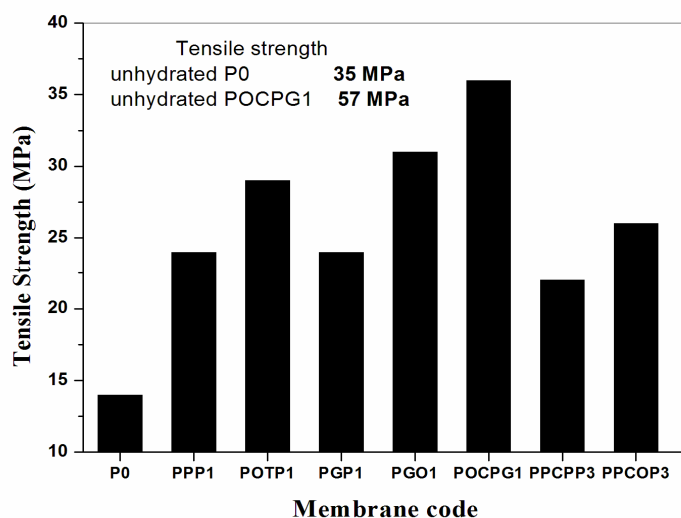


**Figure 8.13:** Tensile strength of PVA/POSS samples at hydrated state

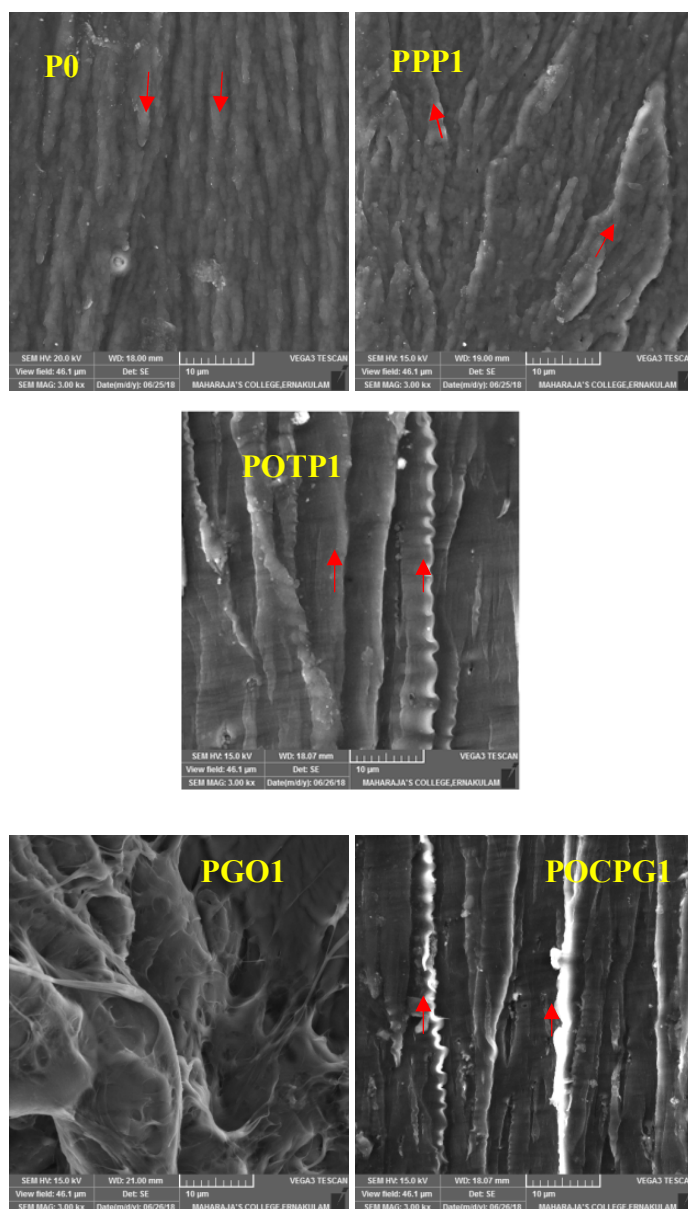


**Figure 8.14:** SEM images of the tensile fractured surface of different PVA/POSS systems at hydrated state

SEM images of tensile fractured surfaces of wet samples are taken and are presented in **Figure 8.14**. The red arrows in the micrograph indicate the direction of crack propagation. The hydrated PVA exhibit linear crack propagation. The crack propagation of hydrated PEG-POSS embedded PVA samples are found to be similar as that of hydrated PVA, it exhibit a slight nonlinear crack propagation due to the presence of oligomeric PEG functional group in the membrane. Fibrillar like morphology is observed in Octa-TMA-POSS and m-POSS doped PVA membrane due to the dominant rigid siloxane core of the POSS, which restrict the crack propagation and the strength of the membrane increases. In the case of Octa-TMA-POSS introduced crosslinked PVA membrane, nonlinear crack propagation is observed, which suggest the high strength of the PGO1 membrane.

### 8.3 Conclusions

Thermo gravimetric analysis was carried out to get an insight into the effect of various POSS particles on the thermal degradation stability of PVA membrane. PEG, Octa-TMA- and cetyltrimethyl ammonium (CTA) functionalised POSS were selected for the present study. The findings revealed that PVA-PEO and crosslinked PVA system exhibited high thermal degradation stability upon the addition of minimum amount of POSS molecule with respect to unfilled PVA. introduction of Octa-TMA-POSS reduced the thermal stability of pure PVA while its introduction on crosslinked PVA enhanced the thermal stability significantly. As compared to uncrosslinked system, crosslinked PVA/POSS system showed more degradation stability due to the formation of three dimensional network structure. Activation energy for the degradation of PVA/POSS and PVA-PEO/POSS systems were found to be higher than the pure PVA. Tensile studies of hydrated samples suggested the stability of POSS embedded PVA and PVA-PEO membranes even in the hydrated state to an appreciable level.



---

## 8.4 References

1. Z. Li, J. Kong, F. Wang, C. He, Polyhedral oligomeric silsesquioxanes (POSSs): an important building block for organic optoelectronic materials, *J. Mater. Chem. C.*, 5 (2017) 5283-5298
2. W. Zhang, G. Camino, R. Yang, Polymer/polyhedral oligomeric silsesquioxane (POSS) nanocomposites: An overview of fire retardance, *Prog. Poly. Sci.*, 67 (2017) 77-125
3. H. Zhou, Q. Ye, J. Xu, Polyhedral oligomeric silsesquioxane-based hybrid materials and their applications, *Mater. Chem. Front.*, 1 (2017) 212-230
4. A. Ullah, S. Ullah, G. S. Khan, S. M. Shah, Z. Hussain, S. Muhammad, M. Siddiq, H. Hussain, Water soluble polyhedral oligomeric silsesquioxane based amphiphilic hybrid polymers: synthesis, self-assembly and applications, *Euro. Poly. J.*, 75 (2016) 67-92
5. I. Blanco, L. Abate, F. A. Bottino, P. Bottino, Thermal behaviour of a series of novel aliphatic bridged polyhedral oligomeric silsesquioxanes (POSSs)/polystyrene (PS) nanocomposites: The influence of the bridge length on the resistance to thermal degradation, *Poly. Degrad. Stab.*, 102 (2014) 132-137
6. Y. Meng, Z. Wei, L. Liu, L. Zhang, T. Nishi, K. Ito, Significantly improving the thermal stability and dispersion morphology of polyhedral oligomeric silsesquioxane/polysiloxane composites by in-situ grafting reaction, *Polymer* 54 (2013) 3055-3064
7. M. Qian, V. J. Murray, W. Wei, B. C. Marshall, T. K. Minton, The resistance of POSS polyimide blends to hyperthermal atomic oxygen attack, *ACS Appl. Mater. Interfac.*, 8 (49) (2016) 33982-33992
8. G. Guerrero, M. B. Hägg, G. Kignelman, C. Simon, T. Peters, N. Rival, C. Denonville, Investigation of amino and amidino functionalized Polyhedral oligomeric silsesquioxanes (POSS<sup>®</sup>) nanoparticles in PVA-based hybrid membranes for CO<sub>2</sub>/N<sub>2</sub> separation, *J. Mem. Sci.*, 544, (2017) 61-173
9. J. Pagacz, E. Hebda, B. Janowski, D. Sternik, M. Jancia, K. Pielichowski, Thermal decomposition studies on polyurethane

- elastomers reinforced with polyhedral silsesquioxanes by evolved gas analysis, *Poly. Degrad. and Stab.*, 149 (2018) 129-142
10. J. Wang, J. Sun, J. Zhou, K. Jin, Q. Fang, Fluorinated and thermo-cross-linked polyhedral oligomeric silsesquioxanes: new organic-inorganic hybrid materials for high-performance dielectric application, *ACS Appl. Mater. Interfaces*, 9 (14) (2017) 12782-12790
  11. Z. Geng, M. Huo, J. Mu, S. Zhang, Y. Lu, J. Luan, P. Huo, Y. Du, G. Wang, Ultra low dielectric constant soluble polyhedral oligomeric silsesquioxane (POSS)-poly(aryl ether ketone) nanocomposites with excellent thermal and mechanical properties, *J. Mater. Chem. C.*, 2 (2014) 1094-1103
  12. N. Konnertz, Y. Ding, W. J. Harrison, P. M. Budd, A. Schönhals, M. Böhning, Molecular mobility and gas transport properties of nanocomposites based on pim-1 and polyhedral oligomeric phenethyl-silsesquioxanes (POSS), *J. Mem. Sci.*, 529 (2017) 274-285
  13. B. Montero, R. Bellas, C. Ramírez, M. Rico, R. Bouza, Flame retardancy and thermal stability of organic-inorganic hybrid resins based on polyhedral oligomeric silsesquioxanes and montmorillonite clay, *Composites: Part B* 63 (2014) 67-76
  14. Z. Li, J. Kong, F. K. Wang, C. He, Polyhedral oligomeric silsesquioxanes (POSSs): an important building block for organic optoelectronic materials, *J. Mater. Chem. C.*, 5 (2017) 5283-5298
  15. W. H. Liao, S. Y. Yang, S. T. Hsiao, Y. S. Wang, S. M. Li, C. C. M. Ma, H. W. Tien, S. J. Zeng, Effect of octa(aminophenyl) polyhedral oligomeric silsesquioxane functionalized graphene oxide on the mechanical and dielectric properties of polyimide composites, *ACS Appl. Mater. Interfac.*, 6 (18) (2014) 15802-15812
  16. S. Kanehashi, Y. Tomita, K. Obokata, T. Kidesaki, S. Sato, T. Miyakoshi, K. Nagai, Effect of substituted groups on characterization and water vapor sorption property of polyhedral oligomeric silsesquioxane (POSS)-containing methacryl polymer membranes, *Polymer* 54 (2013) 2315-2323
  17. A. M. Joseph, B. Nagendra, K. P. Surendran, E. B. Gowd, Syndiotactic polystyrene/hybrid silica spheres of POSS siloxane

- composites exhibiting ultralow dielectric constant, *ACS Appl. Mater. Interfac.*, 7 (34) (2015) 19474-19483
18. D. Yang, W. Zhang, R. Yao, B. Jiang, Thermal stability enhancement mechanism of poly(dimethylsiloxane) composite by incorporating octavinyl polyhedral oligomeric silsesquioxanes, *Poly. Degra. Stab.*, 98 (2013) 109-114
  19. A. Mandal, D. Chakrabarty, Studies on the mechanical, thermal, morphological and barrier properties of nanocomposites based on poly(vinyl alcohol) and nanocellulose from sugarcane bagasse, *J. Indus. Eng. Chem.*, 20 (2014) 462-473
  20. Y. Caydamli, E. Yildirim, J. Shen, X. Fang, M. A. Pasquinelli, R. J. Spontak, A. E. Tonelli, Nanoscale considerations responsible for diverse macroscopic phase behavior in monosubstituted isobutyl-POSS/poly(ethylene oxide) blends, *Soft Matter.*, 3(46) (2017) 8672-8677
  21. H. G. Premakshi, M. Y. Kariduraganavar, G. R. Mitchell, Development of composite anion-exchange membranes using poly(vinyl alcohol) and silica precursor for pervaporation separation of water-isopropanol mixtures, *RSC Adv.*, 6 (2016) 11802-11814
  22. F. P. La Mantia, M. Morreale L. Botta, M. C. Mistretta, M. Ceraulo, R. Scaffaro, Degradation of polymer blends: A brief review, *Poly. Degra. Stab.*, 145 (2017) 79-92
  23. Y. Wang, C. Xiang, T. Li, P. Ma, H. Bai, Y. Xie, M. Chen, W. Dong, Enhanced thermal stability and uv-shielding properties of poly(vinyl alcohol) based on esculetin, *J. Phys. Chem. B.*, 121 (5) (2017) 1148-1157
  24. A. Usman, Z. Hussain, A. Riaz, A. N. Khan, Enhanced mechanical, thermal and antimicrobial properties of poly(vinyl alcohol)/graphene oxide/starch/silver nanocomposites films, *Carbohydr. Polym.*, 153 (2016) 592-599
  25. A. K. Sonker, H. D. Wagner, R. Bajpai, R. Tenne, X. M. Sui, Effects of tungsten disulphide nanotubes and glutaric acid on the thermal and mechanical properties of polyvinyl alcohol, *Compos. Sci. Tech.*, 127 (2016) 47-53

- 
26. H. Lu, C. A. Wilkie, M. Ding, L. Song, Thermal properties and flammability performance of poly(vinyl alcohol)/a-zirconium phosphate nanocomposites, *Poly. Degra. Stab.*, 96 (2011) 885-891
  27. Z. Peng, L. X.Kong, A thermal degradation mechanism of poly(vinyl alcohol)/silica nanocomposites, *Poly. Degra. Stab.*, 92 (2007) 1061-1071
  28. S. D. Jiang, Z. M. Bai, G. Tang, Y. Hu, L. Song, Fabrication and characterization of graphene oxide-reinforced poly(vinyl alcohol)-based hybrid composites by the sol-gel method, *Compos. Sci. Technol.*, 102 (2014) 51-58
  29. S. S. Dong, F. Wu, L. Chen, Y. Z. Wang, S. C. Chen, Preparation and characterization of poly(vinyl alcohol)/grapheme nanocomposite with enhanced thermal stability using PEtVIm-Br as stabilizer and compatibilizer, *Poly. Degra. Stab.*, 131 (2016) 42-52
  30. A. Singhal, M. Kaur, K. A. Dubey, Y. K. Bhardwaj., D.Jain, C. G. S. Pillai, A. K.Tyagi, Polyvinyl alcohol-In<sub>2</sub>O<sub>3</sub> nanocomposite films: synthesis, characterization and gas sensing properties, *RSC Adv.*, 2 (2012) 7180-7189
  31. V. P. Swapna, T. P. Selvin, K. I. Suresh , V. Saranya, M. P. Rahana, R. Stephen, Thermal properties of poly(vinyl alcohol) (PVA)/halloysite nanotubes reinforced nanocomposites, *Int. J. Plast. Technol.*, 19 (2015) 124-136
  32. S. L. Madorsky, S. Straus, Thermal Degradation of Polyethylene Oxide and Polypropylene Oxide, *J. Poly. Sci.*, 36 (1959) 183-194
  33. H. H. Horowitz, G. Metzger, A new analysis of thermogravimetric traces, *Anal. Chem.*, 35 (1963) 1464.

# Conclusions And Future Outlook

---

Poly (vinyl alcohol) (PVA) and poly(ethylene oxide) (PEO) are widely utilised in the separation process due to their water solubility, biodegradability, nontoxicity, gas permeability, thermal properties and ability to form strong H-bonds with various additives. The major challenge in the fabrication of PVA based membrane for separation process is to reduce its swelling behaviour in water and to enhance the separation performance. Incorporation of inorganic moieties in organic polymer membranes is found to be a highly successful strategy to produce advanced material with remarkable mechanical and transport properties. Polyhedral oligomeric silsesquioxane (POSS) is a cage-shaped hybrid organic-inorganic molecule with the chemical formula  $(\text{RSiO}_{1.5})_n$ , consisting of well-defined rigid siloxane core and peripheral organic groups (R). This hybrid material can contribute excellent mechanical stability and separation property to polymers. The rigid silica core imparts enhanced mechanical strength and thermal stability while the versatile and adjustable outer functional groups provide good compatibilisation with polymers.

In this thesis, we presented different strategies for the fabrication of mechanically and thermally stable polyhedral oligomeric silsesquioxane (POSS) embedded poly (vinyl alcohol) (PVA) membranes with excellent permeation properties through solution casting method. Mainly three systems were prepared using various functionalised POSS: (i) PVA/PEG-POSS and PVA/Octa-TMA-POSS, (ii) chemically crosslinked PVA/m-POSS and (iii) PVA-PEO/PEG-POSS and PVA-PEO/Octa-TMA-POSS.

---

The membranes were well characterised by FTIR, XRD, DSC, SEM, TEM, AFM, contact angle measurements and PALS. Influence of POSS on the crystallinity, free volume, mechanical, dynamic mechanical, permeation and thermal properties of PVA and PVA-PEO membranes were analysed and discussed in detail with respect to the functional groups and weight percentage of POSS.

### **9.1 PVA/PEG-POSS and Octa-TMA-POSS systems**

In chapter 3, FTIR results revealed the hydrogen bonding interaction between PVA and PEG-POSS. Crystallinity of the systems were estimated from XRD and DSC measurements, it was observed that the crystallinity of PVA/Octa-TMA-POSS system gets improved as compared with pure PVA. PVA/PEG-POSS system exhibited good ductility and toughness due to the presence of eight flexible PEG tails on the siloxane core of POSS. However, Octa-TMA-POSS incorporated PVA system showed excellent tensile strength and modulus due to the presence of dominant rigid three-dimensional inorganic core in the POSS. The increased hydrophilicity of both systems as compared with pure PVA were confirmed from contact angle studies. The viscoelastic property of PVA/Octa-TMA-POSS system at higher concentration of Octa-TMA-POSS is remarkable, which exhibited higher storage modulus and glass transition temperature due to the presence of rigid inorganic silsesquioxane core in the PVA matrix. The damping behaviour of PVA membrane increased in the presence of POSS particles.

In Chapter 4, the effect of PEG-POSS and Octa-TMA-POSS on the pervaporation (PV) separation performance of PVA was presented and discussed in detail. These membranes achieved excellent water selectivity and permeance during the PV separation of THF-water azeotropic mixture

by overcoming the limitations of trade-off effects in membrane based separation. The presence of hydrophilic functional group on the POSS improved the hydrophilicity of the membrane and produced more binding sites for water molecule in the membrane. As compared with pure PVA, PEG-POSS and Octa-TMA-POSS introduced PVA showed remarkable increase in selectivity.

Gas transport behaviour of PVA/PEG-POSS and PVA/Octa-TMA-POSS membranes were analysed using N<sub>2</sub>, O<sub>2</sub> and CO<sub>2</sub> gases and is presented in chapter 6. PVA/PEG-POSS membranes showed remarkable improvement in CO<sub>2</sub> permeability and selectivity because of the plasticizing action of flexible low molecular weight PEG group on the POSS situated between PVA chains and high dipole-quadrupolar interaction of CO<sub>2</sub> molecules with ethylene oxide groups present in the membrane. Introduction of Octa-TMA-POSS reduced the O<sub>2</sub> and N<sub>2</sub> permeability of the PVA membrane due to the improved crystallinity of PVA/Octa-TMA-POSS system as compared with pure PVA. PALS confirms the significant improvement in polymer free volume in PVA/POSS systems. TGA analysis of membranes were presented in chapter 9. It has been found that PEG-POSS improves the thermal degradation stability of PVA due to the high thermal stability of rigid inorganic core of POSS. While introduction of Octa-TMA-POSS reduced the thermal degradation stability significantly due to the lower degradation temperature of Octa-TMA group on the POSS.

## 9.2 PVA/m-POSS system

In this system, two types of chemical modification was adopted for the fabrication of PVA/POSS membrane: (i) chemical crosslinking of PVA using glutaraldehyde and (ii) chemical modification of Octa-TMA-POSS using cetyltrimethylammonium bromide (CTAB). Characterisation, mechanical and pervaporation properties of PVA/m-POSS were presented

in Chapter 5. The successful modification of Octa-TMA-POSS by CTAB (m-POSS) was confirmed from FTIR and NMR analysis. m-POSS introduced crosslinked PVA membrane exhibited excellent mechanical property and pervaporation performance for the separation of IPA-water azeotropic mixture. The introduction of m-POSS increased the hydrophilicity of the crosslinked PVA. Enhanced wettability observed in the presence of cetyltrimethylammonium group on the POSS due to its amphiphilic nature. Tensile strength and Young's modulus of PVA matrix was increased significantly at higher weight percentage of m-POSS. The introduction of CTAB modified Octa-TMA-POSS in the crosslinked PVA was found to be an effective method to achieve excellent mechanical performance for PVA membrane. The fabricated crosslinked PVA/m-POSS system showed excellent pervaporation performance for the separation of isopropanol (IPA)-water azeotropic mixture. The membranes exhibited excellent water selectivity and permeance at lower loading of POSS. The influence of m-POSS on the permeability of  $N_2$ ,  $O_2$  and  $CO_2$  molecules in crosslinked PVA membrane has been examined and presented in chapter 6. Increased  $CO_2$  permeability and  $CO_2/N_2(O_2)$  selectivity of PVA in the presence of m-POSS molecule has been observed due to the high affinity of anionic POSS towards polar  $CO_2$  molecule. Another interesting observation was the high gas permeability of 3 wt% m-POSS incorporated crosslinked PVA membrane owing to the significant increase in free volume defects in the membrane. The system achieved excellent improvement in thermal degradation stability and mechanical stability in hydrated state due to the presence of rigid siloxane core of the POSS and the  $CH_2-CH_2$  interaction of long alkyl tail of the m-POSS molecule with the PVA chains (chapter 8).



### 9.3 PVA-PEO/PEG-POSS and Octa-TMA-POSS systems

The fabricated PVA-PEO/POSS membranes exhibited excellent azeotropic mixture (THF-water) separation and CO<sub>2</sub> separation (CO<sub>2</sub>/N<sub>2</sub> and CO<sub>2</sub>/O<sub>2</sub> gas mixtures) properties by overcoming the limitations of trade-off effects in membrane based separation. PVA-PEO/POSS membranes exhibited higher CO<sub>2</sub> permeance and selectivity, which can be attributed to the improved free volume properties and dipole-quadrupole interaction between CO<sub>2</sub> and ethylene oxide (polar ether oxygen) group on POSS as well as PEO polymer chain. Factors such as high hydrophilicity, increased roughness, improved free volume and sustained crystallinity of the PVA-PEO/POSS membranes contributed to the excellent separation performance of liquid and gas mixtures. As evident from the results presented in chapter 7, PVA-PEO/POSS membranes exhibited excellent mechanical properties in the presence of CMC and POSS. The interfacial activity of the PVA-PEO system enhanced in the presence of CMC. Moreover, thermal stability and hydrated state mechanical stability of PVA-PEO membrane also get improved to a great extent through the incorporation of nanostructured POSS molecules.

### 9.4 Mechanical stability and permeation properties- A comparison

**Table 9.1:** The percentage of water separation attained from THF-water azeotropic mixture by the membranes

Membranes	% of water separation attained from THF–water azeotropic mixture
P0	50
PPP3	97
POTP3	98
PPCPP3	98.1
PPCOP3	96.7

**Table 9.2:** The percentage of water separation attained from IPA-water azeotropic mixture by PVA/m-POSS membrane

Membrane	% of water separation attained from IPA-water azeotropic mixture
PG	72
POCPG1	93

**Table 9.3:** CO<sub>2</sub> permeability and CO<sub>2</sub>/N<sub>2</sub>(O<sub>2</sub>) selectivity data of PVA/POSS and PVA-PEO/POSS membranes

Membranes	CO <sub>2</sub> permeability (Barrer)	CO <sub>2</sub> /N <sub>2</sub> selectivity	CO <sub>2</sub> /O <sub>2</sub> selectivity
PVA	24	4.19	0.49
PVA/PEG-POSS	110	14.82	1.97
PVA/Octa-TMA-POSS	54	10.57	1.17
Crosslinked PVA/m-POSS	61	11.54	1.31
PVA-PEO/PEG-POSS	270	38.60	4.74
PVA-PEO/Octa-TMA-POSS	215	26.87	3.64

**Table 9.4:** Tensile strength and Young's modulus data of all systems

Membranes	Tensile strength (MPa)	Young's modulus (MPa)
PVA	35±4	198±5.8
PVA/Octa-TMA-POSS	43±1	637±5.3
PVA/m-POSS	57±3	1169±5.1
PVA-PEO/PEG-POSS	47±4	1342±6
PVA-PEO/Octa-TMA-POSS	48±4	1146±5

### 9.5 Future Aspects

- ❖ Synthesis of various organically functionalised POSS molecules to make the membrane more cost effective.
- ❖ The PVA/POSS and PVA-PEO/POSS membranes exhibited excellent separation properties for various gases as well as azeotropic mixtures. Also, these membranes possess remarkable mechanical and thermal stability when compared to neat PVA. Therefore, the commercial application of membrane in separation process is yet to be explored.
- ❖ Antimicrobial activity and biodegradation of the membranes are to be studied in detail. The suppression of bacterial action on the PVA membrane is an important aspect in medical applications and water purification processes.

# Curriculum Vitae

## SWAPNA. V.P

Research Scholar  
Postgraduate & Research Department of Chemistry  
St. Joseph's College, Devagiri  
Calicut-673 008, Kerala, India  
Tel: +91 9400583677  
E-mail: vpswapna@gmail.com



---

### Permanent Address

Jyothi House  
Edakkulam P.O  
Koyilandy  
Calicut- 673306, Kerala, India  
Tel: 9400583677/ 9539460530

### Personal Information

Date of birth : 23-04-1990  
Nationality : Indian  
Religion : Hindu  
Gender : Female  
Marital status : Married

### Educational Summary

2014(June)-Present: Ph.D thesis submitted on 15<sup>th</sup>  
September 2018  
Title of the Ph.D Thesis : Permeation Properties and Stability  
of Nanostructured Polyhedral  
Oligomeric Silsesquioxane  
Incorporated Poly(Vinyl Alcohol)  
Membranes  
Supervisor : Dr. Ranimol Stephen  
Assistant Professor  
St. Joseph's College, Devagiri  
Calicut – 673 008, Kerala, India  
2010-2012 : **Master of Science,**  
Chemistry (3<sup>rd</sup> rank holder)

2007-2010 : School of Chemical Sciences  
Mahatma Gandhi University  
Kerala, India  
**Bachelor of Science**, Chemistry  
University of Calicut, India (86%)

### **Academic Achievements**

1. **University 3<sup>rd</sup>** Rank for **M.Sc.** Physical Chemistry, School of Chemical Sciences, Mahatma Gandhi University (2012).
2. **UGC-NET** Lectureship 2013, June.
3. Qualified **GATE** exams in 2013 (**93.5%**) & 2014 (**94.6%**)

### **Work History**

1. Junior Research Fellow in DST-Fast Track Project for Young Scientist at St. Joseph's College, Devagiri, Calicut.
2. Project Trainee at National Chemical Laboratory, Pune, India. Project title: Synthesis, Characterisation and Catalytic Activity of Nanoparticles Embedded Hierarchical Scaffold

### **Research Awards**

1. **Best Poster Presentation Award** in the **30<sup>th</sup> Kerala Science Congress**, "Poly (Vinyl Alcohol) (PVA)/Cage Structured Polyhedral Oligomeric Silsesquioxane (POSS) Membranes for the Separation of Azeotropic Mixture of Isopropanol (IPA)–Water System" held at Government Brennen College, Thalassery, 28- 30 January **2018**
2. **KSCSTE-Springer Award** in the **30<sup>th</sup> Kerala Science Congress**, "Poly (Vinyl Alcohol) (PVA)/Cage Structured Polyhedral Oligomeric Silsesquioxane (POSS) Membranes for the Separation of Azeotropic Mixture of Isopropanol (IPA)–Water System" held at Government Brennen College, Thalassery, 28- 30 January **2018**
3. **Rev. Fr. Joseph Kappulumakkal CMI** endowment for **Best Paper Publisher** in the year **2015-16** and **2016-17** from St. Joseph's College, Devagiri
4. **Best Poster Presentation Award** in the **103<sup>rd</sup> Indian Science Congress** held at University of Mysuru, 3-7 January **2016**
5. **Best Paper Award** in the **26<sup>th</sup> Swadeshi Science Congress**, "High Performance Green Polymer Membranes for the Separations of Solvents" held at Central Marine Fisheries Research Institute, Kochi, 07- 09 November **2016**
6. **Best Poster Presentation Award (3<sup>rd</sup> prize)** at the **Third International Conference**, "Polymer Processing and

Characterisation” held by International and Inter University Centre for Nanoscience and Nanotechnology, Mahatma Gandhi University, Kerala, India, 11-13 October **2014**.

### **Membership in Professional Group**

Indian Science Congress Association member

### **Research Experience**

- Separation of azeotropic mixtures
- Membrane based CO<sub>2</sub> separation technology
- Experienced in preparation, characterisation and properties of hybrid membranes
- Conducted advanced research on gas barrier and solvent transport properties of nanoparticle incorporated polymer membranes.
- Nanoparticle synthesis and modification
- Published the research findings in highly reputed international journals and presented at scientific conferences.

### **Papers Presented in International (3 Nos.) and National Conferences (6 Nos.)**

1. **Presented a Poster** in the **30<sup>th</sup> Kerala Science**, “Poly (Vinyl Alcohol) (PVA)/Cage Structured Polyhedral Oligomeric Silsesquioxane (POSS) Membranes for the Separation of Azeotropic Mixture of Isopropanol (IPA)–Water System” held at Government Brennen College, Thalassery, 28- 30 January **2018**
2. **Presented a poster** in the **EFCS International Conference**, “Pervaporation Performance Polyhedral Oligomeric Silsesquioxane (POSS) Embedded Poly (vinyl alcohol)-Poly (ethylene oxide) Blend Membrane for Pervaporation Separation of THF-Water Azeotropic Mixture” held at Farook (Autonomous) College, Calicut, 22-24 September **2017**
3. **Presented a paper** in the **MESMAC International Conference**, “Dynamic and Dielectric Properties of Poly (vinyl alcohol)-Polyhedral Oligomeric Silsesquioxane Membranes” held at MES College(Autonomous), Mampad, Malappuram, 14-16 February **2017**
4. **Presented a paper** in the **26<sup>th</sup> Swadeshi Science Congress**, “High Performance Green Polymer Membranes for the Separations of Solvents” held at Central Marine Fisheries Research Institute, Kochi, 07- 09 November **2016**
5. **Presented a poster** at the UGC and KSCSTE sponsored **National Seminar** on the “Green Strategies and Technologies” held at the

Department of Chemistry, St. Joseph's College, Devagiri, Calicut, 18-19 February 2016

6. **Presented a paper** at the UGC and KSCSTE sponsored **National Seminar**, "Green Strategies and Technologies" held at the Department of Chemistry, St. Joseph's College, Devagiri, Calicut, 18-19 February 2016
7. **Presented a paper** in **28<sup>th</sup> Kerala Science Congress** held at University of Calicut, **28–30 January 2016**.
8. **Presented a paper** in **25<sup>th</sup> Swadeshi Science Congress** held at Sree Sankaracharya University of Sanskrit, Kalady, 15-18 December **2015**.
9. **Invited talk in Third International Conference** on "Polymer Processing and Characterisation" held at International and inter University Centre for Nanoscience and Nanotechnology, Mahatma Gandhi University, Kerala, India, 11-13 **October 2014**.

#### **Conferences and Workshops Attended**

1. Participated in the **International Conference** on Polymer Science and Technology, **MACRO 2017** conducted by The Society for Polymer Science, India Thiruvananthapuram Chapter, in collaboration with Indian Space Research Organisation, Council of Scientific and Industrial Research, Department of Science and Technology and American Chemical Society, 8-11 January **2017**
2. Participated in a **workshop** on Polymer Processing-Macro to Micro/Nano Scale conducted by NIT, Calicut on 27<sup>th</sup> November **2015**.
3. Participated in a **workshop** on Science Writing conducted by **Swadeshi Science Movement, Kerala & ICAR-Indian Institute of Spices Research** at Swapna Nagari, Kozhikode, October **2015**
4. Completed a **Training Programme** in 'Recent Trends and Developments in Bioplastic and their Applications' organised by **Central Institute of Plastic Engineering and Technology (CIPET, Kochi)** during 22-23 August **2014**

#### **Project Work Co-Guided (MSc & BSc)**

1. Influence of Chemically Modified Polyhedral Oligomeric Silsesquioxane (POSS) on the Mechanical Stability of Poly (Vinyl Alcohol), **2017**
2. Thermal Stability of Chemically Crosslinked Polyvinyl Alcohol/Polyhedral Oligomeric Silsesquioxane Membrane, **2017**

3. Characterisation and Thermal Properties of Poly(Vinyl Alcohol) (PVA)/Organically Modified Cage-like Silsesquioxane Nanocomposite Membranes, **2016**
4. Characterisation and Mechanical Properties of Poly(Vinyl Alcohol) (PVA)/Organically Modified Cage-like Silsesquioxane Nanocomposite Membranes, **2016**
5. Properties of Poly(Vinyl Alcohol) (PVA)/Organically Modified Cage- Like Silsesquioxane Nanocomposite Membranes, **2016**
6. Characterisation and Thermal Properties of Polysulphone/Polyhedral Oligomeric Silsesquioxane Nanocomposite Membranes, **2015**
7. Polysulfone/Polyhedral Oligomeric Silsesquioxane Nanocomposite Membranes: Preparation, Characterisation and Properties, **2015**
8. Isocyanate Free Synthesis of Diurethane: A “Green Approach”, **2015**
9. A Study on the Water Uptake and Porosity of Polysulfone Nanocomposite Membranes-Prepared by Phase Inversion Method, **2014**
10. Characterisation and Thermal Stability of Polysulfone/Halloysite Nanotube Nanocomposite Membranes-Prepared by Phase Inversion Method, **2014**

#### **Instrumental/Experimental Skills**

- Demonstrable expertise in the operation and application of TGA, FT-IR, ATR, UV-Visible spectrometer, water purification by pervaporation technology, gas separation technology, Freeze dryer, centrifugation and Probe Sonicator.
- Expertise in the synthesis and chemical modification of polymers and nanoparticles.
- Experienced in the preparation of hybrid polymer membranes through different techniques.

#### **Publications (7 *International*)**

1. **Swapna V.P**, P.M.G. Nambissan, Selvin Thomas P, Vayyaprontavida Kaliyathan Abitha, Thomaskutty Jose, Soney C. George, Sabu Thomas, Ranimol Stephen, Free Volume Defect and Transport Properties of Mechanically Stable Polyhedral Oligomeric Silsesquioxane Embedded Poly (vinyl alcohol)-Poly (ethylene oxide) Blend Membranes, *Polymer International* (Accepted) (**2019**) (**IF.2.434**), <https://doi.org/10.1002/pi.5815>.
2. **Swapna V.P**, Thomasukutty Jose, Grace Moni, Soney C. George, Selvin Thomas P, Sabu Thomas, Ranimol Stephen, Mechanical Properties and Pervaporation Separation Performance of CTAB



- Modified Caged Structured POSS Incorporated PVA membrane, *J. Mater. Sci.*, 54(11)(**2019**)8319-8331 (**IF. 3.442**)
3. **Swapna V.P**, Thomaskutty Jose, Soney C. George, Sabu Thomas, Ranimol Stephen, Pervaporation Separation of an Azeotropic Mixture of a Tetrahydrofuran–Water system with Nanostructured Polyhedral Oligomeric Silsesquioxane Embedded Poly(vinyl alcohol), *J. Appl. Poly. Sci.*, 136 (**2019**) 47060(**IF : 1.2**)
  4. **Swapna V. P**, Deepalekshmi Ponnamma, Kishor Kumar Sadasivuni, Sabu Thomas, Ranimol Stephen, Effect of Nanostructured Polyhedral Oligomeric Silsesquioxane on the Physical Properties of Poly(Vinyl Alcohol), *J. Appl. Poly. Sci.*, 134 (**2017**) 45447 (**IF : 1.2**)
  5. **Swapna V.P**, Saranya E. P, Nithya A B, Ranimol Stephen, Properties of Polysulfone/Halloysite Nanocomposite Membranes: Prepared by Phase Inversion Method, *Macromolecular Symposia* 361 (**2016**) 11–19 (**IF : 0.92**)
  6. **Swapna V.P**, T. Greeshma, C. S. Dev, M. S. Sreekala, Ranimol Stephen, Mechanical and Swelling Behavior of Green Nanocomposites of Natural Rubber Latex and Tubular Shaped Halloysite Nano Clay, *Polymer Composites* 37 (**2016**) 602–611(**IF :2.005**)
  7. **Swapna V.P**, Saranya V, Rahana M. P, Selvin Thomas P, K. I. Suresh, Ranimol Stephen, Thermal Properties of Poly(Vinyl Alcohol) (PVA)/Halloysite Nanotubes Reinforced Nanocomposites, *International Journal of Plastic Technology* 19 (**2015**) 124-136, **DOI**: 10.1007/s12588-015-9106-3

### **Book Chapters**

1. **Swapna V.P**, Abhisha V. S, Ranimol Stephen, Polymer/ POSS Nanocomposite Membranes for Pervaporation, Elsevier (March **2020**) eBook (Accepted) ISBN: 9780128167854
2. **Swapna V.P**, Ranimol Stephen, Nanostructured Polyhedral Oligomeric Silsesquioxane (POSS): Structure, Properties and Applications, UGC-HRDC, University of Calicut (**2018**) ISBN 978-3-16-148410-0
3. Abhisha V. S, **Swapna V.P**, Ranimol Stephen, Modern Trends and Applications of Gas Transport Through Various Polymers, Elsevier (**2017**) eBook ISBN:9780128098851
4. **Swapna V.P**, Ranimol Stephen, Recycling of Polymers: Methods, Characterisation and Applications, Chapter, Recycling of Rubbers, Published by Wiley in (**2016**) ISBN: 978-3-527-33848-1

### **Papers communicated**

1. **Swapna V.P**, P. M. G. Nambissan, Vayyaprontavida Kaliyathan Abitha, Hanna J. Maria, Sabu Thomas, Ranimol Stephen, Effect of Cage Structured POSS on the Free Volume and Gas Permeation of Poly(Vinyl Alcohol), Polymer Composite, Wiley
2. **Swapna V.P**, Meera Krishnan, Abhisha V. S, Ranimol Stephen, Thermal and Water stability of PVA/POSS, PVA/m-POSS and PVA-PEO/POSS Systems, Journal of Thermal Analysis and Calorimetry, Springer